Corso di Laurea Magistrale in Ingegneria Civile

TESI DI LAUREA MAGISTRALE

Mechanical and environmental properties of alkali-activated powders from construction and demolition waste aggregates

Indagine sperimentale sulle caratteristiche meccaniche e ambientali di polveri derivate da aggregati da costruzione e demolizione attivate per via alcalina

Relatori

Prof. Marco Bassani

Prof. Paola Palmero

Ing. Luca Tefa

Candidata

Maria José Rojas Medrano

Ottobre 2018

Acknowledgments

I would first like to thank my parents, Edgar Rojas and Fanny Medrano for being always my constant support and give me the encouragement to pursue my dreams, this achievement is yours.

I wish to thank my sisters Maureen Rojas and Estefanny Rojas for always giving me emotional support and being there for me when I most needed it. You have always known to give me the best advice, you are my role models and I want to be like you someday.

I'm deeply grateful to the "Universidad Central de Venezuela" for being my second home and giving me the opportunity to become a professional and be part of the double degree program.

I would also like to thank the Polytechnic of Turin for allowing me to finish my studies and for the cultural exchange offered.

I would like to express my deep gratitude to Prof. Marco Bassani, Prof. Paola Palmero and Eng. Luca Tefa, my research supervisors, for their patient guidance, enthusiastic encouragement and useful critiques of this research work.

Special thanks to Maria Paula Marin, for always supporting me when I needed it and your friendship during all this years. To Nahimbraska Gil, my dear friend, for helping me believe in me and for always giving me the best advice, thank you so much. To you, Maurizio Faleo, for always giving me a reason to smile, for supporting me constantly since we met and for believe in me, without you none of this was possible, I'm very grateful.

Thank you all,

Maria José Rojas Medrano

Table of Contents

List of figures

List of tables

Introduction

The construction industry is not only one of the great consumers of natural resources but is also a sector that generates huge amounts of waste. Nowadays it is of great importance to find a more sustainable way of building preserving the environment. In fact, construction and demolition wastes (CDW) have received significant attention in the last few decades due to their potential as an alternative aggregate in the construction industry. Their reuse would significantly decrease the environmental impact of constructions by reducing the exploitation of natural resources and decreasing the amount of wastes material destined for landfills.

The European Union statistical data evidences the progressive increase of waste generation by all economic activities and households in the EU over the years, revealing that CDW represents at least one third of the total waste generation in EU. However, in 2008 the European Parliament issued the Directive n° 2008/98/EC (European Parliament, 2008), which main objective is to increase the recycling of non-hazardous waste by 2020 and achieve a CDW minimum reuse of 70%.

CDW are composed of a variety of materials such as concrete, ceramics, soils, asphalt, metals, and occasionally wood, glass, and other materials normally used in civil constructions. Before their use, it is important they are properly treated and receive the CE certification according to the EU regulation nº 305/2011 (European Parliament and Council of the European Union, 2011). This certification guarantees that CDW aggregates would have constant performance characteristics, regardless to their nature and origin.

From an economical point of view, the reuse of CDW is convenient when it is competitive with the natural aggregate in terms of cost and quantity. CDW is more competitive where there's a lack of raw materials and landfilling sites (Tam and Tam, 2006). The reuse of CDW will reduce the cost of production in the construction sector and will offer important economic benefits.

Several studies have been carried out to evaluate the CDW feasibility in civil constructions. In fact, it has been already demonstrated that such material has the potential to be used as alternative aggregate in unbound layers of pavement structures, trench backfilling, road embankments and even in low-strength concrete production.

In the road construction sector, some researchers have proven that such material offers sufficient durability and acceptable mechanical performance to be used in granular bases and subbase layers of unpaved rural roads (Jiménez et al., 2012a). Furthermore, it has been observed that its performances are comparable to those of natural aggregates (Arulrajah et al., 2013; Bennert et al., 2000).

However, some road applications might require a prior stabilization to improve their mechanical performance and meet minimum requirements for base and subbase layers of pavements. Many authors have studied the mechanical behaviour and physical properties of CDW stabilized with ordinary Portland cement (Mohammadinia et al., 2015; Agrela et al., 2012), with by-products stabilizers such as cement kiln dust (Bassani et al., 2017) or fly ash (Arulrajah et al., 2017) and some recent contributions considered a chemical stabilization through the alkaline activation of the aluminosilicates presented in such material. In fact, the CDW recycled aggregates may have the function of inert and, at the same time, also the role of stabilizer of the rest of the inert mixture.

Several authors have demonstrated the mechanical performance improvement of various materials when stabilized with alkaline solutions (AS) made up of NaOH and Na_2SiO_3 (Hoy et al., 2016; Zaharaki et al., 2016; Komnitsas et al., 2015). They found that parameters such as the grain size, the chemical composition, the concentration of the activating solution, the curing temperature and curing time control the strength of the alkali-activated CDW samples. However, none of these studies have considered the possible alkaline activation of the fine particles present in the CDW aggregates and the environmental assessment for the alkali-activated CDW material.

The aim of this thesis is to investigate the mechanical performance of the pulverized CDW constituents, when subjected to an alkaline activation to stabilize CDW recycled aggregates. To pursue this objective, a chemical and a physical-volumetric analysis was carried out on different constituents of CDW: (a) recycled concrete (RC),

(b) bricks and tails (BT), (c) reclaimed asphalt aggregates (RA), (d) natural aggregates (NA), and, additionally, the mix of such four components which form the unseparated fraction (UND). Thirty-five prismatic samples for each CDW constituent were prepared combining different liquid to solid (l/s) ratios, and alkaline solution concentrations. Finally, the hardened pastes were subjected to flexural and uniaxial compressive tests to evaluate the effectiveness of the alkaline activation and identify the most reactive component in stabilizing the CDW granular mixtures.

This manuscript is organized in three chapters. The first provides an overview on studies describing the use of CDW aggregates in road construction. Statistics to the annual production of CDW in Italy and Europe, and some basic concepts of the alkaline activation process are also presented. The second chapter introduces the materials and methods used in this research, with specific emphasis on the sample's preparation process, the experimental methods to measure physical and volumetric characteristics of fines, the mechanical performance of hardened specimens, and the chemical characterization of CDW. The third and last chapter provides all the results and discussion of the data collected from the laboratory tests.

Chapter 1: Literature Review

Over the last few years, the reduction of non-renewable resources has been of global concern for those who support the sustainable development and the preservation of the environment, thus encouraging the use of recycled materials in a number of human activities. CDW have been identified by the European Commission as a priority waste stream because of the large amount of wastes that are generated and their high potential for re-use and recycling. There's a growing interest in the road construction sector of the CDW to use it as base and/or sub-base material in road constructions due to their low-cost solution respect to natural aggregates.

CDW are generated by construction, maintenance, and demolition of building and civil works. The composition depends on the site that is generated, for example, a building demolition will cause a huge amount of recycled concrete but not recycled asphalt aggregate for sure (Gálvez-Martos et al., 2018). According to the European Waste Catalogue (Environmental Protection Agency, 2002), the principal components of CDW are: concrete, bricks, tiles and ceramics, wood, glass and plastic, bituminous mixtures, coal tar and tarred products, metals (including their alloys), soil (including excavated soil from contaminated sites), stones and dredging spoil, and basically all the materials normally found in civil works.

The recycling and re-use of CDW definitely will provide lots of benefits to the environment and the construction industry (EPA., 2018) such as:

- the massive reduction of extraction and consumption of natural aggregates in the construction industry, decreasing the environmental impact;
- the reduction of the waste material destined for landfill conserving these spaces for future urban development;
- the decrease of the building project expenses, considering waste material have a lower cost than natural aggregates;

- the energy saving, by avoiding the exploitation of quarries and transport over long distances;
- the creation of employment and economic activities in recycling industries.

1.1. CDW in Italy and Europe

Construction and demolition wastes are one of the most voluminous waste streams generated in the world, as a matter of fact, the statistical office of the European Union (Eurostat), provided an overview of the waste generation by all economic activities and households in the EU, indicating that in 2014 were generated 2 503 million tons of waste from which 34.7% represents CDW, that's approximately 869 million tons.

The European commission issued the Directive (2008/98/EC), which main objective is to provide a framework to achieve a high level of resource efficiency in the EU and become a recycling society. Article 11.2 states that "Member States shall take the necessary measures designed to achieve that by 2020 a minimum of 70% (by weight) of non-hazardous construction and demolition waste, shall be prepared for re-use, recycled or undergo other material recovery". However, only about 50% of CDW is currently being recycled. Some EU countries have already implemented a framework which provides them with a recycling rate of 90% (Gálvez-Martos et al., 2018).

The European commission also introduced in 2016 the "EU construction and demolition waste protocol", being the first guideline of CDW management. The protocol contains good practices from across the EU that will contribute to the waste framework directive objective of 70% of CDW recycled by 2020

In some countries of the EU the objective of 70% recycling of CDW is already achieved according to the estimates of Eurostat for 2017. Figure 1 shows the CDW treatments that the European countries estimated in 2014 (Gálvez-Martos et al., 2018; Eurostat., 2017). It is worth noting that some countries like Greece or Belgium have a huge amount of CDW that is sent to disposal. Furthermore, it must be considered that in some countries, there is a certain amount of illegal dumping which is not considered in the official statistics (Gálvez-Martos et al., 2018). On the other hand, countries like Netherlands, Slovenia or Denmark had more than 80% in CDW material recovered in 2014.

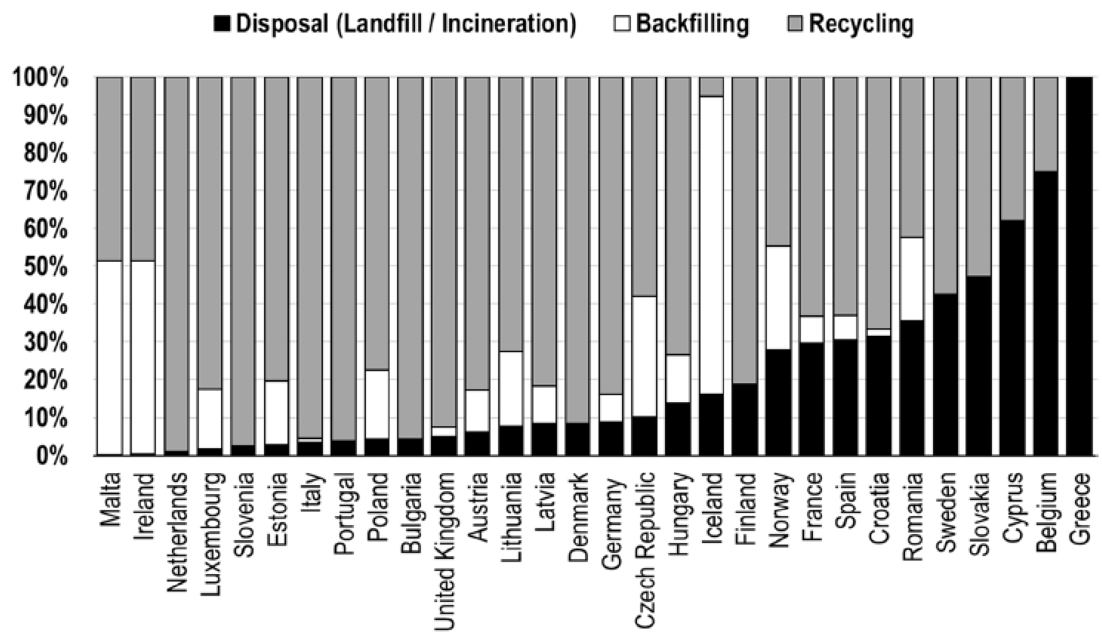

Figure 1: Construction and Demolition Waste's Mineral fraction treatment in 2014. (Gálvez-Martos et al., 2018; Eurostat., 2017)

The CDW management in the Italian Regions and Provinces varies greatly due to factors that may affect the practice like site size and structure, proximity to recycling sites, importance of this issue for the client, ethics and importance of the issue for the construction company, etc.

In Italy the amounts of CDW material and the statistical data are accessible thanks to the Italian Institute for the Protection of Environment (ISPRA) which is in charge of producing national data related to waste. Moreover, each Region has his own waste data centre "*Osservatorio rifiuti*". In 2015, according to ISPRA, 54.091.324 tons of non-hazardous construction waste material that represents approximately 41% of the special waste production in Italy were generated.

Italy does not have a national waste management plan, because each region has its own waste management strategies as established in article n.196 of the law n.152/2006;

however, the legal framework counts for all the country. Some of the most important decrees on waste management are:

- Ministerial Decree, No. 203 dated 8/05/2003 which set a quota of 30% for re-use of recycled materials and products in public procurement;
- Legislative Decree, No. 152/2006 that basically establishes the environmental standards and environmental codes;
- Ministerial Decree, dated 5/2/98 that contains the criteria to distinct hazardous from non-hazardous wastes.

1.2. CDW in road construction

In civil engineering, a road pavement is formed by a surface course laid on a solid foundation. This multi-layer system directly supports the traffic and transmits loads to the subgrade made of selected soils. In road construction, the base and sub-base courses are normally made of natural granular material such as crushed rocks, selected gravels and stabilized materials, which give the pavement sufficient strength and bearing capacity to withstand the effects of vertical loads generated by traffic.

Over the past few decades, several researches have performed laboratory tests on aggregates from CDW to evaluate their feasibility in different civil constructions applications, mainly for unbound layers of pavement structures, road embankments, trench backfilling, and even in low-strength concrete production. However, these recycled materials must ensure enough resistance to the traffic loads, adequate drainage and frost-free characteristics, in other words, the performance must be at least the same provided by natural aggregates to be considered as a replacement.

The CDW aggregates is composed of many elements that have different physical and mechanical properties. Compared to natural aggregates, CDW aggregates have a lower dry density and a high porosity, therefore a greater absorption of water. This phenomenon is increased by the presence of porous materials such as bricks and concrete (Poon et al., 2004).

Several mechanical tests were performed by Bennert et al., (2000) on recycled asphalt pavement aggregate (RA) and recycled concrete aggregate (RC) to assess their behavior under traffic-type loading. Finally, their results shown that a combination of 25% of RA or 25% of RC with dense-graded aggregate would achieve the same resilient modulus and permanent deformation as dense-graded aggregate. The authors concluded that CDW might be a cost-effective material to be used in pavement layers.

CDW aggregates are composed by different types of materials with diverse physical and mechanical properties. Arulrajah et al. (2013) studied their mechanical behavior individually, separating the waste material in 4 different components: recycled concrete, crushed brick, waste rock and reclaimed asphalt pavement. The resilient modulus and permanent deformation results indicated that recycled concrete and waste rock had geotechnical properties equivalent or superior to natural aggregates normally used in base/subbase pavement structures.

Cerni et al., (2012) studied the resilient behavior of unbound CDW aggregates, proving that the waste material presented a resilient behavior very similar to that of typical natural granular material from quarries. They found out that CDW blends presented an optimum moisture content (OMC) greater than in natural aggregates and a lower dry density. Another laboratory study on CDW mixtures was performed by Leite et al., (2011). They found out that, by increasing the amount of ceramic materials to the CDW mixture, the water absorption increases significantly. Furthermore, the authors determined that the compaction and the composition of the CDW mixtures are two important factors to their final mechanical performance.

Poon and Chan., (2006) studied the feasibility of recycled concrete and crushed clay brick blends as subbase material. They determined the volumetric characteristics of the aggregates and the mechanical properties of the blend, finally concluding that compacted CDW have a lower Californian Bearing Ratio (CBR) index with respect to the values shown by mixtures of natural aggregates and this magnitude decreases sensitively with the increase of the ratio between brick and cement present in the mixture.

The physical and mechanical properties of recycled aggregates are normally worse than those of natural aggregates (Cardoso et al., 2016). A stabilization process might be a solution to improve their mechanical performance and meet the minimum requirements for base and subbase layers of pavements. Traditional stabilizers like Ordinary Portland Cement (OPC) (Mohammadinia et al., 2015), cement kiln dust (Bassani et al., 2017) and fly ash (Arulrajah et al., 2017) have been used to improve their properties. However, alkali-activation of CDW is gaining recognition and interest worldwide due to the better environmental performance than traditional stabilizers because these binders have the potential for notable greenhouse emission savings when compared for example with OPC (Rapazote et at., 2011; Provis et al., 2014). Furthermore, geopolymers (or alkali activated products) exhibit rapid mechanical strength development, remarkable chemical and thermal stability and durability in corrosive environments (Kioupis et al., 2018; van Deventer et al., 2007). The negative aspects of the alkaline solution may concern the environmental impact that can cause to the surrounding environment.

1.3. Stabilization of CDW

Soil stabilization is commonly used when the soil does not present a suitable condition to meet a civil engineering purpose. The stabilization consists in a chemical, physical, biological or combined alteration of the soil to improve its mechanical properties, increasing for example the shear strength and improving the bearing capacity of subgrades. Chemical stabilization is extremely used to increase the strength of soils with poor mechanical properties for road embankments and pavements (Mohammadinia et al., 2016). The same goes to CDW, stabilization may be necessary to improve mechanical properties, making such materials totally equivalent or even better than those of natural origin.

A way to improve properties derives from geopolymerization. The term “geopolymer” was introduced in 1987 by Davidovits to identify that group of binders able to harden by the alkali activation of amorphous minerals with high content of aliminium (Al) and silicon (Si). The alkaline activation of alumino-silicates compounds has attracted great attention to the construction industry in the last few decades, due to their potential as alternative (environmental friendly) binders.

Arulrajah et al. (2016) and Mohammadinia et al. (2016) studied the stabilization of CDW with alternative binders activated in a basic environment, such as calcium carbide residue (CCR), fly ash, and slag geopolymers. They found out that the compressive strength and the stiffness of the recycled materials increased significantly with the stabilization.

Rapazote et al., (2011) investigated the mechanical and physical properties of BT, RC, and sludge alkali-activated with an alkaline solution made of sodium hydroxide and sodium silicate. The authors proved that after a thermal treatment for 48 hours all the mixtures had better mechanical performance than ordinary Portland cement (OPC). They also concluded that the alkali-activated materials were less susceptible to high temperatures than OPC.

The strength development of recycled asphalt pavement stabilized with fly ash was also studied by Hoy et al., (2016). After some mechanical tests, they found out that the unconfined compression strength meets the minimum values to be used as pavement base course, confirming their potential in road constructions.

1.3.1. Chemistry of alkaline activation processes

The alkaline activation is referred to the reaction of solid aluminosilicates under basic conditions. Additional terminology generally used to the resulting hardened binder is "geopolymer", especially in case of low-calcium alkali-activated aluminosilicates binders (J. Provis., 2016).

The formation of a geopolymer involves a mixture of solid raw powder (the aluminosilicate source) and a liquid activator which is usually a highly concentrated alkaline solution. The schematic diagram of geopolymer formation is shown in Figure 2.

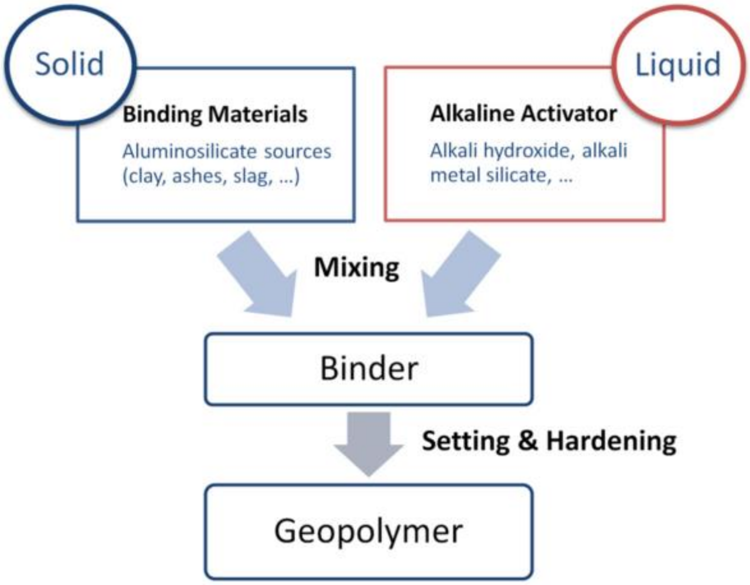

Figure 2:Schematic diagram of geopolymer formation (Liew et al., 2016)

During the process, aluminosilicates bonds break down upon contact with the alkaline reactant. As the reaction progresses, there is a reorganization and diffusion of dissolved ions, which results in the formation of small coagulated structures, then starts the polycondensation to form aluminosilicates gel phases. The final stage concerns the solidification and hardening processes with an ongoing gel rearrangement and crystallization (Liew et al., 2016). The schematic process of the geopolymerization is evidenced in Figure 3.

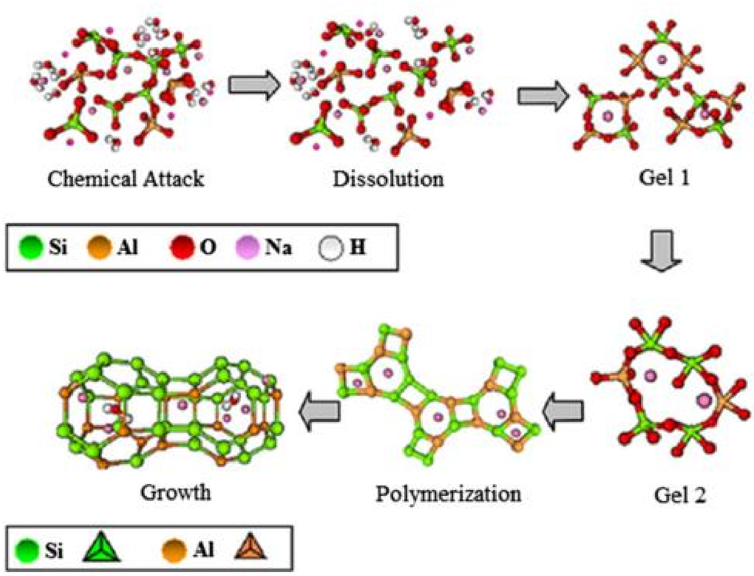

Figure 3: Graphic model of geopolymer formation (Liew et al., 2016)

1.3.2. Alkaline activation of CDW materials

Alkaline activation generally concerns amorphous/pseudo-amorphous aluminosilicate powders, which show higher reactivity in an alkaline environment than crystalline powders. CDW are made predominantly of crystalline powders and consequently are not able to develop high mechanical resistances, however, its alkaline activation has attracted considerable attention over the last few years because the mechanical properties can meet the requirements of base and subbases layers of road pavements. Studies has shown that the structure and mechanical properties of geopolymers depends on the grain size, the chemical composition, the concentration of the activating solution, the curing temperature and time (Komnitsas et al., 2015).

The compressive strength of alkali activated CDW powders with different concentrations of sodium hydroxide (8M, 10M and 12M NaOH) has been studied by Zaharaki et al (2016), concluding that the optimum NaOH molarity for alkali activation of CDW components is 10 M which gives to the specimens the greatest compressive strength. Low concentrations of NaOH do not provide sufficient alkalinity in the mixture, while high concentrations may result in residual alkali concentration that remains unreacted and thus strength weakens (Komnitsas et al., 2015).

The curing temperature is another factor that affects the mechanical properties of the final geopolymer. In fact, Komnitsas et al., (2015), evaluated the variation of the compressive strength with different curing temperatures (60, 80 and 90 °C), determining that for BT and RC, the higher the temperature, the greater the compressive strength; Lampris et al., (2009) also studied the resistance of CDW alkali-activated when maturated at room temperature and at 60 °C, finding again a greater resistance with the increase of the curing temperature. However, even if the curing temperature is an important factor to provide great resistances to the specimens, the usage of the furnace and the energy spent must be considered in the final cost evaluation.

The particle size of the solid raw material is extremely important during the geopolymerization reaction, because even if it is crystalline powder, finer fractions have a higher surface area and the rate of the chemical reaction increases, resulting in a stronger bonding and therefore, in better mechanical properties (Komnitsas et al., 2015). The presence of sufficient water in the mixture is important during the alkali activation, because it facilitates the initiation of the reaction (Zaharaki et al., 2016).

Another study on the possible use of CDW as reagents in a geopolymer paste was carried out by Allahverdi and Kani (2009). They assessed the chemical composition of BT and RC particles, resulting that both waste materials are mainly composed of silica, alumina, ferric oxide and calcium oxide. They activated the raw material with a solution of sodium hydroxy and sodium silicate and the compressive strength after 28 days of curing demonstrated that BT are more suitable for geopolymerization reactions than RC.

The alkaline activation of BT powder was studied by Pathak et al., (2014). The curing was made at 60 ºC for 24 hours; then specimens were conserved at room temperature for 7, 14, 21 and 28 days. Finally, the author measured the strength development with the maximum compressive strength up to 11.43 MPa. The authors also proved that with the increase of the curing period the compressive strength increased too.

1.4. Environmental assessment of CDW

The possibility of using CDW aggregates in base/subbase pavement layers must be assessed to check if they contain hazardous materials such as metals and chemical compounds. They can contaminate the surrounding environment; because of this, it is necessary to assess the pollutant release of these wastes materials. By means of a leaching test, it is possible to evaluate the physical, chemical, and biological reaction that mobilize the contaminants under the effect of the leachant or solvent that initiates the leaching process. In road constructions, the solvent that can extract soluble contaminants may take the form of rain water percolating through the road structure (Annette Hill, 2004).

The environmental impact caused by CDW is determined by the amount of pollutants that water can dissolve and leach into the environment, by reaching the surface and/or underground water (Galvín et al., 2012). The European Union Council, 2003/33/EC, imposed limits on concentrations of various metals resulting from leaching processes for inert landfill.

The environmental performance of CDW materials was evaluated by Jimenez et al. (2012) using the UNI EN 12457-3 leaching test. The results were compared with the waste acceptance criteria for land-filling (EU Council, 2003), finding that all materials were classified as inert except the recycled concrete aggregate, which failed because its arsenic content exceeded the upper limit for inert materials with a L/S ratio of 2.

Another assessment of the environmental impact of crushed concrete from demolition waste was made by Wahlström et al. (1997). They performed batch leaching tests according to the EN 12457 and determined that the leaching amounts from the CDW were low, while only sulphate and chromium were released. They also found that the influence of pH change on the leachability is low.

It is known that alkali-activated products cause less damage to the environment than ordinary Portland cement, however further investigations are needed to be used in real applications (Rapazote et al., 2011).

The application of CDW alkali-activated in road construction is possible if such material does not affect negatively the road adjacent environment, so an environmental assessment through some leaching tests must be carried out.

Chapter 2: Materials and methods

2.1. Objectives

The aim of this thesis is to evaluate the potential of the pulverized CDW constituents, when are alkali activated without thermal treatment to be used as an alternative binder to stabilize pavement base and subbase layers. To pursue this objective a series of laboratory test and methods were adopted to investigate the following aspects:

- the chemical composition of the pulverized CDW constituents;
- the physical and volumetric characteristics of the CDW fine particles;
- the workability of the CDW blends alkali-activated;
- the mechanical performance of the CDW hardened pastes and
- the environmental impact of the CDW alkali-activated.

This chapter describes the laboratory tests used to achieve the research objective and provide some theoretical basis for a better understanding of the subsequent results obtained. Materials used and the stages of the experimental investigation are also included.

2.2. Materials

2.2.1. Construction and Demolition Waste (CDW)

The recycled material used for the experimental investigation comes from four quarries located around the metropolitan area of the city of Turin, all of them in compliance with the Community Directives and in possession of the required CE certification:

- Cavit S.P.A (La Loggia, TO)
- Cave Druento S.R.L (Druento, TO)
- F.G S.R.L – Fassino (Pianezza, TO)

- Cave Sangone S.P.A (Rivalta di Torino, TO)

There are four main types of material derived from construction and demolition waste (CDW): recycled concrete (RC), crushed bricks and tiles (BT), reclaimed asphalt (RA), natural aggregates (NA). An additional sample derives from undivided material (UND1), which contains the four materials mentioned before in a random way and unknow particles, whose cannot be identified the origin.

These five components were used in the experimental process and all of them were obtained by mixing respectively the material coming from the four quarries mentioned before, considering that previous studies demonstrated that the quarry of provenience doesn't affect composition and performance of each components. Furthermore, another material of interest was evaluated (UND2), which was obtained combining RC, BT, NA and RA in equal proportion. Figure 4 exhibits the raw powders used for the specimens' preparation.

The granular size distribution of all CDW components was under 125 μm considering that the particle size has a noticeable effect on the compressive and flexural strength of geopolymers because of surface area (Paragraph 1.3.2). The samples were equally composed in weight of two solid components: one with a grain size under 63 μm and another with a grain size between 125 and 63 μm.

Both grain sizes were obtained by sieving (Figure 4); they were preserved in a dry environment. All the materials were previously separated subjected to a milling process with the Los Angeles test machine.

(a) (b) (c) (d) (e)

Figure 4: CDW raw powder: BT (a), NA (b), RA (c), RC (d) and UND1 (e).

2.2.2. Alkaline Solution (AS)

The alkaline activation process consists on the reaction of a solid aluminosilicate in a basic environment. The basic environment needed to activate the CDW powders was achieved by using sodium hydroxide $NaOH$, also known as lye and caustic soda (Figure 5).

Figure 5: Sodium hydroxide flakes / caustic soda

The AS was prepared using a magnetic stirrer to dissolve the sodium hydroxide flakes $NaOH$ in distilled water to form a liquid solution of sodium hydroxide with a 50% of concentration in weight, the following step was adding a sodium silicate solution $Na_2O \cdot nSiO_2$ with a concentration of 29%, in different phases to avoid an over increase of the temperature of solution; the proportions can be shown in the following pie chart (Figure 6):

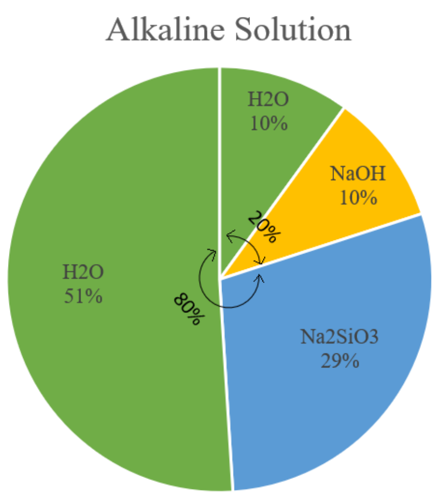

Figure 6: Alkaline solution components proportions (Alkaline concentration 100%)

The alkaline solutions were cooled down for 24 hours before using because of the generated heat during preparation. The activating solution was then mixed with the pulverized CDW under mechanical mixing to obtain a homogeneous paste.

The AS presents a high level of basicity with a pH around 14. Because of it, the activating solution may cause damage to the environment. Hence, samples were made with different alkaline concentrations (AC) to analyze the mechanical performance and the chemical reaction when the concentrations decrease and thus the level of basicity. Therefore, three different concentrations were used: 100%, 75% and 50%, all of them referred to the percentage by weight. In other words, it expresses the ratio between the mass of the alkaline solution (AS) and the total mass of the liquid phase added to the mixture during the mixing phase. From a purely economic point of view, the use of higher alkaline concentrations would be translated in higher costs of production. Figure 7 shows the proportion of the liquid phases used for each concentration.

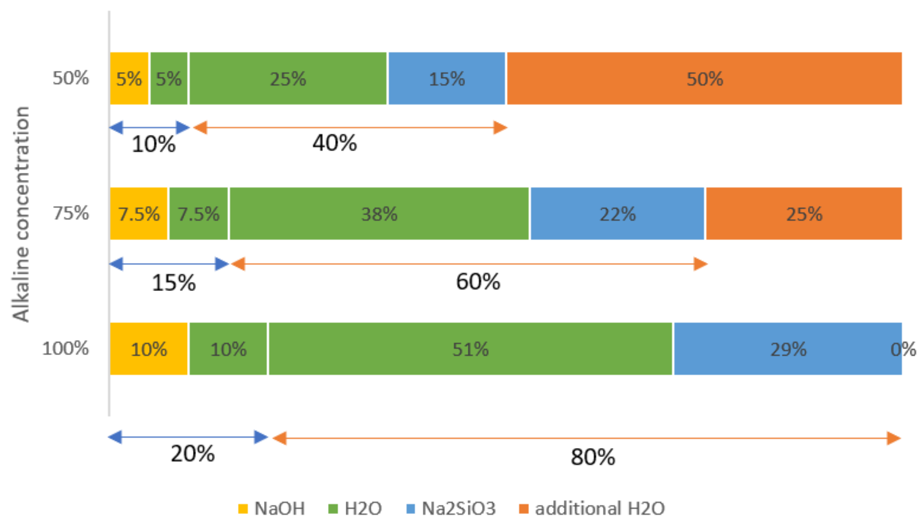

Figure 7: Proportion of components in the AS with concentrations of (A) 100%, (B) 75% and (C) 50%

2.2.3. Mix-design

The CDW fines (RC, RA, BT, NA, UND1, UND2) were mechanically mixed with the AS until they reached the right consistency to cast easily into the molds to obtain hardened specimens with a size of 20x20x80 mm. Later, the hardened specimens were demolded and stored in a hermetic case at room temperature with semi-humid conditions to complete their curing of 28 days. Furthermore, the molds, the pastes and the hardened specimens were weighted in order to evaluate the bleeding phenomena presented in most of the samples. An example of sample preparation is shown in Figure 8 and the hermetic case used for the curing of the samples in Figure 9.

Figure 8: Sample confection

Figure 9: hermetic case for the specimens curing

As already mentioned, the mixtures were made by using two sizes in equal proportion of the solid material: a fraction of 63 – 125 μm and another fraction of particles with dimension lower than 63 μm. A variation on the liquid/solid ratios (l/s) was considered to evaluate the mechanical performance of the hardened pastes when the liquid portion increase, or better, when the viscosity of the pastes decreases, which translates to a better workability of the mixtures. Initially two l/s ratios of 0.6 and 0.5 were studied, yet a l/s = 0.4 with an AS concentration of 100% was lastly considered to evaluate the mechanical behavior of the specimens when the pastes present higher viscosities. The mix-design used for each mixture is summarized in Table 1.

Table 1: mix design of the CDW pastes.

AS concentration	**material**	**quantities [gr]**			**dimensions [mm]**
		l/s = 0.6	l/s = 0.5	l/s = 0.4	
100%	BT, NA, RA, UND1, RC	125	125	150	<0.063
		125	125	150	0.125 - 0.063
	sodium hydroxide	30	25	24	-
	sodium silicate	120	100	96	-
	water	0	0	0	-
75%	BT, NA, RA, UND1, RC	125	125	-	<0.063
		125	125	-	0.125 - 0.063
	sodium hydroxide	22.5	18.75	-	-
	sodium silicate	90	75	-	-
	water	37.5	31.25	-	-
50%	BT, NA, RA, UND1, RC	125	125	-	<0.063
		125	125	-	0.125 - 0.063
	sodium hydroxide	15	12.5	-	-
	sodium silicate	60	50	-	-
	water	75	62.5	-	-

For each combination, a total of five specimens were assembled in order to repeat the test several times for the same material and perform a robust statistical analysis of the results obtained on the mechanical tests. Finally, thirty-five specimens were prepared for each CDW constituent, considering all the combinations studied. A total of 220 samples were assembled and tested for this research (Figure 10).

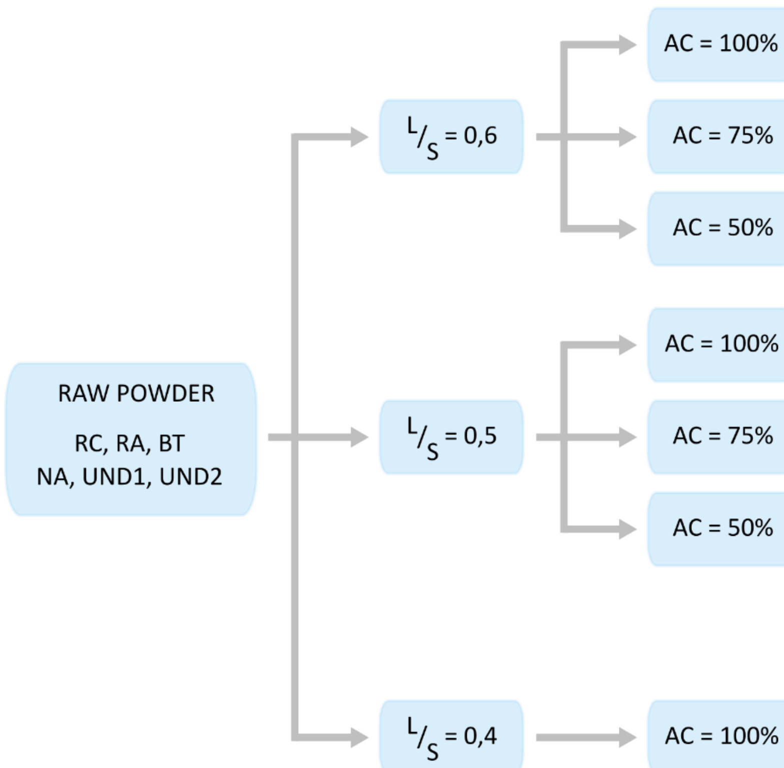

Figure 10: combinations considered to prepare the pastes

2.3. Experimental investigation

Several laboratory tests were carried out to evaluate the physical, volumetric and chemical characteristics of the CDW particles. Moreover, flexural and uniaxial compression tests were performed on CDW hardened specimens to evaluate their mechanical properties. An environmental assessment to the alkali-activated waste materials was carried out, because of the possible heavy metals that can be leached to the soil foundation and the basic environment that may be generated under contact with rain water.

A first step in experiments consisted of the grain separation of the waste material coming from the quarries (Paragraph 2.2.1) to obtain the two grain sizes needed for each CDW component. Following the grain subdivision, a series of laboratory tests were carried out to determine the chemical composition, the particle size distribution, the density and the Rigden voids of the fine particles. The next step consisted in the evaluation of the blend's viscosity and the bleeding phenomena presented in the samples. After that, the compression and flexural tests were carried out to the hardened specimens. Finally, the environmental assessment of the powders alkali-activated was perform through leaching tests and pH tests.

The experimental investigation was divided in three sections (Figure 11): the first one, describes the methods used to determine the physical-volumetric characterization of the powders and the pastes, the second section includes the methodology used to determine the mechanical performance of the hardened specimens and the third and last section describes the methods used to assess the environmental impact of the alkali-activated fines.

Figure 11: sections of the experimental investigation

The alkali activation of the CDW might be an exceptional option for the road construction industry to decrease the costs of production and preserve the environment. Nevertheless, it must be proven that the alkaline activation is a viable option from an economical, mechanical and environmental point of view.

2.3.1. Physical and volumetric characteristics

The mechanical performance of the alkali-activated powders directly depends on its physical and volumetric characteristics. To better understand the mechanical behavior of the final products, it is necessary to investigate the preliminary volumetric and physical characteristics of the starting raw powder.

Particle size analysis

By far, an important physical property of grain materials is the particle size, because it directly affects the final strength of the hardened pastes, the packing of the pastes, the bulk density of the raw material and the geopolymer reaction. As said in paragraph 1.3.2, larger surface areas lead to higher reaction rates and thus, stronger bonding.

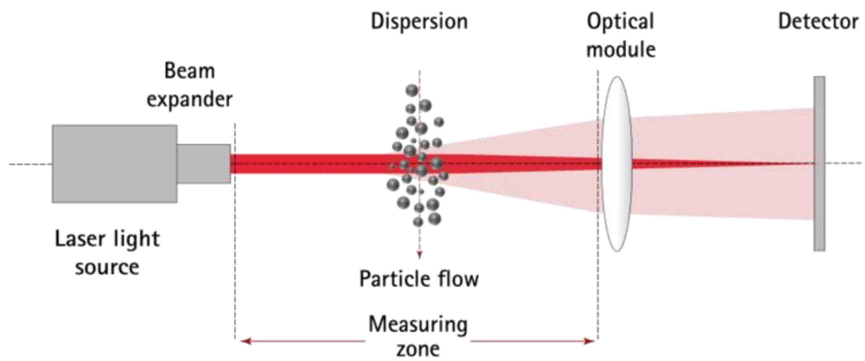

Figure 12: Laser diffraction particle sizer

The particle size analysis for small particles is typically achieved by means of particle size analyzers by laser diffraction (Figure 13), which is commonly used for particles in the range of 0.5 to 1000 μm. It is based on the principle of scattering of a beam light (a laser) that collides a group of particles as shown in Figure 12. Starting by the assumption that the angle of light scattering is inversely proportional to the particle size (the smaller the particle size, the larger it would be the angle of light scattering), it is possible to define the particle size distribution of a sample of fines.

Figure 13: Laser particle sizer FRITSCH

Figure 14: Wet dispersion unit

Different studies were carried out using the laser instrument (Figure 13). They consisted in the evaluation of CDW particles (differentiated in RC, RA, BT, NA and UND1) under 63 µm, under 125 µm and between 63 and 125 µm. Before any measure, the instrument was cleaned with distilled water at least three times to avoid contamination in the samples, background measurements of the distilled water indicated whether further washing was necessary or not. Then, the samples were prepared in the wet dispersion unit (Figure 14) by inserting approximately 1 g of grain material in about 125 ml distilled water. The suspension was then stirred and scanned, giving the background number of particles determined. The relevant output was the particle size distribution (Figure 15), which expresses the cumulated frequency as function of the size of the grain material, usually expressed in the logarithmic scale.

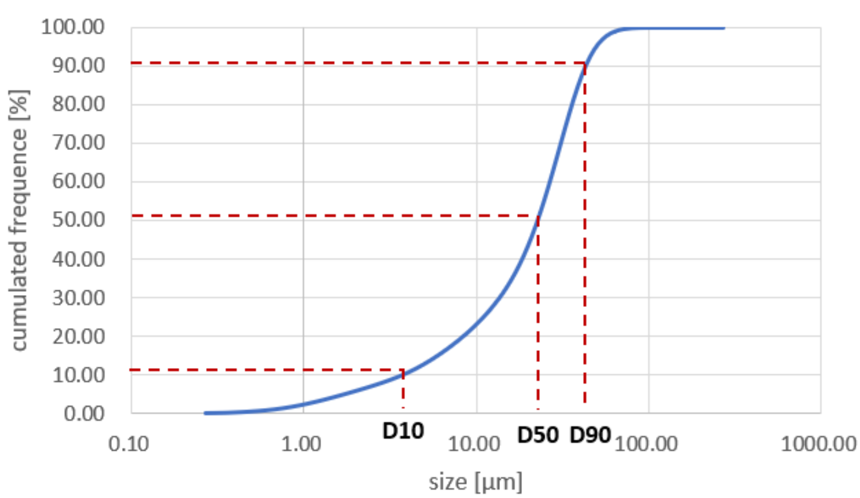

Figure 15: Particle size distribution example

Density of the CDW powders

The density is an elementary physical property of any material. For homogeneous materials it is defined as the ratio of its mass to its volume. To determine the particles density of raw powders, it was performed the pycnometer method according to the UNI EN 1097-7:2008. Density determination by pycnometer is a very precise method, it uses a liquid with well-known density, such as distilled water, at determined temperature. The pycnometer (Figure 16) consist in a glass flask with a close-fitting ground glass stopper with a capillary hole through it. This fine hole releases the spare liquid after closure and allows the determination of a given volume with a high accuracy.

Figure 16: pycnometers filled with the grain material and distilled water

It was first determined the volume of the pycnometer, then it was measured the weight of the pycnometer with the dry material (approximately 10 g) and after that, it was added the distilled water (once the remaining air has been pulled out) to finally weight the pycnometer filled with distilled water and the CDW fines. It is worth mentioning that the density of the grain material depends on the water's temperature; for this reason, the pycnometer filled with distilled water and the material was brought to a temperature of 25°C before weighing it.

To determine the density of the CDW fine particles it was used the following formula:

$$\rho_f = \frac{m_1 - m_0}{V - \frac{m_2 - m_1}{\rho_l}}$$

where:

- m_0 is the weight of the empty pycnometer with the stopper in g.
- m_1 is the weight of the pycnometer with the examined material in g.
- m_2 is the weight of the pycnometer with the examined material filled with distilled water in g.
- V is the pycnometer volume expressed in ml.
- ρ_w is the volumetric mass of the distilled water used at 25 °C expressed in Mg/m^3 (= 0.997 Mg/m^3)
- ρ_f is the volumetric mass of the filler at 25 °C expressed in Mg/m^3.

The pycnometer volume was determined with the following formula:

$$V = \frac{m_3 - m_0}{\rho_w}$$

where m_3 is the weight of the pycnometer filled with distilled water in g.

The volumetric mass of the RA couldn't be determined using distilled water due to the high presence of organic material that floated inside the pycnometer, thus, the ethylene was employed in lieu of water, since it is characterized by a lower density.

Porosity of the CDW material

The porosity is the measure of the void spaces in a granular material, it is the ratio between the volume of voids and the total volume of the sample. It governs some critical aspects, both in mixing phase and in the structure of the hardened product. During mixing, the porosity provides information on the movement of liquid phase and the quantity of air.

To determine the voids of the dry compacted CDW particles, it was used the method in UNI EN 1097-4. The volume of the voids (or Rigden voids) is determined by compacting the CDW powder in a cylindric mold with a standardized hammer (Figure 17), using 100 blows of the hammer in intervals of approximately 1 s.

Figure 17: Compaction equipment (Rigden test)

To calculate the volume of voids of the compacted fines it was used the following equation:

$$v = \left(1 - \frac{4 \cdot 10^3 \cdot m_2}{\pi \cdot \alpha^2 \cdot \rho_f \cdot h}\right) \cdot 100$$

where:

- v is the intergranular porosity (or Rigden voids) in %.
- m_2 is the mass of the compacted fines in g.
- α is the internal diameter of the cylinder mold in mm.
- ρ_f is the volumetric mass of the fines in Mg/m^3.
- h is the height of the compacted fines in mm.

Viscosity of the blends

The viscosity is a physical characteristic of any fluid that represents the resistance to deformation of the fluids by shear stress. It was measured through a Brookfield viscometer (Figure 18) for all the different combinations of blends made of CDW and the AS, except for the blends that were too viscous to be subjected to this kind of test.

The Brookfield viscometer measures the viscosity by means of a spindle, that rotates at a defined speed (measured in rpm) and measures the resistance to rotation. Various spindle designs can be employed (Figure 19), depending on the nature of the sample and the requirements. In principle, less viscous is the liquid greater should be the diameter of the spindle to measure the viscosity.

The viscosity was measured using different spindles for each blend in order to obtain an average viscosity at each speed. The results were analyzed by means of curves plotted according to the rotation speed for each CDW paste prepared and were organized by AS concentration and l/s ratio.

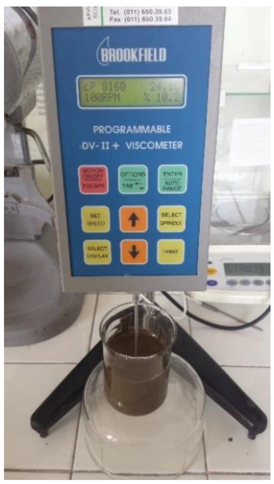

Figure 18: Brookfield viscometer

Figure 19: Spindles of the Brookfield viscometer

The workability of the mixture describes how easily can be placed and consolidated into the molds and this property directly impacts the strength, quality and appearance of the samples. It is expected that pastes prepared with a more concentrated AS would result more viscous and difficult to place into the molds, which in turn can affect in the final mechanical behavior.

2.3.2. Mechanical performance

The mechanical behavior of the hardened pastes made of alkali-activated CDW fine particles, is one of the most important characteristics of the material considering that, depending on their response to flexural and compression tests, it’s possible to understand the effectiveness of the alkaline activation, the level of reactivity for each CDW constituent, and their feasibility as an alternative and sustainable solution to stabilize CDW aggregates.

Both tests were performed in an MTM Zwick/Roell static press (Figure 20) with a load cell of 50 kN and with a displacement control of the crosshead. The data generated by the machine allows the construction of the stress-strain curve and the determination of the maximum stress exhibited by the sample before breaking, and the deformation (strain) at that point.

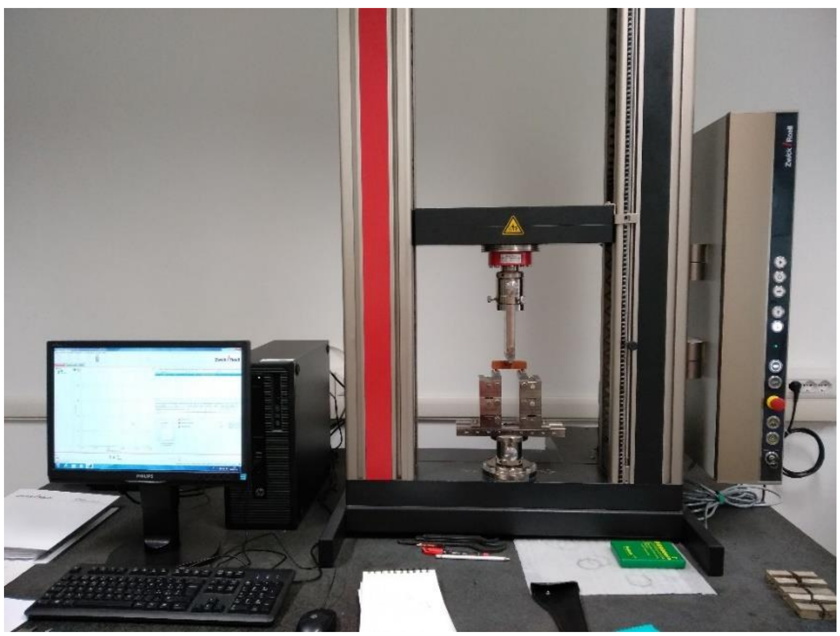

Figure 20: Zwick Roell static press during bending test.

The raw stress-strain curve (Figure 21) doesn’t start from the origin due to the preload imposed for each test. The preload represents the force the machine places on the specimen before recording the test data. Moreover, because the samples are not perfectly shaped, there’s a phase for adjustment before the machine actually starts recording the true behavior of the stress-strain curve. Due to these issues, it is necessary to correct the stress-strain curves (Figure 22) by defining the linear section (would set the final elastic region and tangent modulus) and displace the curve to the origin.

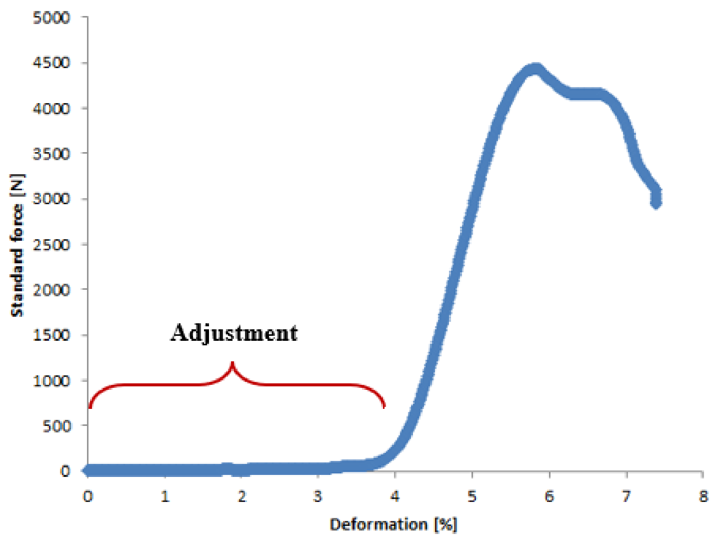

Figure 21: Raw stress-strain curve example

The relationship between the stress and strain is unique for each material, these stress-strain curves (Figure 22) reveal many of the properties of a material like:

- the maximum stress the material can withstand before breaking (σ_{max});
- the strain of the material at the maximum stress point ($\varepsilon(\sigma_{max})$), therefore the relative change in length of the specimen under the maximum applied stress;
- the tangent modulus, which is the slope of the stress–strain curve at the starting point
- the secant modulus that represents the slope of a line drawn from the origin of the stress-strain diagram and intersecting the curve at the point of maximum strength;
- the toughness of the sample, which is the ability of the material to absorb energy and plastically deform without fracturing. It is represented by the area under the stress-strain curve.

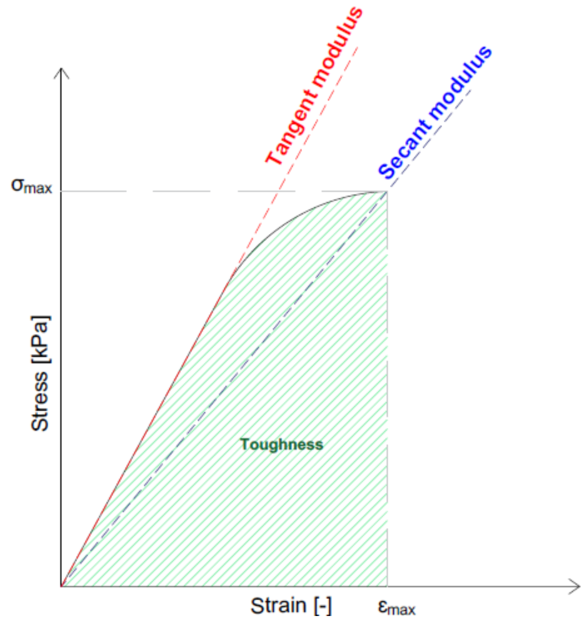

Figure 22: Corrected stress-strain curve example

Compression test

The uniaxial compression test provides the strength and the elastic properties of the tested material. To perform the test, it’s was used a testing device (Figure 23) that allowed the execution of the test for small rectangular prisms. In particular, the instrument is suitable for compression tests of the two parts of a specimen 20x20x80 mm broken previously in the bending test.

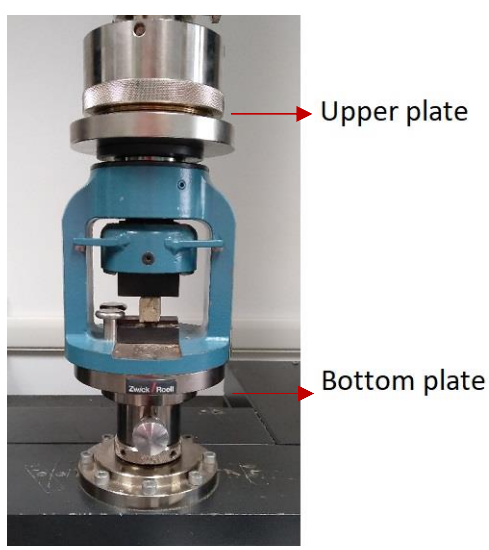

Figure 23: Compression test

The parameter settings for the simple compression test includes:

- a preload of 10 N was selected with a crosshead speed of 2 mm/min;
- a test speed of the crosshead of 0.5 mm/min;
- a time save interval of 0.2 s;
- a specimen thickness of 20 mm.

There were other settings regarding the criteria for the end of the test like, upper force limit, maximum deformation and force shutdown threshold, which were set in order to put some limits to the universal testing machine.

The upper plate linked to the crosshead of the machine approach progressively to the bottom plate that is firm instead, this action causes the compression of the specimen through the adapter device, leading to the consequent deformation. The force is recorded by a load cell and the displacement of the crosshead by a deformation transducer. There is no confinement applied to the samples, they are only subject to atmospheric pressure.

The compressive strength can be determined easily if known the force that was applied and the geometrical characteristics of the specimen, through the following equation:

$$\sigma_c = \frac{F}{A} = \frac{F}{b \cdot h}$$

where,

- σ_c is the compressive stress applied to the specimen in MPa.
- F is the force applied to the specimen in N.
- A is the area of the specimen section demanded in mm^2.

Three-point flexural test

The three-point flexural test (Figure 24), determines the maximum tensile stress that can be sustained by the hardened specimens before it fails in bending. However, the disadvantage of this kind of test is that results are sensitive to the specimen and loading geometry. The prismatic specimens (20x20x80 mm) were placed on two supporting pins at 60 mm distance apart. The stress can be obtained through the Navier formula as follows:

$$\sigma_f = \frac{3Fl}{2bh^2}$$

where,

- σ_f is the flexural stress applied to the specimen at midpoint, in MPa.
- F is the force applied to the specimen in N.
- b is the width of the test beam, in mm.
- h is the height of the test beam, in mm.
- l is the support spam of the test beam, in mm.

The strain can be determined instead with the following equation:

$$\varepsilon_f = \frac{6Dh}{l^2}$$

where,

- ε_f is the strain of the specimen at the midpoint, in %.
- D is the deflection of the center of the beam, in mm.

Figure 24: three-point flexural test example.

Some of the settings considered for the flexural test are the same as in the compression test, what really changes is the preload which was established at 5 N to limit the initial stress, and the test-speed that was set to 0.25 mm/min to allow a slow deformation.

2.3.3. Chemical and environmental assessment

A preliminary X-ray fluorescence analysis was conducted to the CDW powders (RC, RA, BT, NA, UND1) to determine their chemical composition. The environmental assessment in this thesis was studied through leaching tests to the CDW alkali-activated, in order to measure the amount of pollutants the water can dissolve and release to the environment. Moreover, it was determined the pH of leachate given by the hardened pastes after 28 days of curing and the CDW particles.

Chemical composition through X-ray fluorescence (XRF) analysis

The X-ray fluorescence analysis is a non-destructive technique to analyze the elemental composition of a particular material. The resulting XRF spectrum (Figure 25) shows the intensity of the X-Rays (usually in counts per second) as a function of energy (usually in eV).

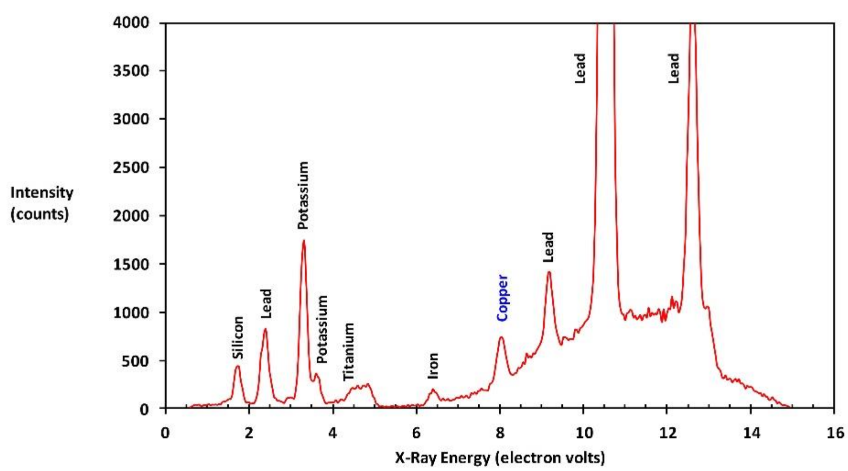

Figure 25: example of an XRF spectrum result

The wavelength dispersive XRF (Figure 26) was used for the present research, in which the fluorescent emission is directed to a crystal that diffracts the x-rays in different directions according to their wavelengths (energies). The crystal is rotated so different wavelengths are catch by the detector. The peak height for any element in the XRF spectrum, relates to the concentration of that element in the sample volume.

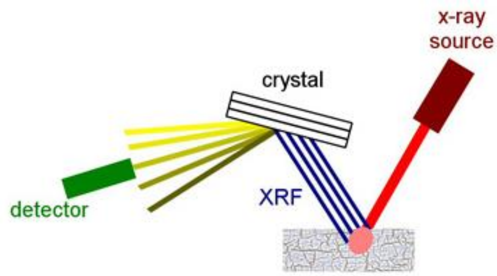

Figure 26: wavelength dispersive XRF

Leaching test

The European Standard UNI EN 12457-1 is the proposed batch test for leaching of the alkali-activated granular waste material preserved after the mechanical tests and the raw material. The test must be carried out on materials with a particle size lower than 4 mm, therefore the broken specimens were milled and passed to the sieve. The properties of the eluates were measured with the methods developed for water analysis, adapted to meet the criteria of eluate analysis (EN 12506 and EN 13370).

The leaching tests were carried out in an external laboratory and the results were compared to the maximum concentrations of release given by the European Council 2003/33/EC and the D.M 05/02/1998. Table 2 exhibits the leaching limit values for CDW acceptable at landfills by the EU/2003 and the D.M/98.

Table 2: Leaching limit values

	Leaching limit values	
parameter	D.M/98	EU/2003
cyanides [µg/l]	50	-
chlorides [mg/l]	100	800
fluorides [mg/l]	1.5	10
nitrates [mg/l]	50	-
sulphates [mg/l]	250	1000
Arsenic [µg/l]	50	500
Barium [mg/l]	1	20
Beryllium [µg/l]	10	-
Cadmium [µg/l]	5	40
Cobalt [µg/l]	250	-
Chrome [µg/l]	50	500
Mercury [µg/l]	1	10
Nickel [µg/l]	10	400
Lead [µg/l]	50	500
Copper [mg/l]	0.05	2
Selenium [µg/l]	10	100
Vanadium [µg/l]	250	-
Zinc [mg/l]	3	4
Asbestos [mg/l]	30	-
pH	5.5 - 12	-

pH tests

The measure of the pH was made following the British Standards 1377-2003 by the electrometric method, which gives a direct reading of the pH value of a soil suspension in water. The mechanical performance of the CDW fine particles improve thanks to the mixing with the AS, nevertheless, the basicity of the hardened specimens (paragraph 2.2.3) may vary according to the AS concentration. It is important to evaluate the pH of the material's eluates because the leachability of metals contained in the CDW is influenced by it. In fact, after the leaching test the pH of the resulting leachates was measured following the UNI EN 12506:2004 standards.

The specimens were brought to a small dimension lower than 2 mm after the mechanical tests, and then a portion of 30 g was placed in a baker of 100 ml with 75 ml of distilled water, the suspension was then stirred for a few minutes to later leave it to rest for at least 8 hours. Finally, a pH-meter was used to measure the pH of the suspension taking three readings with a brief stirring between them.

Figure 27: pH test

Figure 28: pH-meter

Chapter 3: Results and discussion

The chapter displays the results obtained from the laboratory tests to determine the physical-volumetric characteristics of powders and mixtures, and the mechanical properties of the alkali-activated specimens. A detailed analysis of the mechanical behavior for each combination of alkali-activated CDW powders, which is correlated to the chemical and physical-volumetric characteristics of particles and the alkali-activated blends, is presented.

3.1. Results

3.1.1. Chemical Composition of CDW powders

Chemical composition of CDW constituents (RC, RA, BT, NA, UND1 and UND2) was one of the objectives of this thesis. The results of the XRF analysis are reported in Table 3. It illustrates the amount (in percentage) of the chemical components present on the CDW constituents. The UND2 component was calculated as the weighted mean of the four CDW constituents (RC, RA, BT and NA).

The data evidence a great presence of silica (SiO_2) for all the components but significantly high for BT (more than half of the mass is composed by silica). The CDW components are also characterized by a high presence of aluminum oxide (Al_2O_3), evidentially higher for BT. The presence of amorphous aluminosilicates in the powders rendered possible the geopolymerization reaction and the respective formation of Si-O-Si and Al-O-Si bonds, which provides beneficial properties to the resulting material. It's worth noting that all the CDW components (especially for RC), the presence of calcium oxide (CaO) is considerable. Carbon dioxide (CO_2) is also present in the CDW components with exception of BT. The presence of MgO, SO_3, K_2O and Fe_2O_3 were modest for all the waste material, the rest of the chemical components were barely present (with a percentage of mass lower than 1%).

Table 3: XRF results

Component	mass [%]					
	RC	RA	BT	NA	UND1	UND2
CO_2	23.5	38.7	0	16.9	15.9	19.8
Na_2O	0	0.816	0	0	0	0.204
MgO	4.9	6.9	4.8	10.6	6	6.8
Al_2O_3	6.3	6.3	19.2	8.41	12.8	10.1
SiO_2	32.9	36.4	56.4	44.3	42.6	42.5
P_2O_5	0.11	0.085	0	0.125	0.347	0.08
SO_3	1.4	1.2	0.143	0.198	0.589	0.745
K_2O	1.1	1.1	3.1	1.43	2.2	1.665
CaO	24.8	4.1	4.1	11.2	11.5	11.1
TiO_2	0.43	0.31	1.3	0.464	0.758	0.613
Cr_2O_3	0	0.067	0.076	0.123	0	0.066
MnO	0.19	0.135	0.25	0.296	0.28	0.217
Fe_2O_3	4.3	3.7	10.4	5.9	6.8	6.1
NiO	0.03	0.043	0.042	0.064	0.046	0.045
CuO	0	0	0	0	0.020	0
ZnO	0	0.011	0.033	0	0.025	0.011
Rb_2O	0	0	0.023	0.011	0.021	0.009
SrO	0.056	0.019	0.033	0.040	0.041	0.037
ZrO_2	0.014	0.015	0.115	0.018	0.033	0.040
PbO	0	0	0.049	0	0	0
TOTAL	100	100	100	100	100	100

3.1.2. Physical and volumetric characteristics

Particle size analysis

Previous studies have shown that the alkaline activation of CDW may be affected by the particle size distribution. In fact, Assi et al., (2018) have proven that the compressive strength of fly-ash based geopolymers has enhanced by using finer particle size. By increasing the surface area, the geopolymerization proceeds much faster resulting in a stronger bonding. In this study, the particle size distribution was determined for each CDW component and for two grain sizes of interest (< 63 and 63 ÷ 125 µm). The following charts (Figure 29, Figure 30, Figure 31, Figure 32 and Figure 33) show the volume distribution (in percentage) of the CDW powders according to the particle's size (in micron).

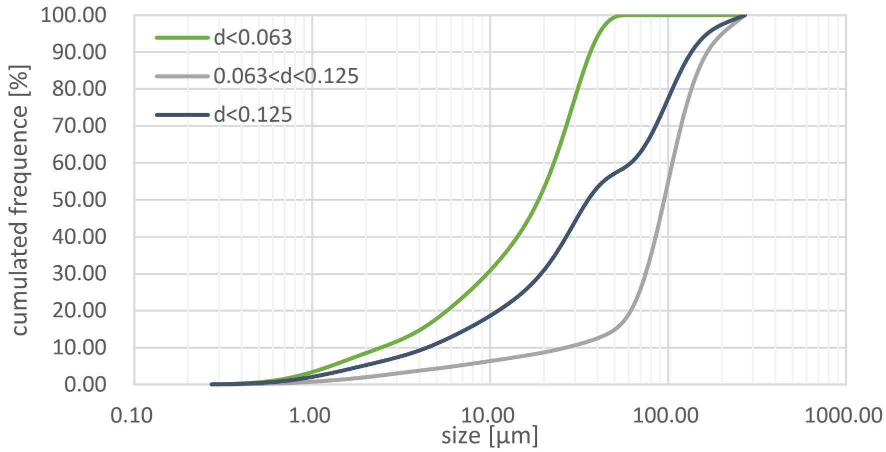

Figure 29: RC particle size distribution

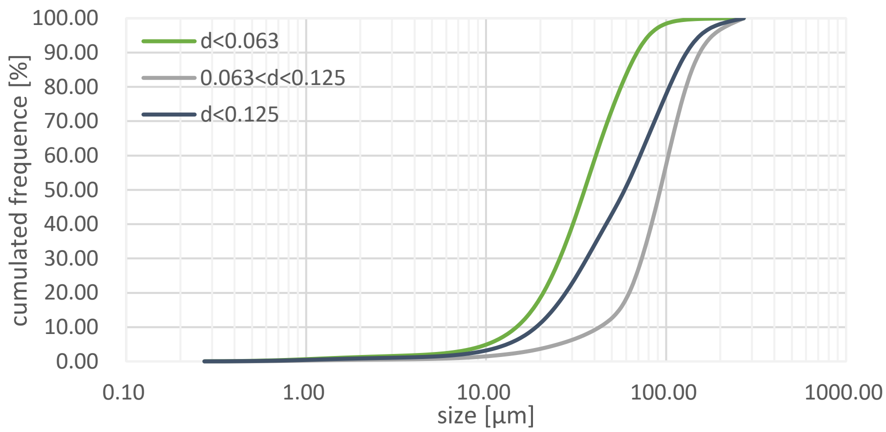

Figure 30: RA particle size distribution

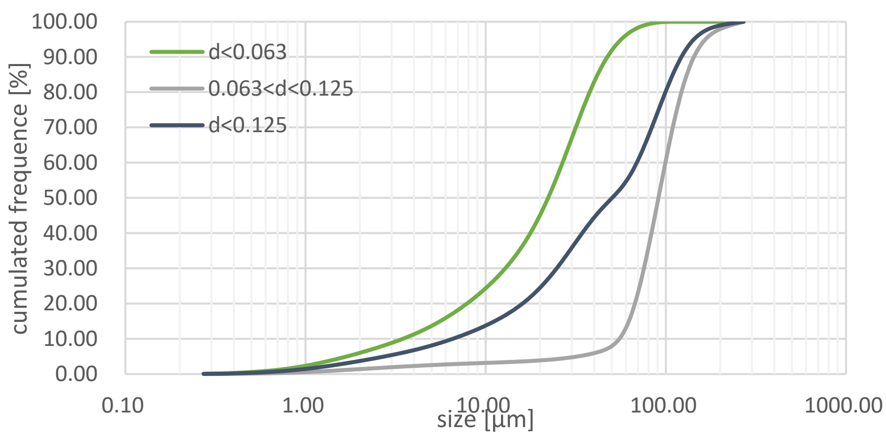

Figure 31: BT particle size distribution

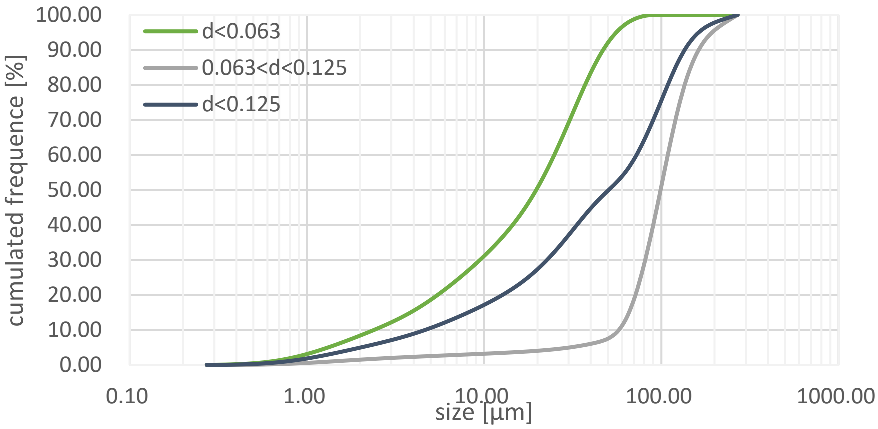

Figure 32: NA particle size distribution

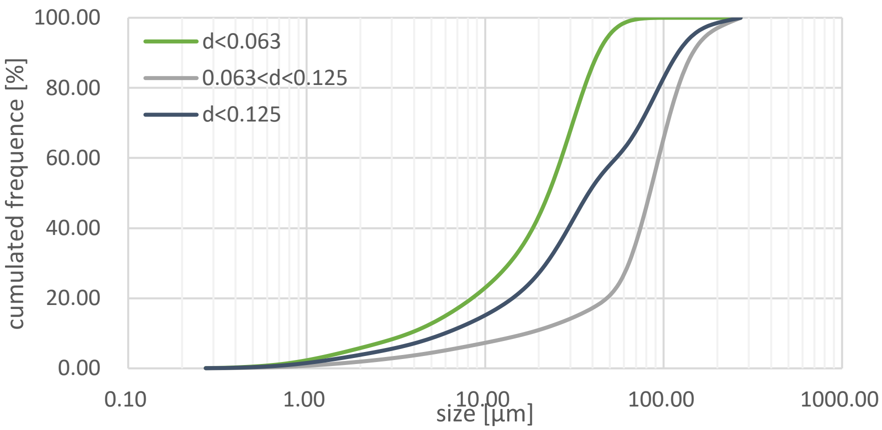

Figure 33: UND1 particle size distribution

The particle size distribution obtained for the CDW components confirms that the milling and sieving procedures were performed successfully since all the curves respected the size limits (d<63 and 63<d<125 µm). In Figure 34 and Figure 35, all the curves with the same particle class were put together to evaluate the difference between materials. The grain size distribution seems to be similar for all the CDW components with a grain size between 63 and 125 µm (Figure 34). Almost all the components presented an average diameter of the volume distribution (d_{50}) of 100 µm. Furthermore, there's a progressive increase of the grain size in d_{10} approximately for almost all the CDW components, basically when moving from the finer (UND1) to the larger (NA). It is worth noting the increment of the volume distribution after 63 µm, proving the efficient sieving for all CDW components.

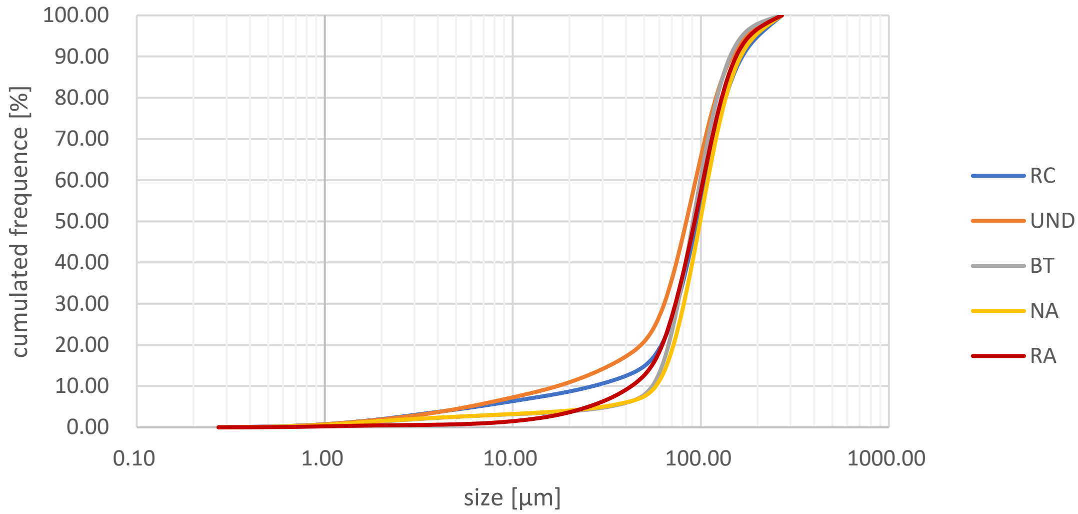

Figure 34: Particle size distribution for the CDW components with a grain size between 125 and 63 µm

Almost all the curves presented in Figure 35 (< 63 µm) behave in the same way, with a d_{50} around 20 µm. The only exception is RA, which clearly have larger grain sizes with a d_{50} of 35 µm approximately. The reason may be due to the less effective milling and sieving process caused by the fact that this material contains a viscoelastic organic binder that counteracts in some way the milling action. As a result, RA exhibit a coarser size distribution.

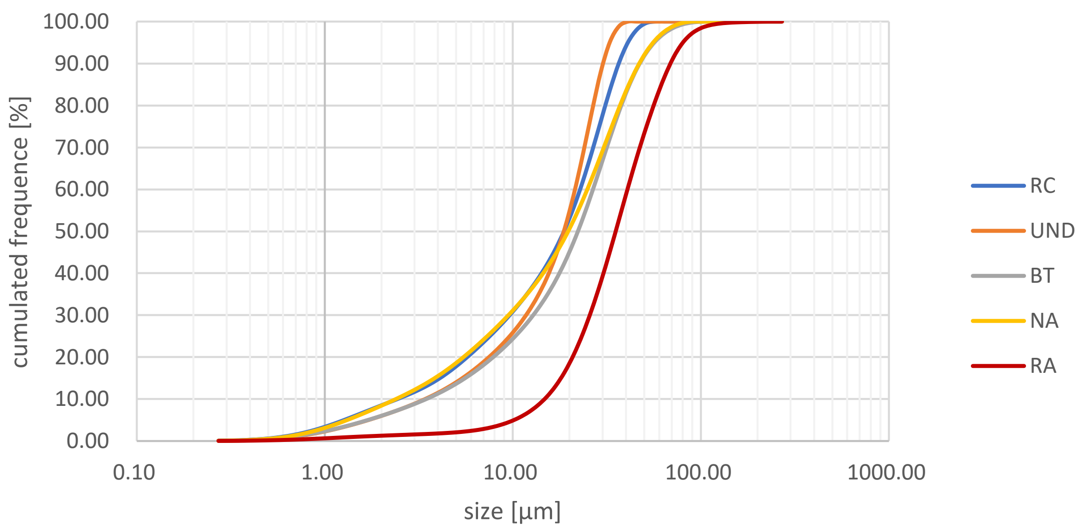

Figure 35: Particle size distribution for the CDW components with a grain size lower than 63 µm

Density and porosity of CDW

The particle density (ρ_p), the bulk density (ρ_p) and the Rigden voids (ν) of the dry compacted fines are in Table 4. Each measure was made to a sample equally composed by both grain sizes (d < 63 and 63 < d < 125 µm). The particle density was obtained by means of two pycnometers, and before making any measures, the volume of both pycnometers was determined. The porosity was determined with the Rigden test on a sample of 10 g.

The results evidence a significant difference on the particle's density between all the CDW components. The minimum value of 2.35 Mg/m^3 was measured in the case of RA, while the maximum of 2.76 Mg/m^3 was measured in case for BT. Figure 36 shows the Rigden voids of CDW component and grain size considered. The voids content depends on the particle size distribution and the shape of particles as well. In the specific case of the investigated materials, the components present a similar grain distribution and similar void contents. The exception is the RA: the lower percentage of voids is due to the different particles size distribution of the fraction < 63 µm, and by the presence of the viscoelastic binder in this material allows a further deformation of the particles resulting in greater reduction of voids: in fact, the greater deformability of the RA particles is what characterizes it from the other CDW components.

Table 4: particle density, bulk density and Rigden porosity of the CDW fine particles

Material	Diameter [µm]	ρ_p [Mg/m^3]	ρ_b [Mg/m^3]	ν [%]
RC	< 63	2.58	1.94	24.60
	125 ÷ 63	2.69	1.95	27.32
RA	< 63	2.42	1.94	19.98
	125 ÷ 63	2.35	1.99	15.21
BT	< 63	2.76	2.01	27.26
	125 ÷ 63	2.72	1.95	28.52
NA	< 63	2.73	1.99	27.09
	125 ÷ 63	2.71	2.03	25.26
UND1	< 63	2.64	1.96	25.65
	125 ÷ 63	2.67	1.96	26.54

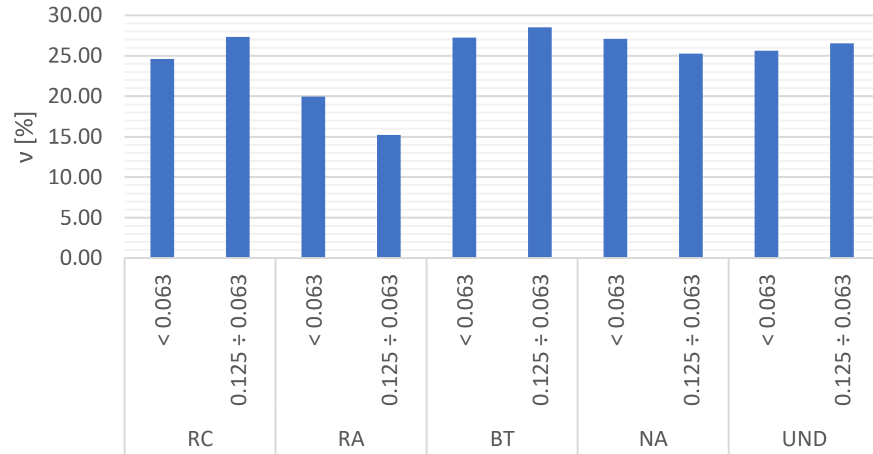

Figure 36: percentage of voids in CDW

The other particles presented particles sizes. Another important fact is that BT and RC are the components with the higher amount of voids, and therefore, a higher water absorption is expected.

Viscosity of the blends

The viscosity of the pastes relates to its workability and flowability and may help to understand the subsequent behavior of the hardened pastes. As indicated in paragraph 2.3.1, it was measured with the Brookfield viscometer as a function of the rotation speed and the spindle used (changing it when necessary); as a result, an average curve was built for each paste evaluated and a graphic for each l/s ratio and for each waste material was made to facilitate the analysis of results.

The viscosity of the pastes with a l/s ratio of 0.4 presented a great viscosity due to the presence of a low liquid content. In some cases, the test was impossible to be performed and difficult to cast the pastes into the molds. In case of pastes with a l/s ratio of 0.5, just few pastes with AC of 100% were not tested at the Brookfield viscometer. The viscosity was measured on pastes with an AC of 75% and 50%, on the other hand, the pastes undiluted in water (with an AC of 100%) and the paste formed with BT powder and an AC of 75%, were not tested because they were extremely viscous and fell out from the measurement field of the device. Figure 37 shows the results obtained with the viscometer for each paste as function of the rotation speed in revolutions per minute (on a logarithmic scale) and the AC presented in the mixture.

The increase of the liquid/solid ratio in case of pastes with a l/s ratio of 0.6 brought to the pastes a lower viscosity and a better flowability. With such a liquid portion in the paste, it was possible to measure the viscosity even on mixtures made with an AC of 100% (which normally have the highest viscosity); the results are plotted in Figure 38 in function of the rotation speed and the alkaline solution.

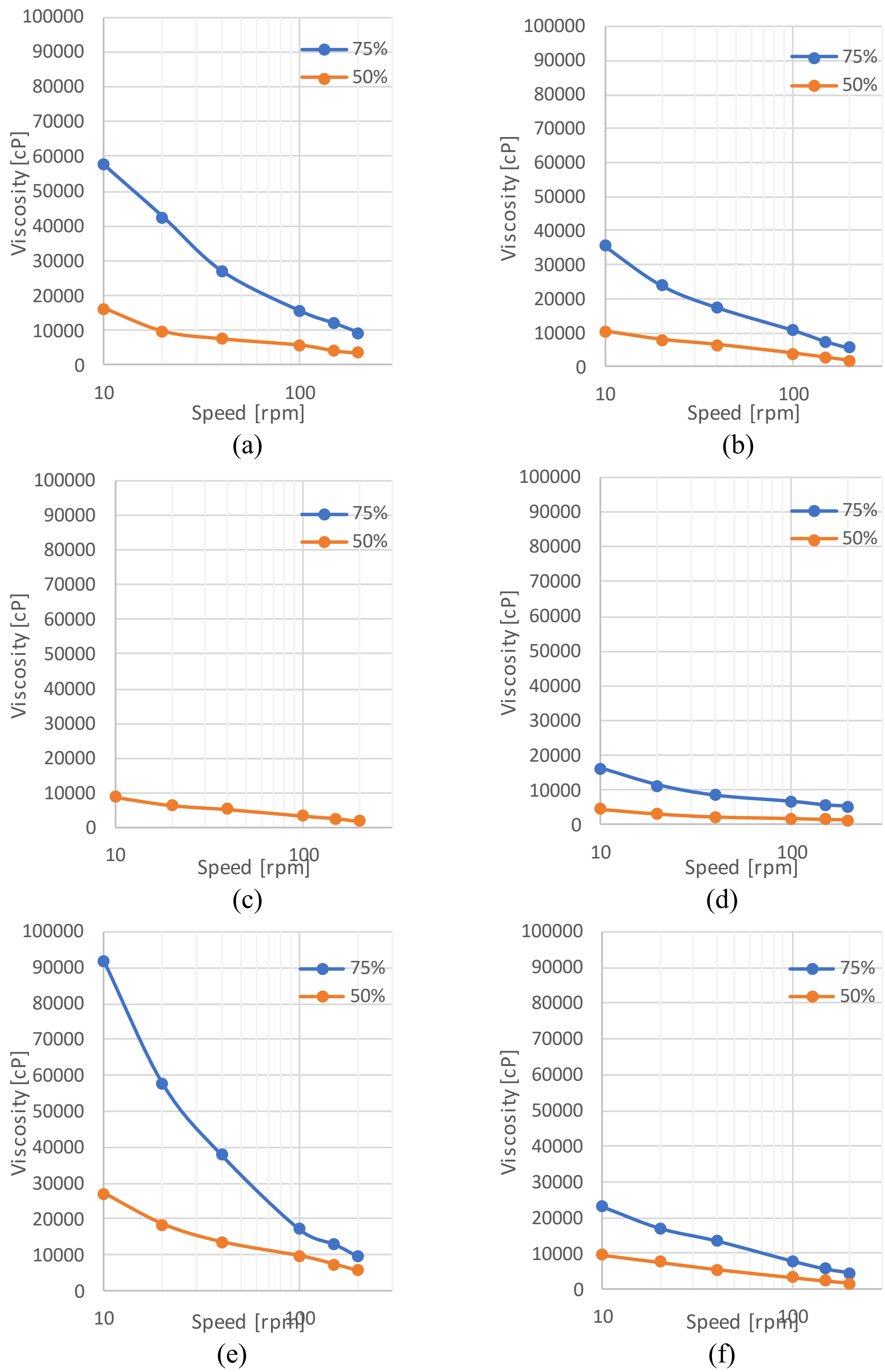

Figure 37: viscosity of the blends prepared with a l/s=0.5 for RC (a), RA (b), BT (c), NA (d), UND1 (e), UND2 (f).

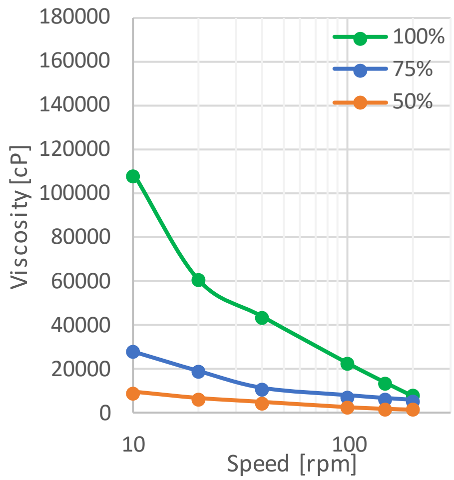

(a)

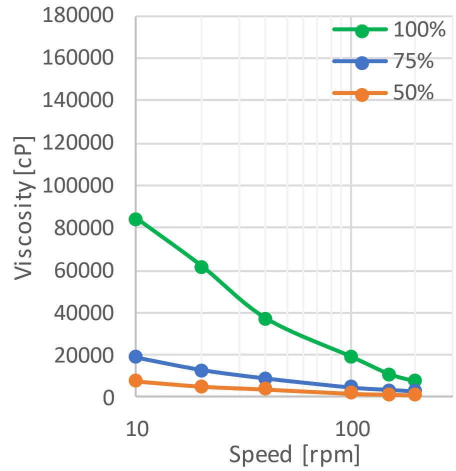

(b)

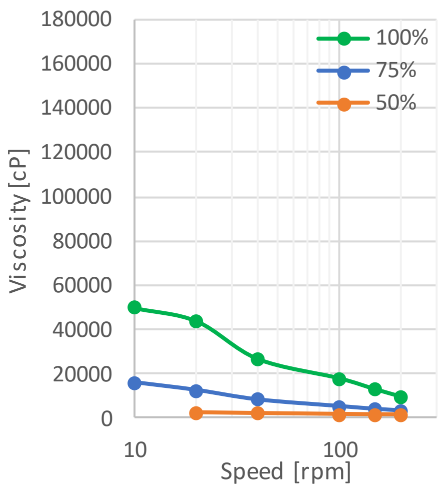

(c)

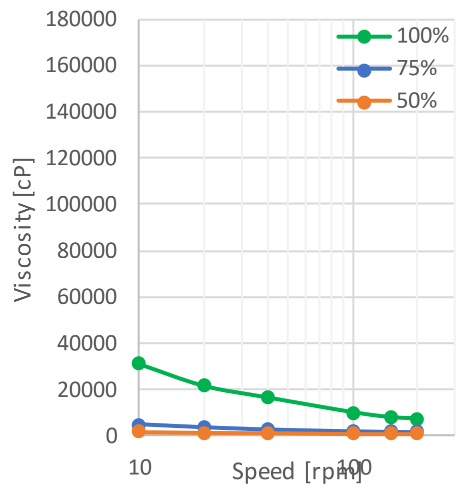

(d)

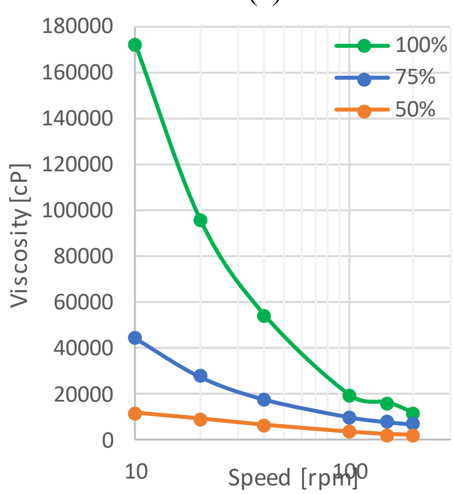

(e)

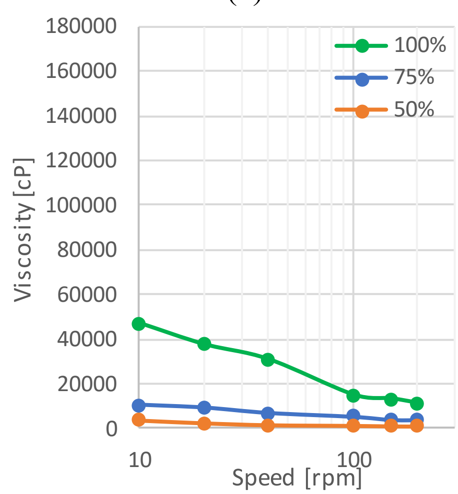

(f)

Figure 38: viscosity of the blends prepared with a l/s=0.6 for RC (a), RA (b), BT (c), NA (d), UND1 (e), UND2 (f).

Results evidence a similar behavior of all the curves; with the increase of the rotation speed, the viscosity tends to decrease because the resistance to deformation of the paste decrease at higher rotational speeds. Another tendency on the results is the drop of the curves for lower alkaline concentrations; as the matter of fact, the pastes formed with a more diluted AS presented a better workability and were easy to cast into the prism molds. The results presented for each material revealed the differences on the viscosity for different AC. However, the viscosity of similar materials was plotted in Figure 39 and Figure 40. The viscosity of the CDW pastes with a l/s ratio of 0.5 are plotted in Figure 39, where the two charts are referred to an AS concentration of 75% and 50% respectively. Results demonstrates a huge increase of viscosity for all the pastes when passing from an AC of 50% to 75%. It's evident that UND1 presented by far the highest viscosity and it follows the RC pastes, on the contrary, the NA mixtures shown the lowest viscosity of all. Almost all the pastes were sufficiently fluid, and it was easy to cast them into the molds. However, some of them presented bleeding phenomena due to the excessive liquid content: consequently, the specimens hardening lasted around 1-2 days for UND1, UND2 and RC, and approximately 3-5 days for BT, RA and NA. The fact that UND1 and UND2 exhibited widely different viscosities is because there is clearly some material present in UND1 and not in UND2 (e.g. clays or fine soils).

Figure 40 shows the viscosity of the blends prepared with a l/s ratio of 0.6, it's evident they presented a lower viscosity compared to the ones formed with a l/s ratio of 0.5, meaning they were sufficiently fluid for pouring into the molds. The specimens shown bleeding phenomenon due to the liquid excess presented in the mixtures. The hardening lasted around 1-2 for UND1, UND2 and RC and lasted more than 4 days for BT, NA and RA.

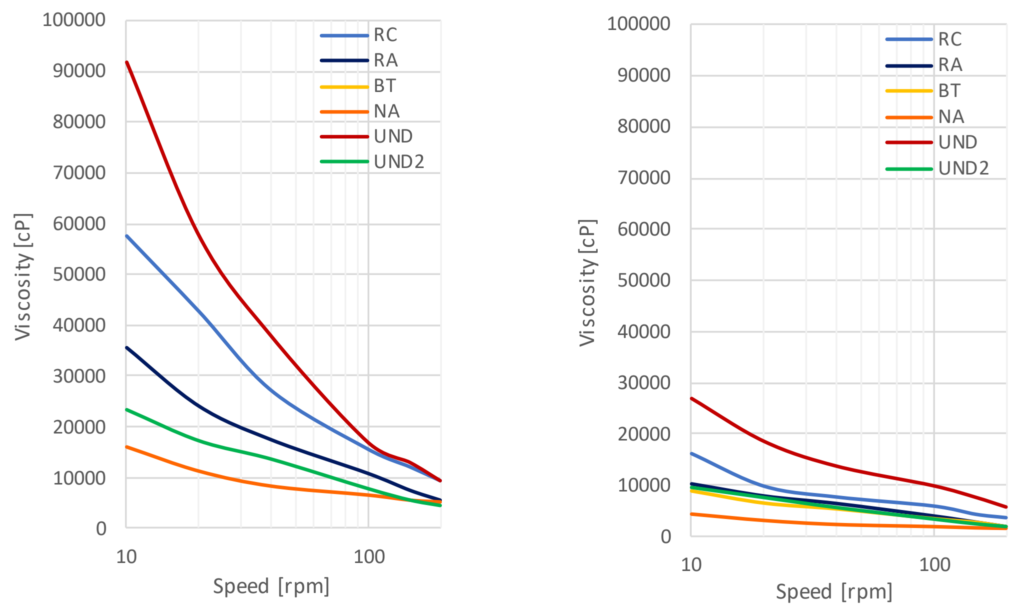

(a) (b)

Figure 39: viscosity of the CDW mixtures with a l/s = 0.5 and AC of 75% (a) and of 50% (b)

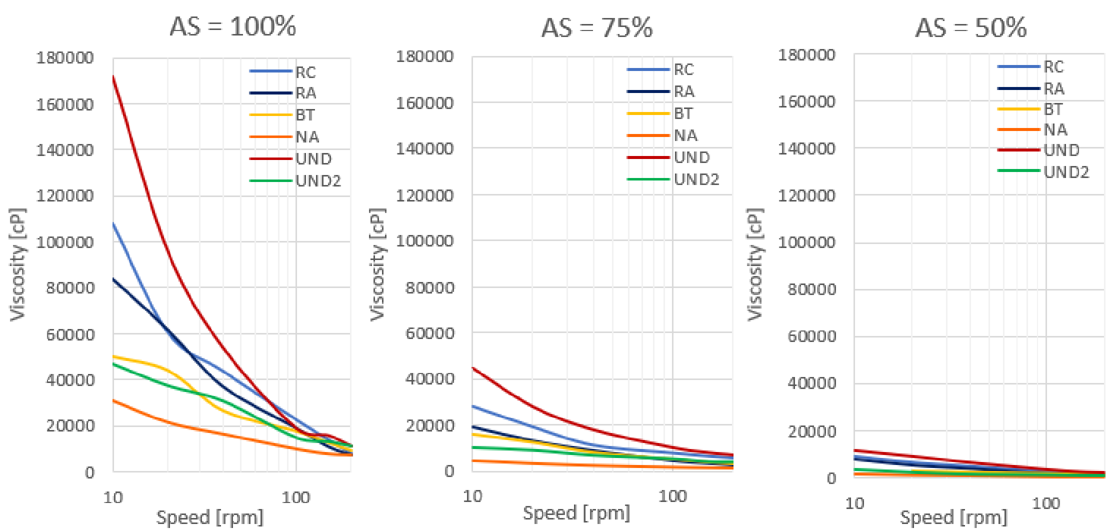

(a) (b) (c)

Figure 40: viscosity of the CDW mixtures with a l/s ratio of 0.6 with an AS concentration of 100% (a), 75% (b) and 50% (c)

The pastes with a l/s ratio of 0.4 were impossible to test with the Brookfield viscometer due to the excessive viscosity. These mixtures were also difficult to cast into the molds, so a small compaction of the paste to avoid hardened specimens with fissures inside was necessary. All the materials presented a low percentage of bleeding, and the hardening time was less than 1 day for almost all the materials.

The specimens presented a bleeding phenomenon while hardening, the percentage of mass lost by the samples is exhibited in Table 5 for each CDW combination. The results evidence that RA presented high percentages of bleeding compared to the other components. The bleeding tends to increase for more diluted alkaline solutions due to the lower viscosity presented in the pastes. It's worth noting that RC pastes do not loose liquid while hardening even when the pastes AS is diluted, because of the re-hydration process of the non-hydrated cement particles present in the raw material.

Table 5: Bleeding presented on the blends

	Bleeding [%]						
	l/s=0.6			l/s=0.5			l/s=0.4
material \ AS	100%	75%	50%	100%	75%	50%	100%
RC	0.0	0.0	0.0	0.0	0.3	10.7	0.5
RA	8.4	12.6	13.7	1.3	11.4	10.6	2.8
BT	3.1	6.3	8.6	2.7	8.1	7.3	2.5
NA	3.7	3.7	14.5	5.3	10.2	8.2	3.2
UND1	0.2	2.4	5.0	0.0	0.2	6.9	3.8
UND2	0.8	6.3	9.4	2.1	5.6	10.7	1.5

3.1.3. Mechanical performance

This paragraph illustrates the results deriving from the mechanical tests appropriately treated according to the methods described in the experimental program. As already specified in paragraph 2.3.2, the parameters of interest are:

- the maximum stress and strain deformation at the peak stress point,
- tangent and secant modulus, and
- breaking energy (toughness).

The results include the average for each parameter concerning the same paste, the standard deviation to quantify the amount of variation, and the coefficient of variation (CV) that standardized the dispersion of a probability distribution (Table 1). The samples

ID goes according the CDW component, the l/s ratio used, and the AC considered, for example: BT_06C_100% refers to the BT specimens made with a l/s ratio of 0.6 and an AC of 100% that were subjected to compression test (C).

Compression test

This section presents the results obtained with the uniaxial compression tests carried out to the two halves of the specimens previously tested at the three-point bending test. For each material and combination, the stress stress-strain curve is presented in order to appreciate the differences of the mechanical behavior when the l/s ratio and the AS varies. The quantitative results are exposed in tables for each component with the parameters of interest mentioned above.

Recycled concrete (RC). The stress-strain curves of the specimens made of RC alkali-activated are in Figure 41. The average results, the standard deviation and the coefficient of variation for each l/s ratio and AC considered are shown in Table 6 and Table 7. One irregular result was neglected in order to obtain more reliable stats for RC_06C_50%. The coefficient of variation evidences the high homogeneity in the maximum stress and strain results for all the combinations of RC. The tangent and secant modulus presented results with an order of variation around 20%. The maximum stress and highest toughness were obtained for a l/s ratio of 0.5 and a AS of 100%, evidencing that there's a progressive increase of the strength when increasing the AS concentration. The same behavior goes for the tangent modulus, giving the highest values for an alkaline concentration of 100%.

Table 6: Uniaxial compression test results of RC (1).

Sample ID	σmax			ε(σmax)			Esec		
	Average	Stand. Dev	CV	Average	Stand. Dev	CV	Average	Stand. Dev	CV
	[MPa]	[MPa]	[%]	[%]	[%]	[%]	[MPa]	[MPa]	[%]
RC_06C_100%	6.9	0.26	3.7	2.3	0.277	12.1	305.9	37.6	12.3
RC_06C_75%	5.4	0.24	4.4	2.3	0.303	13.1	239.7	37.5	15.6
RC_06C_50%	0.3	0.034	10.8	2.5	0.394	15.5	12.9	2.8	21.9
RC_05C_100%	15.8	1.15	7.3	2.4	0.257	10.8	671.9	72.2	10.7
RC_05C_75%	6.1	0.40	6.7	2.2	0.307	14.2	287.5	38.3	13.3
RC_05C_50%	0.9	0.18	19.3	1.9	0.309	16.0	49.1	17.9	36.4
RC_04C_100%	14.0	2.24	16.0	2.2	0.280	13.0	656.4	114.5	17.4

Table 7: Uniaxial compression test results of RC (2).

Sample ID	**Etan**			**T**			**Number of Observations**
	Average	Stand. Dev	CV	Average	Stand. Dev	CV	
	[MPa]	[MPa]	[%]	[kPa*mm/mm]	[kPa*mm/mm]	[%]	
RC_06C_100%	379.7	52.6	13.8	92.3	10.9	11.8	10
RC_06C_75%	295.7	53.6	18.1	79.9	15.9	19.9	8
RC_06C_50%	17.1	4.1	23.8	4.9	0.97	19.7	9
RC_05C_100%	778.1	62.4	8.0	211.6	36.6	17.3	10
RC_05C_75%	361.4	49.6	13.7	83.1	20.5	24.7	10
RC_05C_50%	68.5	18.0	26.3	10.8	0.91	8.4	10
RC_04C_100%	823.7	140.9	17.1	179.9	53.9	29.9	10

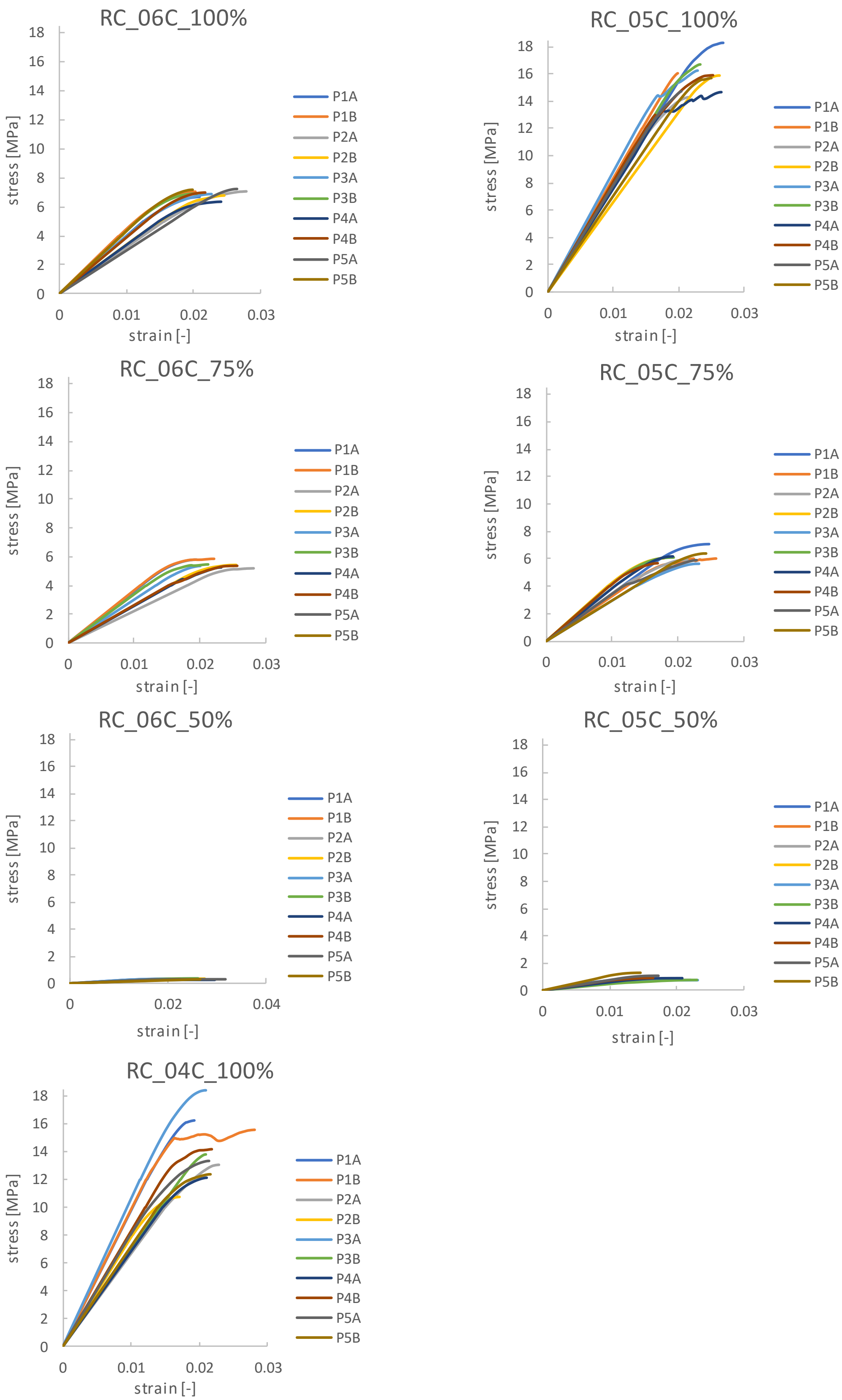

Figure 41: Compression stress-strain curves of RC

Recycled Asphalt (RA). the average results, the coefficent of variation and the standard deviation of the parameters are exhibit in Table 8 and Table 9. The stress-strain curves are plotted for each combination made with RA in Figure 42. One irregular result for RA_06C_75% and one for RA_06C_50% were neglected for their irregular behavior compared to the other samples. The RA specimens presented low strengths compared to the other materials, obtaining a maximum stress of 2.31 MPa for a l/s ratio of 0.6 and an alkaline concentration of 75%. The highest tangent modulus, secant modulus and toughness are given by the same combination. Nevertheless, the specimens achieved great deformations up to 11% for the samples prepared with a higher AS concentration. This might be due to the presence of bitumen in the RA particles which results in a remarkable viscoelastic behavior. The standard deviation for all the parameters is significantly low, evidencing that the results are close to the mean.

Table 8: Uniaxial compression test results of RA (1).

Sample ID	σmax			ε(σmax)			Esec		
	Average	Stand. Dev	CV	Average	Stand. Dev	CV	Average	Stand. Dev	CV
	[MPa]	[MPa]	[%]	[%]	[%]	[%]	[MPa]	[MPa]	[%]
RA_06C_100%	1.08	0.120	11.1	11.3	1.633	14.3	9.8	2.4	25.1
RA_06C_75%	2.31	0.234	10.1	6.3	0.780	12.4	37.6	7.5	20.1
RA_06C_50%	0.55	0.046	8.3	2.6	0.455	17.3	21.4	2.9	13.9
RA_05C_100%	1.32	0.119	9.0	10.3	0.846	8.2	12.9	1.9	14.3
RA_05C_75%	0.76	0.039	5.2	10.4	0.491	4.7	7.3	0.49	6.8
RA_05C_50%	0.42	0.033	7.9	3.5	0.512	14.7	12.2	2.2	17.6
RA_04C_100%	1.79	0.138	7.7	7.63	0.421	5.5	23.4	1.8	7.7

Table 9: Uniaxial compression test results of RA (2).

Sample ID	Etan			T			Number of Observations
	Average	Stand. Dev	CV	Average	Stand. Dev	CV	
	[MPa]	[MPa]	[%]	[kPa*mm/mm]	[kPa*mm/mm]	[%]	
RA_06C_100%	12.8	4.04	31.5	72.2	7.5	10.3	10
RA_06C_75%	55.3	13.04	23.6	90.0	10.9	12.2	9
RA_06C_50%	27.7	3.87	14.0	8.7	2.5	28.7	5
RA_05C_100%	15.9	2.62	16.5	78.6	8.3	10.5	10
RA_05C_75%	8.5	0.86	10.2	44.1	2.9	6.8	10
RA_05C_50%	18.0	5.78	32.1	9.1	1.4	15.4	8
RA_04C_100%	30.9	2.26	7.3	82.2	8.4	10.2	10

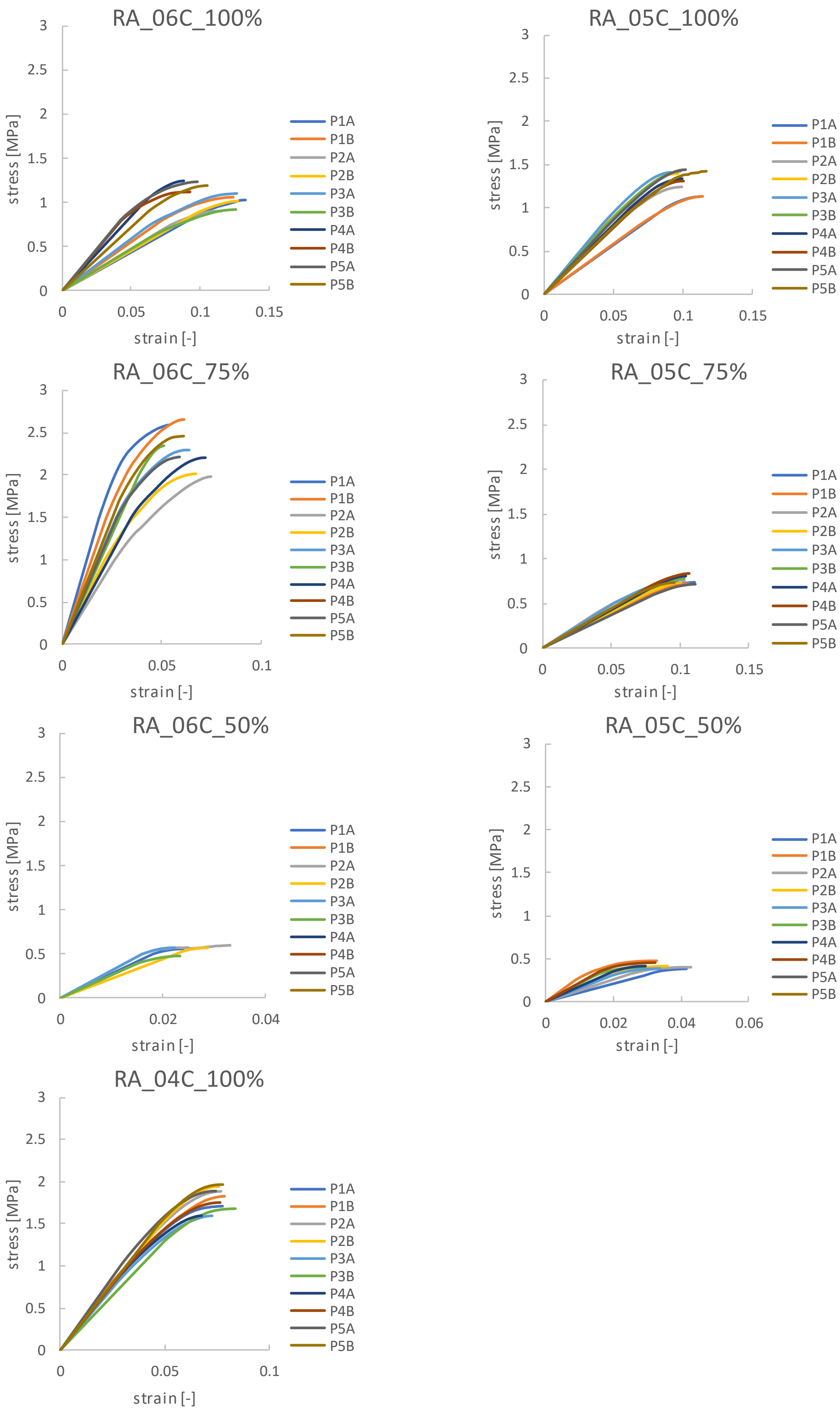

Figure 42: Compression stress-strain curves of RA

Bricks and tiles (BT). The average results, standard deviation and coefficient of variation are in Table 10 and Table 11, and the corresponding stress-strain curves are in Figure 43. Results of four samples: BT_06C_50%, two for BT_05C_100% and three for BT_05C_50% were neglected since they were too much irregular with the rest of the data. It's worth noting that, the highest values of strength are given by the samples prepared with an alkaline concentration of 100%, evidencing a greater reactivity of the grains for higher AS concentrations. The highest compressive strength achived is 10.31 MPa for the pastes made with a l/s ratio of 0.4 and an alkaline concentration of 100%, the strenght obtained is significantly higher compared to the other combinations. The greatest toughness is shown by samples formed with a l/s ratio equal to 0.5 and an AS of 100%, evidencing the fact that greater deformations are seen for this combination, almost the double (4.58%) than the maximum strain obtained for the combination which provided the highest stregnth.

Table 10: Uniaxial compression test results of BT (1).

Sample ID	σmax			ε(σmax)			Esec		
	Average	Stand. Dev	CV	Average	Stand. Dev	CV	Average	Stand. Dev	CV
	[MPa]	[MPa]	[%]	[%]	[%]	[%]	[MPa]	[MPa]	[%]
BT_06C_100%	4.3	0.401	9.4	4.6	1.59	34.2	98.9	26.0	26.3
BT_06C_75%	2.2	0.283	12.8	5.2	1.13	21.7	44.9	12.9	28.7
BT_06C_50%	0.7	0.186	25.4	2.6	0.71	26.9	29.9	11.5	38.3
BT_05C_100%	4.7	0.592	12.6	4.6	0.53	11.5	104.5	21.9	21.0
BT_05C_75%	1.8	0.085	4.7	5.6	1.00	18.0	34.0	9.7	28.6
BT_05C_50%	1.2	0.220	20.8	1.9	0.86	46.2	67.1	30.3	45.1
BT_04C_100%	10.3	1.477	14.3	1.9	0.24	12.3	544.0	91.9	16.9

Table 11: Uniaxial compression test results of BT (2).

Sample ID	Etan			T			Number of Observations
	Average	Stand. Dev	CV	Average	Stand. Dev	CV	
	[MPa]	[MPa]	[%]	[kPa*mm/mm]	[kPa*mm/mm]	[%]	
BT_06C_100%	124.8	22.5	18.1	120.8	53.3	44.1	10
BT_06C_75%	56.5	16.9	29.9	67.9	16.2	23.91	10
BT_06C_50%	55.8	14.6	26.1	13.4	5.3	39.8	4
BT_05C_100%	147.3	35.6	24.1	131.4	13.1	9.9	8
BT_05C_75%	72.3	15.0	20.7	71.6	15.9	22.20	10
BT_05C_50%	118.5	48.0	40.5	13.0	6.3	48.19	5
BT_04C_100%	654.3	92.9	14.2	113.9	26.9	23.6	10

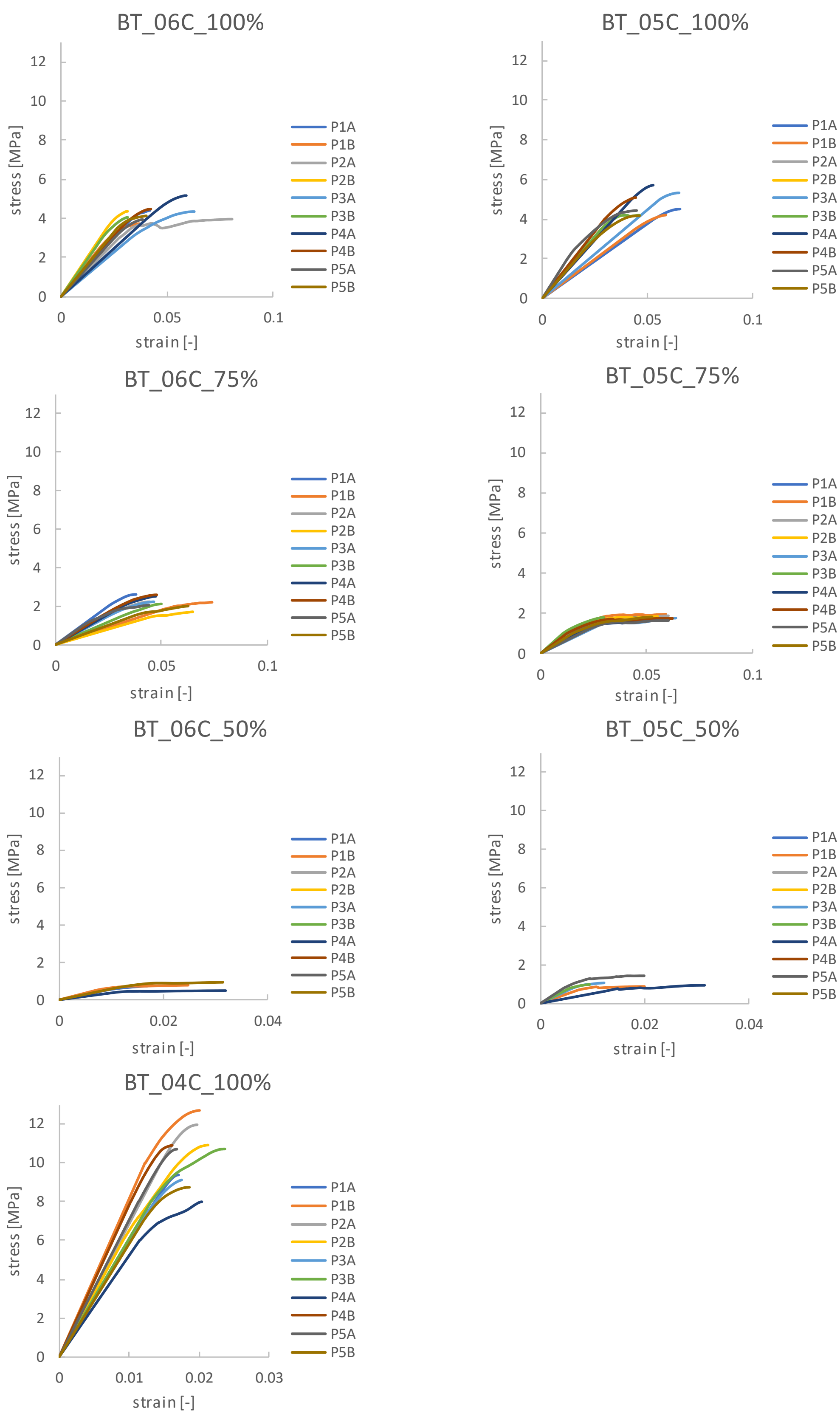

Figure 43: Compression stress-strain curves of BT

Natural aggregates (NA). The stress-strain curves considered are presented in Figure 44. The statistical results are shown in Table 12 and Table 13. Some specimens were neglected in the final results due to their inconsistency: three for NA_06C_100%, four for NA_06C_75%, one for NA_05C_50% and another one for NA_04C_100%. The results shown low resistances for a l/s ratio of 0.6 and 0.5, and a significant increment of the compression strength for a l/s equal to 0.4. It's noticeable a progressive increase of the resistance for more concentrated AS. The greatest values of tangent modulus, secant modulus and toughness were obtained for the same combination, however greater deformations were given by the samples prepared with a l/s ratio of 0.5 and AS of 75%. The coefficient of variation of the parameters is particularly low for the samples made with an alkaline concentration of 75%.

Table 12: Uniaxial compression test results of NA (1).

Sample ID	σmax			ε(σmax)			Esec		
	Average	Stand. Dev	CV	Average	Stand. Dev	CV	Average	Stand. Dev	CV
	[MPa]	[MPa]	[%]	[%]	[%]	[%]	[MPa]	[MPa]	[%]
NA_06C_100%	3.6	0.653	18.1	5.1	1.325	26.1	73.0	12.4	17.0
NA_06C_75%	2.5	0.091	3.7	5.2	0.305	5.9	47.7	3.4	7.2
NA_06C_50%	0.38	0.072	19.0	3.4	0.909	26.6	11.7	3.5	29.6
NA_05C_100%	2.0	0.172	8.6	5.3	0.580	11.1	38.8	6.3	16.3
NA_05C_75%	1.1	0.036	3.5	8.4	0.475	5.7	12.6	0.85	6.8
NA_05C_50%	0.43	0.080	18.6	2.8	0.589	21.4	16.5	5.6	33.8
NA_04C_100%	10.1	1.197	11.8	2.9	0.426	14.8	359.5	79.5	22.1

Table 13: Uniaxial compression test results of NA (2).

Sample ID	Etan			T			Number of Observations
	Average	Stand. Dev	CV	Average	Stand. Dev	CV	
	[MPa]	[MPa]	[%]	[kPa*mm/mm]	[kPa*mm/mm]	[%]	
NA_06C_100%	84.4	17.7	20.9	104.7	38.7	37.0	7
NA_06C_75%	61.1	5.2	8.4	77.2	6.3	8.1	6
NA_06C_50%	17.6	7.5	42.4	8.1	2.2	27.0	10
NA_05C_100%	57.4	10.6	18.4	66.5	9.6	14.5	10
NA_05C_75%	14.1	0.97	6.9	48.5	3.7	7.5	8
NA_05C_50%	29.5	11.6	39.3	7.9	1.3	17.1	7
NA_04C_100%	508.5	99.8	19.6	180.7	29.8	16.5	9

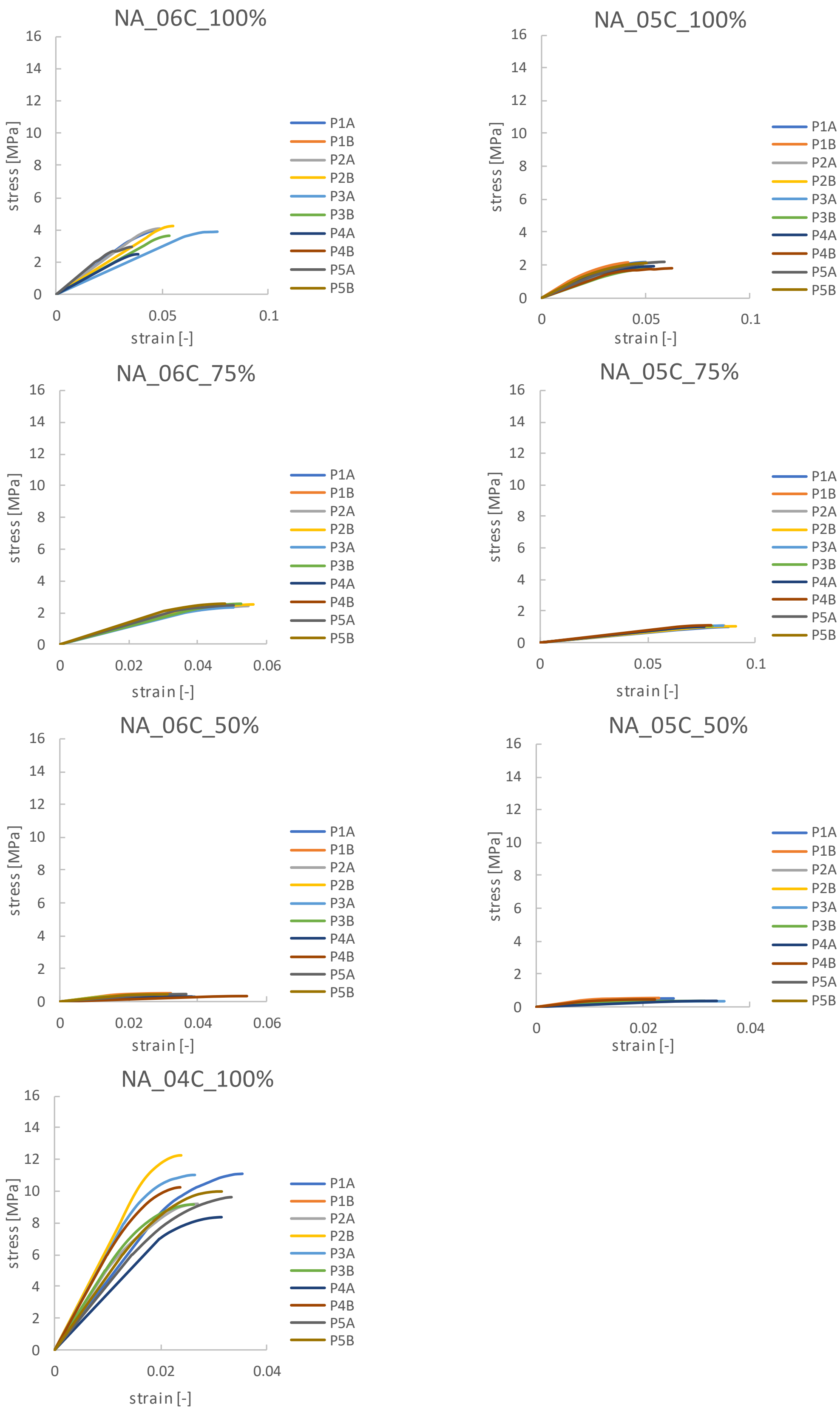

Figure 44: Compression stress-strain curves of NA

Undivided material (UND1): in this case only two samples were not considered in the final results, one for UND1_06C_50% and another for UND1_05C_50%. In Table 14 and Table 15 are shown the average results, the standard deviation and coefficient of variation of the pastes and the stress-strain curves are exhibit in Figure 45. The highest values of strength, tangent modulus, secant modulus and toughness were obtained by the specimens prepared with a l/s ratio of 0.4, achieving a compression resistance of 12.06 MPa, also with modest coefficient of variation, stating a precision in the measurement. It is worth noticing that for a l/s ratio of 0.6, the greatest strength is not determined by the less diluted AS but for a concentration of 75%.

Table 14: Uniaxial compression test results of UND1 (1).

Sample ID	σmax			ε(σmax)			Esec		
	Average	Stand. Dev	CV	Average	Stand. Dev	CV	Average	Stand. Dev	CV
	[MPa]	[MPa]	[%]	[%]	[%]	[%]	[MPa]	[MPa]	[%]
UND1_06C_100%	1.9	0.100	5.2	4.2	0.443	10.6	47.1	6.2	13.1
UND1_06C_75%	4.9	0.405	8.3	3.5	0.364	10.3	140.1	18.2	13.0
UND1_06C_50%	0.54	0.101	18.9	2.9	0.697	23.9	19.3	5.1	26.2
UND1_05C_100%	6.9	0.628	9.1	2.4	0.240	10.0	287.9	42.1	14.6
UND1_05C_75%	3.2	0.318	9.8	2.5	0.384	15.2	129.7	16.6	12.8
UND1_05C_50%	0.71	0.100	14.0	2.2	0.347	15.5	32.4	6.8	20.9
UND1_04C_100%	12.1	1.156	9.6	2.0	0.173	8.5	596.0	73.5	12.3

Table 15: Uniaxial compression test results of UND1 (2).

Sample ID	Etan			T			Number of Observations
	Average	Stand. Dev	CV	Average	Stand. Dev	CV	
	[MPa]	[MPa]	[%]	[kPa*mm/mm]	[kPa*mm/mm]	[%]	
UND1_06C_100%	65.9	9.0	13.7	58.4	27.6	47.3	10
UND1_06C_75%	170.8	13.4	7.8	101.4	15.9	15.7	10
UND1_06C_50%	28.3	6.8	23.9	10.3	3.5	33.6	9
UND1_05C_100%	381.8	58.8	15.4	92.2	22.2	24.1	10
UND1_05C_75%	179.5	27.7	15.4	51.6	11.3	21.8	10
UND1_05C_50%	51.6	8.8	17.0	10.4	1.9	18.6	9
UND1_04C_100%	707.7	95.6	13.5	140.4	19.6	14.0	10

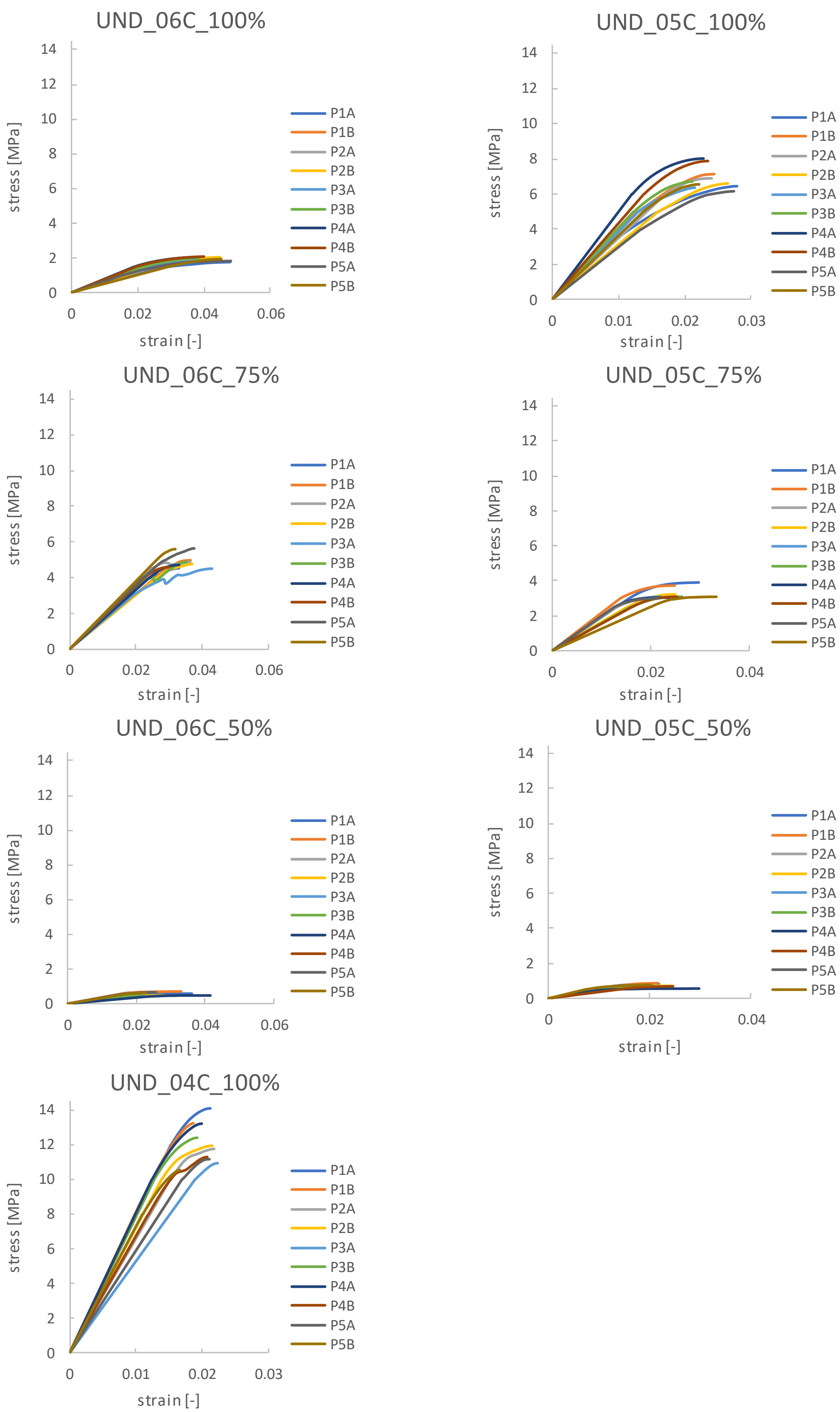

Figure 45: Compression stress-strain curves of UND1

Undivided material 2 (UND2). Two specimens for UND2_06C_50% were not considered and other two for UND2_05C_50%. The statistical results are shown in Table 16 and

Table 17 and stress-strain curves are presented in Figure 46. The pastes formed with a l/s ratio of 0.5 determined optimum strengths up to 8.64 MPa for the most concentrated AS and 8.13 MPa for a concentration of 75%, highlining the fact that for different concentrations the result is very similar. For a l/s ratio of 0.6, it was also obtained the maximum values of strength for an AS concentration of 75% as for UND1. The highest tangent modulus was obtained for a l/s = 0.4, while the highest secant modulus was determined by the most concentrated AS with a l/s = 0.5. It is also evident that the maximum strain is similar for all the combinations with the exception of specimens prepared with a l/s equal to 0.6 and the most concentrated AS.

Table 16: Uniaxial compression test results of UND2 (1).

Sample ID	σmax			ε(σmax)			Esec		
	Average	Stand. Dev	CV	Average	Stand. Dev	CV	Average	Stand. Dev	CV
	[MPa]	[MPa]	[%]	[%]	[%]	[%]	[MPa]	[MPa]	[%]
UND2_06C_100%	1.9	0.087	4.5	4.4	0.344	7.9	43.8	2.8	6.4
UND2_06C_75%	3.2	0.326	10.2	2.7	0.442	16.3	121.7	28.1	23.1
UND2_06C_50%	0.54	0.066	12.4	2.1	0.661	31.5	27.3	6.7	24.7
UND2_05C_100%	8.6	0.855	9.9	2.8	0.437	15.5	311.5	47.9	15.4
UND2_05C_75%	8.1	0.860	10.6	2.8	0.371	13.3	296.9	60.3	20.3
UND2_05C_50%	2.4	0.215	8.9	2.1	0.491	23.0	118.6	30.4	25.7
UND2_04C_100%	7.1	0.355	5.0	2.4	0.200	8.5	304.8	32.6	10.7

Table 17: Uniaxial compression test results of UND2 (2).

Sample ID	Etan			T			Number of Observations
	Average	Stand. Dev	CV	Average	Stand. Dev	CV	
	[MPa]	[MPa]	[%]	[kPa*mm/mm]	[kPa*mm/mm]	[%]	
UND2_06C_100%	64.2	8.0	12.5	52.8	6.4	12.0	10
UND2_06C_75%	173.6	41.1	23.6	54.0	8.0	14.9	10
UND2_06C_50%	40.1	10.8	27.0	6.9	3.2	45.6	6
UND2_05C_100%	387.9	38.1	9.8	144.3	29.7	20.6	10
UND2_05C_75%	391.9	71.1	18.1	139.1	23.6	17.0	10
UND2_05C_50%	171.6	47.3	27.6	33.1	9.9	30.1	6
UND2_04C_100%	414.4	28.7	6.9	112.4	26.8	23.82	10

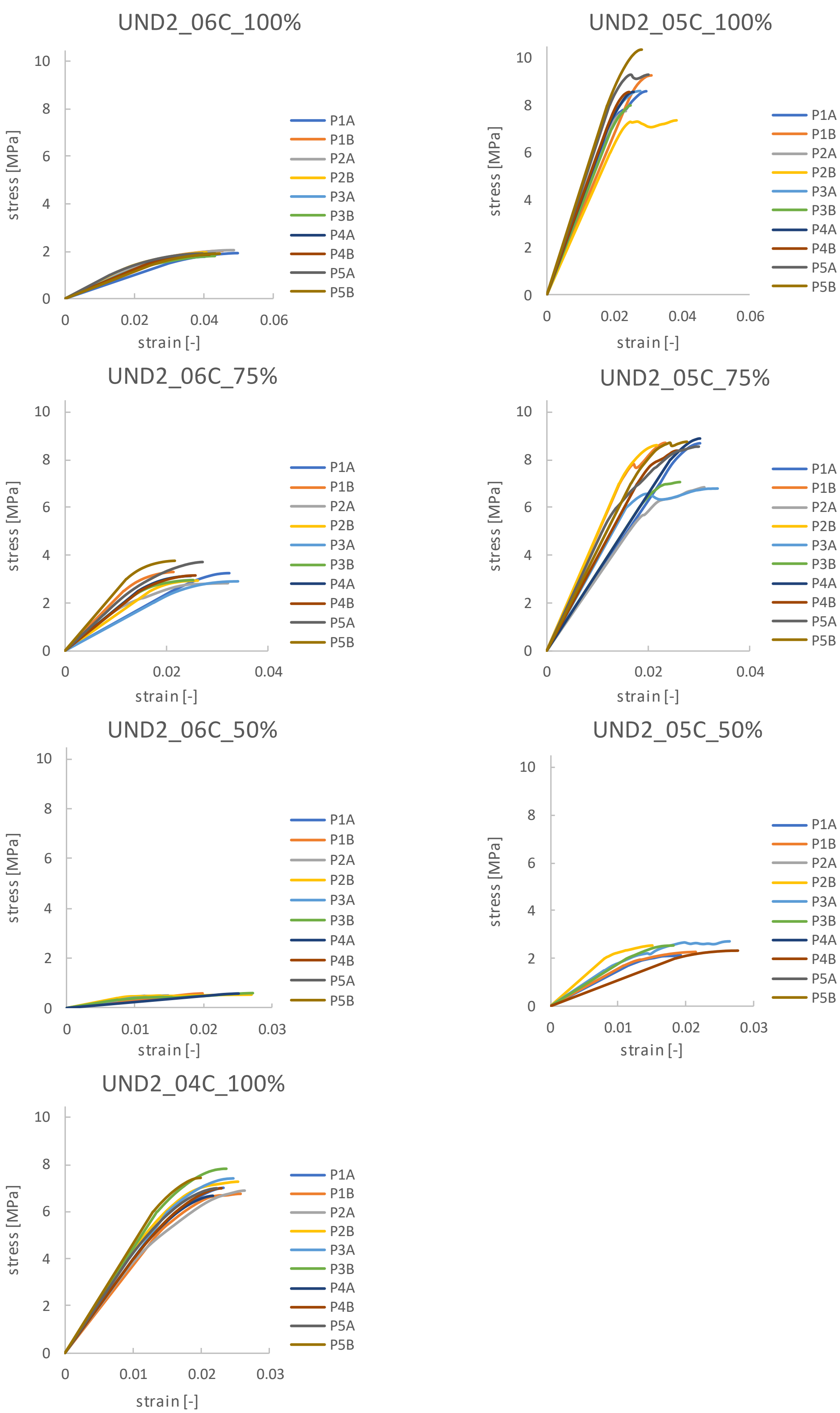

Figure 46: Compression stress-strain curves of UND2

Three-point flexural test

This section the three-point flexural test results for all the CDW components and combinations considered for this research are presented. The average maximum flexural strength, the maximum strain, the tangent modulus, the toughness and the density are reported. The stress-strain curves for all the specimens are plotted.

Recycled concrete (RC). Table 18 and Table 19 summarize the statistical results obtained from the flexural test performed to the RC activated samples. Figure 47 exhibits the stress-strain curve for each specimen considered in the analysis. Some irregular results were neglected: one specimen for RC_06_75%, one for RC_05_100%, two for RC_05_50% and other two for RC_04_100%. The highest flexural strength was determined by the l/s ratio of 0.5 and an AC of 100%. This combination also has a tangent modulus significantly higher than the others, equal to 1079 MPa.

Table 18: Flexural test results of RC (1)

Sample ID	σmax			ε(σmax)			Etan		
	Average	Stand. Dev	CV	Average	Stand. Dev	CV	Average	Stand. Dev	CV
	[MPa]	[MPa]	[%]	[%]	[%]	[%]	[MPa]	[MPa]	[%]
RC_06_100%	1.2	0.158	13.3	0.56	0.177	31.4	234.6	97.6	41.6
RC_06_75%	2.3	0.255	11.0	0.63	0.076	11.9	370.8	78.8	21.2
RC_06_50%	0.16	0.010	6.4	0.86	0.191	22.2	19.1	5.5	29.0
RC_05_100%	5.8	0.592	10.2	0.54	0.007	1.4	1078.9	114.1	10.6
RC_05_75%	2.6	0.319	12.3	0.53	0.042	8.0	490.4	42.6	8.7
RC_05_50%	0.34	0.060	17.8	1.09	0.352	32.4	38.8	3.1	8.0
RC_04_100%	2.9	0.320	11.2	0.33	0.027	8.2	903.1	173.4	19.2

Table 19: Flexural test results of RC (2)

Sample ID	T			ρ			Number of Observations
	Average	Stand. Dev	CV	Average	Stand. Dev	CV	
	[kPa*mm/mm]	[kPa*mm/mm]	[%]	[kg/m^3]	[kg/m^3]	[%]	
RC_06_100%	3.3	1.01	30.2	1908	18.6	1.0	5
RC_06_75%	7.3	0.75	10.3	1767	11.3	0.6	3
RC_06_50%	0.66	0.12	17.5	1488	49.4	3.3	5
RC_05_100%	15.7	1.51	9.6	1900	5.0	0.3	4
RC_05_75%	6.9	1.24	18.1	1904	17.2	0.9	5
RC_05_50%	2.8	1.75	62.5	1575	26.5	1.7	3
RC_04_100%	4.8	0.31	6.6	1835	51.4	2.8	3

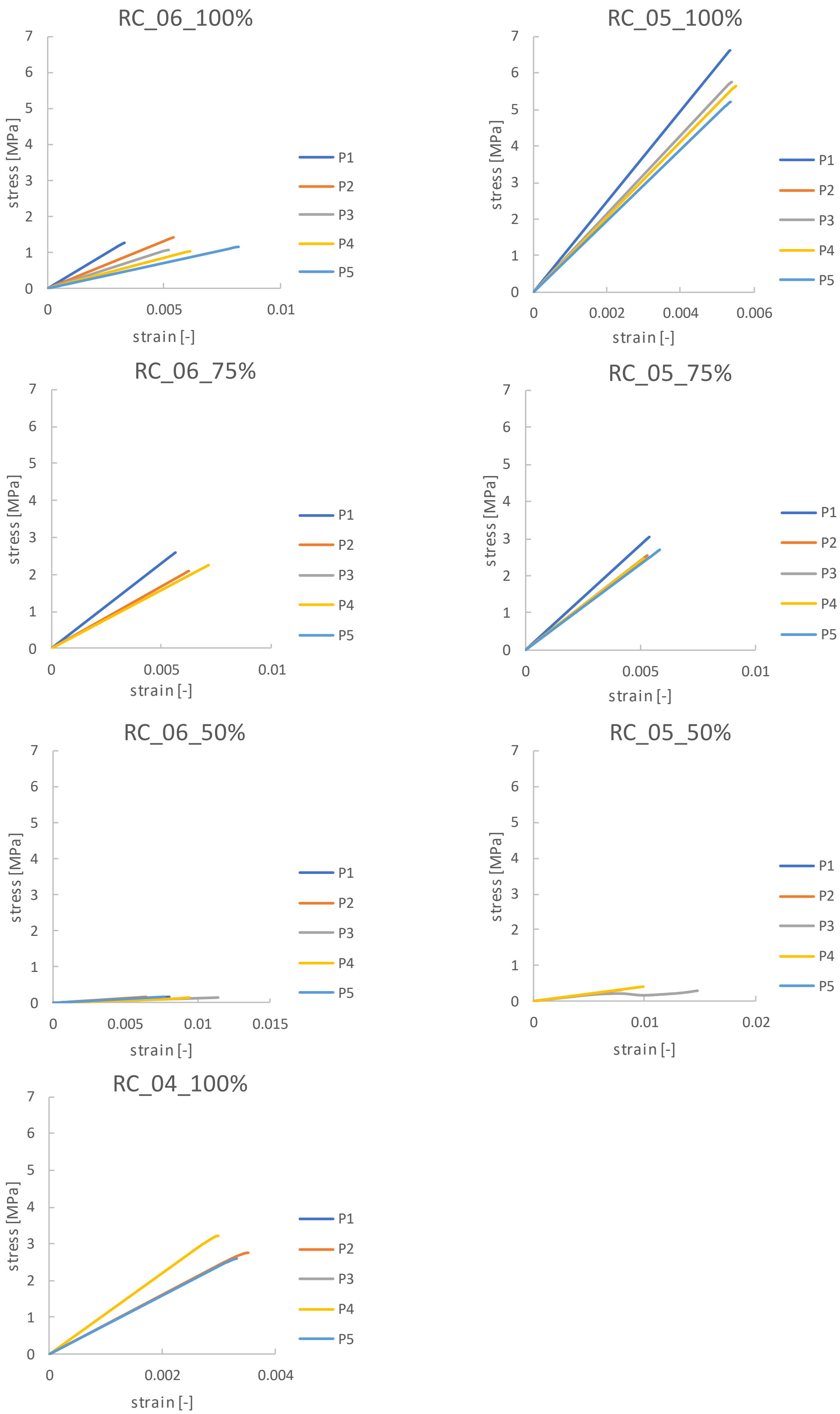

Figure 47: flexural stress-strain curves of RC

Recycled Asphalt (RA). Table 20 and Table 21 report the average results obtained for all RA combinations. The flexural strength is illustrated in Figure 48 through the stress-strain curves generated for each sample. Some specimens were neglected due to their unreliable results: two specimens for RA_06_100%, one for RA_06_75% and another for RA_05_75. The results evidenced an extremely low flexural resistance for this material, however, they showed larger deformations before breaking than the other CDW components, as a consequence for the presence of bitumen. Nevertheless, the best mechanical behavior was obtained for a l/s ratio of 0.6 and an AC of 75%.

Table 20: Flexural test results of RA (1)

Sample ID	**σmax**			**ε(σmax)**			**Etan**		
	Average	Stand. Dev	CV	Average	Stand. Dev	CV	Average	Stand. Dev	CV
	[MPa]	[MPa]	[%]	[%]	[%]	[%]	[MPa]	[MPa]	[%]
RA_06_100%	0.43	0.026	6.0	2.46	0.240	9.8	19.5	1.06	5.4
RA_06_75%	0.95	0.108	11.4	1.45	0.231	15.9	83.8	15.4	18.3
RA_06_50%	0.10	0.029	28.6	0.58	0.155	26.7	20.3	8.6	42.4
RA_05_100%	0.32	0.044	13.8	7.05	1.314	18.6	5.2	1.01	20.0
RA_05_75%	0.14	0.009	6.4	3.63	1.037	28.5	4.0	0.98	24.3
RA_05_50%	0.12	0.012	9.8	0.77	0.292	37.8	17.1	5.8	33.6
RA_04_100%	0.47	0.049	10.3	4.41	0.460	10.4	11.9	1.03	8.6

Table 21: Flexural test results of RA (2)

Sample ID	**T**			**ρ**			**Number of Observations**
	Average	Stand. Dev	CV	Average	Stand. Dev	CV	
	[kPa*mm/mm]	[kPa*mm/mm]	[%]	[kg/m^3]	[kg/m^3]	[%]	
RA_06_100%	5.7	1.023	17.8	1890	43.4	2.3	3
RA_06_75%	8.1	2.114	26.2	1862	36.3	1.9	4
RA_06_50%	0.32	0.077	24.3	1679	43.7	2.6	3
RA_05_100%	12.1	2.738	22.5	1939	28.8	1.5	5
RA_05_75%	2.7	0.793	30.0	1951	5.8	0.3	4
RA_05_50%	0.47	0.185	39.3	1737	13.5	0.8	4
RA_04_100%	11.4	1.877	16.5	1975	26.5	1.3	5

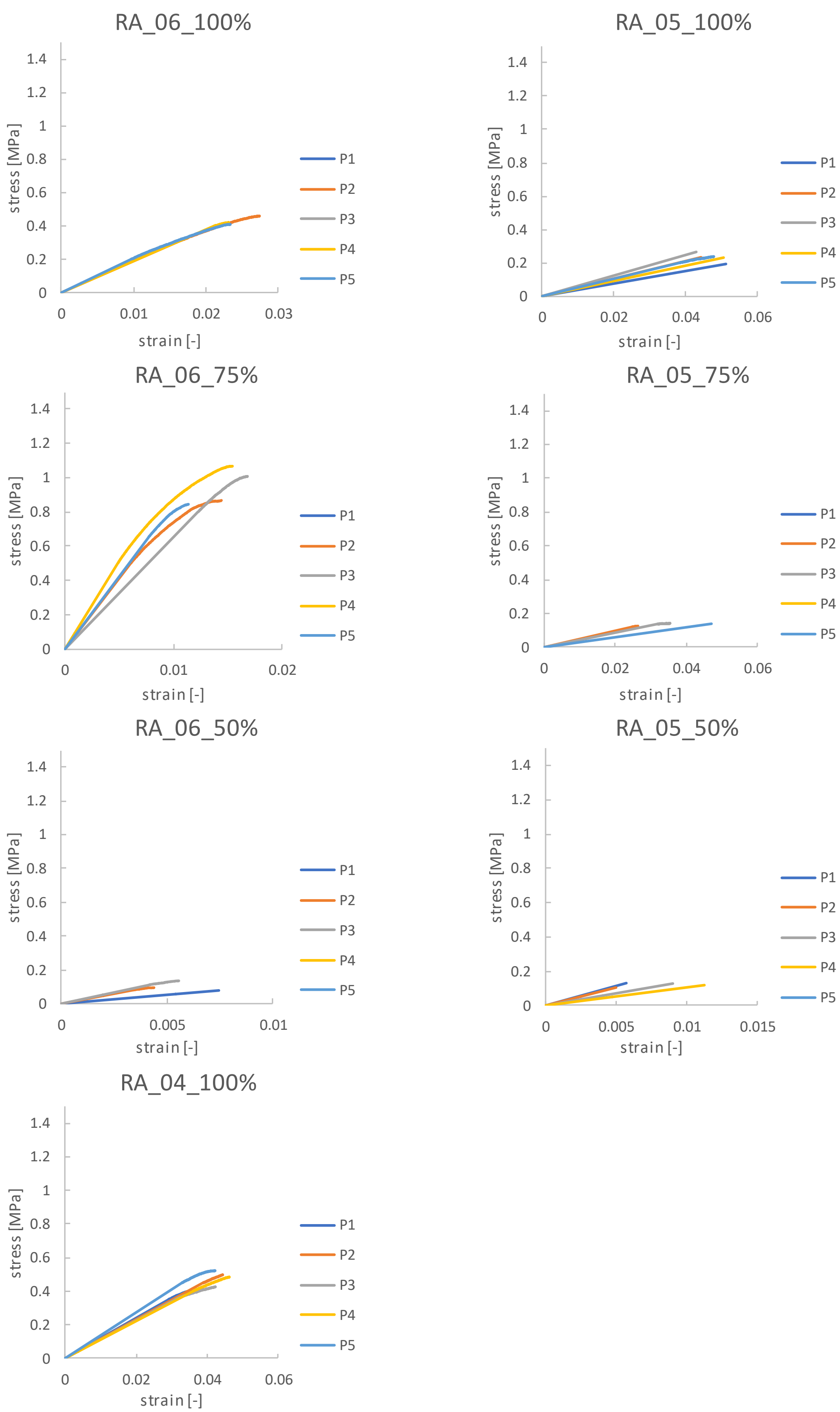

Figure 48: flexural stress-strain curves of RA

Bricks and tails (BT). Table 22 and Table 23 show the results obtained for each paste. The stress-strain curves were built for all the specimens and are exhibit in Figure 49. Again, some specimens were neglected due to their irregularity: one for BT_06_75%, two for BT_06_50%, two for BT_05_100% and another for BT_05_50%. The best flexure strength was observed by specimens prepared with a l/s ratio of 0.4; however, the coefficient of variation is high, suggesting a large variation on the specimen's results. The flexural strength seems to increase for more concentrated AS. The specimens made with a l/s ratio of 0.5 and an alkaline concentration of 100% obtained the highest toughness overall because, compared to sol_0.4_100%, the specimens reported higher deformations.

Table 22: Flexural test results of BT (1)

Sample ID	σmax			ε(σmax)			Etan		
	Average	Stand. Dev	CV	Average	Stand. Dev	CV	Average	Stand. Dev	CV
	[MPa]	[MPa]	[%]	[%]	[%]	[%]	[MPa]	[MPa]	[%]
BT_06_100%	1.42	0.128	9.0	1.85	0.820	44.4	102.5	62.6	61.1
BT_06_75%	0.84	0.159	18.9	1.17	0.218	18.6	76.3	9.2	12.0
BT_06_50%	0.70	0.107	15.3	0.95	0.121	12.8	112.1	20.1	17.9
BT_05_100%	1.45	0.309	21.3	1.06	0.072	6.8	147.1	37.3	25.4
BT_05_75%	0.39	0.026	6.8	0.65	0.085	13.0	62.8	9.1	14.4
BT_05_50%	0.73	0.154	21.2	0.92	0.390	42.6	104.3	38.8	37.2
BT_04_100%	2.92	0.639	21.9	0.44	0.083	18.8	671.5	30.9	4.6

Table 23: Flexural test results of BT (2)

Sample ID	T			ρ			Number of Observations
	Average	Stand. Dev	CV	Average	Stand. Dev	CV	
	[kPa*mm/mm]	[kPa*mm/mm]	[%]	[kg/m^3]	[kg/m^3]	[%]	
BT_06_100%	13.1	4.7	35.6	1973	33.0	1.7	5
BT_06_75%	5.2	1.7	32.2	1958	77.6	4.0	4
BT_06_50%	4.3	1.1	25.2	1609	15.5	1.0	3
BT_05_100%	11.6	4.2	36.1	1875	25.2	1.3	3
BT_05_75%	1.3	0.18	13.7	1932	13.3	0.7	5
BT_05_50%	3.6	1.4	39.0	1734	9.6	0.6	4
BT_04_100%	6.8	2.6	38.6	1536	25.9	1.7	5

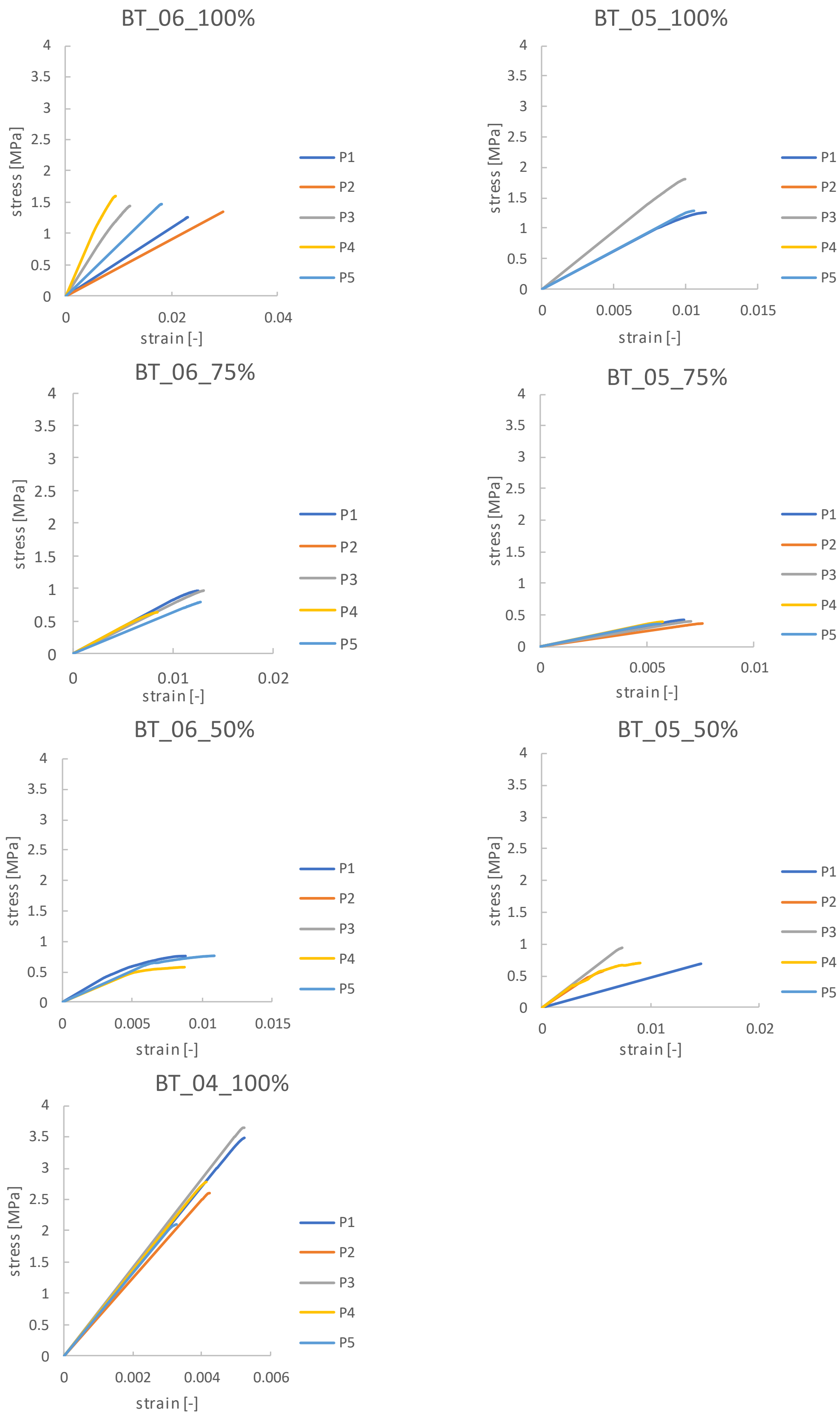

Figure 49: flexural stress-strain curves of BT

Natural aggregates (NA). In this case only three specimens were not considered in the final results: two specimens for NA_06_100% and one for NA_05_50%. The results obtained from the analysis are in Table 24 and Table 25 and the stress-strain curves are in Figure 50. The flexural strength obtained by the NA aggregates alkali-activated were essentially low. The best mechanical performance was determined by the samples made with a l/s ratio of 0.4 (sol_0.4_100%) and the second best was obtained for a l/s ratio of 0.6 and the most concentrated AS (sol_0.6_100%). Even though sol_0.4_100% achieved greater strength, sol_0.6_100% obtained a higher toughness because the specimens presented larger deformations. It is worth noticing that, the tangent modulus is significantly higher for sol_0.4_100%, almost eight times what was obtained for sol_0.6_100%.

Table 24: Flexural test results of NA (1)

Sample ID	σmax			ε(σmax)			Etan		
	Average	Stand. Dev	CV	Average	Stand. Dev	CV	Average	Stand. Dev	CV
	[MPa]	[MPa]	[%]	[%]	[%]	[%]	[MPa]	[MPa]	[%]
NA_06_100%	1.9	0.323	16.4	1.98	0.273	13.8	110.2	15.0	13.7
NA_06_75%	1.00	0.171	17.1	0.98	0.243	24.7	112.4	31.2	27.8
NA_06_50%	0.11	0.003	2.3	0.90	0.137	15.3	13.1	2.2	16.9
NA_05_100%	0.45	0.034	7.7	1.34	0.173	12.9	40.6	7.6	18.8
NA_05_75%	0.13	0.023	17.8	2.81	0.661	23.6	5.30	0.5	8.8
NA_05_50%	0.16	0.016	10.0	0.59	0.184	31.1	29.6	11.9	40.3
NA_04_100%	4.9	0.886	18.2	0.66	0.158	23.8	795.6	287.1	36.1

Table 25: Flexural test results of NA (2)

Sample ID	T			ρ			Number of Observations
	Average	Stand. Dev	CV	Average	Stand. Dev	CV	
	[kPa*mm/mm]	[kPa*mm/mm]	[%]	[kg/m^3]	[kg/m^3]	[%]	
NA_06_100%	20.9	3.9	19.1	2034	137.7	6.8	3
NA_06_75%	5.3	1.8	34.7	1991	21.7	1.1	4
NA_06_50%	0.51	0.072	13.9	1710	22.3	1.3	5
NA_05_100%	3.4	0.17	5.1	2016	13.9	0.7	5
NA_05_75%	2.04	0.81	40.0	2085	24.9	1.2	4
NA_05_50%	0.48	0.16	32.9	1902	7.9	0.4	3
NA_04_100%	15.86	2.29	14.4	1994	37.9	1.9	5

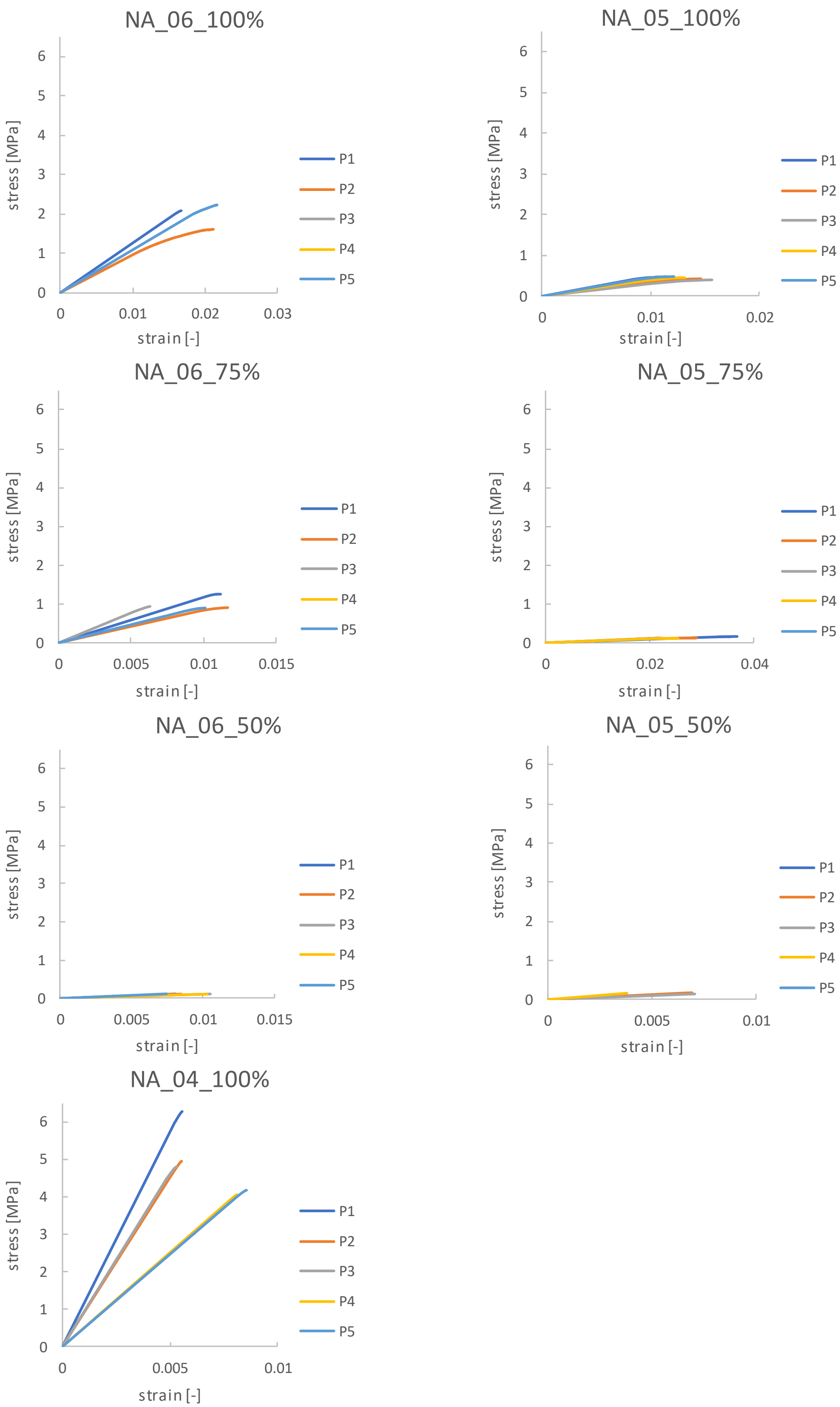

Figure 50: flexural stress-strain curves of NA

Undivided material (UND1). The average results, the coefficient of variation and the standard deviation of the parameters of interest are in Table 26 and Table 27, while the stress-strain curves are illustrated in Figure 51. Some specimens were neglected in the final results: two samples for UND1_06_50% and one for UND1_05_50%. Results evidence a higher flexural strength for the specimens made with a l/s ratio of 0.4 with a modest coefficient of variation. The greatest tangent modulus was obtained for the same combination, however, the highest toughness was determined by the pastes made with a l/s ratio of 0.6 and an alkaline concentration of 75%, this results is justified by the flexural strength (2.49 MPa) and the large deformation (compared to the other combinations).

Table 26: Flexural test results of UND1 (1)

Sample ID	σmax			ε(σmax)			Etan		
	Average	Stand. Dev	CV	Average	Stand. Dev	CV	Average	Stand. Dev	CV
	[MPa]	[MPa]	[%]	[%]	[%]	[%]	[MPa]	[MPa]	[%]
UND1_06_100%	0.30	0.046	15.3	0.83	0.101	12.3	39.1	8.9	22.7
UND1_06_75%	2.49	0.450	18.1	1.24	0.266	21.4	211.9	50.9	24.0
UND1_06_50%	0.43	0.088	20.4	1.03	0.039	3.8	56.9	10.1	17.7
UND1_05_100%	1.83	0.313	17.1	0.49	0.124	25.1	394.1	75.2	19.1
UND1_05_75%	1.28	0.234	18.2	0.67	0.076	11.3	194.0	29.2	15.1
UND1_05_50%	0.34	0.029	8.4	0.71	0.290	40.8	54.6	21.6	39.5
UND1_04_100%	4.19	0.328	7.8	0.44	0.108	24.4	981.2	163.9	16.7

Table 27: Flexural test results of UND1 (2)

Sample ID	T			ρ			Number of Observations
	Average	Stand. Dev	CV	Average	Stand. Dev	CV	
	[kPa*mm/mm]	[kPa*mm/mm]	[%]	[kg/m^3]	[kg/m^3]	[%]	
UND1_06_100%	1.31	0.204	15.6	1934	23.2	1.2	5
UND1_06_75%	15.7	4.118	26.2	1833	10.5	0.6	5
UND1_06_50%	2.55	0.496	19.4	1605	22.9	1.4	3
UND1_05_100%	4.66	1.583	33.9	1916	16.8	0.9	5
UND1_05_75%	4.38	1.116	25.5	1951	4.4	0.2	5
UND1_05_50%	1.23	0.540	44.0	1826	12.9	0.7	4
UND1_04_100%	9.46	3.010	31.8	1974	25.8	1.3	5

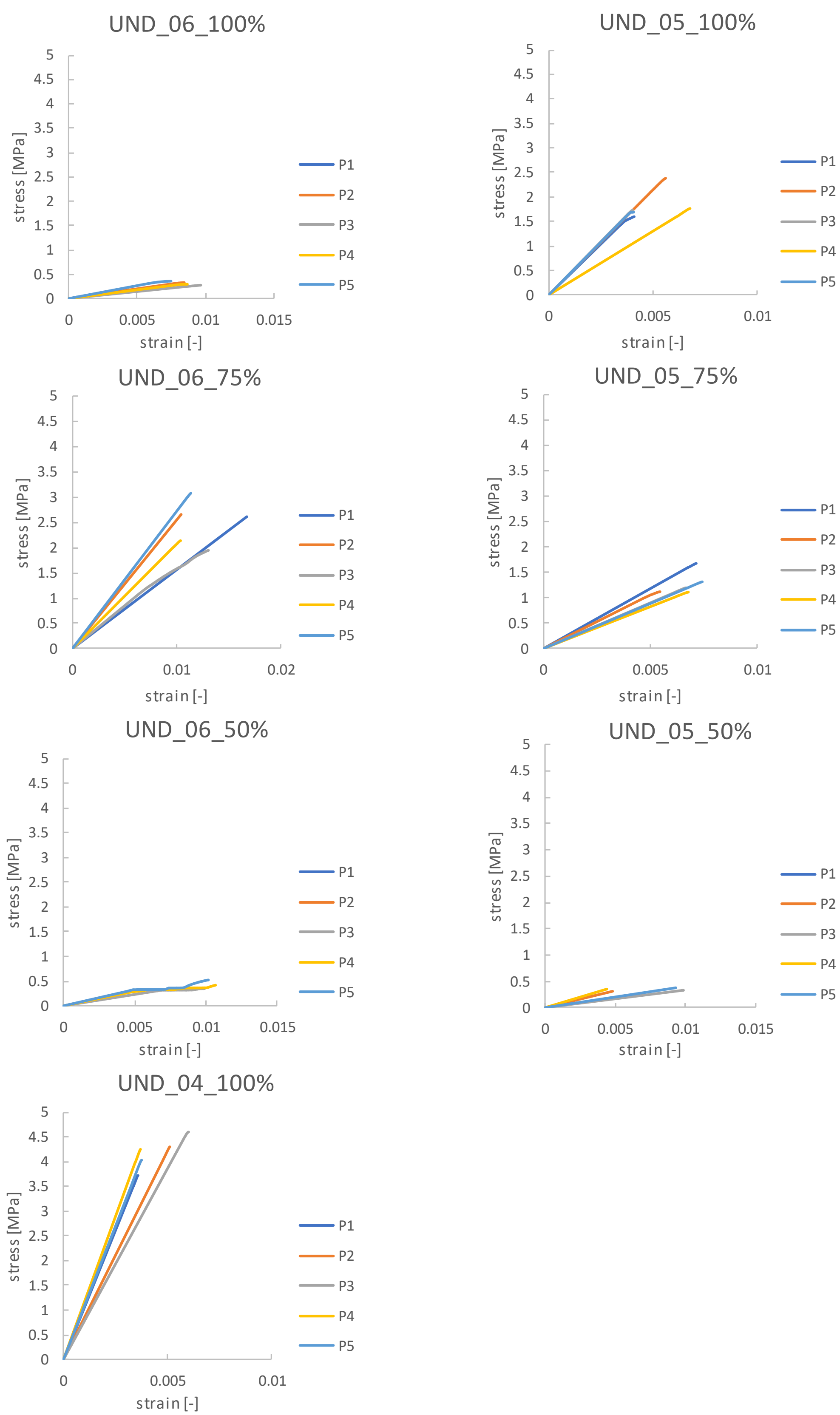

Figure 51: flexural stress-strain curves of UND1

Undivided material 2 (UND2). The stress-strain curves are presented in Figure 52 and the average results, standard deviation and coefficient of variation of the parameters of interest are shown in Table 28 and Table 29. Only two specimens were neglected in the final results: one for UND2_06_75% and another for UND2_04_100%. The best mechanical response was given by specimens prepared with a l/s ratio of 0.5 and an alkaline concentration of 75%, hence a better result was obtained by diluting in water the AS, meaning that the RC portion present in the UND2 component, was subjected to a further rehydration with the addition of water. The specimens prepared with a l/s ratio of 0.6 and concentrated AS showed the highest tangent modulus of 532 MPa.

Table 28: Flexural test results of UND2 (1)

Sample ID	σmax			ε(σmax)			Etan		
	Average	Stand. Dev	CV	Average	Stand. Dev	CV	Average	Stand. Dev	CV
	[MPa]	[MPa]	[%]	[%]	[%]	[%]	[MPa]	[MPa]	[%]
UND2_06_100%	0.38	0.057	14.7	1.38	0.142	10.3	29.0	4.2	14.3
UND2_06_75%	1.35	0.031	2.3	0.90	0.034	3.8	150.9	6.8	4.5
UND2_06_50%	0.53	0.083	15.6	0.65	0.249	38.3	96.0	38.3	39.9
UND2_05_100%	3.10	0.158	5.1	0.60	0.116	19.1	532.4	87.6	16.5
UND2_05_75%	3.71	0.536	14.4	1.04	0.251	24.2	369.5	59.9	16.2
UND2_05_50%	0.89	0.103	11.6	0.81	0.233	28.9	122.8	53.2	43.3
UND2_04_100%	1.88	0.139	7.4	0.40	0.045	11.5	482.4	36.2	7.5

Table 29: Flexural test results of UND2 (2)

Sample ID	T			ρ			Number of Observations
	Average	Stand. Dev	CV	Average	Stand. Dev	CV	
	[kPa*mm/mm]	[kPa*mm/mm]	[%]	(kg/m3)	[kg/m^3]	[%]	
UND2_06_100%	2.75	0.458	16.6	1925.6	15.9	0.8	5
UND2_06_75%	6.11	0.281	4.6	1893.4	22.6	1.2	4
UND2_06_50%	1.74	0.561	32.2	1528.9	24.2	1.6	4
UND2_05_100%	10.00	2.918	29.2	1907.5	39.8	2.1	5
UND2_05_75%	19.85	7.387	37.2	1737.1	13.7	0.8	5
UND2_05_50%	3.55	0.840	23.7	1543.7	22.2	1.4	4
UND2_04_100%	3.76	0.690	18.3	1961.9	17.2	0.9	4

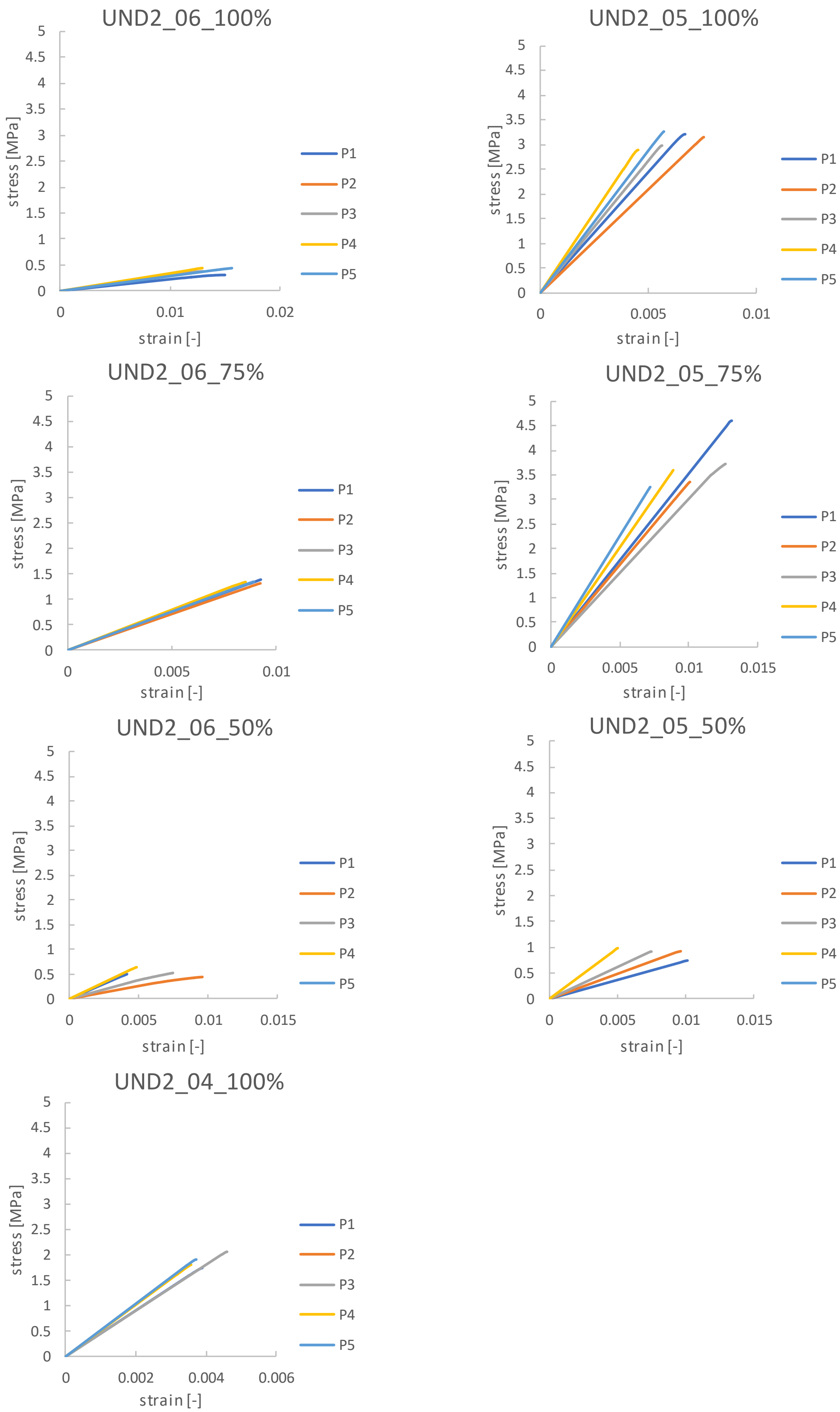

Figure 52: flexural stress-strain curves of UND2

3.1.4. Environmental assessment

The environmental assessment was carried out through leaching tests. The metal's release of the raw material (RC, RA, BT, NA and UND1) is exhibit in Table 30. The leaching test results concerning the alkali-activated powders are showed in table Table 31. However, not all the pastes were subjected to the test, only those made with a l/s ratio of 0.5 and a AS concentration of 100% were considered because they presented the best mechanical results compared to the other combinations. The results were then compared to the European council and Italian D.M/98 limits (Table 2) and was finally determined that all the materials tested provided results under the EC (2003/33/EC) limits, indicating that all the components can be classified as inert waste. Nevertheless, not all the metals release was under the D.M/98 limits, suggesting that the Italian criteria is more severe. Significant concentrations of chlorides, nitrates and sulphates were found in the eluates of the components compared to the other parameters analyzed. Furthermore, there seems to be a higher pollutants release for all the alkali activated particles.

Table 30: Leaching test results (1)

Parameter	**RC**	**RA**	**BT**	**NA**	**UND1**
cyanides [µg/l]	0	0	0	0	0
chlorides [mg/l]	55	43	48	44	50
fluorides [mg/l]	0.61	0.092	0.68	0.2	0.14
nitrates [mg/l]	34	6.4	12	9.6	37
sulphates [mg/l]	540	28	120	79	390
Arsenic [µg/l]	0.6	2.4	3.5	1.3	4.1
Barium [mg/l]	0.099	0.74	2.5	0.089	0.073
Beryllium [µg/l]	0	0	0	0	0
Cadmium [µg/l]	0	0	0	0	0
Cobalt [µg/l]	0.28	0.13	0.11	0.18	0.31
Chrome [µg/l]	110	0.93	42	1.3	4.1
Mercury [µg/l]	0	0	0	0	0
Nickel [µg/l]	0	4	0	3.7	2.1
Lead [µg/l]	0	0.26	0.16	0.14	0.19
Copper [mg/l]	0.008	0.002	0.004	0.002	0.009
Selenium [µg/l]	0.97	0	1.1	0	1.3
Vanadium [µg/l]	17	4.6	110	2.9	11
Zinc [mg/l]	0.001	0.003	0.005	0.003	0.003
Asbestos [mg/l]	0	0	0	0	0
pH	11	8.7	10.1	8.3	8.6

Table 31: Leaching test results (2)

Parameter	RC_05_100	RA_05_100	BT_05_100	NA_05_100	UND_05_100
cyanides [µg/l]	0	0	0	0	0
chlorides [mg/l]	69	58	58	49	68
fluorides [mg/l]	3.1	0.53	0.87	0	0.91
nitrates [mg/l]	22	3.8	6.3	9.3	27
sulphates [mg/l]	520	600	100	79	560
Arsenic [µg/l]	120	66	210	69	180
Barium [mg/l]	0.013	0.037	0.086	0.047	0.081
Beryllium [µg/l]	0	0.250	0	0.11	0.14
Cadmium [µg/l]	0	0	0	0	0.11
Cobalt [µg/l]	1.8	6.5	1	2.1	7.9
Chrome [µg/l]	160	21	25	15	13
Mercury [µg/l]	0	0	0	0	0.24
Nickel [µg/l]	0	76	0	19	58
Lead [µg/l]	2.7	19	64	11	16
Copper [mg/l]	0.067	0.047	0.026	0.064	0.23
Selenium [µg/l]	8.1	3.3	2.9	0	3.9
Vanadium [µg/l]	360	150	1200	140	580
Zinc [mg/l]	0.04	0.094	0.067	0.12	0.058
Asbestos [mg/l]	0	0	0	0	0
pH	11.8	12.2	11.5	12.1	12

The pH was measured to the eluates of the alkali-activated powders and the raw material following the British Standards 1377-2003. The pH tests results are represented in Table 32 for a l/s ratio of 0.6, in Table 33 for a l/s ratio of 0.5 and in Table 34 for a l/s of 0.4. It is evident how the pH of the resulting leachate is greater for the activated powders than for the raw material, the reason is that the alkaline solution has a pH around 14 so it was expected that by mixing it with the raw powder it would increase. The pH decreased for lower l/s ratios and it is similar for all alkaline concentrations. The raw material presented a pH from 9.46 (for BT) to 11.14 (for RA), however after the alkaline activation, the lowest pH was obtained by UND2 and the other components presented similar results. The pH is one of the most relevant factors that controls the pollutant release in the leaching test (Galvin et al., 2012), in fact, after the leaching test, it was recorded with a pH-meter following the UNI EN 12506:2004 standards (Table 30 and Table 31). The results showed slightly differences between the pH values due to the diverse pH setting for each standard (e.g., liquid/solid ratio).

Table 32: pH results for l/s=0.6

l/s=0.6	pH			
Sample	AS=100%	AS=75%	AS=50%	Raw material
RC	12.44	12.68	12.07	10.35
RA	12.42	12.58	11.45	11.14
BT	12.32	12.42	11.34	9.46
NA	12.43	12.56	11.81	10.32
UND1	12.34	12.35	11.75	10.15
UND2	12.12	11.85	10.95	10.44

Table 33: pH results for l/s=0.5

l/s=0.5	pH			
Sample	AS=100%	AS=75%	AS=50%	Raw material
RC	12.35	12.39	11.67	10.35
RA	12.35	12.30	11.85	11.14
BT	12.53	12.20	11.24	9.46
NA	12.31	12.39	11.42	10.32
UND1	12.15	12.17	11.42	10.15
UND2	12.15	11.60	10.88	10.44

Table 34: pH results for l/s=0.4

l/s=0.4	pH	
Sample	AS=100%	Raw material
RC	11.82	10.35
RA	12.24	11.14
BT	11.29	9.46
NA	12.19	10.32
UND1	11.93	10.15
UND2	12.18	10.44

3.2. Discussion

Prior work has documented the physical, volumetric and mechanical characterization of CDW and some of its components like, recycled concrete, bricks and tails and recycled asphalt, proving the feasibility of these alternative aggregates in road construction. Other studies have shown the mechanical properties improvement through chemical stabilization. However, neither of these studies have considered the individual characterization of the fines nor the NA and UND2 components. In this section the analysis and discussion of the mechanical results considering the physical, chemical, and volumetric properties of CDW fine particles are presented. Few comments regarding the mechanical behavior differences between the materials are also included.

The best way to represent the data and perform a deep analysis of the results obtained is through charts, which were built and here commented to provide a description and a comparison of the results for each CDW component. In this section, the analysis and the assumptions made of the results obtained from the laboratory tests are presented.

3.2.1. Mechanical properties

The mechanical outputs give evidence to the improvement of the compression and flexural strength of fines from CDW components when are alkali-activated. The same behavior has been also observed by Zaharaki et al., (2016), Komnitsas et al, (2015) and Rapazote et al., (2011). The mechanical strength of the CDW alkali-activated specimens, highly depends on the conditions such as the AS concentration used (demonstrated in the present research), the curing time considered (Pathak et al., (2014), the curing temperature Komnitsas et al., (2015), the amount of aluminosilicates present (Zaharaki et al., 2016), etc.

Figure 53 shows the mean flexural and compressive strength achieved by each CDW component when mixed with the alkali-activating solution. Flexural and compressive strength of alkali-activated CDW components exhibit the same trend, only with a different scale. The strength of the alkali-activated specimens is affected by the AS concentration used to prepare the pastes.

At a 50% alkaline concentration, the strength of specimens for all mixing combinations were extremely low, not even the 10% of what obtained with an undiluted AS. This may be due to the presence of unreacted aluminosilicates which resulted in a solidification process slower and in partial loss of strength. When the AS concentration increase to 75%, a noticeable beneficial effect in the compressive and flexural strength is shown for almost all the combinations, as a matter of fact, the best results obtained for the RA specimens were prepared with 25% diluted AS. A further increase of the mechanical strength is exhibited for the samples prepared with an undiluted AS, only RA, UND1 and UND2 with a l/s = 0.6 presented better results for a 75% alkaline concentration. The fact that with higher AS concentrations the mechanical strength improve, may be an effect of the blends viscosity, due to the presence of the liquid glass ($Na_2O \cdot nSiO_2$), and the geopolymerization reaction resulted in a stronger bonding. In conclusion, the mechanical tests results presented an evident improvement on the compressive and flexural strength for an undiluted AS.

The RC mixtures gave the best results for l/s ratio equal to 0.5. The strength of the hardened specimens may be only partly explained by geopolymerization, but there's the suspect that the rehydration process of the cement present in the mixture may also have played a role. This inference is also supported by the limited bleeding exhibited by pastes, which was not observed for the other CDW components. Furthermore, according to the XRF results (Table 3), the presence of a significant amount of calcite fractions in this recycled material may support such a hypothesis. When calcite enters into contact with the AS, the solubilized calcium and the unreacted silicates originate new calcium silicate hydrate (C-S-H) thanks to water and silicon present in the AS.

The RA hardened specimens provided always the smallest values compared to the other blends. An extremely slow speed of hardening process, the high presence of organic content in this component, and a low presence of aluminosilicates (if compared to other CDW components) may explain this result. It was also observed that most of the RA specimens were still humid after 28 days, meaning that the water was released progressively and slowly during time. This might have an effect in the development of strengths. However, the maximum strength is given by an AC of 100% and a l/s ratio of 0.6.

The NA hardened specimens presented a progressive increase in strength for more concentrated AS. The specimens achieved an optimum maximum compressive strength of 10.66 MPa when prepared with a l/s = 0.4 and an undiluted AS. However, the rest of the NA combinations presented low values of strength compared to the maximum achieved: in such cases the pastes exhibited a low viscosity and a greater bleeding than other CDW components.

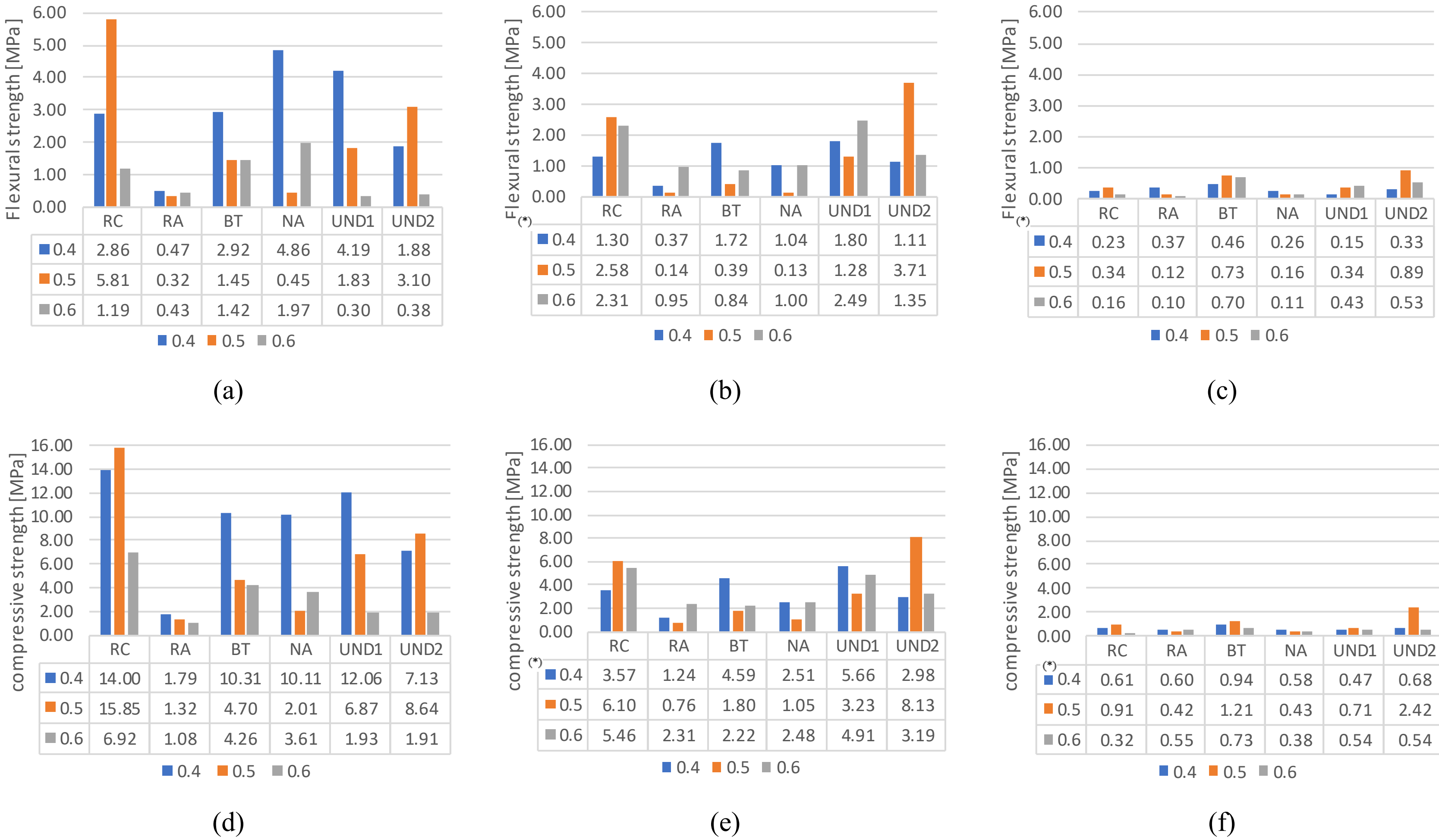

Figure 53: Flexural and compressive strength of the six CDW components with an alkaline concentration of 100% (a and d), 75% (b and e) and 50% (c and f), for a l/s ratio of 0.6, 0.5 and 0.4. (*) Data obtained by C. Bertello (2017).

BT and UND1 have similar behavior. In both cases, a progressive increase of compressive strength was observed passing from 0.6 to 0.4 in l/s ratio in case of 100% of AC. However, in case of AC = 75%, it's evident that the highest strength is given by a l/s=0.4 and the lowest by l/s=0.5 for both components. The considerable strength obtained by both materials is evidently associated to the significant amount of aluminum oxide and silica (Table 3). BT and UND1 contain the higher values of aluminum oxide, 19.2% and 12.8 respectively, and silica, 56.4% and 42.6% respectively.

Another important comparison is between the results given by UND1 and UND2. If the composition of UND1 is unknown, UND2 is determined by ¼ of each CDW constituent (RC, RA, BT, and NA). Results shows (Figure 53) that their mechanical properties are significantly different. UND1 obtained a maximum strength for a l/s=0.4, while UND2 for a l/s=0.5; in both cases the optimum was for an AC of 100%. The fact that UND1 behave similarly to BT might be connected to a higher presence of this component in UND1.

The samples prepared with an AS concentration of 50% presented the lowest strength compared to the other AC and also a greater bleeding compared to the rest of blends; it seems like that the excess of water and part of the AS leaked out from the specimens and the resting AS was not enough to activate the aluminum-silicates of the CDW powders.

The l/s ratio is also an important parameter that influence the mechanical response of hardened specimens. Figure 54 illustrates the tendency in compressive strength results when the l/s ratio changes for each AS concentration. For RC and UND2, the charts evidence an increment of the compressive strength passing from l/s ratio of 0.4 to 0.5. This might be explained with the fact that blends prepared with l/s = 0.4 presented a lower workability due to the poor liquid content, resulting in lower strength. In fact, the specimens were formed with a moderate action with a spatula to reduce voids and favor the bonding process. For l/s = 0.6, the drop in strength is caused by the high liquid content in the paste, which prolongs the solidification process and results in partial loss of strength. The RA and NA hardened specimens shown a progressive decrease of strength when incrementing the l/s ratio for the most concentrated AS. Conversely, it tends to increase for a 75% alkaline concentration.

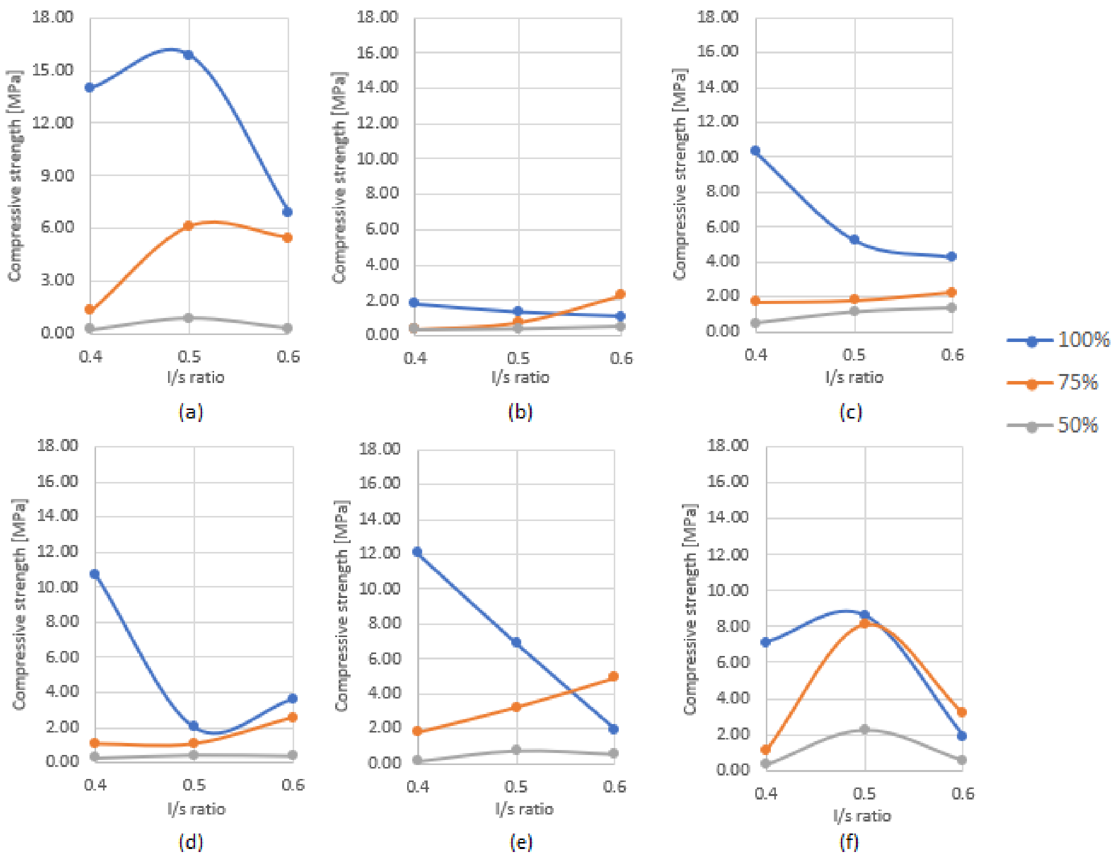

Figure 54: Compressive strength of RC (a), RA (b), BT (c), NA (d), UND1 (e) and UND2 (f)

The UND1 specimens exhibited a linear decrease of strength when increasing the l/s ratio of the mixtures prepared with an undiluted AS. This behavior can be explained by the viscosity, which is lower when the l/s ratio increases. The pastes made with a 75% alkaline concentration presented the opposite behavior. A new investigation and a more detailed analysis will be necessary to explain this behavior.

As mentioned in paragraph 2.2.1, UND2 is a material equally composed by the four investigated CDW components. The hypothesis that the UND2 mechanical strength could be the weighted average strength of the CDW constituents' mechanical results should be assessed. Hence, the UND2 compressive and tensile test results were compared to the weighted average strengths observed on RC, RA, BT and NA in Figure 55. The expected and measured results for each alkaline concentration and l/s ratio is distinguished in the figure. Almost all the results presented a great deviation from the linear regression providing a coefficient of determination (R^2) lower than 0.6 for all the samples. Such results lead to the conclusion that the hypothesis is rejected, and that the strength development on CDW components is certainly regulated by secondary effects (i.e., phenomena of the second order) that are governed by the interaction between components and the AS.

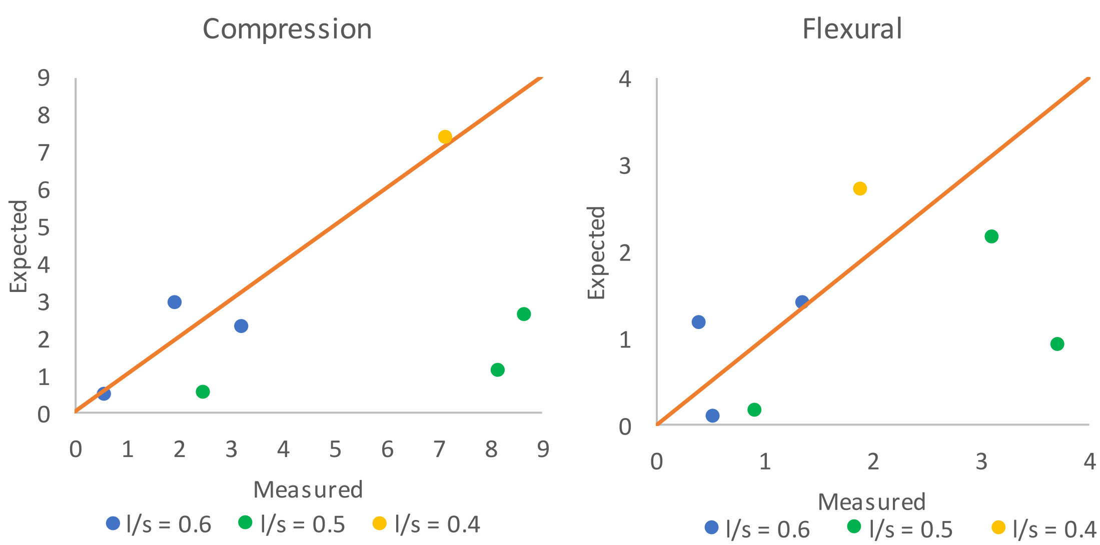

(a) (b)

Figure 55: comparison between UND2 expected results and the UND2 actual results of compression strength (a) and flexural strength (b)

3.2.2. Chemical and environmental assessment

Figure 56 exhibit the amount of metals released for each CDW constituent and their respective limits given by the European council (2003) and the D.M (1998). It’s evident that none of the components exceed the EU/2003 limits, which are significantly higher than those reported by the DM/98.

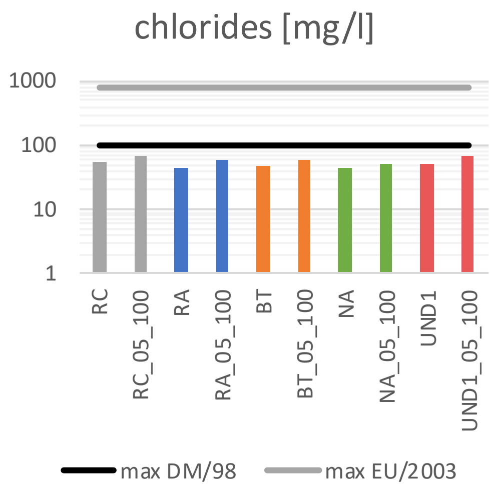
chlorides [mg/l]
1000
100
10
1
RC
RC_05_100
RA
RA_05_100
BT
BT_05_100
NA
NA_05_100
UND1
UND1_05_100
max DM/98
max EU/2003

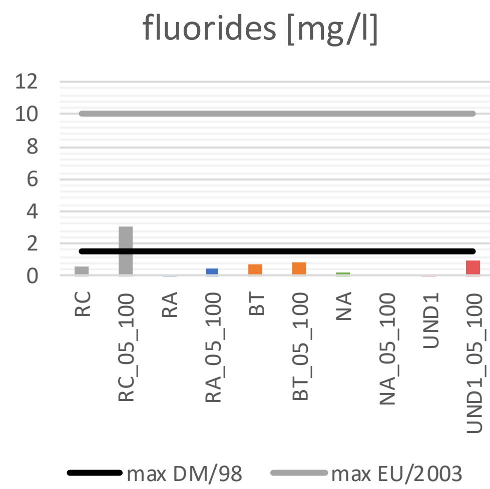
fluorides [mg/l]
12
10
8
6
4
2
0
RC
RC_05_100
RA
RA_05_100
BT
BT_05_100
NA
NA_05_100
UND1
UND1_05_100
max DM/98
max EU/2003

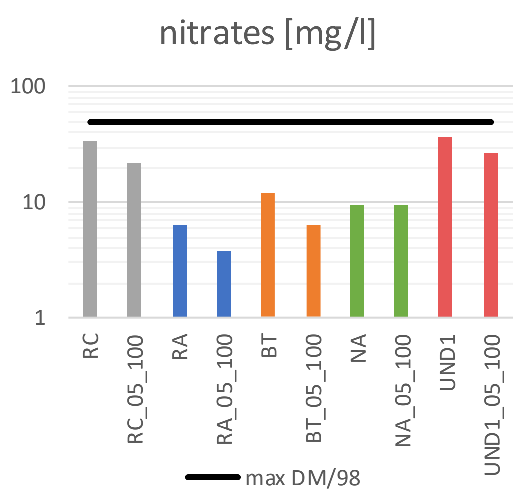
nitrates [mg/l]
100
10
1
RC
RC_05_100
RA
RA_05_100
BT
BT_05_100
NA
NA_05_100
UND1
UND1_05_100
max DM/98

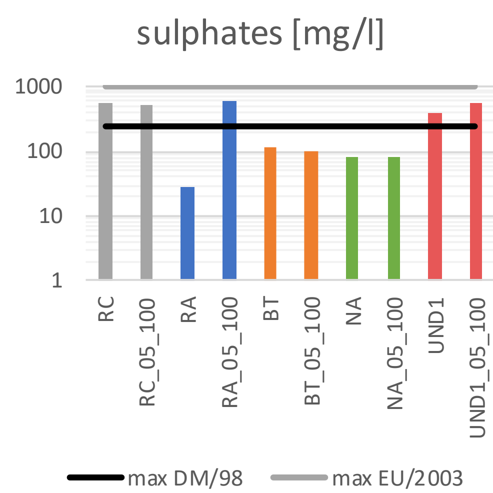
sulphates [mg/l]
1000
100
10
1
RC
RC_05_100
RA
RA_05_100
BT
BT_05_100
NA
NA_05_100
UND1
UND1_05_100
max DM/98
max EU/2003

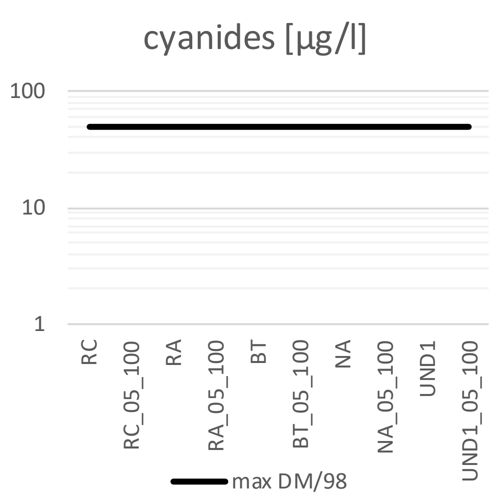
cyanides [µg/l]
100
10
1
RC
RC_05_100
RA
RA_05_100
BT
BT_05_100
NA
NA_05_100
UND1
UND1_05_100
max DM/98

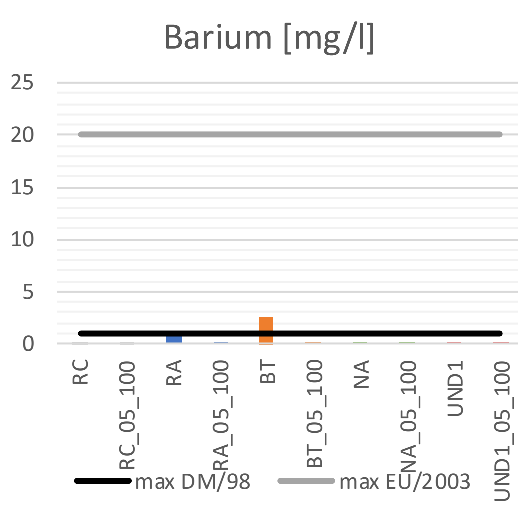
Barium [mg/l]
25
20
15
10
5
0
RC
RC_05_100
RA
RA_05_100
BT
BT_05_100
NA
NA_05_100
UND1
UND1_05_100
max DM/98
max EU/2003

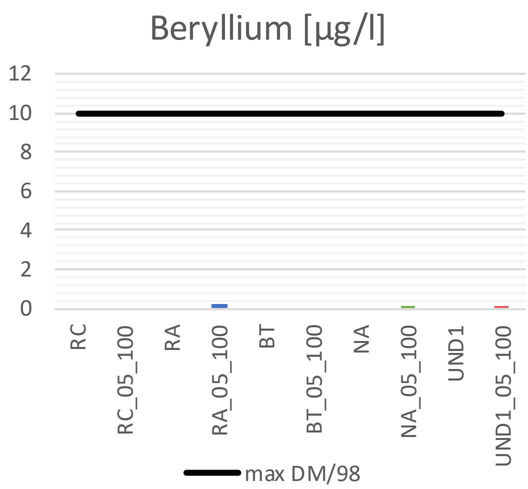
Beryllium [µg/l]
12
10
8
6
4
2
0
RC
RC_05_100
RA
RA_05_100
BT
BT_05_100
NA
NA_05_100
UND1
UND1_05_100
max DM/98

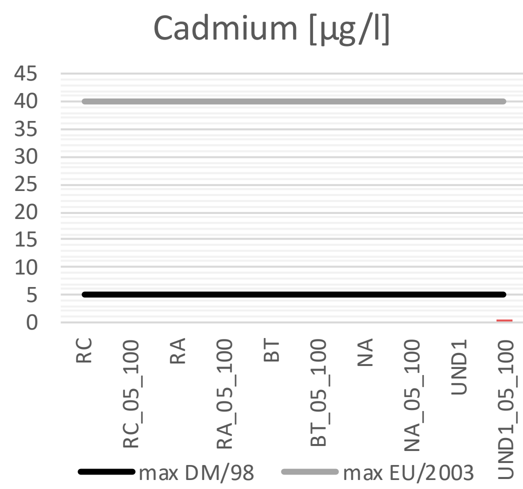
Cadmium [µg/l]
45
40
35
30
25
20
15
10
5
0
RC
RC_05_100
RA
RA_05_100
BT
BT_05_100
NA
NA_05_100
UND1
UND1_05_100
max DM/98
max EU/2003

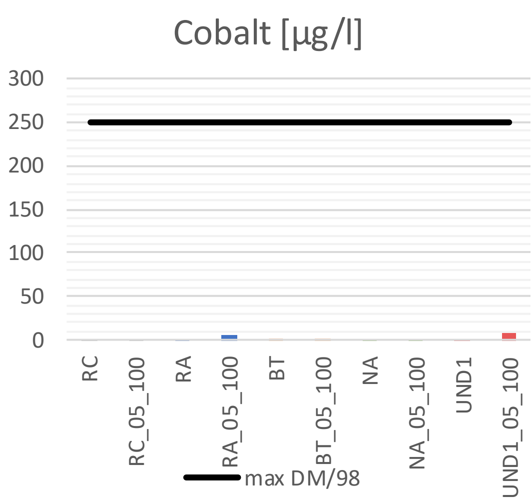
Cobalt [µg/l]
300
250
200
150
100
50
0
RC
RC_05_100
RA
RA_05_100
BT
BT_05_100
NA
NA_05_100
UND1
UND1_05_100
max DM/98

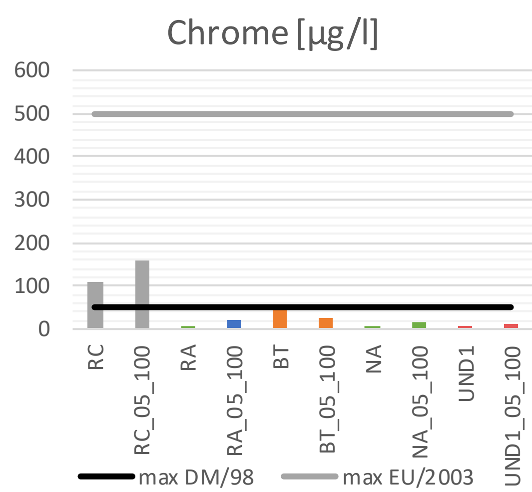
Chrome [µg/l]
600
500
400
300
200
100
0
RC
RC_05_100
RA
RA_05_100
BT
BT_05_100
NA
NA_05_100
UND1
UND1_05_100
max DM/98
max EU/2003

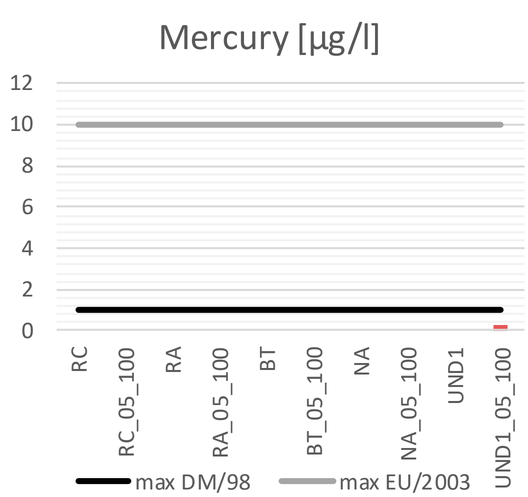
Mercury [µg/l]
12
10
8
6
4
2
0
RC
RC_05_100
RA
RA_05_100
BT
BT_05_100
NA
NA_05_100
UND1
UND1_05_100
max DM/98
max EU/2003

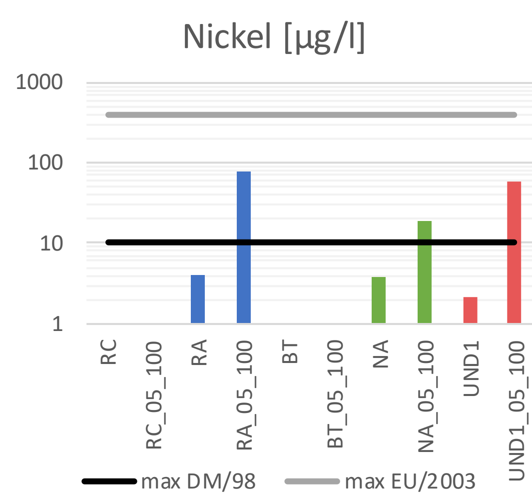
Nickel [µg/l]
1000
100
10
1
RC
RC_05_100
RA
RA_05_100
BT
BT_05_100
NA
NA_05_100
UND1
UND1_05_100
max DM/98
max EU/2003

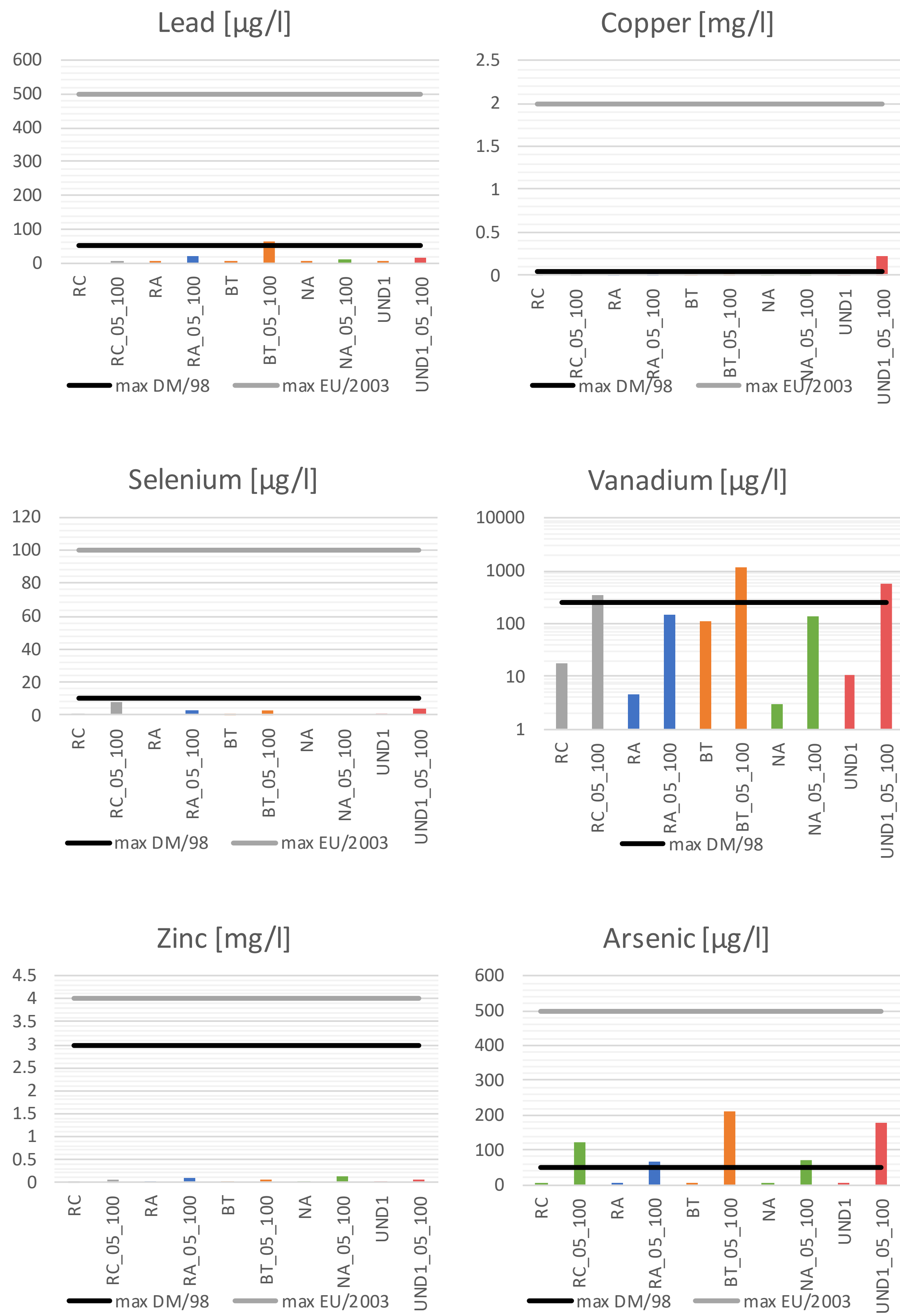

Figure 56: Leaching tests results

The alkaline activation seems to lead to a greater release of cations (As, Ba, Be, Cd, Co, Cr, Hg, Ni, Pb, Cu, Se, V, Zn). The reason might be correlated to the fact that, there's a double exposure of particles to an aqueous medium: (a) when the samples were prepared, and the grains entered into contact with the AS, a partial release may have occurred, and (b) when exposed again during the leaching test, a further dissolution caused a higher release. The dry powders instead, were only exposed once to the aqueous medium during the leaching test. However, in few cases the opposite was observed: this is the case of nitrates whose release is greater for the powders than for the alkali-activated materials. This could be justified that with the geopolymerization these components remained blocked in the new mineral structure. The leaching behavior is considered to be a pH-dependent process controlled by metal hydroxide solubility (Galvin et al., 2012). The concentration of the anions (Cl^-, F^-, SO_4^{2-} and NO_3^-) after the alkaline activation essentially does not vary, in fact, chlorides and sulphates remained in general constant and nitrates decreased. This behavior might be because they react with soda to form composites (sodium chloride, sodium fluoride, sodium nitrate and sodium sulfate) which precipitate into the structure and are therefore released to a lesser extent

The leaching tests results are clearly related to the CDW components chemical composition. The presence of sulphates is evidenced by the XRF analysis in all the waste materials, however, its release is over the DM/98 limit for the RC, RA and UND1 alkali activated powders, due to the evident higher presence of sulphates in the raw material. The XRF analysis determined low portions of nickel in the CDW components. The raw material exhibited a nickel's release under the D.M /98 limits, however the alkali activated fine particles showed leaching results over the Italian limits. UND1 is the only component that presents concentrations of copper, which is consistent with the XRF results. This is the only component that leached cooper and also over the D.M limit. The only CDW component that contains lead is BT; however, the leaching test evidenced that it is only released when the grain is alkali-activated, exceeding the DM/98 limit.

It's evident that the pollutant release of the waste materials is far below the DM/98 limit for cobalt, cadmium, zinc beryllium and mercury. It seems that the release of arsenic is significantly greater when the powder is alkali-activated, the same goes for the fluorides, chlorides, copper, selenium, nickel, lead, chrome and vanadium. On the contrary, the nitrates and the barium’s release decrease considerably for the alkali-activated particles, probably because they easily dissolved during the blends preparation and remained on the bleeding or they remained blocked in the new structure under the exposure to water in the leaching test.

Conclusions

Prior work has documented the successful alkali activation of CDW and the mechanical performance improvement due to such stabilization. This experimental research aimed to investigate the mechanical behavior of the pulverized CDW constituents (RC, RA, BT, NA, UND1 and UND2) when are alkali activated with different l/s ratios (0.4, 0.5 and 0.6) and three different alkaline concentrations (pure 100% and diluted 75% and 50%). The objective was to identify the most reactive components capable of performing a potential binding function in CDW granular mixtures.

The chemical composition of the raw material was determined through an X-ray fluorescent analysis to verify the presence of aluminosilicates, which allows the alkaline activation process. The test revealed that all the CDW components had a high presence of silica with an average of 42% by weight, and aluminum oxide with an average of 10% by weight. The test also evidenced high values of calcium oxide for RC and large values of carbon dioxide for RA.

The flexural and compressive strength of the hardened pastes tended to increase with the AS concentration, since the lowest strength values for all the CDW components were obtained for an AC of 50% and the highest strengths were observed for the specimens with an AC of 100%, regardless of the l/s ratio. The best mechanical performance was determined by the RC component, with a l/s=0.5 and an AC of 100% that achieved a compressive strength of 15.85 MPa and a flexural strength of 5.61 MPa. Good results were also obtained by BT, NA and UND1 for a l/s=0.4 and for and AC of 100%, evidencing that the viscosity played a key role in their final mechanical behavior. UND2 behaved completely different from UND1 and obtained the best results for a l/s=0.5 and an AC of 100%.

A further environmental assessment was performed through the leaching test and related analysis to evaluate the pollutant’s release of the CDW constituents and the alkali-activated powders (with a l/s=0.5 and an AC of 100%). The results were then compared to the limit values suggested by the ministerial decree 05/02/1998 and the European council (2003/33/EC). All the metals released by the components were under the EU/2003 limit, however the DM/98 limits are more conservative, and some materials exceed this limit. The concentration of sulfates, nitrates, and chlorides were important in all materials tested while for cobalt, zinc, cadmium and beryllium were negligible. According to the European criteria all the components can be classified as inert waste.

The results obtained in this thesis demonstrated that CDW fine particles successfully reacted with the alkaline solution to form hardened specimens with significant mechanical properties for a l/s ratio equal to 0.4 and without any thermal treatment. Therefore, the geopolymerization of CDW fine particles represent an effective alternative solution to stabilize the layers made of CDW aggregates. This technology excludes the use of cementitious binders, so it can be considered as more sustainable and economical with respect to current technology based on the use of traditional binders in road constructions.

Future research may deepen in some unexplored aspects such as: (a) the effects of temperature on the kinetics of reaction to assess the mechanical behavior of the CDW powders after thermal treatment and (b) the use of different alkali-solution not including sodium silicate in order to evaluate the reactivity of the powders with an alternative activator.

References

Agrela, F., Barbudo, A., Ramírez, A., Ayuso, J., Carvajal, M. D., & Jiménez, J. R. (2012). Construction of road sections using mixed recycled aggregates treated with cement in Malaga, Spain. *Resources, Conservation and Recycling*, *58*, 98–106. http://doi.org/10.1016/j.resconrec.2011.11.003

Allahverdi, A., & Najafi Kani, E. (2009). Construction wastes as raw materials for geopolymers binders. *International Journal of Civil Engineering*, *7*(3), 154–160.

Arulrajah, A., Piratheepan, J., Disfani, M. M., & Bo, M. W. (2013). Resilient Moduli Response of Recycled Construction and Demolition Materials in Pavement Subbase Applications. *Journal of Materials in Civil Engineering*, *25*(12), 1920–1928. http://doi.org/10.1061/(ASCE)MT.1943-5533.0000766

Arulrajah, A., & Piratheepan, J. (2012). Geotechnical and geoenvironmental properties of recycled construction and demolition materials in pavement subbase applications. *Journal of Materials in …*, *25*(8), 1077–1088. http://doi.org/10.1061/(ASCE)MT.1943-5533.0000652.

Arulrajah, a, Piratheepan, J., Ali, M. M. Y., & Bo, M. W. (2011). Geotechnical Properties of Recycled Concrete Aggregate in Pavement Sub-Base Applications. *Journal of Materials in Civil Engineering*, *35*(5), 1–9. http://doi.org/10.1061/(ASCE)MT.1943-5533.0000319.

Arulrajah, A., Mohammadinia, A., D'Amico, A., & Horpibulsuk, S. (2017). Cement kiln dust and fly ash blends as an alternative binder for the stabilization of demolition aggregates. *Construction and Building Materials*, *145*, 218–225. http://doi.org/10.1016/j.conbuildmat.2017.04.007

Arulrajah, A., Mohammadinia, A., Phummiphan, I., Horpibulsuk, S., & Samingthong, W. (2016). Stabilization of Recycled Demolition Aggregates by Geopolymers comprising Calcium Carbide Residue, Fly Ash and Slag precursors. *Construction and Building Materials*, *114*, 864–873. http://doi.org/10.1016/j.conbuildmat.2016.03.150

Assi, L. N., Eddie Deaver, E., & Ziehl, P. (2018). Effect of source and particle size distribution on the mechanical and microstructural properties of fly Ash-Based geopolymer concrete. *Construction and Building Materials*, *167*, 372–380. http://doi.org/10.1016/j.conbuildmat.2018.01.193

Bassani, M., Riviera, P. P., Tefa, L. (2017). Short-Term and Long-Term Effects of Cement Kiln Dust Stabilization of Construction and Demolition Waste. *Journal of*

Materials in Civil Engineering, *29*(5), 04016286. http://doi.org/10.1061/(ASCE)MT.1943-5533.0001797.

Bennert, T., & Papp, W. J. (2000). Utilization of construction and demolition debris under traffic-type loading in base and subbase applications. *Journal of the Transportation Research Board: Transportation Research Record*, *TRR 1714*(00), 33–39. http://doi.org/10.3141/1714-05

Butera, S., Christensen, T. H., & Astrup, T. F. (2014). Composition and leaching of construction and demolition waste: Inorganic elements and organic compounds. *Journal of Hazardous Materials*, *276*, 302–311. http://doi.org/10.1016/j.jhazmat.2014.05.033

Cardoso, R., Silva, R. V., Brito, J. de, & Dhir, R. (2016). Use of recycled aggregates from construction and demolition waste in geotechnical applications: A literature review. *Waste Management*, *49*, 131–145. http://doi.org/10.1016/j.wasman.2015.12.021

Cerni, G., & Colagrande, S. (2012). Resilient Modulus of Recycled Aggregates Obtained by Means of Dynamic Tests in a Triaxial Apparatus. *Procedia - Social and Behavioral Sciences*, *53*, 475–484. http://doi.org/10.1016/j.sbspro.2012.09.898

Council of the European Union, & 2003/33/EC. (2003). Council Decision establishing criteria and procedures for the acceptance of waste at landfills pursuant to Article 16 of and Annex II to Directive 1999/31/EC. *Official Journal of the European Communities*, 27–49.

Delay, M., Lager, T., Schulz, H. D., & Frimmel, F. H. (2007). Comparison of leaching tests to determine and quantify the release of inorganic contaminants in demolition waste. *Waste Management*, *27*(2), 248–255. http://doi.org/10.1016/j.wasman.2006.01.013

Duxson, P., Fernández-Jiménez, A., Provis, J. L., Lukey, G. C., Palomo, A., & Van Deventer, J. S. J. (2007). Geopolymer technology: The current state of the art. *Journal of Materials Science*, *42*(9), 2917–2933. http://doi.org/10.1007/s10853-006-0637-z

Environmental Protection Agency. (2002). *European waste catalogue and hazardous waste list*. *Hazardous Waste*. Retrieved from http://www.environ.ie/en/Publications/Environment/Waste/WEEE/FileDownLoad,1343,en.pdf

European Commission. (2015). Screening template for Construction and Demolition Waste management, (October).

European Commission (DG ENV). (2011). Service contract on management of construction and demolition waste - SR1. Final Report Task 2. *Bio Intelligence Service*, *33*(0), 1–240. http://doi.org/ENV.G.4/FRA/2008/0112

Fernández-Jiménez, A., & Palomo, A. (2005). Composition and microstructure of alkali activated fly ash binder: Effect of the activator. *Cement and Concrete Research*, *35*(10), 1984–1992. http://doi.org/10.1016/j.cemconres.2005.03.003

Gálvez-Martos, J. L., Styles, D., Schoenberger, H., & Zeschmar-Lahl, B. (2018). Construction and demolition waste best management practice in Europe. *Resources, Conservation and Recycling*, *136*(April), 166–178. http://doi.org/10.1016/j.resconrec.2018.04.016

Galvín, A. P., Ayuso, J., Jiménez, J. R., & Agrela, F. (2012). Comparison of batch leaching tests and influence of pH on the release of metals from construction and demolition wastes. *Waste Management*, *32*(1), 88–95. http://doi.org/10.1016/j.wasman.2011.09.010

Gonçalves Rapazote, J., Laginhas, C., & Teixeira-Pinto, A. (2011). Development of Building Materials through Alkaline Activation of Construction and Demolition Waste (CDW) – Resistance to High Temperatures. *12th International Conference on Durability of Building Materials and Components*, 1–8. Retrieved from https://www.irbnet.de/daten/iconda/CIB22585.pdf

Herrador, R., Pérez, P., Garach, L., & Ordóñez, J. (2012). Use of Recycled Construction and Demolition Waste Aggregate for Road Course Surfacing. *Journal of Transportation Engineering*, *138*(2), 182–190. http://doi.org/10.1061/(ASCE)TE.1943-5436.0000320

Hoy, M., Horpibulsuk, S., & Arulrajah, A. (2016). Strength development of Recycled Asphalt Pavement - Fly ash geopolymer as a road construction material. *Construction and Building Materials*, *117*, 209–219. http://doi.org/10.1016/j.conbuildmat.2016.04.136

Jiménez, J. R., Ayuso, J., Agrela, F., L??pez, M., & Galv??n, A. P. (2012). Utilisation of unbound recycled aggregates from selected CDW in unpaved rural roads. *Resources, Conservation and Recycling*, *58*, 88–97. http://doi.org/10.1016/j.resconrec.2011.10.012

Komnitsas, K., & Zaharaki, D. (2007). Geopolymerisation: A review and prospects for the minerals industry. *Minerals Engineering*, *20*(14), 1261–1277. http://doi.org/10.1016/j.mineng.2007.07.011

Komnitsas, K., Zaharaki, D., Vlachou, A., Bartzas, G., & Galetakis, M. (2015). Effect of synthesis parameters on the quality of construction and demolition wastes (CDW) geopolymers. *Advanced Powder Technology*, *26*(2), 368–376. http://doi.org/10.1016/j.apt.2014.11.012

Kosson, D. S., van der Sloot, H. A., Sanchez, F., & Garrabrants, A. C. (2002). An Integrated Framework for Evaluating Leaching in Waste Management and Utilization of Secondary Materials. *Environmental Engineering Science*, *19*(3), 159–204. http://doi.org/10.1089/109287502760079188

Lampris, C., Lupo, R., & Cheeseman, C. R. (2009). Geopolymerisation of silt generated from construction and demolition waste washing plants. *Waste Management*, *29*(1), 368–373. http://doi.org/10.1016/j.wasman.2008.04.007

Leite, F. D. C., Motta, R. D. S., Vasconcelos, K. L., & Bernucci, L. (2011). Laboratory evaluation of recycled construction and demolition waste for pavements. *Construction and Building Materials*, *25*(6), 2972–2979. http://doi.org/10.1016/j.conbuildmat.2010.11.105

Liew, Y. M., Heah, C. Y., Mohd Mustafa, A. B., & Kamarudin, H. (2016). Structure and properties of clay-based geopolymer cements: A review. *Progress in Materials Science*, *83*, 595–629. http://doi.org/10.1016/j.pmatsci.2016.08.002

Mohammadinia, A., Arulrajah, A., Sanjayan, J., Disfani, M. M., Bo, M. W., & Darmawan, S. (2015). Laboratory Evaluation of the Use of Cement-Treated Construction and Demolition Materials in Pavement Base and Subbase Applications. *Journal of Materials in Civil Engineering*, *27*(6), 04014186. http://doi.org/10.1061/(ASCE)MT.1943-5533.0001148

Mohammadinia, A., Arulrajah, A., Sanjayan, J., Disfani, M. M., Win Bo, M., & Darmawan, S. (2016). Stabilization of Demolition Materials for Pavement Base/Subbase Applications Using Fly Ash and Slag Geopolymers: Laboratory Investigation. *Journal of Materials in Civil Engineering*, *28*(7), 04016033. http://doi.org/10.1061/(ASCE)MT.1943-5533.0001526

Pathak, A., Kumar, S., & Jha, V. K. (2014). Development of Building Material from Geopolymerization of Construction and Demolition Waste (CDW). *Transactions of the Indian Ceramic Society*, *73*(2), 133–137. http://doi.org/10.1080/0371750X.2014.922429

Poon, C. S., Shui, Z. H., & Lam, L. (2004). Effect of microstructure of ITZ on compressive strength of concrete prepared with recycled aggregates. *Construction and Building Materials*, *18*(6), 461–468. http://doi.org/10.1016/j.conbuildmat.2004.03.005

Poon, C. S., & Chan, D. (2006). Feasible use of recycled concrete aggregates and crushed clay brick as unbound road sub-base. *Construction and Building Materials*, *20*(8), 578–585. http://doi.org/10.1016/j.conbuildmat.2005.01.045

Provis, J. L. (2016). Alkali-activated materials. *Cement and Concrete Research*. http://doi.org/10.1016/j.cemconres.2017.02.009

Reig, L., Tashima, M. M., Soriano, L., Borrachero, M. V., Monzó, J., & Payá, J. (2013). Alkaline activation of ceramic waste materials. *Waste and Biomass Valorization*, *4*(4), 729–736. http://doi.org/10.1007/s12649-013-9197-z

Tam, V. W. Y., & Tam, C. M. (2006). A review on the viable technology for construction waste recycling. *Resources, Conservation and Recycling*, *47*(3), 209–221. http://doi.org/10.1016/j.resconrec.2005.12.002

Van Der Sloot, H. A. (1996). Developments in evaluating environmental impact from utilization of bulk inert wastes using laboratory leaching tests and field verification. *Waste Management*, *16*(1–3), 65–81. http://doi.org/10.1016/S0956-053X(96)00028-1

Vieira, C. S., & Pereira, P. M. (2015). Use of recycled construction and demolition materials in geotechnical applications: A review. *Resources, Conservation and Recycling*, *103*, 192–204. http://doi.org/10.1016/j.resconrec.2015.07.023

Wahlström, M., Laine-Ylijoki, J., Määttänen, A., Luotojärvi, T., & Kivekäs, L. (1997). Environmental quality assurance system for use of crushed mineral demolition wastes in earth constructions. *Studies in Environmental Science*, *71*(C), 725–734. http://doi.org/10.1016/S0166-1116(97)80256-7

Zaharaki, D., Galetakis, M., & Komnitsas, K. (2016). Valorization of construction and demolition (C&D) and industrial wastes through alkali activation. *Construction and Building Materials*, *121*, 686–693. http://doi.org/10.1016/j.conbuildmat.2016.06.051

APPENDIX 1: compression test results

ID	Material	l/s	AS	F_{max} [N]	σ_{max} [kPa]	σ_{max} [MPa]	$\varepsilon_{(\sigma max)}$ [mm/mm]	$\varepsilon_{(\sigma max)}$ [%]	E_{sec} [kPa]	E_{sec} [MPa]	E_{tan} [kPa]	E_{tan} [MPa]	T [kPa*mm/mm]
RC_06C_100%_P1A	RC	0.6	100%	2690.8	6694.5	6.7	0.021	2.1	320379.2	320.4	399347.9	399.3	82.1
RC_06C_100%_P1B	RC	0.6	100%	2832.9	7048.2	7.0	0.020	2.0	347611.3	347.6	451289.7	451.3	85.3
RC_06C_100%_P2A	RC	0.6	100%	2813.7	7069.8	7.1	0.028	2.8	253740.4	253.7	321068.4	321.1	116.4
RC_06C_100%_P2B	RC	0.6	100%	2687.3	6786.1	6.8	0.025	2.5	276092.9	276.1	339431.3	339.4	97.6
RC_06C_100%_P3A	RC	0.6	100%	2752.4	6885.2	6.9	0.023	2.3	303551.6	303.6	396775.9	396.8	93.9
RC_06C_100%_P3B	RC	0.6	100%	2763.1	6912.0	6.9	0.020	2.0	337364.0	337.4	431559.6	431.6	84.9
RC_06C_100%_P4A	RC	0.6	100%	2735.7	6354.7	6.4	0.024	2.4	263673.3	263.7	337505.0	337.5	90.1
RC_0C_100%_P4B	RC	0.6	100%	2966.4	6990.4	7.0	0.022	2.2	321618.3	321.6	388403.7	388.4	88.4
RC_06C_100%_P5A	RC	0.6	100%	3055.6	7237.6	7.2	0.026	2.6	273373.7	273.4	298596.1	298.6	103.5
RC_06C_100%_P5B	RC	0.6	100%	3003.7	7182.8	7.2	0.020	2.0	361634.1	361.6	433715.6	433.7	81.6
RA_06C_100%_P1A	RA	0.6	100%	386.7	1028.6	1.0	0.133	13.3	7731.7	7.7	8708.2	8.7	74.7
RA_06C_100%_P1B	RA	0.6	100%	382.2	1060.3	1.1	0.124	12.4	8541.1	8.5	11029.5	11.0	79.0
RA_06C_100%_P2A	RA	0.6	100%	341.6	903.7	0.9	0.116	11.6	7802.4	7.8	9521.5	9.5	60.5
RA_06C_100%_P2B	RA	0.6	100%	380.4	1016.0	1.0	0.128	12.8	7966.6	8.0	9030.5	9.0	71.8
RA_0C_100%_P3A	RA	0.6	100%	396.9	1102.5	1.1	0.127	12.7	8695.1	8.7	11788.2	11.8	83.9
RA_06C_100%_P3B	RA	0.6	100%	326.5	920.7	0.9	0.126	12.6	7301.7	7.3	9475.0	9.5	69.0
RA_06C_100%_P4A	RA	0.6	100%	467.5	1245.6	1.2	0.088	8.8	14118.7	14.1	16854.9	16.9	62.8
RA_06C_100%_P4B	RA	0.6	100%	407.2	1119.9	1.1	0.093	9.3	12067.3	12.1	18568.6	18.6	67.3
RA_06C_100%_P5A	RA	0.6	100%	436.5	1235.1	1.2	0.098	9.8	12576.4	12.6	18952.7	19.0	78.9
RA_06C_100%_P5B	RA	0.6	100%	437.3	1192.6	1.2	0.105	10.5	11324.6	11.3	14377.8	14.4	74.6
BT_06C_100%_P1A	BT	0.6	100%	1720.0	4410.2	4.4	0.042	4.2	105010.9	105.0	120586.4	120.6	102.6
BT_06C_100%_P1B	BT	0.6	100%	1529.3	3729.9	3.7	0.037	3.7	100832.8	100.8	136668.9	136.7	84.8
BT_06C_100%_P2A	BT	0.6	100%	1578.1	3965.0	4.0	0.081	8.1	49076.0	49.1	109587.2	109.6	238.9
BT_06C_100%_P2B	BT	0.6	100%	1726.9	4362.6	4.4	0.031	3.1	138915.6	138.9	162390.4	162.4	77.5
BT_06C_100%_P3A	BT	0.6	100%	1722.4	4349.6	4.3	0.063	6.3	69125.1	69.1	90894.5	90.9	164.9
BT_06C_100%_P3B	BT	0.6	100%	1604.4	4051.6	4.1	0.032	3.2	128617.9	128.6	153834.6	153.8	72.7
BT_06C_100%_P4A	BT	0.6	100%	2056.7	5168.5	5.2	0.059	5.9	87368.7	87.4	98539.6	98.5	168.6
BT_06C_100%_P4B	BT	0.6	100%	1810.0	4480.3	4.5	0.042	4.2	105652.9	105.7	123696.2	123.7	107.1
BT_06C_100%_P5A	BT	0.6	100%	1543.6	3937.9	3.9	0.039	3.9	101891.0	101.9	119388.4	119.4	86.5
BT_06C_100%_P5B	BT	0.6	100%	1619.1	4130.4	4.1	0.040	4.0	102589.2	102.6	132138.4	132.1	104.8

ID	Material	l/s	AS	F_{max} [N]	σ_{max} [kPa]	σ_{max} [MPa]	$\varepsilon_{(\sigma max)}$ [mm/mm]	$\varepsilon_{(\sigma max)}$ [%]	E_{sec} [kPa]	E_{sec} [MPa]	E_{tan} [kPa]	E_{tan} [MPa]	T [kPa*mm/mm]
NA_06C_100%_P1A	NA	0.6	100%	1368.7	4002.1	4.0	0.047	4.7	84328.6	84.3	97709.9	97.7	106.4
NA_06C_100%_P1B	NA	0.6	100%	1904.1	5424.9	5.4	0.045	4.5	119760.8	119.8	142694.3	142.7	137.1
NA_06C_100%_P2A	NA	0.6	100%	1369.8	4081.4	4.1	0.049	4.9	83637.9	83.6	95407.7	95.4	111.1
NA_06C_100%_P2B	NA	0.6	100%	1426.3	4241.2	4.2	0.055	5.5	77038.0	77.0	82845.5	82.8	128.0
NA_06C_100%_P3A	NA	0.6	100%	1319.7	3887.2	3.9	0.076	7.6	51184.4	51.2	59522.9	59.5	167.8
NA_06C_100%_P3B	NA	0.6	100%	1294.2	3635.3	3.6	0.053	5.3	68230.9	68.2	73148.1	73.1	103.8
NA_06C_100%_P4A	NA	0.6	100%	836.3	2487.7	2.5	0.039	3.9	64491.3	64.5	71996.5	72.0	52.7
NA_06C_100%_P4B	NA	0.6	100%	894.5	2644.8	2.6	0.042	4.2	62421.4	62.4	84091.5	84.1	67.3
NA_06C_100%_P5A	NA	0.6	100%	973.1	2943.3	2.9	0.036	3.6	82750.2	82.8	110282.0	110.3	63.3
NA_06C_100%_P5B	NA	0.6	100%	921.9	2772.7	2.8	0.080	8.0	34693.4	34.7	38650.4	38.7	121.2
UND_06C_100%_P1A	UND	0.6	100%	795.4	1753.4	1.8	0.048	4.8	36631.6	36.6	52751.0	52.8	51.8
UND_06C_100%_P1B	UND	0.6	100%	826.4	1901.0	1.9	0.037	3.7	51409.2	51.4	71481.9	71.5	44.1
UND_06C_100%_P2A	UND	0.6	100%	835.4	1931.0	1.9	0.039	3.9	49210.1	49.2	68157.0	68.2	47.4
UND_06C_100%_P2B	UND	0.6	100%	875.8	2034.2	2.0	0.045	4.5	45365.4	45.4	61185.6	61.2	55.9
UND_06C_100%_P3A	UND	0.6	100%	822.4	1891.8	1.9	0.038	3.8	50206.5	50.2	67137.0	67.1	44.3
UND_06C_100%_P3B	UND	0.6	100%	859.4	1977.0	2.0	0.039	3.9	51154.4	51.2	68240.7	68.2	46.7
UND_06C_100%_P4A	UND	0.6	100%	882.4	2039.6	2.0	0.037	3.7	54563.7	54.6	78489.2	78.5	49.0
UND_06C_100%_P4B	UND	0.6	100%	896.0	2071.0	2.1	0.040	4.0	51796.2	51.8	76106.6	76.1	135.8
UND_06C_100%_P5A	UND	0.6	100%	798.3	1818.9	1.8	0.048	4.8	37826.6	37.8	64303.3	64.3	58.8
UND_06C_100%_P5B	UND	0.6	100%	830.7	1929.7	1.9	0.045	4.5	42688.2	42.7	50826.1	50.8	50.0
UND2_06C_100%_P1A	UND2	0.6	100%	787.6	1920.7	1.9	0.050	5.0	38603.6	38.6	49916.6	49.9	57.3
UND2_06C_100%_P1B	UND2	0.6	100%	819.8	2019.1	2.0	0.045	4.5	44433.9	44.4	64835.5	64.8	59.0
UND2_06C_100%_P2A	UND2	0.6	100%	802.2	2046.8	2.0	0.049	4.9	42089.3	42.1	66485.2	66.5	66.3
UND2_06C_100%_P2B	UND2	0.6	100%	748.9	1950.4	2.0	0.041	4.1	47903.4	47.9	75769.7	75.8	52.4
UND2_06C_100%_P3A	UND2	0.6	100%	739.0	1768.0	1.8	0.040	4.0	43931.9	43.9	63756.2	63.8	44.4
UND2_06C_100%_P3B	UND2	0.6	100%	744.3	1797.8	1.8	0.043	4.3	41656.1	41.7	62614.8	62.6	48.6
UND2_06C_100%_P4A	UND2	0.6	100%	779.5	1901.1	1.9	0.043	4.3	43902.1	43.9	61783.0	61.8	50.9
UND2_06C_100%_P4B	UND2	0.6	100%	762.6	1860.0	1.9	0.042	4.2	44666.4	44.7	62118.9	62.1	48.4
UND2_06C_100%_P5A	UND2	0.6	100%	760.7	1901.8	1.9	0.040	4.0	47947.6	47.9	77425.3	77.4	49.4
UND2_06C_100%_P5B	UND2	0.6	100%	759.8	1899.6	1.9	0.045	4.5	42607.8	42.6	57142.1	57.1	51.7

ID	Material	l/s	AS	F_{max} [N]	σ_{max} [kPa]	σ_{max} [MPa]	$\varepsilon_{(\sigma max)}$ [mm/mm]	$\varepsilon_{(\sigma max)}$ [%]	E_{sec} [kPa]	E_{sec} [MPa]	E_{tan} [kPa]	E_{tan} [MPa]	T [kPa*mm/mm]
RC_06C_75%_P1A	RC	0.6	75%	2221.4	5789.9	5.8	0.019	1.9	297088.2	297.1	359981.1	360.0	113.1
RC_06C_75%_P1B	RC	0.6	75%	2243.7	5848.1	5.8	0.022	2.2	264204.6	264.2	365783.6	365.8	80.5
RC_06C_75%_P2A	RC	0.6	75%	2022.2	5188.3	5.2	0.028	2.8	184474.1	184.5	221532.4	221.5	84.8
RC_06C_75%_P2B	RC	0.6	75%	2114.5	5421.7	5.4	0.025	2.5	212880.3	212.9	260038.3	260.0	81.1
RC_06C_75%_P3A	RC	0.6	75%	2129.2	5350.0	5.4	0.020	2.0	267068.7	267.1	300763.9	300.8	58.9
RC_06C_75%_P3B	RC	0.6	75%	2161.5	5458.7	5.5	0.021	2.1	257091.0	257.1	337772.6	337.8	71.8
RC_06C_75%_P4A	RC	0.6	75%	2120.2	5248.1	5.2	0.023	2.3	226007.4	226.0	257151.2	257.2	68.0
RC_06C_75%_P4B	RC	0.6	75%	2090.8	5360.9	5.4	0.026	2.6	209079.1	209.1	262934.7	262.9	80.6
RC_06C_75%_P5A	RC	0.6	75%	-	-	-	-	-	-	-	-	-	-
RC_06C_75%_P5B	RC	0.6	75%	-	-	-	-	-	-	-	-	-	-
RA_06C_75%_P1A	RA	0.6	75%	872.6	2592.4	2.6	0.054	5.4	48259.0	48.3	81055.8	81.1	93.3
RA_06C_75%_P1B	RA	0.6	75%	858.3	2655.7	2.7	0.061	6.1	43350.4	43.4	67713.5	67.7	105.2
RA_06C_75%_P2A	RA	0.6	75%	657.8	1981.5	2.0	0.075	7.5	26508.0	26.5	37976.0	38.0	89.0
RA_06C_75%_P2B	RA	0.6	75%	669.0	2015.0	2.0	0.067	6.7	29961.5	30.0	46873.4	46.9	86.5
RA_06C_75%_P3A	RA	0.6	75%	759.8	2295.9	2.3	0.064	6.4	35991.5	36.0	55233.5	55.2	95.8
RA_06C_75%_P3B	RA	0.6	75%	771.9	2346.4	2.3	0.051	5.1	45917.5	45.9	52071.3	52.1	66.7
RA_06C_75%_P4A	RA	0.6	75%	741.0	2205.4	2.2	0.072	7.2	30657.8	30.7	43243.1	43.2	96.7
RA_06C_75%_P4B	RA	0.6	75%	681.0	2076.3	2.1	0.090	9.0	23129.2	23.1	25972.2	26.0	102.1
RA_06C_75%_P5A	RA	0.6	75%	708.4	2213.7	2.2	0.059	5.9	37518.9	37.5	54539.1	54.5	82.1
RA_06C_75%_P5B	RA	0.6	75%	764.7	2460.1	2.5	0.061	6.1	40312.0	40.3	59401.9	59.4	95.2
BT_06C_75%_P1A	BT	0.6	75%	1046.3	2604.8	2.6	0.038	3.8	68499.3	68.5	80259.0	80.3	56.1
BT_06C_75%_P1B	BT	0.6	75%	850.8	2199.2	2.2	0.074	7.4	29709.7	29.7	35995.2	36.0	110.5
BT_06C_75%_P2A	BT	0.6	75%	892.8	2224.1	2.2	0.045	4.5	49921.8	49.9	60585.5	60.6	57.0
BT_06C_75%_P2B	BT	0.6	75%	670.7	1703.6	1.7	0.065	6.5	26245.0	26.2	32000.2	32.0	638.4
BT_06C_75%_P3A	BT	0.6	75%	810.9	2223.4	2.2	0.046	4.6	47837.7	47.8	59385.9	59.4	60.0
BT_06C_75%_P3B	BT	0.6	75%	778.2	2112.0	2.1	0.050	5.0	42231.8	42.2	47278.9	47.3	57.5
BT_06C_75%_P4A	BT	0.6	75%	919.4	2511.5	2.5	0.047	4.7	52937.2	52.9	63232.3	63.2	68.3
BT_06C_75%_P4B	BT	0.6	75%	946.4	2585.2	2.6	0.048	4.8	54062.0	54.1	68585.7	68.6	72.7
BT_06C_75%_P5A	BT	0.6	75%	737.5	2048.5	2.0	0.044	4.4	46382.3	46.4	76931.7	76.9	59.7
BT_06C_75%_P5B	BT	0.6	75%	788.2	2000.6	2.0	0.063	6.3	31913.7	31.9	40482.2	40.5	73.6

ID	Material	l/s	AS	F_{max} [N]	σ_{max} [kPa]	σ_{max} [MPa]	$\varepsilon_{(\sigma max)}$ [mm/mm]	$\varepsilon_{(\sigma max)}$ [%]	E_{sec} [kPa]	E_{sec} [MPa]	E_{tan} [kPa]	E_{tan} [MPa]	T [kPa*mm/mm]
NA_06C_75%_P1A	NA	0.6	75%	268.9	783.0	0.8	0.075	7.5	10452.0	10.5	60613.1	60.6	39.0
NA_06C_75%_P1B	NA	0.6	75%	942.9	2678.6	2.7	0.087	8.7	30845.8	30.8	68573.2	68.6	155.5
NA_06C_75%_P2A	NA	0.6	75%	828.1	2419.4	2.4	0.058	5.8	41743.5	41.7	58525.0	58.5	86.7
NA_06C_75%_P2B	NA	0.6	75%	856.1	2517.8	2.5	0.054	5.4	46234.1	46.2	77419.3	77.4	89.0
NA_06C_75%_P3A	NA	0.6	75%	803.7	2328.9	2.3	0.049	4.9	47479.8	47.5	64483.6	64.5	68.3
NA_06C_75%_P3B	NA	0.6	75%	883.1	2558.8	2.6	0.053	5.3	48646.3	48.6	57093.2	57.1	76.5
NA_06C_75%_P4A	NA	0.6	75%	1340.6	3852.2	3.9	0.031	3.1	123599.0	123.6	214287.0	214.3	80.5
NA_06C_75%_P4B	NA	0.6	75%	1163.9	3344.5	3.3	0.037	3.7	91005.5	91.0	153842.1	153.8	81.2
NA_06C_75%_P5A	NA	0.6	75%	856.6	2470.0	2.5	0.049	4.9	49972.4	50.0	76497.1	76.5	77.7
NA_06C_75%_P5B	NA	0.6	75%	889.4	2564.5	2.6	0.047	4.7	54828.2	54.8	83263.6	83.3	75.1
UND_06C_75%_P1A	UND	0.6	75%	1703.7	4527.0	4.5	0.033	3.3	137219.7	137.2	172070.8	172.1	88.0
UND_06C_75%_P1B	UND	0.6	75%	1861.3	4971.2	5.0	0.036	3.6	136360.4	136.4	154493.8	154.5	100.7
UND_06C_75%_P2A	UND	0.6	75%	1781.8	4884.4	4.9	0.036	3.6	134395.7	134.4	186812.0	186.8	119.4
UND_06C_75%_P2B	UND	0.6	75%	1772.6	4758.7	4.8	0.037	3.7	128656.1	128.7	151707.3	151.7	102.9
UND_06C_75%_P3A	UND	0.6	75%	1659.2	4501.3	4.5	0.043	4.3	104832.7	104.8	157244.0	157.2	125.5
UND_06C_75%_P3B	UND	0.6	75%	1809.0	4882.5	4.9	0.035	3.5	138319.3	138.3	171688.3	171.7	94.1
UND_06C_75%_P4A	UND	0.6	75%	1783.0	4713.4	4.7	0.033	3.3	142790.4	142.8	166107.4	166.1	88.2
UND_06C_75%_P4B	UND	0.6	75%	1754.4	4590.4	4.6	0.030	3.0	153101.9	153.1	177112.0	177.1	77.6
UND_06C_75%_P5A	UND	0.6	75%	2011.7	5634.2	5.6	0.038	3.8	149976.7	150.0	180490.6	180.5	121.0
UND_06C_75%_P5B	UND	0.6	75%	1998.1	5596.2	5.6	0.032	3.2	175638.9	175.6	190280.8	190.3	96.2
UND2_06C_75%_P1A	UND2	0.6	75%	1120.8	3247.2	3.2	0.032	3.2	100323.5	100.3	118574.8	118.6	60.1
UND2_06C_75%_P1B	UND2	0.6	75%	1137.8	3296.5	3.3	0.021	2.1	154268.8	154.3	216638.2	216.6	44.2
UND2_06C_75%_P2A	UND2	0.6	75%	1002.5	2827.0	2.8	0.032	3.2	88059.3	88.1	171349.6	171.3	67.4
UND2_06C_75%_P2B	UND2	0.6	75%	1041.4	2936.8	2.9	0.026	2.6	112216.1	112.2	148972.4	149.0	47.0
UND2_06C_75%_P3A	UND2	0.6	75%	1057.3	2904.8	2.9	0.034	3.4	85230.7	85.2	115399.6	115.4	61.1
UND2_06C_75%_P3B	UND2	0.6	75%	1076.3	2956.9	3.0	0.025	2.5	117103.4	117.1	173909.3	173.9	48.3
UND2_06C_75%_P4A	UND2	0.6	75%	1117.2	3130.6	3.1	0.025	2.5	126160.9	126.2	173763.5	173.8	48.4
UND2_06C_75%_P4B	UND2	0.6	75%	1136.8	3151.1	3.2	0.026	2.6	122619.7	122.6	170381.4	170.4	49.0
UND2_06C_75%_P5A	UND2	0.6	75%	1236.6	3713.6	3.7	0.027	2.7	136961.6	137.0	198296.5	198.3	62.7
UND2_06C_75%_P5B	UND2	0.6	75%	1274.3	3765.7	3.8	0.022	2.2	174098.0	174.1	248872.5	248.9	51.7

ID	Material	l/s	AS	F_{max} [N]	σ_{max} [kPa]	σ_{max} [MPa]	$\varepsilon_{(\sigma max)}$ [mm/mm]	$\varepsilon_{(\sigma max)}$ [%]	E_{sec} [kPa]	E_{sec} [MPa]	E_{tan} [kPa]	E_{tan} [MPa]	T [kPa*mm/mm]
RC_06C_50%_P1A	RC	0.6	50%	134.2	335.8	0.3	0.024	2.4	14162.5	14.2	22577.7	22.6	5.3
RC_06C_50%_P1B	RC	0.6	50%	103.6	263.1	0.3	0.054	5.4	4879.7	4.9	7650.8	7.7	9.4
RC_06C_50%_P2A	RC	0.6	50%	130.6	343.8	0.3	0.020	2.0	16910.0	16.9	20690.2	20.7	4.2
RC_06C_50%_P2B	RC	0.6	50%	131.8	343.1	0.3	0.028	2.8	12475.7	12.5	14283.9	14.3	5.3
RC_06C_50%_P3A	RC	0.6	50%	128.1	335.1	0.3	0.021	2.1	16336.7	16.3	22496.2	22.5	4.3
RC_06C_50%_P3B	RC	0.6	50%	140.1	366.5	0.4	0.026	2.6	14014.3	14.0	16719.3	16.7	5.5
RC_06C_50%_P4A	RC	0.6	50%	100.0	257.8	0.3	0.030	3.0	8716.8	8.7	12503.1	12.5	4.9
RC_06C_50%_P4B	RC	0.6	50%	119.4	294.0	0.3	0.023	2.3	13022.8	13.0	16459.8	16.5	4.1
RC_06C_50%_P5A	RC	0.6	50%	111.7	301.5	0.3	0.032	3.2	9499.9	9.5	17287.3	17.3	7.0
RC_06C_50%_P5B	RC	0.6	50%	106.4	291.8	0.3	0.027	2.7	10979.4	11.0	11402.2	11.4	4.0
RA_06C_50%_P1A	RA	0.6	50%	207.3	556.9	0.6	0.024	2.4	23216.3	23.2	27660.4	27.7	7.7
RA_06C_50%_P1B	RA	0.6	50%	128.7	338.4	0.3	0.053	5.3	6446.5	6.4	13161.9	13.2	12.5
RA_06C_50%_P2A	RA	0.6	50%	226.3	598.7	0.6	0.033	3.3	18073.1	18.1	31210.3	31.2	12.9
RA_06C_50%_P2B	RA	0.6	50%	222.3	569.9	0.6	0.029	2.9	19788.1	19.8	22076.9	22.1	9.0
RA_06C_50%_P3A	RA	0.6	50%	215.0	571.4	0.6	0.022	2.2	25578.9	25.6	31377.6	31.4	7.3
RA_06C_50%_P3B	RA	0.6	50%	176.6	477.0	0.5	0.023	2.3	20428.8	20.4	26093.5	26.1	6.6
RA_06C_50%_P4A	RA	0.6	50%	-	-	-	-	-	-	-	-	-	-
RA_06C_50%_P4B	RA	0.6	50%	-	-	-	-	-	-	-	-	-	-
RA_06C_50%_P5A	RA	0.6	50%	-	-	-	-	-	-	-	-	-	-
RA_06C_50%_P5B	RA	0.6	50%	-	-	-	-	-	-	-	-	-	-
BT_06C_50%_P1A	BT	0.6	50%	276.7	729.2	0.7	0.017	1.7	43222.1	43.2	56923.8	56.9	7.4
BT_06C_50%_P1B	BT	0.6	50%	292.5	779.4	0.8	0.025	2.5	31481.2	31.5	71991.3	72.0	14.3
BT_06C_50%_P2A	BT	0.6	50%	812.9	2276.8	2.3	0.020	2.0	116657.8	116.7	144752.7	144.8	26.0
BT_06C_50%_P2B	BT	0.6	50%	863.9	2394.6	2.4	0.026	2.6	92729.7	92.7	176593.2	176.6	42.7
BT_06C_50%_P3A	BT	0.6	50%	514.0	1381.1	1.4	0.041	4.1	33726.8	33.7	113810.1	113.8	45.7
BT_06C_50%_P3B	BT	0.6	50%	603.2	1647.4	1.6	0.023	2.3	71653.1	71.7	154072.5	154.1	27.5
BT_06C_50%_P4A	BT	0.6	50%	188.7	487.5	0.5	0.032	3.2	15255.3	15.3	36548.2	36.5	11.8
BT_06C_50%_P4B	BT	0.6	50%	-	-	-	-	-	-	-	-	-	-
BT_06C_50%_P5A	BT	0.6	50%	-	-	-	-	-	-	-	-	-	-
BT_06C_50%_P5B	BT	0.6	50%	355.3	936.0	0.9	0.031	3.1	29763.0	29.8	57975.6	58.0	20.1

ID	Material	l/s	AS	F_{max} [N]	σ_{max} [kPa]	σ_{max} [MPa]	$\varepsilon_{(\sigma max)}$ [mm/mm]	$\varepsilon_{(\sigma max)}$ [%]	E_{sec} [kPa]	E_{sec} [MPa]	E_{tan} [kPa]	E_{tan} [MPa]	T [kPa*mm/mm]
NA_06C_50%_P1A	NA	0.6	50%	131.8	394.1	0.4	0.035	3.5	11270.4	11.3	15548.2	15.5	8.5
NA_06C_50%_P1B	NA	0.6	50%	170.6	510.3	0.5	0.032	3.2	15851.4	15.9	27141.8	27.1	11.7
NA_06C_50%_P2A	NA	0.6	50%	115.6	337.6	0.3	0.030	3.0	11327.4	11.3	16967.5	17.0	6.6
NA_06C_50%_P2B	NA	0.6	50%	118.5	342.4	0.3	0.022	2.2	15558.8	15.6	27257.2	27.3	5.2
NA_06C_50%_P3A	NA	0.6	50%	107.6	303.8	0.3	0.039	3.9	7770.8	7.8	8658.6	8.7	6.5
NA_06C_50%_P3B	NA	0.6	50%	121.0	342.6	0.3	0.024	2.4	14487.8	14.5	25358.3	25.4	5.5
NA_06C_50%_P4A	NA	0.6	50%	108.9	301.7	0.3	0.038	3.8	7880.7	7.9	10791.0	10.8	7.1
NA_06C_50%_P4B	NA	0.6	50%	122.7	336.2	0.3	0.054	5.4	6193.7	6.2	6974.5	7.0	10.1
NA_06C_50%_P5A	NA	0.6	50%	158.8	457.6	0.5	0.037	3.7	12481.1	12.5	16251.0	16.3	10.2
NA_06C_50%_P5B	NA	0.6	50%	154.9	446.9	0.4	0.031	3.1	14313.7	14.3	20920.7	20.9	9.0
UND_06C_50%_P1A	UND	0.6	50%	205.7	579.1	0.6	0.036	3.6	16043.2	16.0	26717.0	26.7	14.3
UND_06C_50%_P1B	UND	0.6	50%	253.4	705.7	0.7	0.033	3.3	21398.3	21.4	36582.5	36.6	15.8
UND_06C_50%_P2A	UND	0.6	50%	178.8	458.5	0.5	0.032	3.2	14514.1	14.5	18749.9	18.7	9.0
UND_06C_50%_P2B	UND	0.6	50%	185.8	476.3	0.5	0.028	2.8	17073.3	17.1	26834.8	26.8	9.1
UND_06C_50%_P3A	UND	0.6	50%	170.2	436.4	0.4	0.022	2.2	19725.1	19.7	29269.6	29.3	6.3
UND_06C_50%_P3B	UND	0.6	50%	174.1	446.4	0.4	0.021	2.1	21029.1	21.0	29630.3	29.6	6.1
UND_06C_50%_P4A	UND	0.6	50%	179.1	473.6	0.5	0.041	4.1	11415.1	11.4	17660.9	17.7	13.1
UND_06C_50%_P4B	UND	0.6	50%	148.7	389.2	0.4	0.044	4.4	8884.3	8.9	10118.4	10.1	9.5
UND_06C_50%_P5A	UND	0.6	50%	255.4	658.3	0.7	0.026	2.6	25653.8	25.7	35996.9	36.0	10.6
UND_06C_50%_P5B	UND	0.6	50%	240.1	609.5	0.6	0.023	2.3	26808.4	26.8	33429.0	33.4	8.2
UND2_06C_50%_P1A	UND2	0.6	50%	170.2	497.4	0.5	0.015	1.5	33436.5	33.4	43757.2	43.8	4.4
UND2_06C_50%_P1B	UND2	0.6	50%	200.2	584.9	0.6	0.020	2.0	29403.6	29.4	30997.7	31.0	6.0
UND2_06C_50%_P2A	UND2	0.6	50%	177.1	488.1	0.5	0.041	4.1	11787.8	11.8	37547.4	37.5	15.4
UND2_06C_50%_P2B	UND2	0.6	50%	194.4	535.9	0.5	0.027	2.7	19805.1	19.8	54152.7	54.2	10.5
UND2_06C_50%_P3A	UND2	0.6	50%	160.4	424.7	0.4	0.012	1.2	36342.7	36.3	42480.4	42.5	2.8
UND2_06C_50%_P3B	UND2	0.6	50%	225.9	598.2	0.6	0.027	2.7	21947.2	21.9	45128.1	45.1	10.6
UND2_06C_50%_P4A	UND2	0.6	50%	220.3	579.7	0.6	0.025	2.5	23030.4	23.0	23992.8	24.0	7.5
UND2_06C_50%_P4B	UND2	0.6	50%	342.3	910.3	0.9	0.018	1.8	49875.2	49.9	57136.9	57.1	9.3
UND2_06C_50%_P5A	UND2	0.6	50%	-	-	-	-	-	-	-	-	-	-
UND2_06C_50%_P5B	UND2	0.6	50%	-	-	-	-	-	-	-	-	-	-

ID	Material	l/s	AS	F_{max} [N]	σ_{max} [kPa]	σ_{max} [MPa]	$\varepsilon_{(\sigma max)}$ [mm/mm]	$\varepsilon_{(\sigma max)}$ [%]	E_{sec} [kPa]	E_{sec} [MPa]	E_{tan} [kPa]	E_{tan} [MPa]	T [kPa*mm/mm]
RC_05C_100%_P1A	RC	0.5	100%	7383.2	18286.2	18.3	0.027	2.7	681939.8	681.9	775390.5	775.4	273.6
RC_05C_100%_P1B	RC	0.5	100%	6611.4	16053.4	16.1	0.020	2.0	808112.8	808.1	833652.1	833.7	163.1
RC_05C_100%_P2A	RC	0.5	100%	6165.4	14298.2	14.3	0.021	2.1	665487.2	665.5	775345.7	775.3	172.5
RC_05C_100%_P2B	RC	0.5	100%	6920.9	15888.2	15.9	0.026	2.6	605012.1	605.0	660028.2	660.0	228.4
RC_50C_100%_P3A	RC	0.5	100%	6971.5	16250.6	16.3	0.023	2.3	709424.0	709.4	882994.1	883.0	211.3
RC_05C_100%_P3B	RC	0.5	100%	7201.4	16700.8	16.7	0.023	2.3	716320.7	716.3	794656.8	794.7	212.6
RC_05C_100%_P4A	RC	0.5	100%	6239.3	14669.6	14.7	0.027	2.7	552879.1	552.9	758498.1	758.5	241.3
RC_05C_100%_P4B	RC	0.5	100%	6767.0	15910.3	15.9	0.025	2.5	629962.6	630.0	810942.3	810.9	236.1
RC_05C_100%_P5A	RC	0.5	100%	6352.1	14731.3	14.7	0.020	2.0	721856.7	721.9	784019.4	784.0	161.1
RC_05C_100%_P5B	RC	0.5	100%	6770.1	15700.5	15.7	0.025	2.5	628051.3	628.1	705648.1	705.6	216.4
RA_05C_100%_P1A	RA	0.5	100%	434.3	1128.7	1.1	0.110	11.0	10237.1	10.2	12116.6	12.1	70.5
RA_05C_100%_P1B	RA	0.5	100%	433.7	1132.5	1.1	0.114	11.4	9912.3	9.9	11662.2	11.7	73.1
RA_05C_100%_P2A	RA	0.5	100%	486.5	1242.5	1.2	0.099	9.9	12516.8	12.5	15618.9	15.6	72.2
RA_05C_100%_P2B	RA	0.5	100%	532.8	1396.6	1.4	0.096	9.6	14473.8	14.5	18266.8	18.3	79.9
RA_05C_100%_P3A	RA	0.5	100%	516.0	1410.6	1.4	0.091	9.1	15479.9	15.5	19296.6	19.3	74.3
RA_05C_100%_P3B	RA	0.5	100%	518.4	1424.1	1.4	0.098	9.8	14495.0	14.5	17978.1	18.0	80.9
RA_05C_100%_P4A	RA	0.5	100%	503.0	1337.7	1.3	0.100	10.0	13444.2	13.4	16107.4	16.1	76.6
RA_05C_100%_P4B	RA	0.5	100%	492.6	1310.1	1.3	0.100	10.0	13035.4	13.0	15384.3	15.4	74.6
RA_05C_100%_P5A	RA	0.5	100%	509.1	1441.4	1.4	0.102	10.2	14133.1	14.1	17282.6	17.3	84.9
RA_05C_100%_P5B	RA	0.5	100%	502.8	1423.7	1.4	0.117	11.7	12184.8	12.2	15649.0	15.6	98.5
BT_05C_100%_P1A	BT	0.5	100%	1959.0	4509.5	4.5	0.054	5.4	84156.5	84.2	110059.6	110.1	143.6
BT_05C_100%_P1B	BT	0.5	100%	1801.1	4205.0	4.2	0.053	5.3	79221.6	79.2	93332.5	93.3	126.2
BT_05C_100%_P2A	BT	0.5	100%	3313.8	7815.6	7.8	0.038	3.8	204319.9	204.3	279059.1	279.1	181.8
BT_05C_100%_P2B	BT	0.5	100%	2988.1	7080.7	7.1	0.044	4.4	161865.6	161.9	206950.6	207.0	183.9
BT_05C_100%_P3A	BT	0.5	100%	2247.7	5325.0	5.3	0.047	4.7	114370.2	114.4	159726.4	159.7	154.9
BT_05C_100%_P3B	BT	0.5	100%	1780.5	4197.4	4.2	0.042	4.2	99614.1	99.6	158058.2	158.1	117.3
BT_05C_100%_P4A	BT	0.5	100%	2434.5	5714.8	5.7	0.040	4.0	142869.0	142.9	200012.1	200.0	136.8
BT_05C_100%_P4B	BT	0.5	100%	2165.9	5084.3	5.1	0.040	4.0	126714.4	126.7	167849.7	167.8	121.4
BT_05C_100%_P5A	BT	0.5	100%	1871.2	4433.1	4.4	0.045	4.5	98644.5	98.6	167533.8	167.5	131.4
BT_05C_100%_P5B	BT	0.5	100%	1759.6	4168.8	4.2	0.046	4.6	90048.6	90.0	121413.3	121.4	119.7

ID	Material	l/s	AS	F_{max} [N]	σ_{max} [kPa]	σ_{max} [MPa]	$\varepsilon_{(\sigma max)}$ [mm/mm]	$\varepsilon_{(\sigma max)}$ [%]	E_{sec} [kPa]	E_{sec} [MPa]	E_{tan} [kPa]	E_{tan} [MPa]	T [kPa*mm/mm]
NA_05C_100%_P1A	NA	0.5	100%	838.1	2172.8	2.2	0.050	5.0	43531.0	43.5	66268.2	66.3	69.5
NA_05C_100%_P1B	NA	0.5	100%	827.3	2155.6	2.2	0.041	4.1	51953.8	52.0	78081.4	78.1	55.7
NA_05C_100%_P2A	NA	0.5	100%	845.4	2156.6	2.2	0.055	5.5	38898.8	38.9	59403.9	59.4	76.0
NA_05C_100%_P2B	NA	0.5	100%	765.3	1982.6	2.0	0.048	4.8	40924.0	40.9	52159.2	52.2	57.1
NA_05C_100%_P3A	NA	0.5	100%	730.7	1826.7	1.8	0.052	5.2	34925.3	34.9	49658.1	49.7	58.9
NA_05C_100%_P3B	NA	0.5	100%	711.1	1752.0	1.8	0.052	5.2	34010.3	34.0	44005.7	44.0	54.0
NA_05C_100%_P4A	NA	0.5	100%	769.8	1924.4	1.9	0.054	5.4	35760.1	35.8	57429.7	57.4	67.8
NA_05C_100%_P4B	NA	0.5	100%	724.3	1801.7	1.8	0.063	6.3	28809.9	28.8	45854.0	45.9	77.1
NA_05C_100%_P5A	NA	0.5	100%	857.5	2188.2	2.2	0.059	5.9	37147.1	37.1	54556.2	54.6	80.7
NA_05C_100%_P5B	NA	0.5	100%	832.4	2124.1	2.1	0.050	5.0	42265.2	42.3	66904.7	66.9	68.5
UND_05C_100%_P1A	UND	0.5	100%	2598.9	6445.7	6.4	0.028	2.8	231339.0	231.3	360084.0	360.1	38.2
UND_05C_100%_P1B	UND	0.5	100%	2917.9	7131.4	7.1	0.024	2.4	291822.0	291.8	406360.0	406.4	107.9
UND_05C_100%_P2A	UND	0.5	100%	2784.3	6891.8	6.9	0.024	2.4	286657.5	286.7	350364.7	350.4	95.6
UND_05C_100%_P2B	UND	0.5	100%	2666.0	6599.0	6.6	0.026	2.6	249272.0	249.3	313038.5	313.0	101.7
UND_05C_100%_P3A	UND	0.5	100%	2543.7	6360.6	6.4	0.022	2.2	295593.9	295.6	385439.6	385.4	82.2
UND_05C_100%_P3B	UND	0.5	100%	2685.0	6714.0	6.7	0.021	2.1	317446.4	317.4	407585.3	407.6	84.7
UND_05C_100%_P4A	UND	0.5	100%	3058.4	8017.3	8.0	0.023	2.3	351369.1	351.4	498663.6	498.7	115.1
UND_05C_100%_P4B	UND	0.5	100%	3020.6	7876.0	7.9	0.023	2.3	335262.0	335.3	433862.7	433.9	111.2
UND_05C_100%_P5A	UND	0.5	100%	2484.6	6157.2	6.2	0.027	2.7	224680.9	224.7	298488.3	298.5	100.9
UND_05C_100%_P5B	UND	0.5	100%	2643.5	6551.1	6.6	0.022	2.2	295565.0	295.6	363771.8	363.8	85.0
UND2_05C_100%_P1A	UND2	0.5	100%	3355.2	8603.1	8.6	0.029	2.9	292449.1	292.4	387072.8	387.1	154.4
UND2_05C_100%_P1B	UND2	0.5	100%	3634.6	9272.0	9.3	0.031	3.1	299629.8	299.6	341232.1	341.2	160.0
UND2_05C_100%_P2A	UND2	0.5	100%	3118.6	7763.5	7.8	0.023	2.3	332113.2	332.1	400006.3	400.0	104.9
UND2_05C_100%_P2B	UND2	0.5	100%	2947.2	7374.6	7.4	0.038	3.8	192253.3	192.3	321117.2	321.1	191.2
UND2_05C_100%_P3A	UND2	0.5	100%	3409.7	8612.1	8.6	0.028	2.8	311640.9	311.6	392030.3	392.0	141.9
UND2_05C_100%_P3B	UND2	0.5	100%	3153.7	8004.3	8.0	0.025	2.5	323153.5	323.2	366480.7	366.5	109.6
UND2_05C_100%_P4A	UND2	0.5	100%	3244.3	8576.4	8.6	0.026	2.6	333952.0	334.0	391943.1	391.9	124.2
UND2_05C_100%_P4B	UND2	0.5	100%	3275.5	8570.6	8.6	0.024	2.4	351432.3	351.4	397305.6	397.3	115.8
UND2_05C_100%_P5A	UND2	0.5	100%	3460.6	9302.7	9.3	0.030	3.0	309538.9	309.5	432556.9	432.6	173.4
UND2_05C_100%_P5B	UND2	0.5	100%	3874.5	10359.6	10.4	0.028	2.8	368998.8	369.0	448803.0	448.8	167.9

ID	Material	l/s	AS	F_{max} [N]	σ_{max} [kPa]	σ_{max} [MPa]	$\varepsilon_{(\sigma max)}$ [mm/mm]	$\varepsilon_{(\sigma max)}$ [%]	E_{sec} [kPa]	E_{sec} [MPa]	E_{tan} [kPa]	E_{tan} [MPa]	T [kPa*mm/mm]
RC_05C_75%_P1A	RC	0.5	75%	2914.0	7077.5	7.1	0.025	2.5	286479.1	286.5	347624.5	347.6	100.2
RC_05C_75%_P1B	RC	0.5	75%	2493.4	6023.8	6.0	0.026	2.6	233781.1	233.8	328649.1	328.6	98.5
RC_05C_75%_P2A	RC	0.5	75%	2491.0	5936.5	5.9	0.021	2.1	277327.3	277.3	347576.5	347.6	73.9
RC_05C_75%_P2B	RC	0.5	75%	2534.3	6039.6	6.0	0.018	1.8	338365.8	338.4	429928.2	429.9	64.0
RC_50C_75%_P3A	RC	0.5	75%	2312.4	5643.4	5.6	0.023	2.3	243456.6	243.5	295513.1	295.5	75.1
RC_05C_75%_P3B	RC	0.5	75%	2526.1	6102.8	6.1	0.019	1.9	315450.9	315.5	418929.4	418.9	72.0
RC_05C_75%_P4A	RC	0.5	75%	2542.8	6177.9	6.2	0.019	1.9	321467.0	321.5	385540.9	385.5	126.6
RC_05C_75%_P4B	RC	0.5	75%	2374.9	5682.9	5.7	0.017	1.7	335915.5	335.9	418938.8	418.9	56.5
RC_05C_75%_P5A	RC	0.5	75%	2479.2	5906.3	5.9	0.023	2.3	258895.0	258.9	344268.6	344.3	77.9
RC_05C_75%_P5B	RC	0.5	75%	2683.1	6392.0	6.4	0.024	2.4	263592.1	263.6	296852.7	296.9	85.9
RA_05C_75%_P1A	RA	0.5	75%	259.6	735.9	0.7	0.111	11.1	6656.8	6.7	7506.2	7.5	44.8
RA_05C_75%_P1B	RA	0.5	75%	254.1	720.3	0.7	0.106	10.6	6787.3	6.8	7788.1	7.8	43.0
RA_05C_75%_P2A	RA	0.5	75%	266.6	752.0	0.8	0.103	10.3	7285.5	7.3	10017.0	10.0	47.4
RA_05C_75%_P2B	RA	0.5	75%	266.1	734.0	0.7	0.101	10.1	7302.3	7.3	8082.5	8.1	40.2
RA_05C_75%_P3A	RA	0.5	75%	264.0	752.0	0.8	0.098	9.8	7660.0	7.7	9643.5	9.6	42.2
RA_05C_75%_P3B	RA	0.5	75%	273.7	779.9	0.8	0.103	10.3	7568.9	7.6	8618.8	8.6	44.4
RA_05C_75%_P4A	RA	0.5	75%	285.9	806.3	0.8	0.104	10.4	7738.6	7.7	8534.1	8.5	45.6
RA_05C_75%_P4B	RA	0.5	75%	296.1	835.1	0.8	0.107	10.7	7830.7	7.8	8854.0	8.9	49.0
RA_05C_75%_P5A	RA	0.5	75%	250.3	714.6	0.7	0.111	11.1	6434.5	6.4	7393.1	7.4	44.6
RA_05C_75%_P5B	RA	0.5	75%	261.6	734.0	0.7	0.096	9.6	7652.7	7.7	8849.1	8.8	39.5
BT_05C_75%_P1A	BT	0.5	75%	725.1	1840.4	1.8	0.050	5.0	36604.7	36.6	69898.5	69.9	66.7
BT_05C_75%_P1B	BT	0.5	75%	770.0	1954.3	2.0	0.059	5.9	33030.6	33.0	84516.1	84.5	88.2
BT_05C_75%_P2A	BT	0.5	75%	762.0	1877.0	1.9	0.060	6.0	31081.5	31.1	79126.9	79.1	83.9
BT_05C_75%_P2B	BT	0.5	75%	744.3	1842.4	1.8	0.055	5.5	33295.1	33.3	85538.4	85.5	76.2
BT_05C_75%_P3A	BT	0.5	75%	726.3	1762.9	1.8	0.064	6.4	27566.4	27.6	50848.0	50.8	77.6
BT_05C_75%_P3B	BT	0.5	75%	718.4	1795.9	1.8	0.030	3.0	60086.2	60.1	94732.3	94.7	34.0
BT_05C_75%_P4A	BT	0.5	75%	705.0	1745.3	1.7	0.061	6.1	28703.0	28.7	58238.9	58.2	73.9
BT_05C_75%_P4B	BT	0.5	75%	705.7	1746.9	1.7	0.062	6.2	28023.3	28.0	80507.6	80.5	86.7
BT_05C_75%_P5A	BT	0.5	75%	657.6	1644.0	1.6	0.060	6.0	27183.4	27.2	53095.8	53.1	64.2
BT_05C_75%_P5B	BT	0.5	75%	726.9	1817.5	1.8	0.053	5.3	34490.4	34.5	65994.0	66.0	64.0

ID	Material	l/s	AS	F_{max} [N]	σ_{max} [kPa]	σ_{max} [MPa]	$\varepsilon_{(\sigma max)}$ [mm/mm]	$\varepsilon_{(\sigma max)}$ [%]	E_{sec} [kPa]	E_{sec} [MPa]	E_{tan} [kPa]	E_{tan} [MPa]	T [kPa*mm/mm]
NA_05C_75%_P1A	NA	0.5	75%	375.2	997.8	1.0	0.088	8.8	11399.9	11.4	12609.3	12.6	47.6
NA_05C_75%_P1B	NA	0.5	75%	388.3	1032.8	1.0	0.084	8.4	12307.5	12.3	13713.8	13.7	47.7
NA_05C_75%_P2A	NA	0.5	75%	399.8	1079.9	1.1	0.086	8.6	12626.9	12.6	13813.5	13.8	49.8
NA_05C_75%_P2B	NA	0.5	75%	383.8	1036.6	1.0	0.091	9.1	11402.0	11.4	13236.7	13.2	53.9
NA_05C_75%_P3A	NA	0.5	75%	410.4	1080.0	1.1	0.085	8.5	12705.6	12.7	14678.6	14.7	51.9
NA_05C_75%_P3B	NA	0.5	75%	398.0	1047.3	1.0	0.080	8.0	13076.7	13.1	14500.7	14.5	46.4
NA_05C_75%_P4A	NA	0.5	75%	383.2	1008.4	1.0	0.076	7.6	13219.5	13.2	14516.0	14.5	41.8
NA_05C_75%_P4B	NA	0.5	75%	418.2	1100.4	1.1	0.079	7.9	13848.8	13.8	15737.8	15.7	48.8
NA_05C_75%_P5A	NA	0.5	75%	-	-	-	-	-	-	-	-	-	-
NA_05C_75%_P5B	NA	0.5	75%	-	-	-	-	-	-	-	-	-	-
UND_05C_75%_P1A	UND	0.5	75%	1585.7	3907.4	3.9	0.030	3.0	131388.3	131.4	192181.6	192.2	75.3
UND_05C_75%_P1B	UND	0.5	75%	1513.0	3728.3	3.7	0.025	2.5	150153.6	150.2	216888.3	216.9	59.5
UND_05C_75%_P2A	UND	0.5	75%	1291.8	3049.8	3.0	0.021	2.1	145942.6	145.9	190623.5	190.6	38.8
UND_05C_75%_P2B	UND	0.5	75%	1355.7	3230.9	3.2	0.025	2.5	129445.8	129.4	164155.7	164.2	48.0
UND_05C_75%_P3A	UND	0.5	75%	1303.7	3092.4	3.1	0.022	2.2	140584.7	140.6	196984.7	197.0	43.1
UND_05C_75%_P3B	UND	0.5	75%	1303.3	3091.5	3.1	0.026	2.6	117314.3	117.3	157605.7	157.6	50.2
UND_05C_75%_P4A	UND	0.5	75%	1263.9	3041.7	3.0	0.024	2.4	128048.4	128.0	198180.8	198.2	49.0
UND_05C_75%_P4B	UND	0.5	75%	1283.5	3089.0	3.1	0.025	2.5	121497.1	121.5	154743.2	154.7	47.7
UND_05C_75%_P5A	UND	0.5	75%	1284.5	2992.5	3.0	0.021	2.1	139460.3	139.5	198185.7	198.2	41.0
UND_05C_75%_P5B	UND	0.5	75%	1313.3	3087.7	3.1	0.033	3.3	92689.2	92.7	125776.3	125.8	63.0
UND2_05C_75%_P1A	UND2	0.5	75%	3202.3	8689.0	8.7	0.030	3.0	287659.3	287.7	314510.9	314.5	142.0
UND2_05C_75%_P1B	UND2	0.5	75%	3242.9	8709.8	8.7	0.023	2.3	372479.2	372.5	488444.4	488.4	122.9
UND2_05C_75%_P2A	UND2	0.5	75%	2510.4	6845.9	6.8	0.031	3.1	220505.1	220.5	308764.4	308.8	132.4
UND2_05C_75%_P2B	UND2	0.5	75%	3173.6	8609.8	8.6	0.022	2.2	396638.3	396.6	491803.7	491.8	110.2
UND2_05C_75%_P3A	UND2	0.5	75%	2555.7	6793.5	6.8	0.034	3.4	201763.6	201.8	383215.9	383.2	181.6
UND2_05C_75%_P3B	UND2	0.5	75%	2670.8	7063.6	7.1	0.026	2.6	269034.8	269.0	329393.3	329.4	108.8
UND2_05C_75%_P4A	UND2	0.5	75%	3175.0	8888.6	8.9	0.030	3.0	294287.9	294.3	328847.8	328.8	147.5
UND2_05C_75%_P4B	UND2	0.5	75%	2993.9	8381.5	8.4	0.026	2.6	324994.0	325.0	393116.7	393.1	126.9
UND2_05C_75%_P5A	UND2	0.5	75%	2941.2	8548.9	8.5	0.030	3.0	285321.1	285.3	457571.3	457.6	167.0
UND2_05C_75%_P5B	UND2	0.5	75%	3044.8	8754.4	8.8	0.028	2.8	316793.0	316.8	422852.6	422.9	151.5

ID	Material	l/s	AS	F_{max} [N]	σ_{max} [kPa]	σ_{max} [MPa]	$\varepsilon_{(\sigma max)}$ [mm/mm]	$\varepsilon_{(\sigma max)}$ [%]	E_{sec} [kPa]	E_{sec} [MPa]	E_{tan} [kPa]	E_{tan} [MPa]	T [kPa*mm/mm]
RC_05C_50%_P1A	RC	0.5	50%	327.1	873.7	0.9	0.017	1.7	50206.4	50.2	79846.2	79.8	9.8
RC_05C_50%_P1B	RC	0.5	50%	309.4	826.5	0.8	0.019	1.9	42536.1	42.5	62036.0	62.0	10.1
RC_05C_50%_P2A	RC	0.5	50%	299.1	774.7	0.8	0.022	2.2	35059.8	35.1	57946.1	57.9	11.4
RC_05C_50%_P2B	RC	0.5	50%	313.3	803.5	0.8	0.053	5.3	15159.1	15.2	66660.0	66.7	34.0
RC_50C_50%_P3A	RC	0.5	50%	290.7	753.0	0.8	0.023	2.3	32504.3	32.5	53731.7	53.7	11.7
RC_05C_50%_P3B	RC	0.5	50%	295.8	766.2	0.8	0.023	2.3	33255.2	33.3	47069.4	47.1	11.1
RC_05C_50%_P4A	RC	0.5	50%	346.6	897.7	0.9	0.021	2.1	43048.9	43.0	59544.1	59.5	11.9
RC_05C_50%_P4B	RC	0.5	50%	352.3	912.3	0.9	0.016	1.6	55305.6	55.3	73504.6	73.5	9.2
RC_05C_50%_P5A	RC	0.5	50%	381.8	1074.5	1.1	0.017	1.7	62142.2	62.1	76060.0	76.1	11.2
RC_05C_50%_P5B	RC	0.5	50%	459.3	1292.6	1.3	0.015	1.5	88435.4	88.4	106866.0	106.9	11.1
RA_05C_50%_P1A	RA	0.5	50%	134.7	381.9	0.4	0.042	4.2	9183.4	9.2	10437.9	10.4	8.8
RA_05C_50%_P1B	RA	0.5	50%	167.7	475.3	0.5	0.033	3.3	14501.3	14.5	28689.5	28.7	10.8
RA_05C_50%_P2A	RA	0.5	50%	139.2	401.3	0.4	0.043	4.3	9345.8	9.3	12923.8	12.9	81.1
RA_05C_50%_P2B	RA	0.5	50%	143.8	414.4	0.4	0.036	3.6	11512.6	11.5	15751.9	15.8	9.3
RA_05C_50%_P3A	RA	0.5	50%	137.0	386.4	0.4	0.034	3.4	11476.4	11.5	15551.2	15.6	8.1
RA_05C_50%_P3B	RA	0.5	50%	144.2	400.5	0.4	0.029	2.9	13653.4	13.7	20926.0	20.9	7.4
RA_05C_50%_P4A	RA	0.5	50%	149.3	414.2	0.4	0.029	2.9	14047.1	14.0	17641.3	17.6	7.4
RA_05C_50%_P4B	RA	0.5	50%	163.8	454.3	0.5	0.032	3.2	14047.8	14.0	22094.9	22.1	9.8
RA_05C_50%_P5A	RA	0.5	50%	-	-	-	-	-	-	-	-	-	-
RA_05C_50%_P5B	RA	0.5	50%	-	-	-	-	-	-	-	-	-	-
BT_05C_50%_P1A	BT	0.5	50%	-	-	-	-	-	-	-	-	-	-
BT_05C_50%_P1B	BT	0.5	50%	328.3	874.2	0.9	0.020	2.0	43769.8	43.8	95511.9	95.5	13.8
BT_05C_50%_P2A	BT	0.5	50%	252.0	682.0	0.7	0.033	3.3	20564.0	20.6	42999.4	43.0	17.1
BT_05C_50%_P2B	BT	0.5	50%	296.6	794.0	0.8	0.037	3.7	21208.3	21.2	110734.9	110.7	21.1
BT_05C_50%_P3A	BT	0.5	50%	398.5	1060.5	1.1	0.012	1.2	86857.6	86.9	127609.8	127.6	8.0
BT_05C_50%_P3B	BT	0.5	50%	371.8	975.1	1.0	0.009	0.9	103402.3	103.4	140592.2	140.6	5.7
BT_05C_50%_P4A	BT	0.5	50%	346.6	938.0	0.9	0.032	3.2	29749.5	29.7	50733.7	50.7	16.3
BT_05C_50%_P4B	BT	0.5	50%	-	-	-	-	-	-	-	-	-	-
BT_05C_50%_P5A	BT	0.5	50%	540.5	1430.0	1.4	0.020	2.0	71806.1	71.8	177870.8	177.9	316.2
BT_05C_50%_P5B	BT	0.5	50%	754.1	1995.0	2.0	0.014	1.4	140420.3	140.4	235352.8	235.4	18.7

ID	Material	l/s	AS	F_{max} [N]	σ_{max} [kPa]	σ_{max} [MPa]	$\varepsilon_{(\sigma max)}$ [mm/mm]	$\varepsilon_{(\sigma max)}$ [%]	E_{sec} [kPa]	E_{sec} [MPa]	E_{tan} [kPa]	E_{tan} [MPa]	T [kPa*mm/mm]
NA_05C_50%_P1A	NA	0.5	50%	195.2	518.6	0.5	0.026	2.6	20196.0	20.2	34088.9	34.1	9.1
NA_05C_50%_P1B	NA	0.5	50%	205.6	546.4	0.5	0.023	2.3	23800.2	23.8	48004.7	48.0	242.2
NA_05C_50%_P2A	NA	0.5	50%	140.8	368.4	0.4	0.056	5.6	6542.0	6.5	8310.9	8.3	12.0
NA_05C_50%_P2B	NA	0.5	50%	150.0	392.6	0.4	0.021	2.1	18636.3	18.6	28592.1	28.6	5.5
NA_05C_50%_P3A	NA	0.5	50%	133.5	349.3	0.3	0.035	3.5	9930.2	9.9	21167.3	21.2	8.9
NA_05C_50%_P3B	NA	0.5	50%	139.3	364.4	0.4	0.032	3.2	11562.2	11.6	23177.2	23.2	8.3
NA_05C_50%_P4A	NA	0.5	50%	141.2	369.3	0.4	0.034	3.4	10940.7	10.9	13431.3	13.4	7.3
NA_05C_50%_P4B	NA	0.5	50%	175.3	458.6	0.5	0.022	2.2	20685.2	20.7	38108.2	38.1	7.1
NA_05C_50%_P5A	NA	0.5	50%	-	-	-	-	-	-	-	-	-	-
NA_05C_50%_P5B	NA	0.5	50%	-	-	-	-	-	-	-	-	-	-
UND_05C_50%_P1A	UND	0.5	50%	325.6	831.0	0.8	0.022	2.2	38459.3	38.5	57480.4	57.5	11.5
UND_05C_50%_P1B	UND	0.5	50%	339.3	865.9	0.9	0.022	2.2	40158.3	40.2	50608.1	50.6	11.1
UND_05C_50%_P2A	UND	0.5	50%	249.9	637.5	0.6	0.017	1.7	36482.1	36.5	50055.2	50.1	6.9
UND_05C_50%_P2B	UND	0.5	50%	279.7	713.5	0.7	0.024	2.4	29286.0	29.3	52274.6	52.3	12.1
UND_05C_50%_P3A	UND	0.5	50%	238.2	616.8	0.6	0.021	2.1	28790.8	28.8	48082.7	48.1	8.5
UND_05C_50%_P3B	UND	0.5	50%	268.3	694.8	0.7	0.021	2.1	33588.8	33.6	54414.9	54.4	9.3
UND_05C_50%_P4A	UND	0.5	50%	219.8	560.7	0.6	0.030	3.0	18861.9	18.9	47421.5	47.4	13.1
UND_05C_50%_P4B	UND	0.5	50%	270.7	690.5	0.7	0.025	2.5	28095.6	28.1	36751.9	36.8	10.2
UND_05C_50%_P5A	UND	0.5	50%	231.6	599.8	0.6	0.046	4.6	13165.1	13.2	14809.9	14.8	14.9
UND_05C_50%_P5B	UND	0.5	50%	296.9	769.1	0.8	0.020	2.0	38075.2	38.1	70220.3	70.2	10.8
UND2_05C_50%_P1A	UND2	0.5	50%	853.0	2132.6	2.1	0.019	1.9	110630.4	110.6	148050.8	148.1	25.3
UND2_05C_50%_P1B	UND2	0.5	50%	919.3	2275.8	2.3	0.021	2.1	105896.7	105.9	157174.6	157.2	31.0
UND2_05C_50%_P2A	UND2	0.5	50%	515.3	1334.7	1.3	0.034	3.4	39841.3	39.8	51352.7	51.4	26.9
UND2_05C_50%_P2B	UND2	0.5	50%	987.2	2544.4	2.5	0.015	1.5	168678.6	168.7	249928.4	249.9	25.0
UND2_05C_50%_P3A	UND2	0.5	50%	1017.8	2718.5	2.7	0.026	2.6	102598.4	102.6	188714.2	188.7	50.3
UND2_05C_50%_P3B	UND2	0.5	50%	952.7	2544.5	2.5	0.018	1.8	139763.8	139.8	177283.1	177.3	27.6
UND2_05C_50%_P4A	UND2	0.5	50%	950.5	2449.2	2.4	0.045	4.5	54007.8	54.0	88203.7	88.2	72.8
UND2_05C_50%_P4B	UND2	0.5	50%	912.9	2328.5	2.3	0.028	2.8	83994.7	84.0	108552.4	108.6	39.2
UND2_05C_50%_P5A	UND2	0.5	50%	-	-	-	-	-	-	-	-	-	-
UND2_05C_50%_P5B	UND2	0.5	50%	-	-	-	-	-	-	-	-	-	-

ID	Material	l/s	AS	F_{max} [N]	σ_{max} [kPa]	σ_{max} [MPa]	$\varepsilon_{(\sigma max)}$ [mm/mm]	$\varepsilon_{(\sigma max)}$ [%]	E_{sec} [kPa]	E_{sec} [MPa]	E_{tan} [kPa]	E_{tan} [MPa]	T [kPa*mm/mm]
RC_04C_100%_P1A	RC	0.4	100%	6697.8	16256.8	16.3	0.019	1.9	844526.2	844.5	979611.4	979.6	174.9
RC_04C_100%_P1B	RC	0.4	100%	6421.3	15585.7	15.6	0.028	2.8	554985.8	555.0	986274.8	986.3	308.3
RC_04C_100%_P2A	RC	0.4	100%	5305.1	13070.0	13.1	0.023	2.3	571896.7	571.9	669297.1	669.3	168.2
RC_04C_100%_P2B	RC	0.4	100%	4433.8	10761.6	10.8	0.017	1.7	629958.1	630.0	786997.2	787.0	108.2
RC_04C_100%_P3A	RC	0.4	100%	7545.2	18425.3	18.4	0.021	2.1	879916.4	879.9	1063529.0	1063.5	222.3
RC_04C_100%_P3B	RC	0.4	100%	5630.7	13816.0	13.8	0.021	2.1	659844.8	659.8	698586.4	698.6	151.9
RC_04C_100%_P4A	RC	0.4	100%	4928.5	12139.2	12.1	0.021	2.1	576391.5	576.4	686068.9	686.1	146.5
RC_04C_100%_P4B	RC	0.4	100%	5847.8	14190.6	14.2	0.022	2.2	650610.9	650.6	830495.8	830.5	189.4
RC_04C_100%_P5A	RC	0.4	100%	5122.8	13347.7	13.3	0.021	2.1	623595.4	623.6	814135.2	814.1	171.5
RC_04C_100%_P5B	RC	0.4	100%	4753.1	12388.4	12.4	0.022	2.2	573098.0	573.1	721678.8	721.7	158.2
RA_04C_100%_P1A	RA	0.4	100%	673.8	1710.1	1.7	0.078	7.8	21979.2	22.0	30638.9	30.6	82.7
RA_04C_100%_P1B	RA	0.4	100%	720.4	1828.4	1.8	0.079	7.9	23218.9	23.2	32656.0	32.7	87.8
RA_04C_100%_P2A	RA	0.4	100%	689.4	1886.6	1.9	0.077	7.7	24492.4	24.5	30993.5	31.0	86.3
RA_04C_100%_P2B	RA	0.4	100%	710.6	1944.7	1.9	0.076	7.6	25565.6	25.6	30992.1	31.0	85.9
RA_04C_100%_P3A	RA	0.4	100%	634.6	1595.2	1.6	0.073	7.3	21914.2	21.9	29492.1	29.5	69.6
RA_04C_100%_P3B	RA	0.4	100%	661.7	1680.5	1.7	0.084	8.4	20012.1	20.0	25920.4	25.9	85.9
RA_04C_100%_P4A	RA	0.4	100%	638.1	1596.3	1.6	0.068	6.8	23571.1	23.6	31336.7	31.3	64.7
RA_04C_100%_P4B	RA	0.4	100%	683.8	1753.3	1.8	0.077	7.7	22876.9	22.9	31035.2	31.0	82.1
RA_04C_100%_P5A	RA	0.4	100%	718.2	1890.0	1.9	0.075	7.5	25341.2	25.3	34782.9	34.8	86.3
RA_04C_100%_P5B	RA	0.4	100%	735.8	1967.5	2.0	0.078	7.8	25250.8	25.3	31745.4	31.7	90.8
BT_04C_100%_P1A	BT	0.4	100%	3474.1	9376.7	9.4	0.017	1.7	548867.5	548.9	592224.3	592.2	85.0
BT_04C_100%_P1B	BT	0.4	100%	4657.6	12701.5	12.7	0.020	2.0	632288.9	632.3	814259.5	814.3	153.3
BT_04C_100%_P2A	BT	0.4	100%	4736.8	11961.7	12.0	0.020	2.0	605636.5	605.6	685678.3	685.7	130.8
BT_04C_100%_P2B	BT	0.4	100%	4258.1	10916.4	10.9	0.021	2.1	512032.7	512.0	656726.3	656.7	136.9
BT_04C_100%_P3A	BT	0.4	100%	3701.6	9117.2	9.1	0.018	1.8	520160.8	520.2	594277.8	594.3	88.9
BT_04C_100%_P3B	BT	0.4	100%	4350.0	10714.4	10.7	0.024	2.4	451564.7	451.6	609044.5	609.0	154.1
BT_04C_100%_P4A	BT	0.4	100%	3307.7	7989.7	8.0	0.020	2.0	391343.4	391.3	521819.3	521.8	97.7
BT_04C_100%_P4B	BT	0.4	100%	4403.0	10898.4	10.9	0.016	1.6	673929.1	673.9	781958.8	782.0	99.2
BT_04C_100%_P5A	BT	0.4	100%	4131.4	10701.5	10.7	0.017	1.7	635578.4	635.6	705500.3	705.5	98.0
BT_04C_100%_P5B	BT	0.4	100%	3390.1	8737.5	8.7	0.019	1.9	468687.4	468.7	581966.0	582.0	95.3

ID	Material	l/s	AS	F_{max} [N]	σ_{max} [kPa]	σ_{max} [MPa]	$\varepsilon_{(\sigma max)}$ [mm/mm]	$\varepsilon_{(\sigma max)}$ [%]	E_{sec} [kPa]	E_{sec} [MPa]	E_{tan} [kPa]	E_{tan} [MPa]	T [kPa*mm/mm]
NA_04C_100%_P1A	NA	0.4	100%	3857.4	11096.5	11.1	0.035	3.5	313191.5	313.2	436477.0	436.5	239.9
NA_04C_100%_P1B	NA	0.4	100%	5485.1	15610.9	15.6	0.032	3.2	480835.8	480.8	658190.2	658.2	316.1
NA_04C_100%_P2A	NA	0.4	100%	3374.7	9203.9	9.2	0.027	2.7	340822.7	340.8	513513.2	513.5	155.7
NA_04C_100%_P2B	NA	0.4	100%	4494.3	12257.3	12.3	0.024	2.4	513221.6	513.2	646705.0	646.7	175.5
NA_04C_100%_P3A	NA	0.4	100%	3948.5	11023.2	11.0	0.026	2.6	416498.2	416.5	612235.7	612.2	186.8
NA_04C_100%_P3B	NA	0.4	100%	3281.6	9161.3	9.2	0.026	2.6	349108.7	349.1	526781.3	526.8	155.2
NA_04C_100%_P4A	NA	0.4	100%	3049.2	8364.0	8.4	0.031	3.1	265560.6	265.6	354238.3	354.2	162.0
NA_04C_100%_P4B	NA	0.4	100%	3677.6	10242.8	10.2	0.024	2.4	432186.4	432.2	606266.7	606.3	148.4
NA_04C_100%_P5A	NA	0.4	100%	3275.4	9624.0	9.6	0.033	3.3	288339.0	288.3	411767.8	411.8	201.3
NA_04C_100%_P5B	NA	0.4	100%	3323.8	9981.3	10.0	0.032	3.2	316537.8	316.5	468977.2	469.0	201.5
UND_04C_100%_P1A	UND	0.4	100%	5551.7	14092.0	14.1	0.021	2.1	662861.7	662.9	783988.1	784.0	170.1
UND_04C_100%_P1B	UND	0.4	100%	5187.8	13234.3	13.2	0.019	1.9	707391.3	707.4	810891.3	810.9	137.1
UND_04C_100%_P2A	UND	0.4	100%	4723.8	11756.7	11.8	0.022	2.2	538446.8	538.4	657861.3	657.9	151.6
UND_04C_100%_P2B	UND	0.4	100%	4821.9	11942.4	11.9	0.022	2.2	554422.5	554.4	720119.5	720.1	156.7
UND_04C_100%_P3A	UND	0.4	100%	4308.0	10934.1	10.9	0.022	2.2	488668.2	488.7	527461.6	527.5	131.2
UND_04C_100%_P3B	UND	0.4	100%	4860.5	12399.2	12.4	0.019	1.9	643154.2	643.2	782580.2	782.6	141.0
UND_04C_100%_P4A	UND	0.4	100%	5020.1	13210.8	13.2	0.020	2.0	661485.7	661.5	804707.3	804.7	152.5
UND_04C_100%_P4B	UND	0.4	100%	4285.6	11289.6	11.3	0.021	2.1	542852.8	542.9	673098.6	673.1	136.3
UND_04C_100%_P5A	UND	0.4	100%	4461.2	11166.7	11.2	0.021	2.1	528541.1	528.5	588833.4	588.8	129.3
UND_04C_100%_P5B	UND	0.4	100%	4191.7	10539.8	10.5	0.017	1.7	632375.3	632.4	727435.7	727.4	97.8
UND2_04C_100%_P1A	UND2	0.4	100%	2860.0	7015.4	7.0	0.023	2.3	302204.9	302.2	398673.0	398.7	98.3
UND2_04C_100%_P1B	UND2	0.4	100%	2782.7	6760.6	6.8	0.026	2.6	262831.0	262.8	373328.4	373.3	109.8
UND2_04C_100%_P2A	UND2	0.4	100%	2647.2	6897.3	6.9	0.026	2.6	262081.2	262.1	393039.1	393.0	113.2
UND2_04C_100%_P2B	UND2	0.4	100%	2806.6	7276.6	7.3	0.025	2.5	287049.7	287.0	438521.1	438.5	119.6
UND2_04C_100%_P3A	UND2	0.4	100%	2892.8	7417.4	7.4	0.025	2.5	300807.7	300.8	400010.7	400.0	112.0
UND2_04C_100%_P3B	UND2	0.4	100%	3006.8	7827.1	7.8	0.024	2.4	331226.2	331.2	445716.5	445.7	113.6
UND2_04C_100%_P4A	UND2	0.4	100%	2737.5	6676.9	6.7	0.022	2.2	308171.0	308.2	400024.7	400.0	182.3
UND2_04C_100%_P4B	UND2	0.4	100%	2853.7	6994.4	7.0	0.023	2.3	305218.1	305.2	400068.6	400.1	95.5
UND2_04C_100%_P5A	UND2	0.4	100%	2882.3	6995.9	7.0	0.022	2.2	314409.9	314.4	428586.3	428.6	93.4
UND2_04C_100%_P5B	UND2	0.4	100%	3050.1	7439.2	7.4	0.020	2.0	374291.8	374.3	465989.0	466.0	86.6

Stress-Strain curves for l/s = 0.6

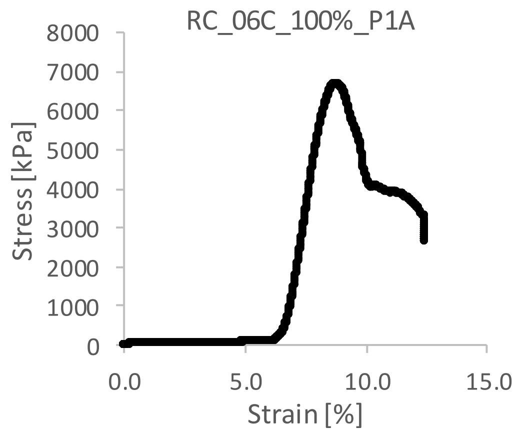

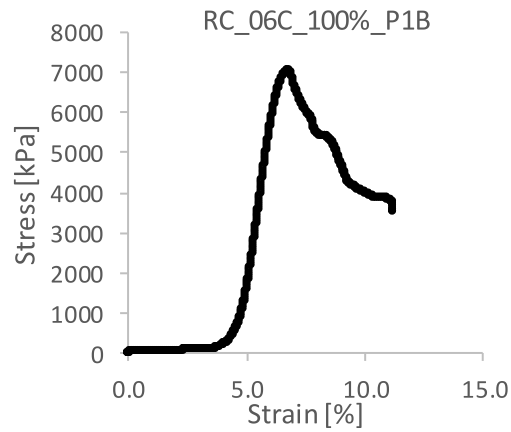

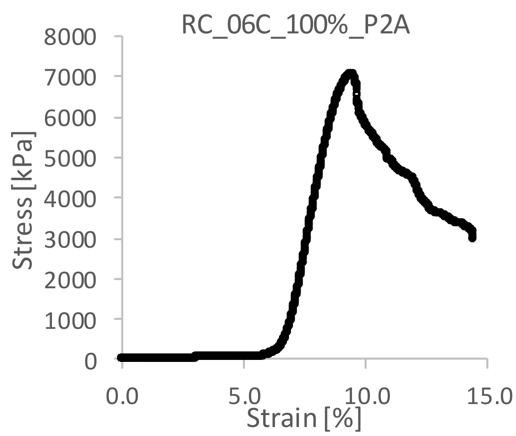

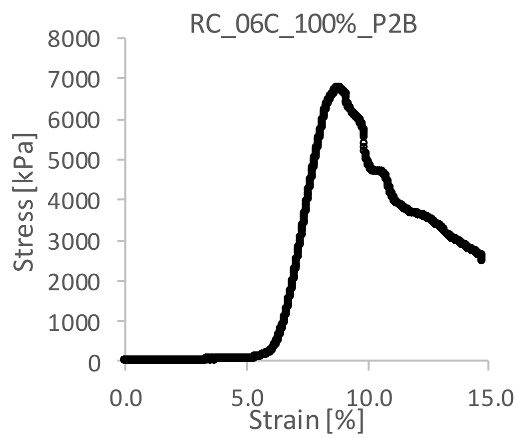

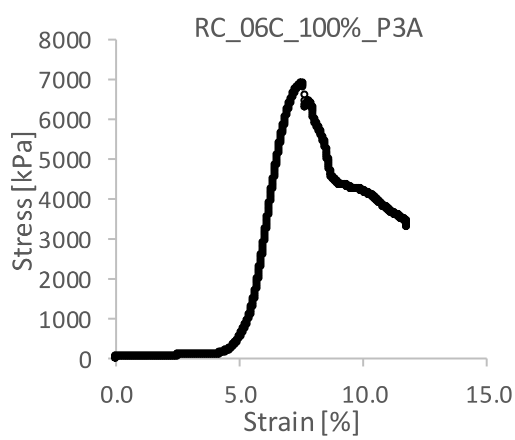

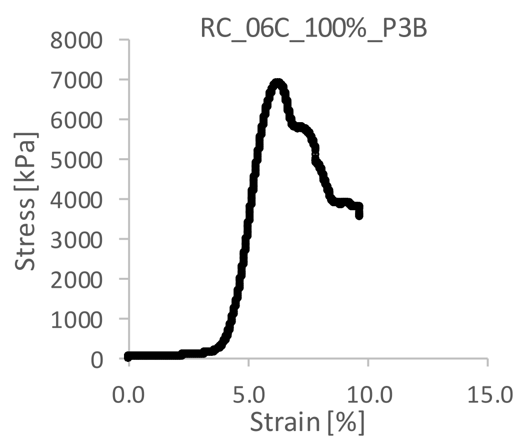

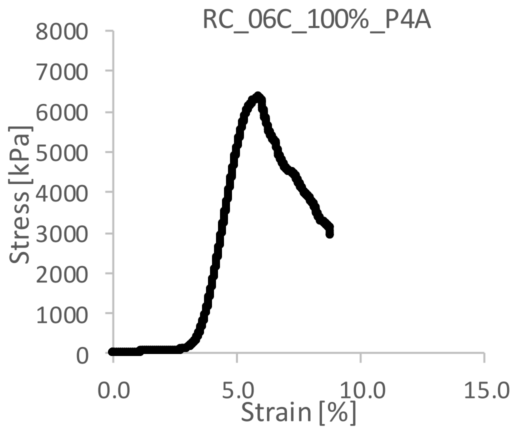
RC_06C_100%_P4A
Stress [kPa]
Strain [%]

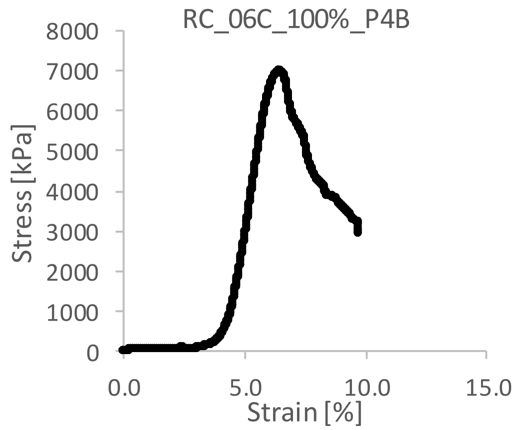
RC_06C_100%_P4B
Stress [kPa]
Strain [%]

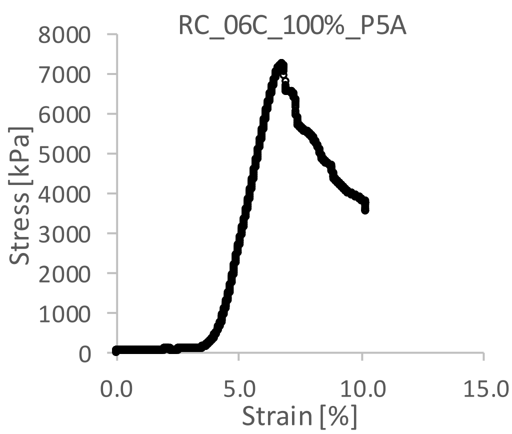
RC_06C_100%_P5A
Stress [kPa]
Strain [%]

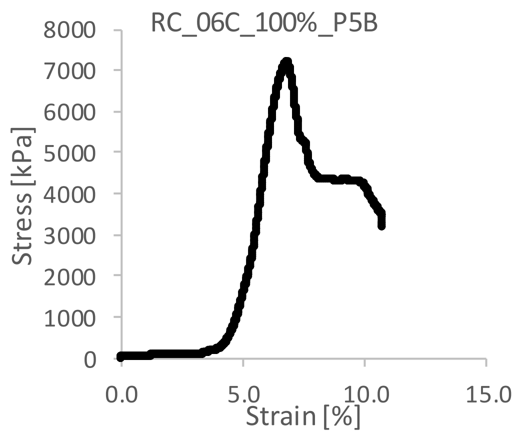
RC_06C_100%_P5B
Stress [kPa]
Strain [%]

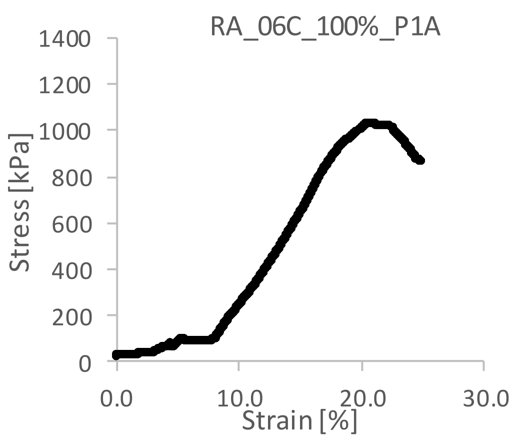
RA_06C_100%_P1A
Stress [kPa]
Strain [%]

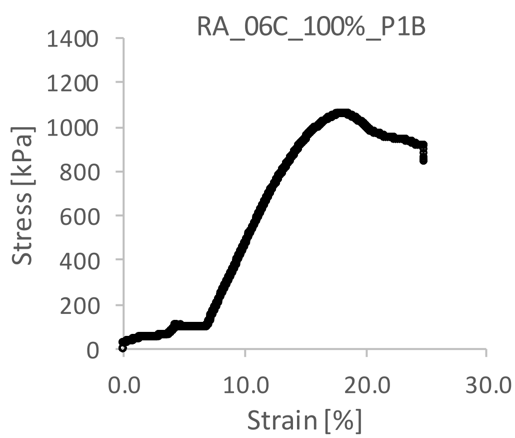
RA_06C_100%_P1B
Stress [kPa]
Strain [%]

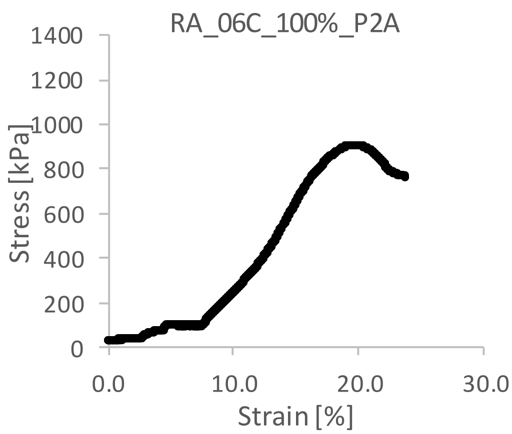
RA_06C_100%_P2A
Stress [kPa]
Strain [%]

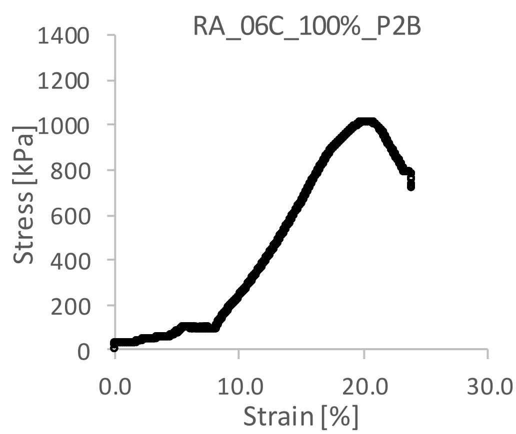
RA_06C_100%_P2B
Stress [kPa]
Strain [%]

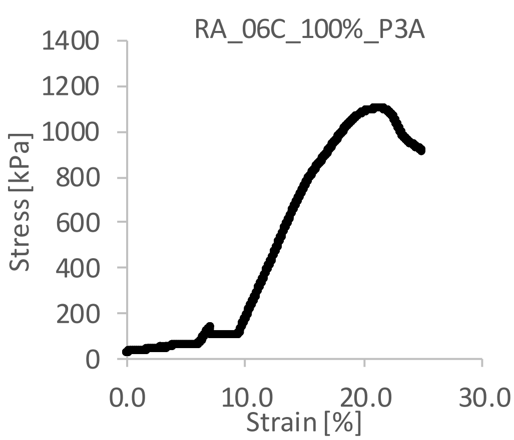
RA_06C_100%_P3A
Stress [kPa]
Strain [%]

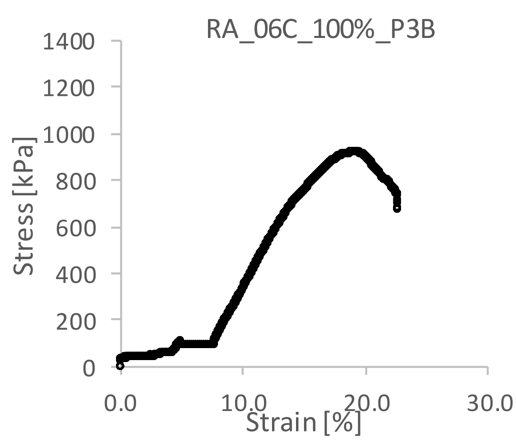
RA_06C_100%_P3B
Stress [kPa]
Strain [%]

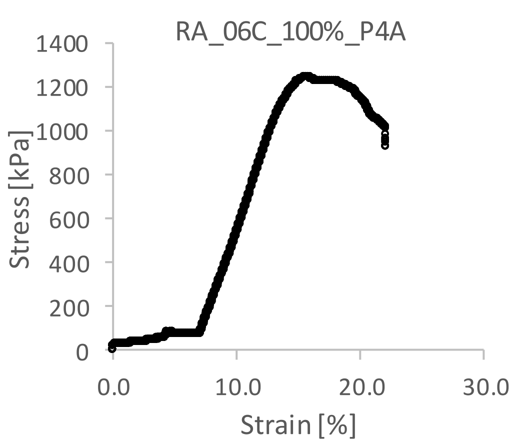
RA_06C_100%_P4A
Stress [kPa]
Strain [%]

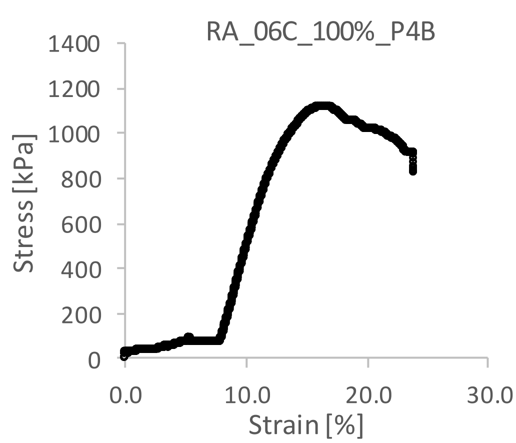
RA_06C_100%_P4B
Stress [kPa]
Strain [%]

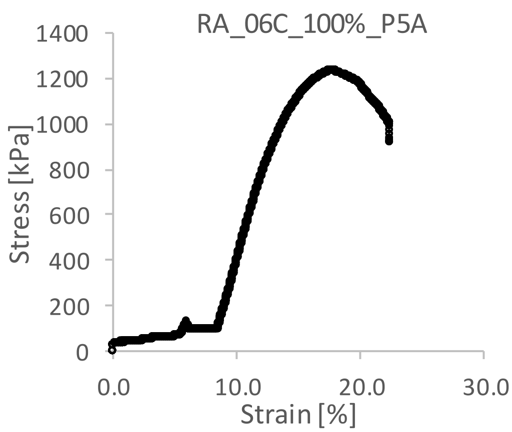
RA_06C_100%_P5A
Stress [kPa]
1400
1200
1000
800
600
400
200
0
0.0
10.0
20.0
30.0
Strain [%]

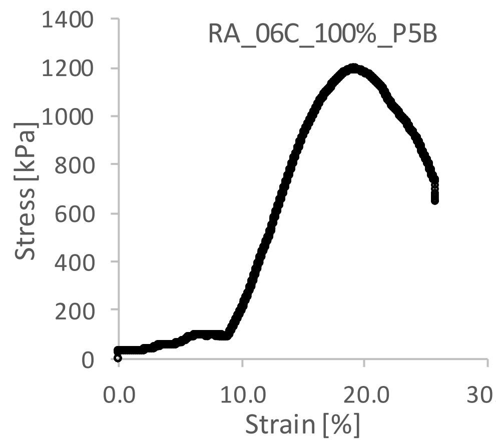
RA_06C_100%_P5B
Stress [kPa]
1400
1200
1000
800
600
400
200
0
0.0
10.0
20.0
30.0
Strain [%]

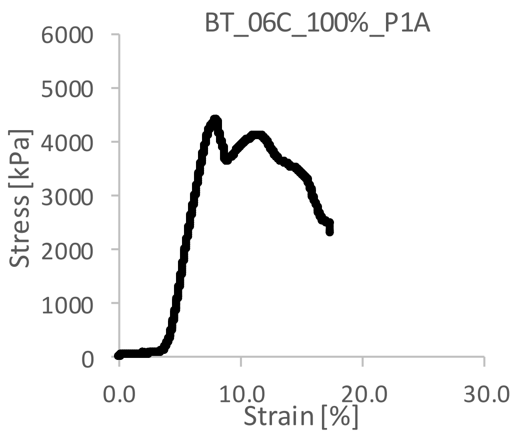
BT_06C_100%_P1A
Stress [kPa]
6000
5000
4000
3000
2000
1000
0
0.0
10.0
20.0
30.0
Strain [%]

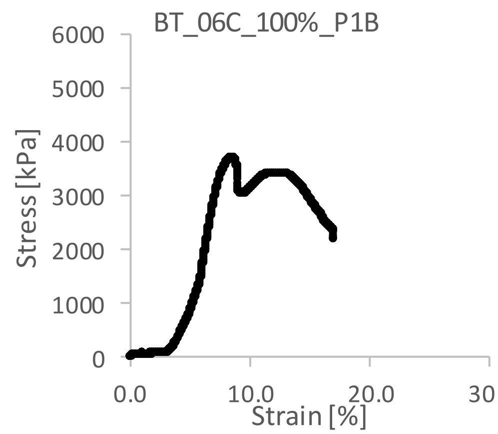
BT_06C_100%_P1B
Stress [kPa]
6000
5000
4000
3000
2000
1000
0
0.0
10.0
20.0
30.0
Strain [%]

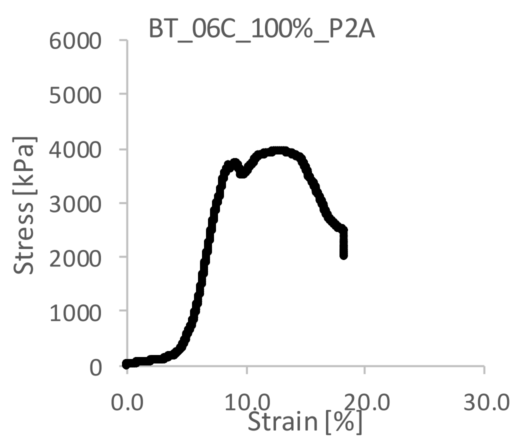
BT_06C_100%_P2A
Stress [kPa]
6000
5000
4000
3000
2000
1000
0
0.0
10.0
20.0
30.0
Strain [%]

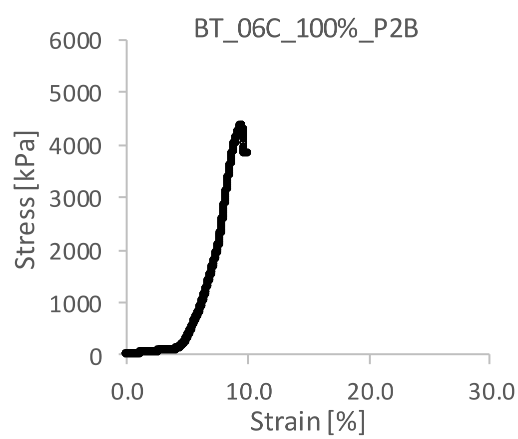
BT_06C_100%_P2B
Stress [kPa]
6000
5000
4000
3000
2000
1000
0
0.0
10.0
20.0
30.0
Strain [%]

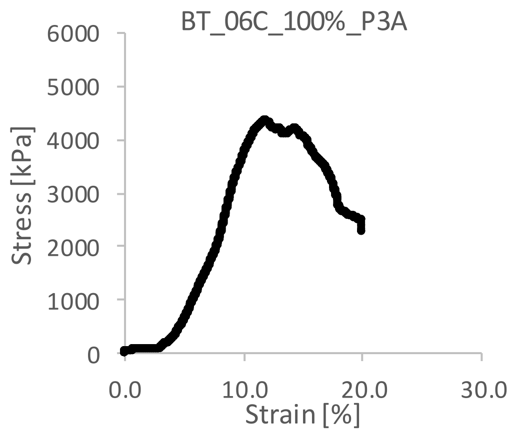
BT_06C_100%_P3A
Stress [kPa]
6000
5000
4000
3000
2000
1000
0
0.0
10.0
20.0
30.0
Strain [%]

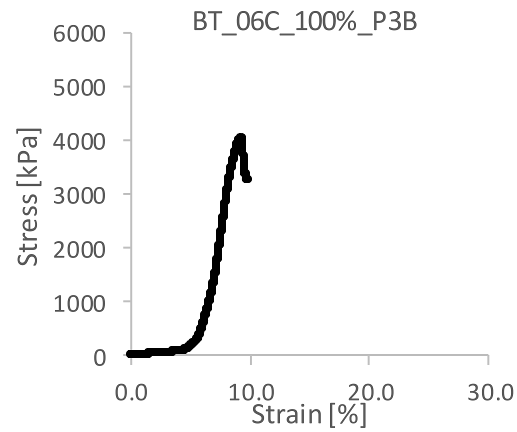
BT_06C_100%_P3B
Stress [kPa]
6000
5000
4000
3000
2000
1000
0
0.0
10.0
20.0
30.0
Strain [%]

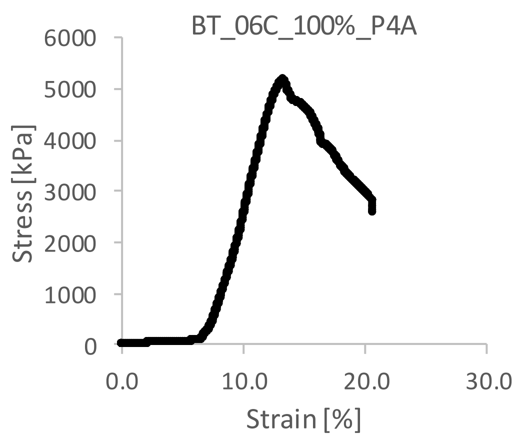
BT_06C_100%_P4A
Stress [kPa]
6000
5000
4000
3000
2000
1000
0
0.0
10.0
20.0
30.0
Strain [%]

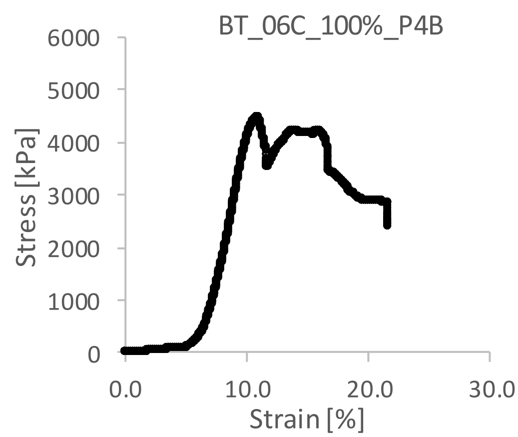
BT_06C_100%_P4B
Stress [kPa]
6000
5000
4000
3000
2000
1000
0
0.0
10.0
20.0
30.0
Strain [%]

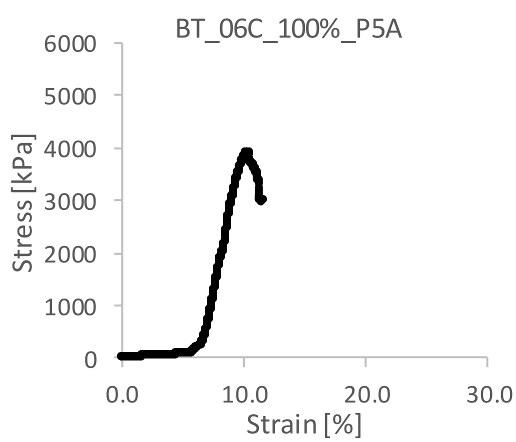
BT_06C_100%_P5A
Stress [kPa]
6000
5000
4000
3000
2000
1000
0
0.0
10.0
20.0
30.0
Strain [%]

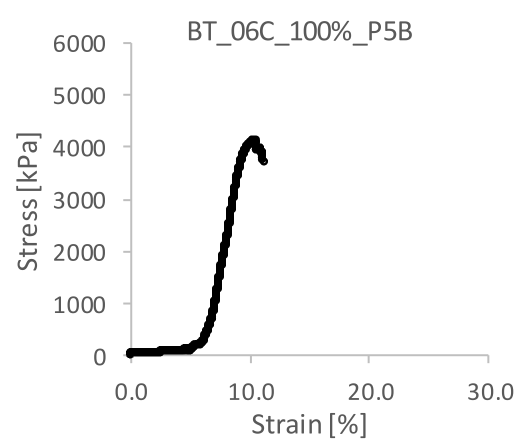
BT_06C_100%_P5B
Stress [kPa]
6000
5000
4000
3000
2000
1000
0
0.0
10.0
20.0
30.0
Strain [%]

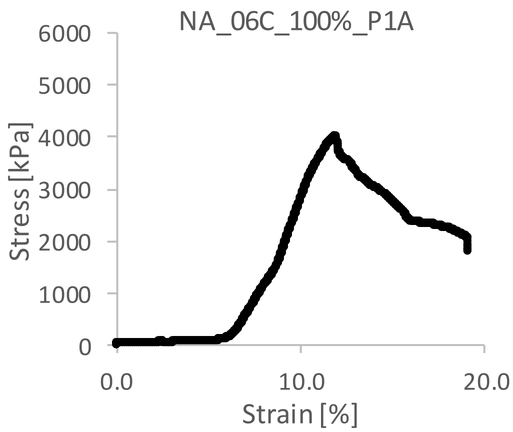
NA_06C_100%_P1A
Stress [kPa]
6000
5000
4000
3000
2000
1000
0
0.0
10.0
20.0
Strain [%]

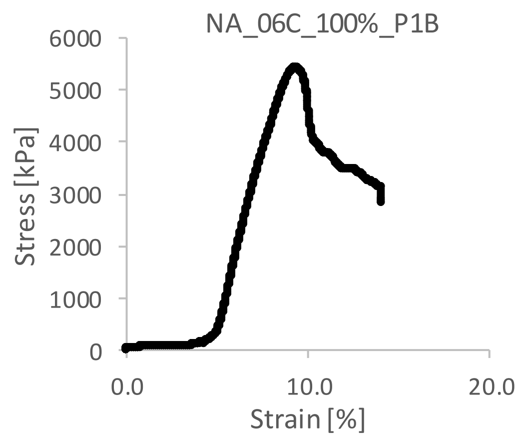
NA_06C_100%_P1B
Stress [kPa]
6000
5000
4000
3000
2000
1000
0
0.0
10.0
20.0
Strain [%]

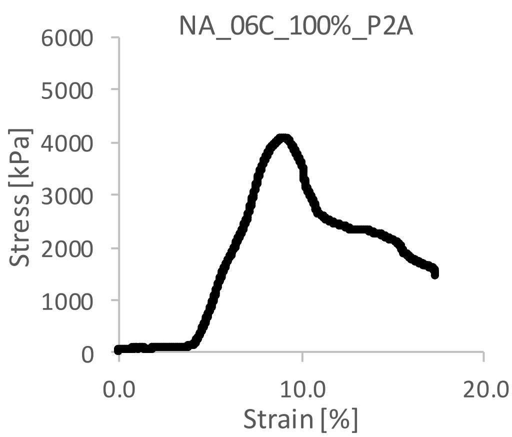
NA_06C_100%_P2A
Stress [kPa]
6000
5000
4000
3000
2000
1000
0
0.0
10.0
20.0
Strain [%]

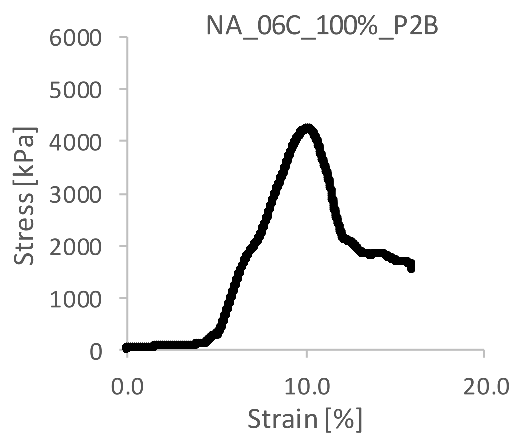
NA_06C_100%_P2B
Stress [kPa]
6000
5000
4000
3000
2000
1000
0
0.0
10.0
20.0
Strain [%]

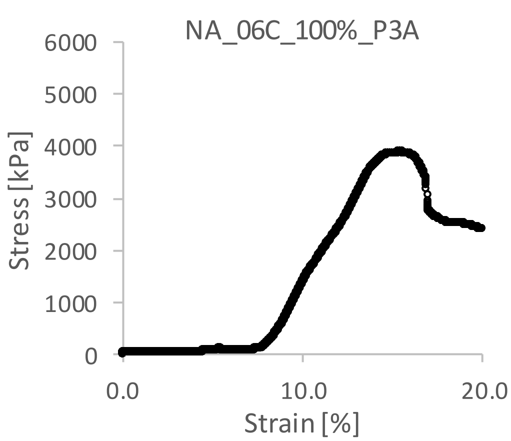
NA_06C_100%_P3A
Stress [kPa]
6000
5000
4000
3000
2000
1000
0
0.0
10.0
20.0
Strain [%]

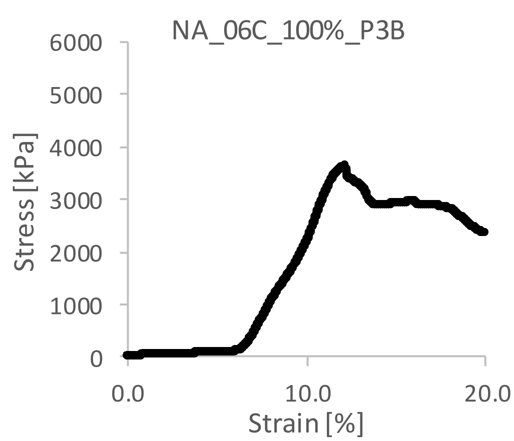
NA_06C_100%_P3B
Stress [kPa]
6000
5000
4000
3000
2000
1000
0
0.0
10.0
20.0
Strain [%]

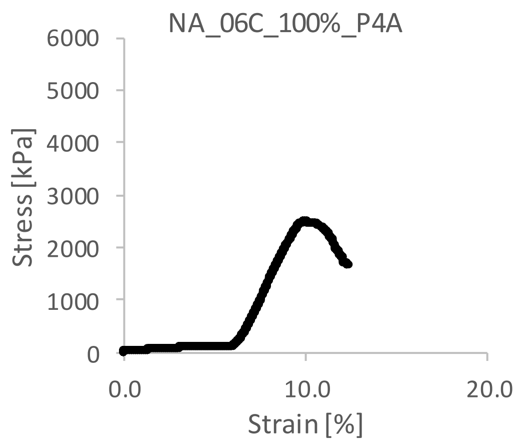
NA_06C_100%_P4A
Stress [kPa]
0
1000
2000
3000
4000
5000
6000
Strain [%]
0.0
10.0
20.0

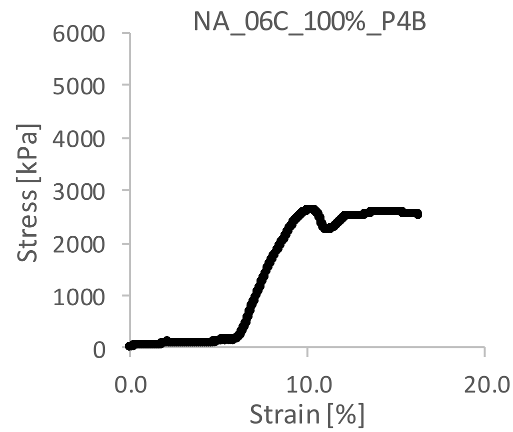
NA_06C_100%_P4B
Stress [kPa]
0
1000
2000
3000
4000
5000
6000
Strain [%]
0.0
10.0
20.0

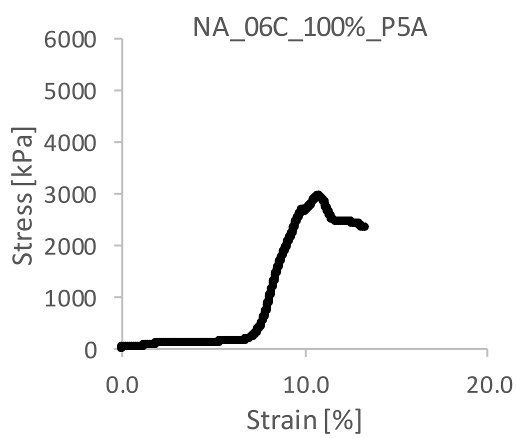
NA_06C_100%_P5A
Stress [kPa]
0
1000
2000
3000
4000
5000
6000
Strain [%]
0.0
10.0
20.0

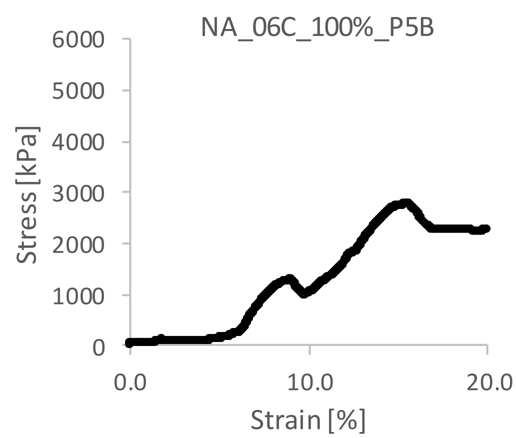
NA_06C_100%_P5B
Stress [kPa]
0
1000
2000
3000
4000
5000
6000
Strain [%]
0.0
10.0
20.0

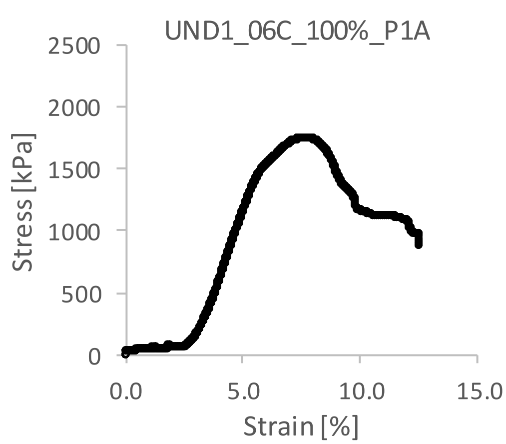
UND1_06C_100%_P1A
Stress [kPa]
0
500
1000
1500
2000
2500
Strain [%]
0.0
5.0
10.0
15.0

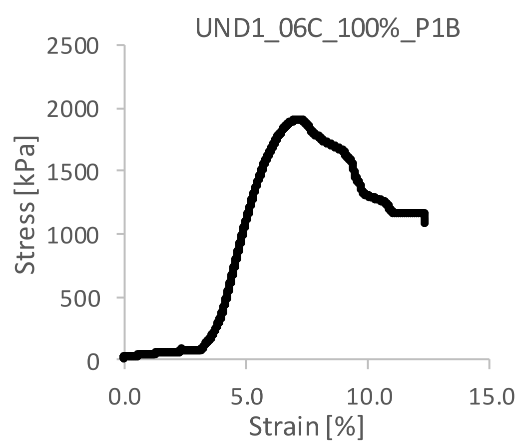
UND1_06C_100%_P1B
Stress [kPa]
0
500
1000
1500
2000
2500
Strain [%]
0.0
5.0
10.0
15.0

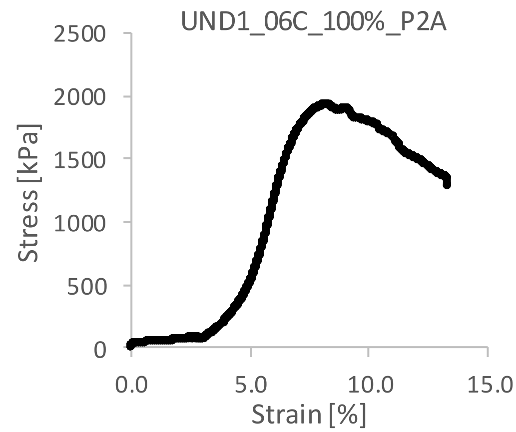
UND1_06C_100%_P2A
Stress [kPa]
Strain [%]
0
500
1000
1500
2000
2500
0.0
5.0
10.0
15.0

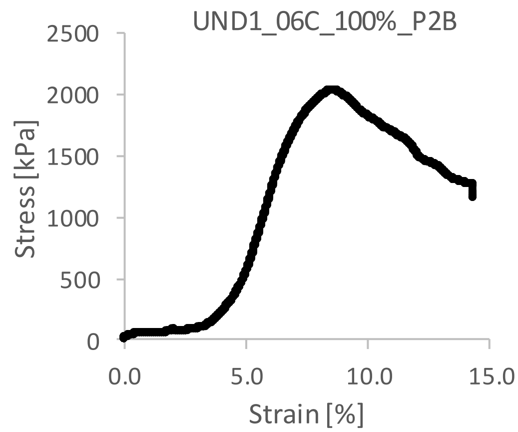
UND1_06C_100%_P2B
Stress [kPa]
Strain [%]
0
500
1000
1500
2000
2500
0.0
5.0
10.0
15.0

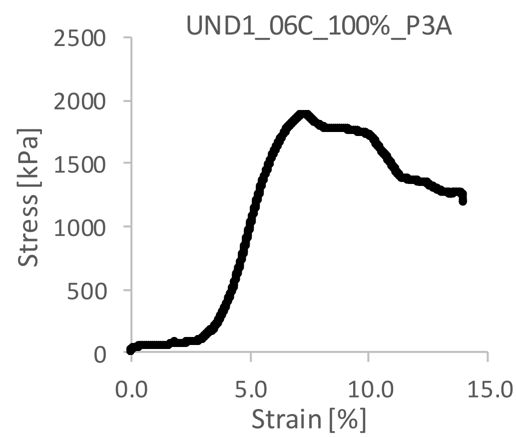
UND1_06C_100%_P3A
Stress [kPa]
Strain [%]
0
500
1000
1500
2000
2500
0.0
5.0
10.0
15.0

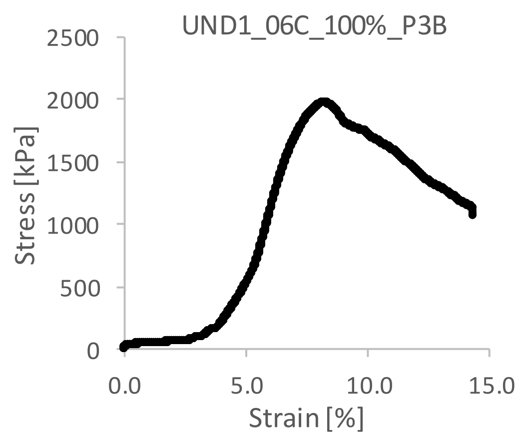
UND1_06C_100%_P3B
Stress [kPa]
Strain [%]
0
500
1000
1500
2000
2500
0.0
5.0
10.0
15.0

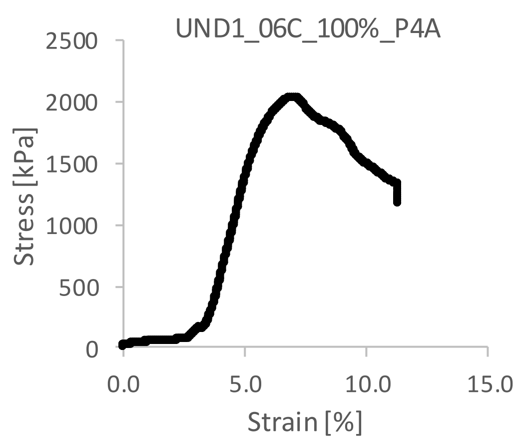
UND1_06C_100%_P4A
Stress [kPa]
Strain [%]
0
500
1000
1500
2000
2500
0.0
5.0
10.0
15.0

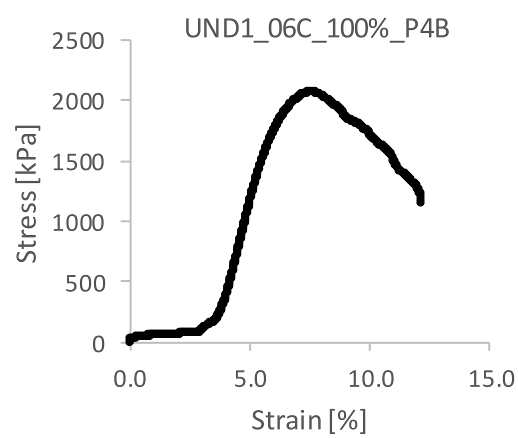
UND1_06C_100%_P4B
Stress [kPa]
Strain [%]
0
500
1000
1500
2000
2500
0.0
5.0
10.0
15.0

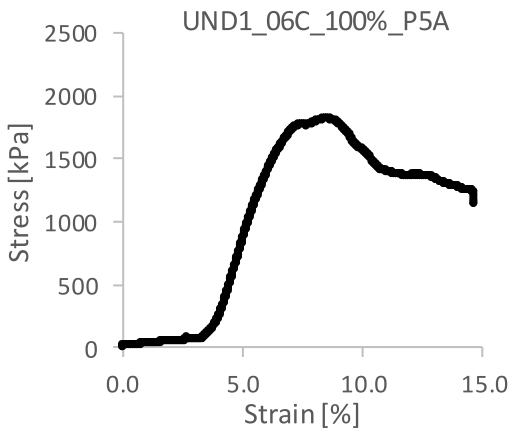
UND1_06C_100%_P5A
Stress [kPa]
Strain [%]
0
500
1000
1500
2000
2500
0.0
5.0
10.0
15.0

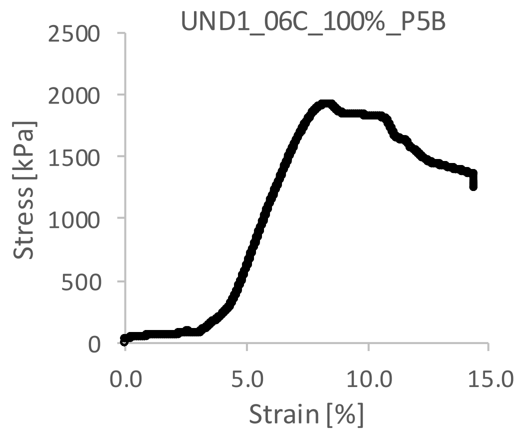
UND1_06C_100%_P5B
Stress [kPa]
Strain [%]
0
500
1000
1500
2000
2500
0.0
5.0
10.0
15.0

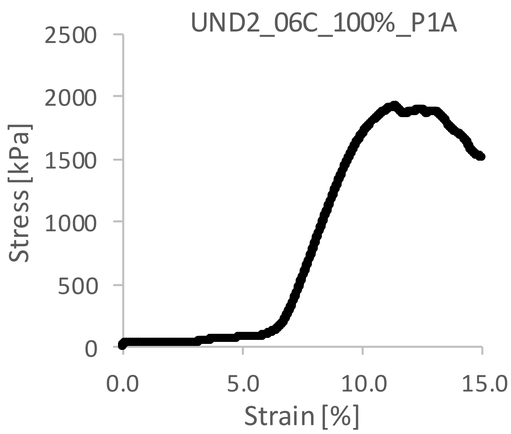
UND2_06C_100%_P1A
Stress [kPa]
Strain [%]
0
500
1000
1500
2000
2500
0.0
5.0
10.0
15.0

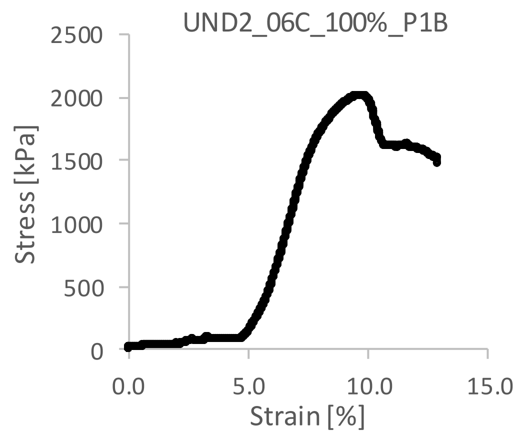
UND2_06C_100%_P1B
Stress [kPa]
Strain [%]
0
500
1000
1500
2000
2500
0.0
5.0
10.0
15.0

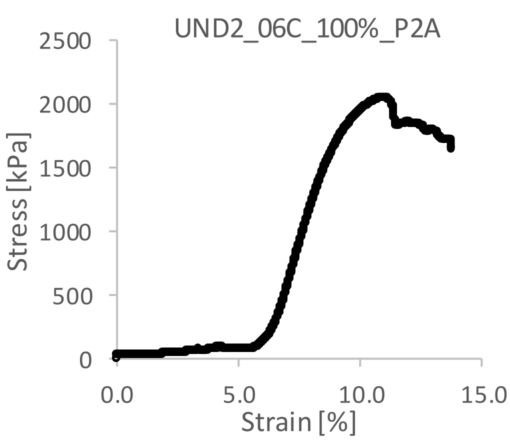
UND2_06C_100%_P2A
Stress [kPa]
Strain [%]
0
500
1000
1500
2000
2500
0.0
5.0
10.0
15.0

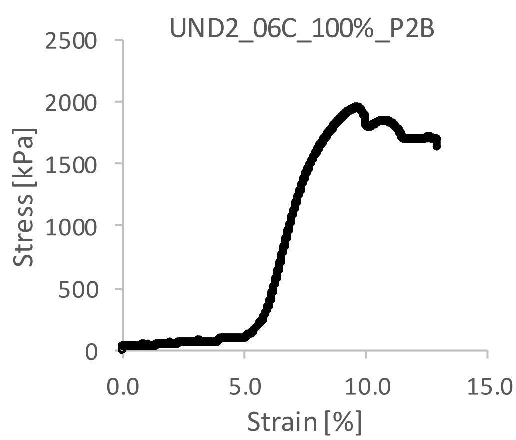
UND2_06C_100%_P2B
Stress [kPa]
Strain [%]
0
500
1000
1500
2000
2500
0.0
5.0
10.0
15.0

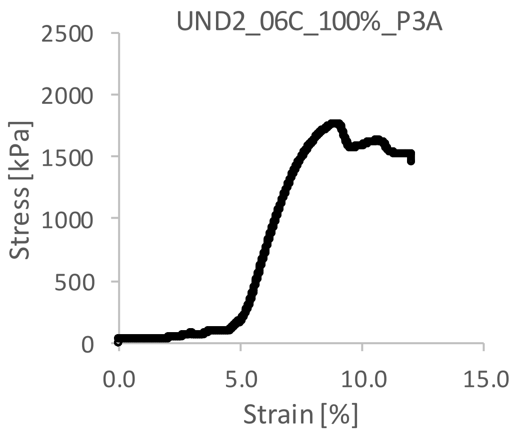
UND2_06C_100%_P3A
Stress [kPa]
Strain [%]

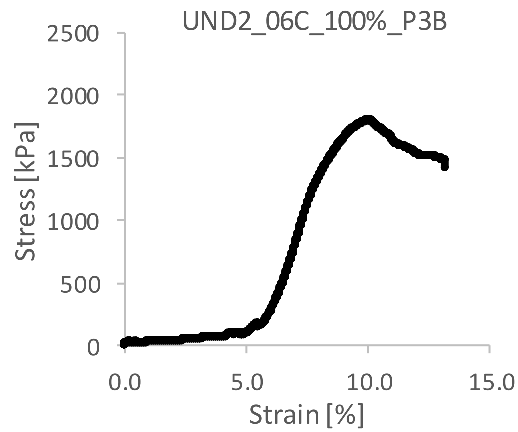
UND2_06C_100%_P3B
Stress [kPa]
Strain [%]

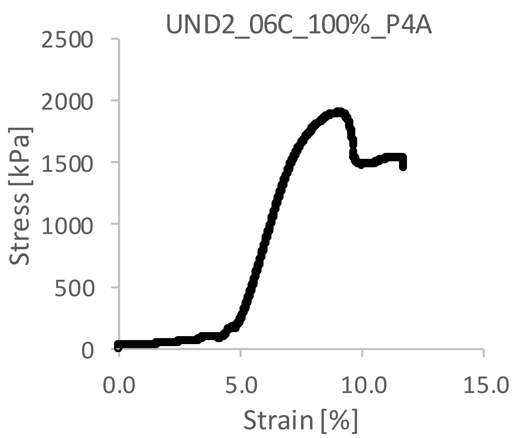
UND2_06C_100%_P4A
Stress [kPa]
Strain [%]

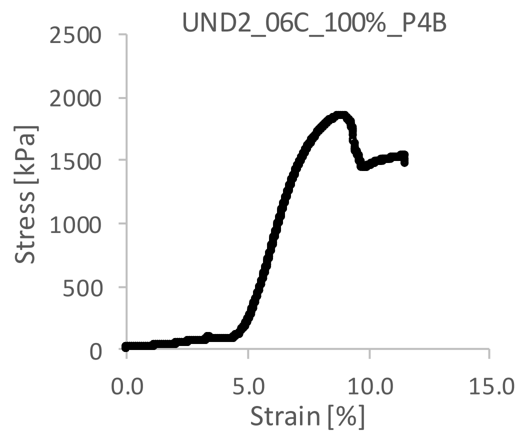
UND2_06C_100%_P4B
Stress [kPa]
Strain [%]

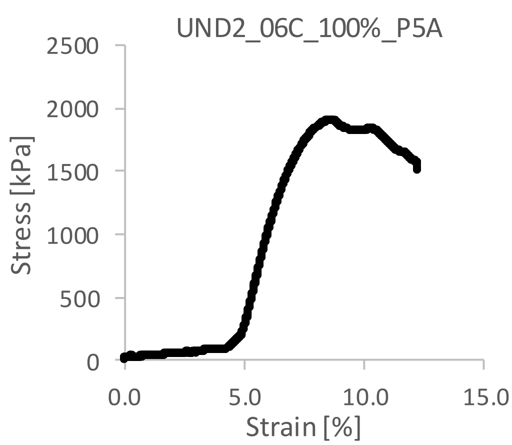
UND2_06C_100%_P5A
Stress [kPa]
Strain [%]

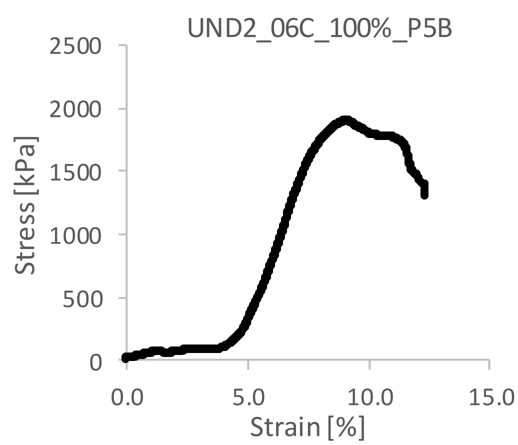
UND2_06C_100%_P5B
Stress [kPa]
Strain [%]

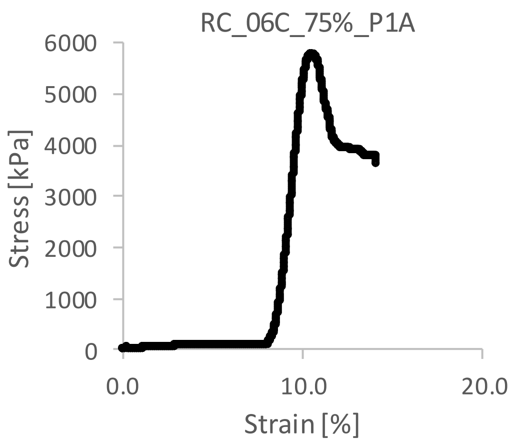
RC_06C_75%_P1A
Stress [kPa]
6000
5000
4000
3000
2000
1000
0
0.0
10.0
20.0
Strain [%]

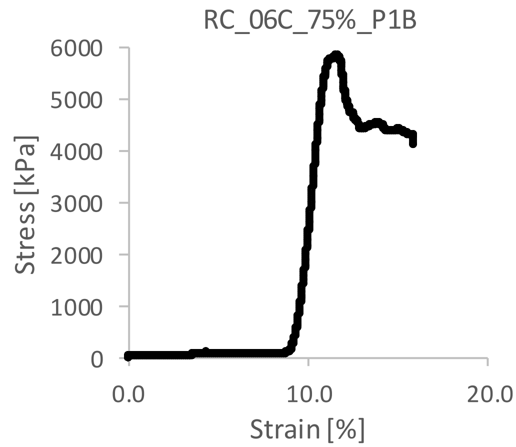
RC_06C_75%_P1B
Stress [kPa]
6000
5000
4000
3000
2000
1000
0
0.0
10.0
20.0
Strain [%]

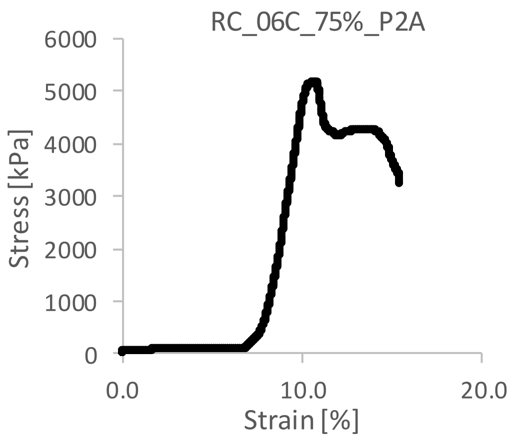
RC_06C_75%_P2A
Stress [kPa]
6000
5000
4000
3000
2000
1000
0
0.0
10.0
20.0
Strain [%]

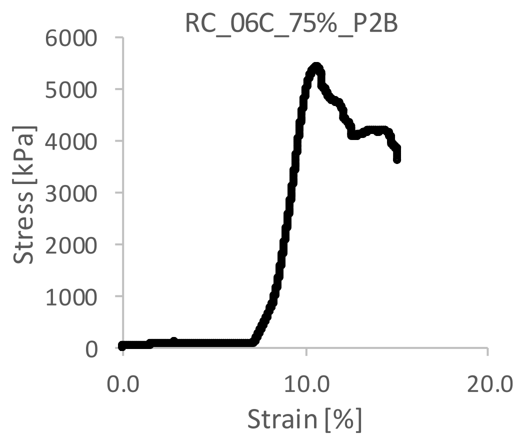
RC_06C_75%_P2B
Stress [kPa]
6000
5000
4000
3000
2000
1000
0
0.0
10.0
20.0
Strain [%]

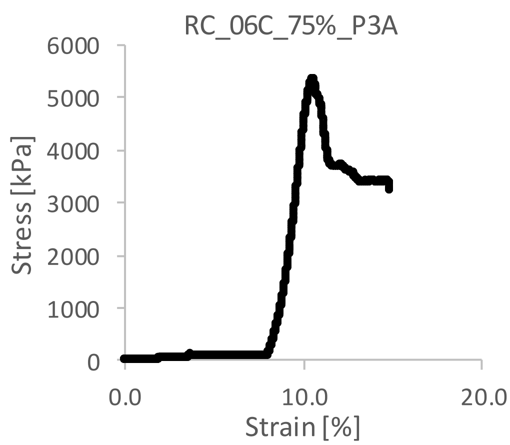
RC_06C_75%_P3A
Stress [kPa]
6000
5000
4000
3000
2000
1000
0
0.0
10.0
20.0
Strain [%]

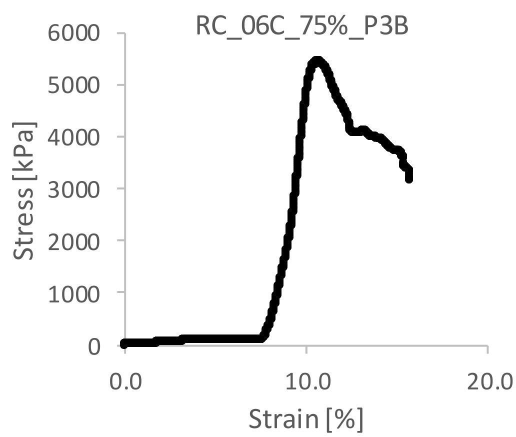
RC_06C_75%_P3B
Stress [kPa]
6000
5000
4000
3000
2000
1000
0
0.0
10.0
20.0
Strain [%]

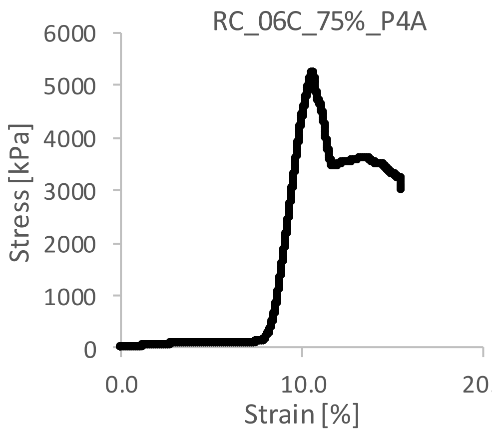
RC_06C_75%_P4A
Stress [kPa]
6000
5000
4000
3000
2000
1000
0
0.0
10.0
20.0
Strain [%]

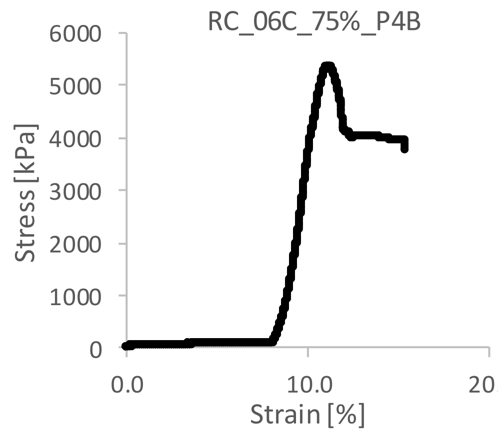
RC_06C_75%_P4B
Stress [kPa]
6000
5000
4000
3000
2000
1000
0
0.0
10.0
20.0
Strain [%]

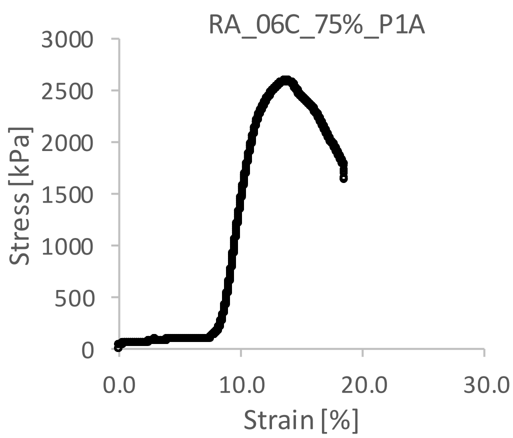
RA_06C_75%_P1A
Stress [kPa]
3000
2500
2000
1500
1000
500
0
0.0
10.0
20.0
30.0
Strain [%]

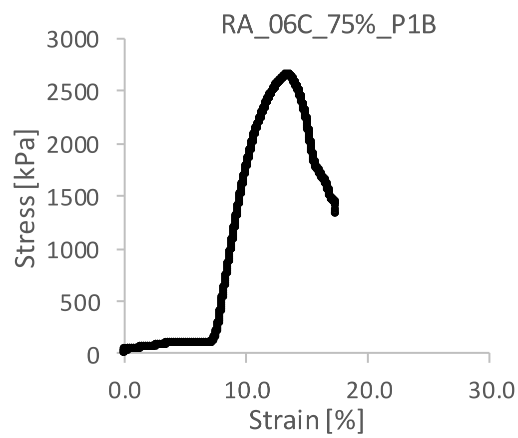
RA_06C_75%_P1B
Stress [kPa]
3000
2500
2000
1500
1000
500
0
0.0
10.0
20.0
30.0
Strain [%]

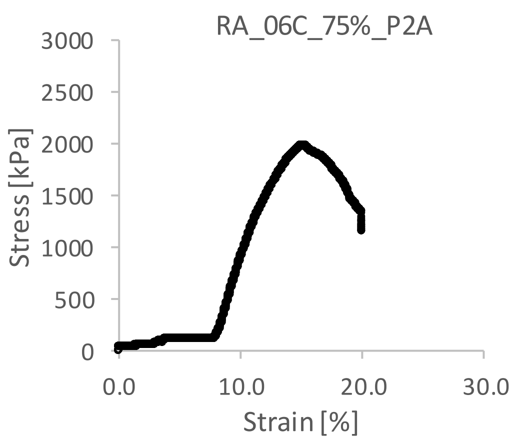
RA_06C_75%_P2A
Stress [kPa]
3000
2500
2000
1500
1000
500
0
0.0
10.0
20.0
30.0
Strain [%]

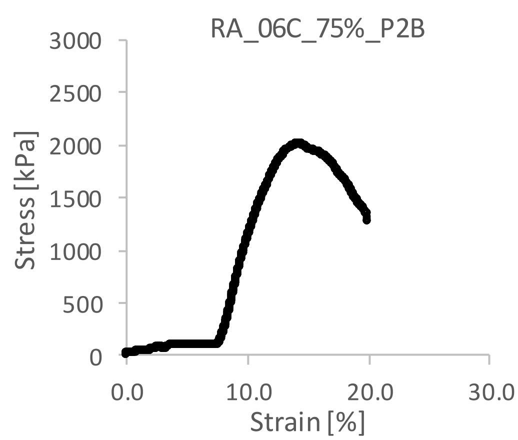
RA_06C_75%_P2B
Stress [kPa]
3000
2500
2000
1500
1000
500
0
0.0
10.0
20.0
30.0
Strain [%]

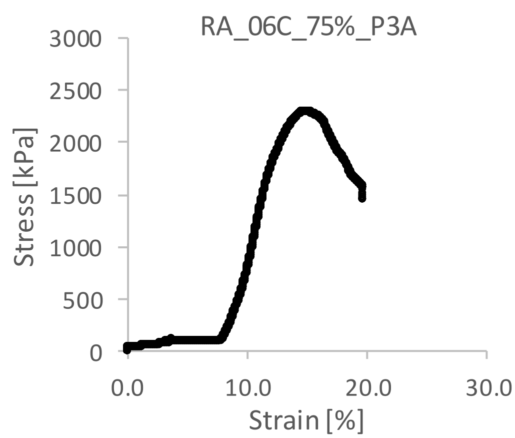
RA_06C_75%_P3A
3000
2500
2000
1500
1000
500
0
Stress [kPa]
0.0
10.0
20.0
30.0
Strain [%]

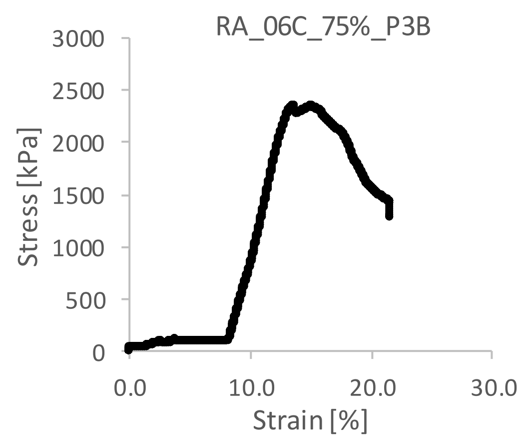
RA_06C_75%_P3B
3000
2500
2000
1500
1000
500
0
Stress [kPa]
0.0
10.0
20.0
30.0
Strain [%]

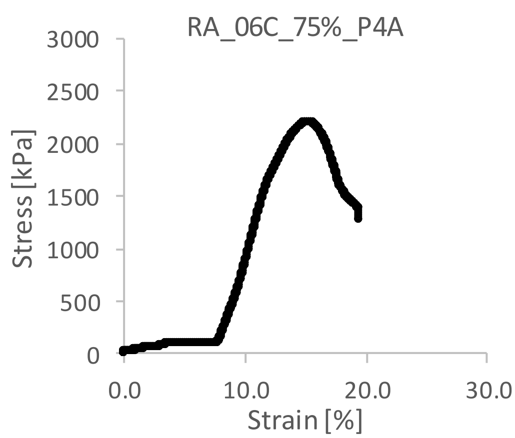
RA_06C_75%_P4A
3000
2500
2000
1500
1000
500
0
Stress [kPa]
0.0
10.0
20.0
30.0
Strain [%]

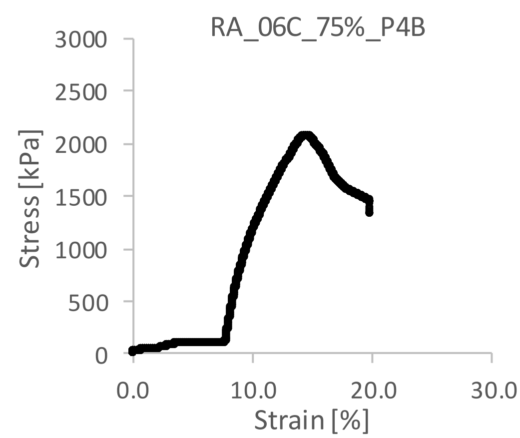
RA_06C_75%_P4B
3000
2500
2000
1500
1000
500
0
Stress [kPa]
0.0
10.0
20.0
30.0
Strain [%]

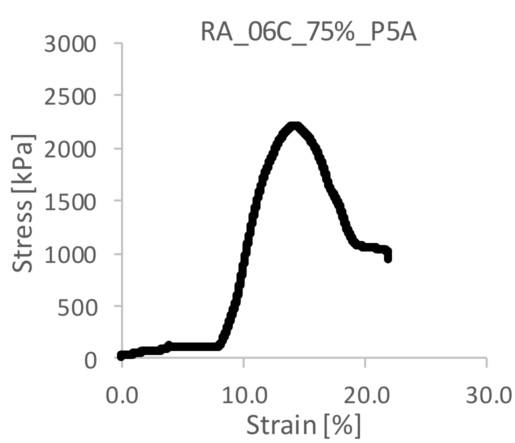
RA_06C_75%_P5A
3000
2500
2000
1500
1000
500
0
Stress [kPa]
0.0
10.0
20.0
30.0
Strain [%]

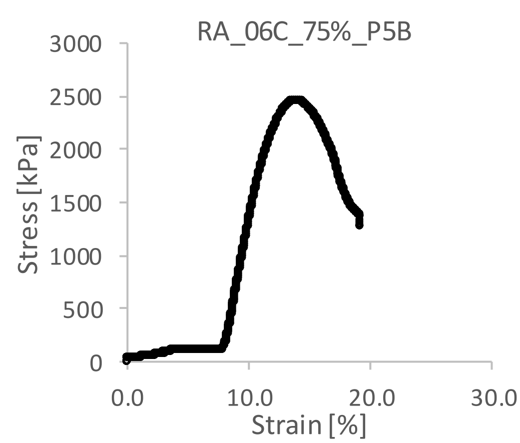
RA_06C_75%_P5B
3000
2500
2000
1500
1000
500
0
Stress [kPa]
0.0
10.0
20.0
30.0
Strain [%]

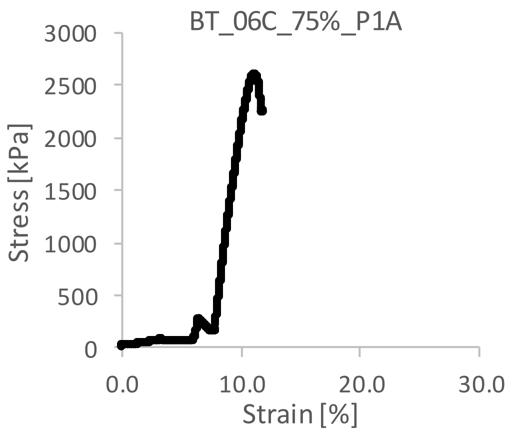
BT_06C_75%_P1A
Stress [kPa]
0
500
1000
1500
2000
2500
3000
0.0
10.0
20.0
30.0
Strain [%]

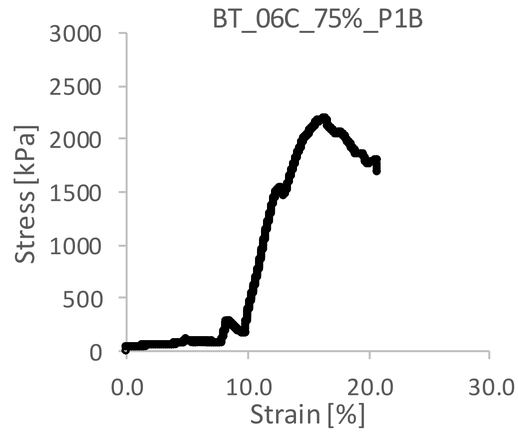
BT_06C_75%_P1B
Stress [kPa]
0
500
1000
1500
2000
2500
3000
0.0
10.0
20.0
30.0
Strain [%]

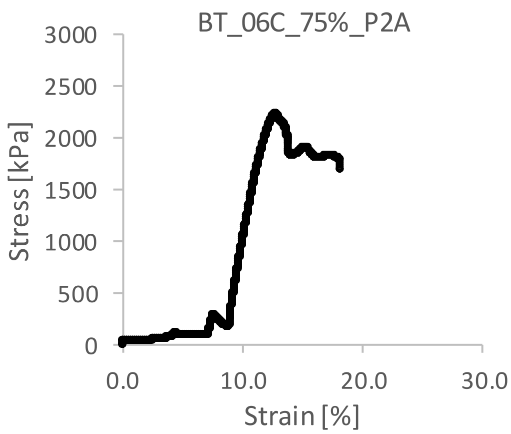
BT_06C_75%_P2A
Stress [kPa]
0
500
1000
1500
2000
2500
3000
0.0
10.0
20.0
30.0
Strain [%]

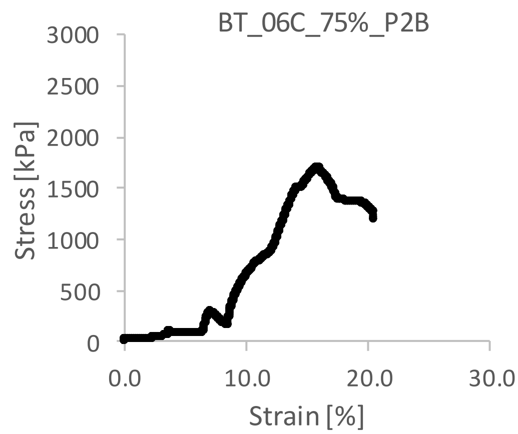
BT_06C_75%_P2B
Stress [kPa]
0
500
1000
1500
2000
2500
3000
0.0
10.0
20.0
30.0
Strain [%]

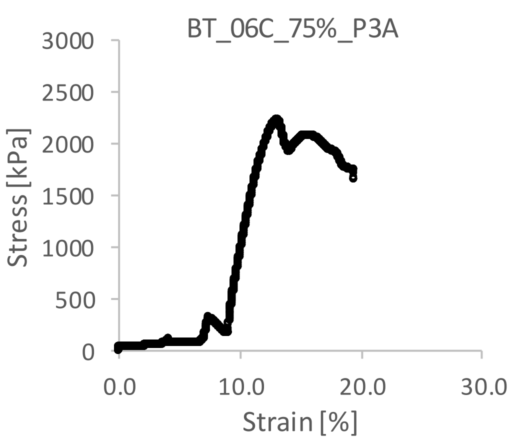
BT_06C_75%_P3A
Stress [kPa]
0
500
1000
1500
2000
2500
3000
0.0
10.0
20.0
30.0
Strain [%]

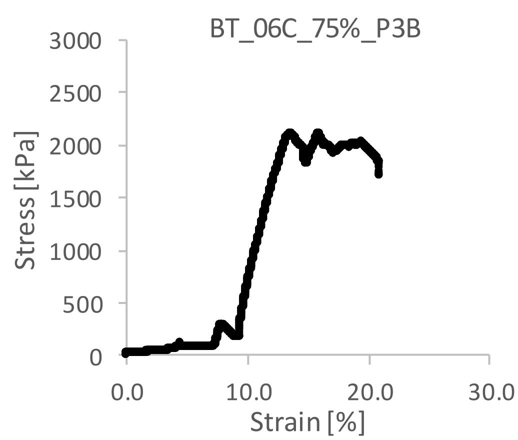
BT_06C_75%_P3B
Stress [kPa]
0
500
1000
1500
2000
2500
3000
0.0
10.0
20.0
30.0
Strain [%]

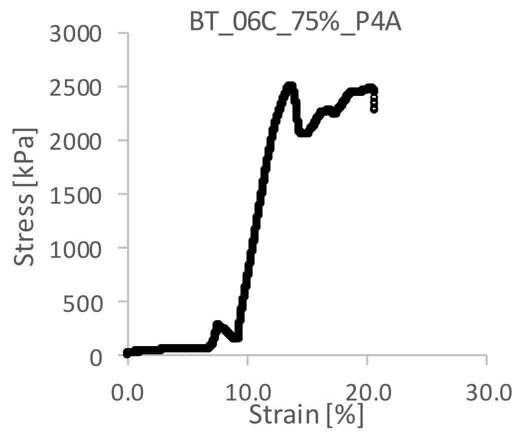
BT_06C_75%_P4A
Stress [kPa]
Strain [%]

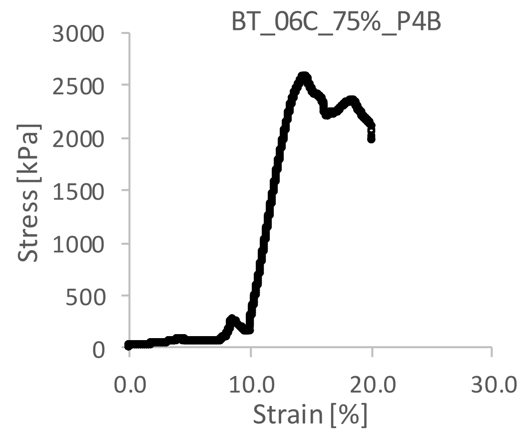
BT_06C_75%_P4B
Stress [kPa]
Strain [%]

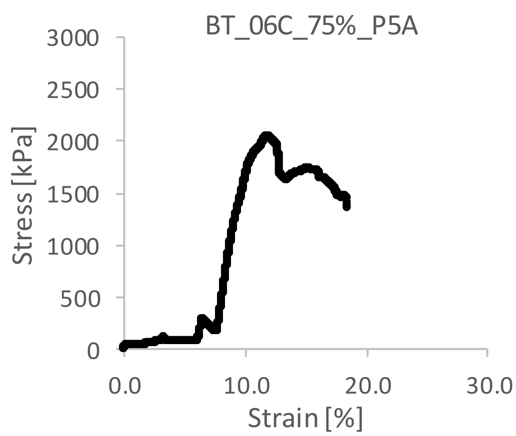
BT_06C_75%_P5A
Stress [kPa]
Strain [%]

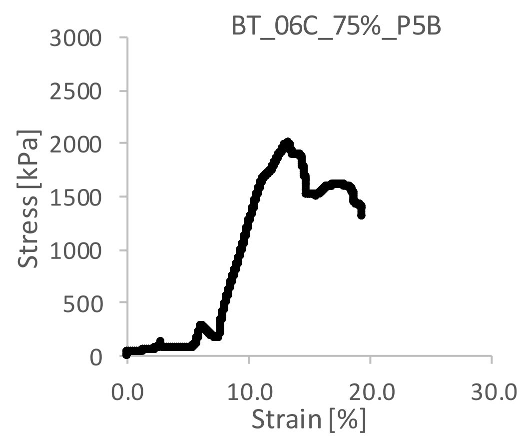
BT_06C_75%_P5B
Stress [kPa]
Strain [%]

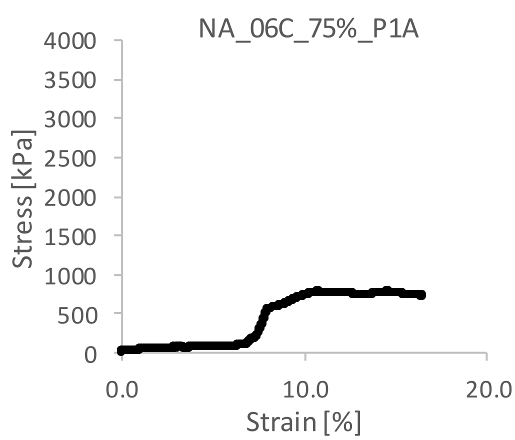
NA_06C_75%_P1A
Stress [kPa]
Strain [%]

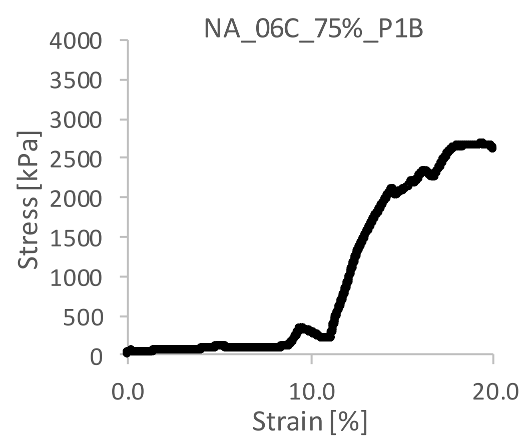
NA_06C_75%_P1B
Stress [kPa]
Strain [%]

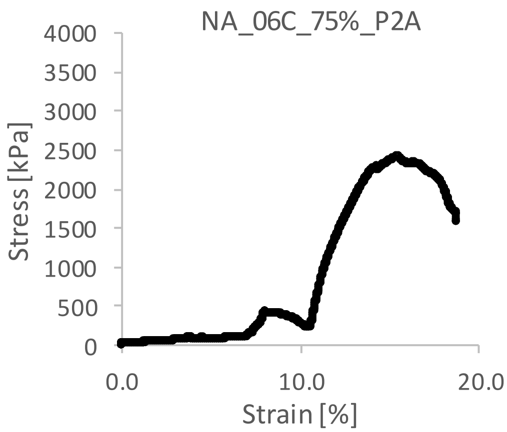
NA_06C_75%_P2A
Stress [kPa]
Strain [%]
4000
3500
3000
2500
2000
1500
1000
500
0
0.0
10.0
20.0

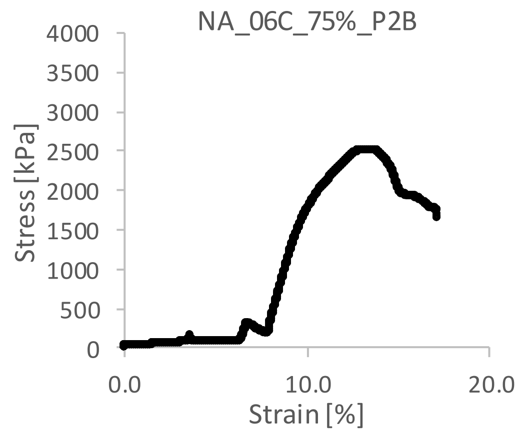
NA_06C_75%_P2B
Stress [kPa]
Strain [%]
4000
3500
3000
2500
2000
1500
1000
500
0
0.0
10.0
20.0

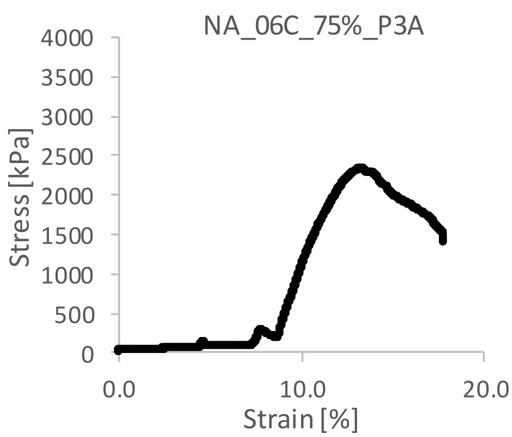
NA_06C_75%_P3A
Stress [kPa]
Strain [%]
4000
3500
3000
2500
2000
1500
1000
500
0
0.0
10.0
20.0

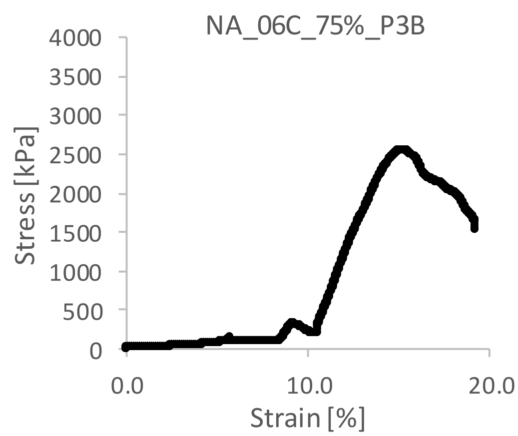
NA_06C_75%_P3B
Stress [kPa]
Strain [%]
4000
3500
3000
2500
2000
1500
1000
500
0
0.0
10.0
20.0

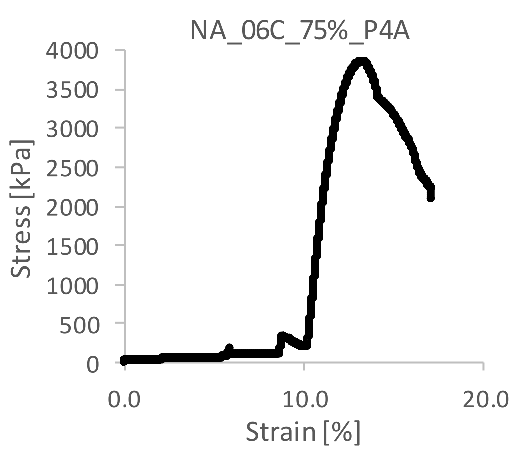
NA_06C_75%_P4A
Stress [kPa]
Strain [%]
4000
3500
3000
2500
2000
1500
1000
500
0
0.0
10.0
20.0

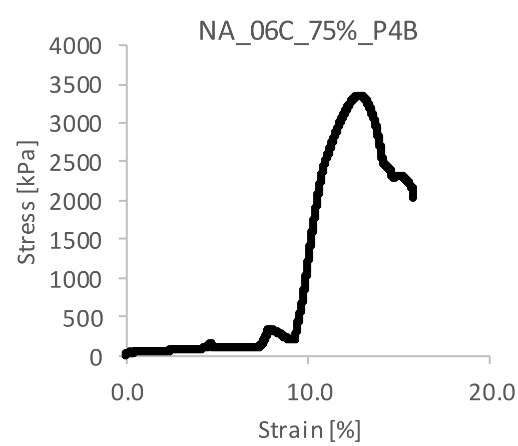
NA_06C_75%_P4B
Stress [kPa]
Strain [%]
4000
3500
3000
2500
2000
1500
1000
500
0
0.0
10.0
20.0

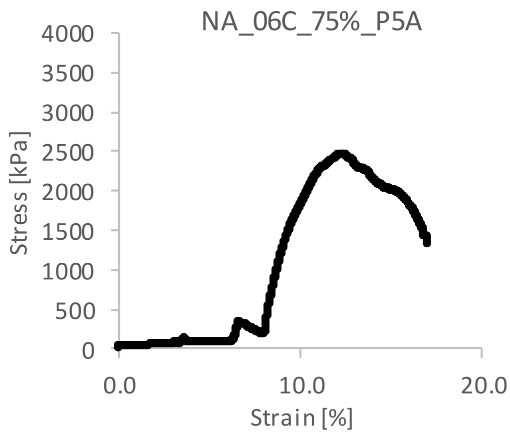
NA_06C_75%_P5A
Stress [kPa]
4000
3500
3000
2500
2000
1500
1000
500
0
0.0
10.0
20.0
Strain [%]

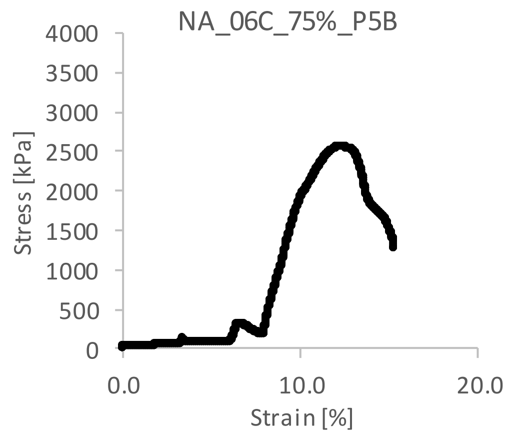
NA_06C_75%_P5B
Stress [kPa]
4000
3500
3000
2500
2000
1500
1000
500
0
0.0
10.0
20.0
Strain [%]

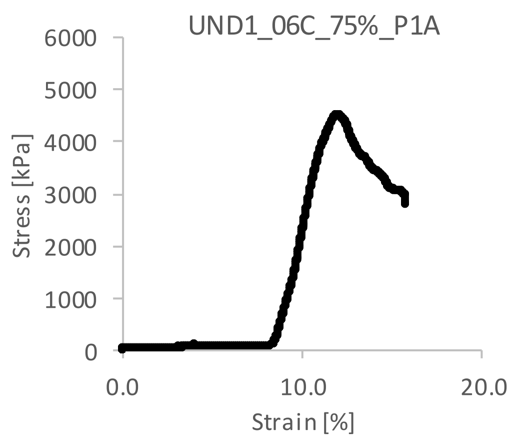
UND1_06C_75%_P1A
Stress [kPa]
6000
5000
4000
3000
2000
1000
0
0.0
10.0
20.0
Strain [%]

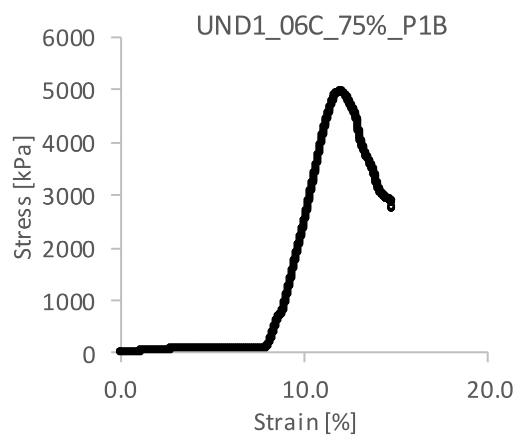
UND1_06C_75%_P1B
Stress [kPa]
6000
5000
4000
3000
2000
1000
0
0.0
10.0
20.0
Strain [%]

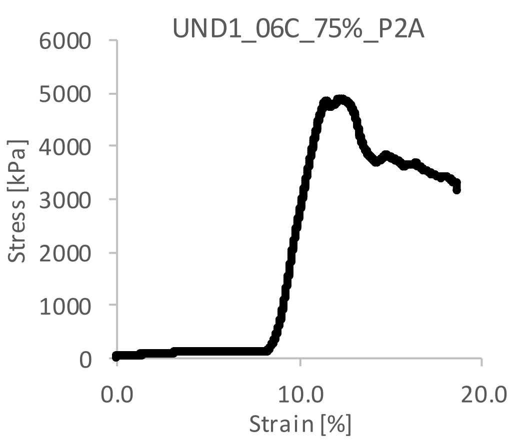
UND1_06C_75%_P2A
Stress [kPa]
6000
5000
4000
3000
2000
1000
0
0.0
10.0
20.0
Strain [%]

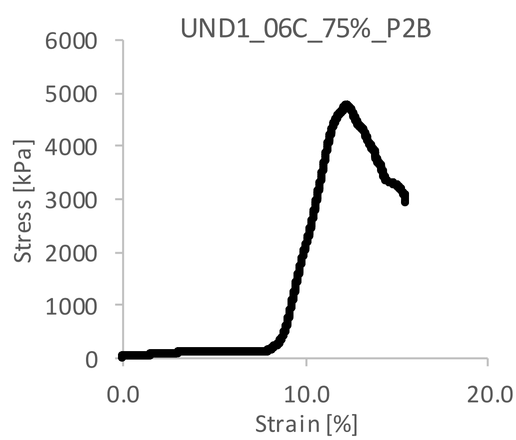
UND1_06C_75%_P2B
Stress [kPa]
6000
5000
4000
3000
2000
1000
0
0.0
10.0
20.0
Strain [%]

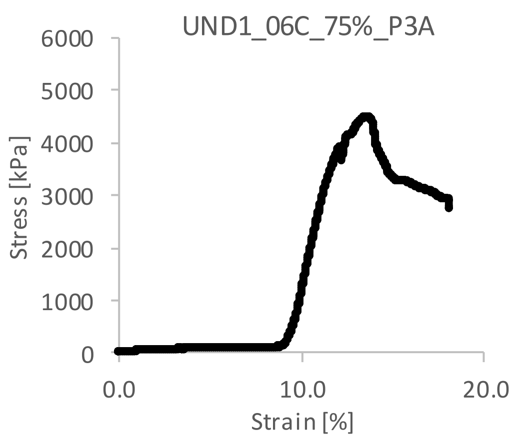
UND1_06C_75%_P3A
Stress [kPa]
Strain [%]

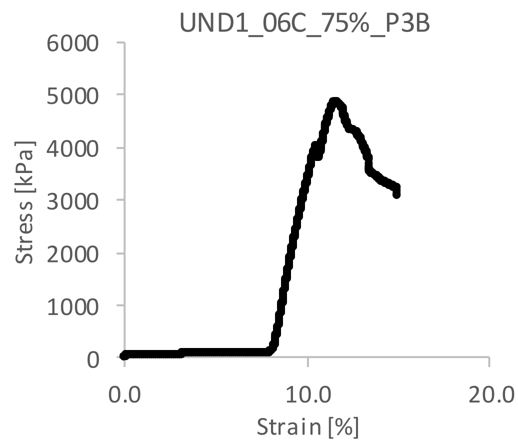
UND1_06C_75%_P3B
Stress [kPa]
Strain [%]

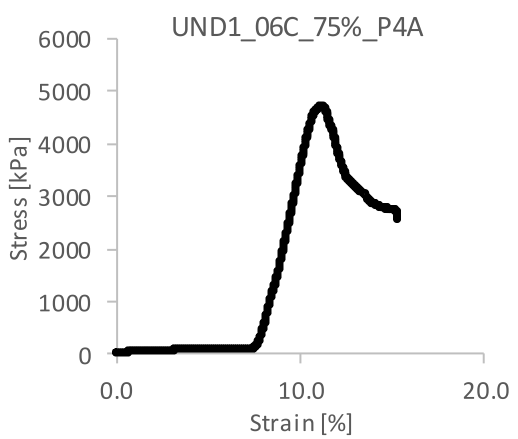
UND1_06C_75%_P4A
Stress [kPa]
Strain [%]

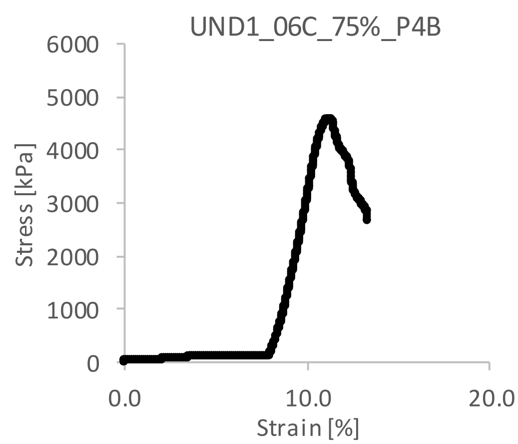
UND1_06C_75%_P4B
Stress [kPa]
Strain [%]

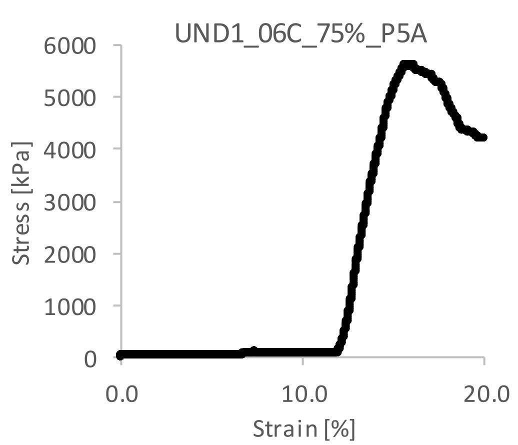
UND1_06C_75%_P5A
Stress [kPa]
Strain [%]

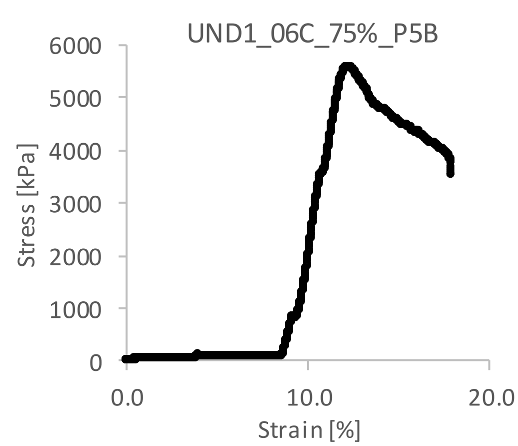
UND1_06C_75%_P5B
Stress [kPa]
Strain [%]

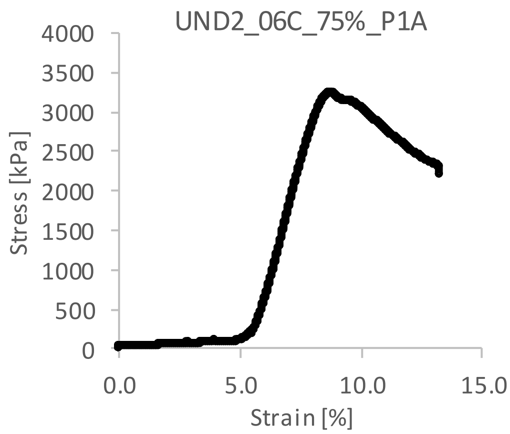
UND2_06C_75%_P1A
Stress [kPa]
Strain [%]

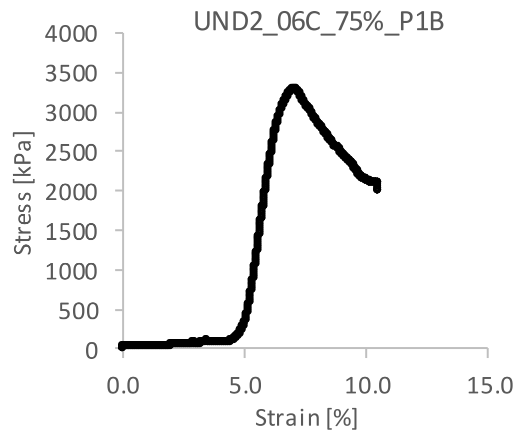
UND2_06C_75%_P1B
Stress [kPa]
Strain [%]

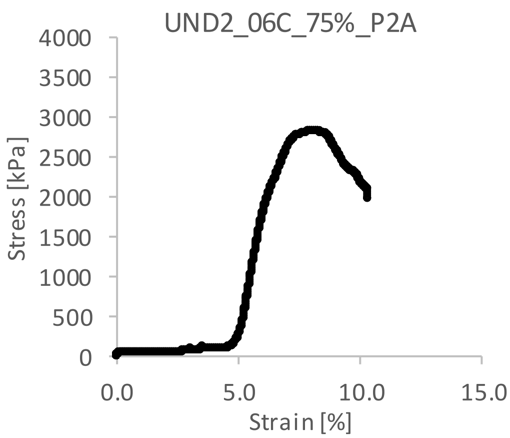
UND2_06C_75%_P2A
Stress [kPa]
Strain [%]

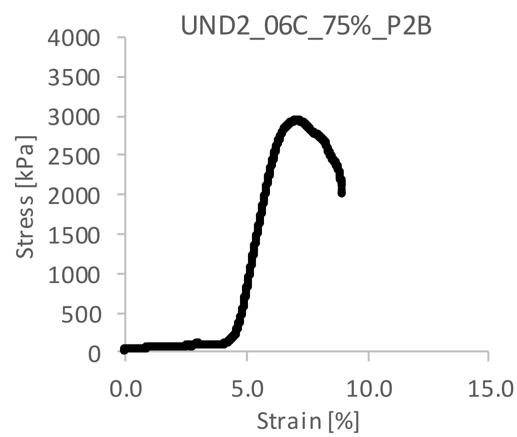
UND2_06C_75%_P2B
Stress [kPa]
Strain [%]

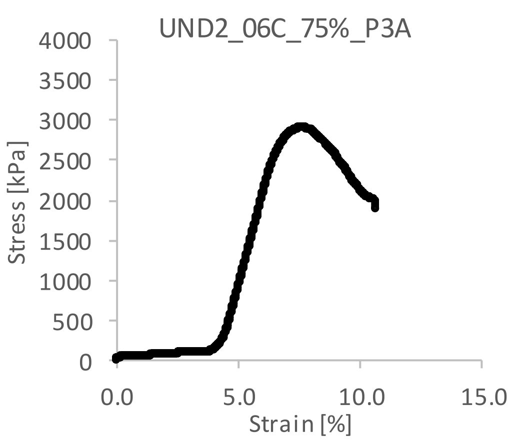
UND2_06C_75%_P3A
Stress [kPa]
Strain [%]

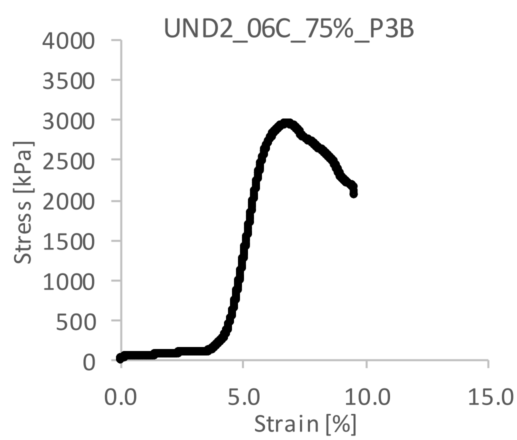
UND2_06C_75%_P3B
Stress [kPa]
Strain [%]

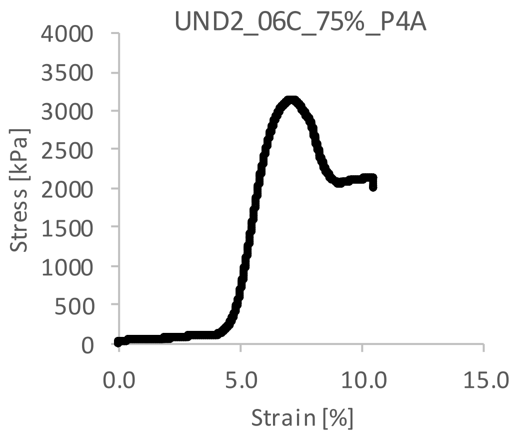
UND2_06C_75%_P4A
Stress [kPa]
4000
3500
3000
2500
2000
1500
1000
500
0
0.0
5.0
10.0
15.0
Strain [%]

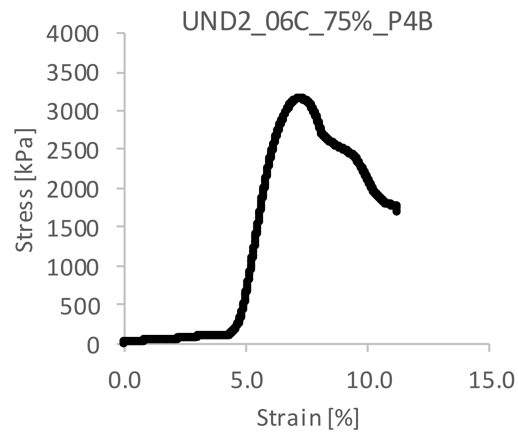
UND2_06C_75%_P4B
Stress [kPa]
4000
3500
3000
2500
2000
1500
1000
500
0
0.0
5.0
10.0
15.0
Strain [%]

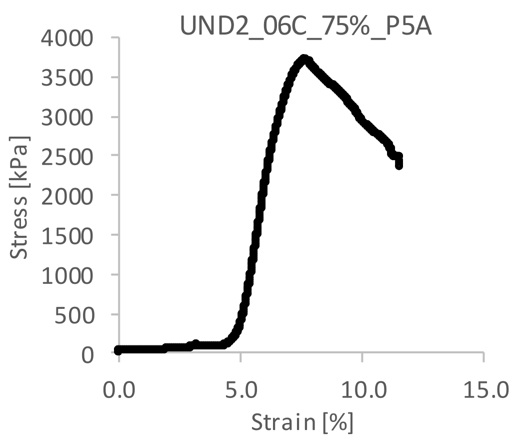
UND2_06C_75%_P5A
Stress [kPa]
4000
3500
3000
2500
2000
1500
1000
500
0
0.0
5.0
10.0
15.0
Strain [%]

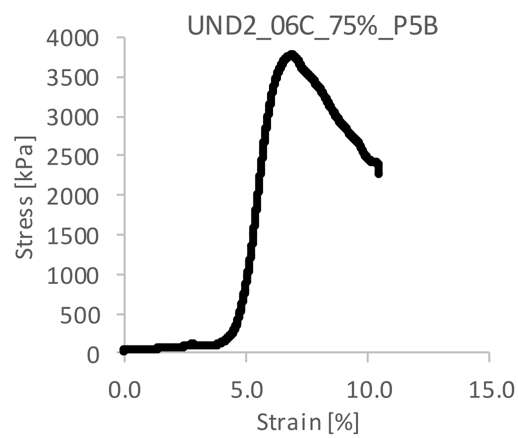
UND2_06C_75%_P5B
Stress [kPa]
4000
3500
3000
2500
2000
1500
1000
500
0
0.0
5.0
10.0
15.0
Strain [%]

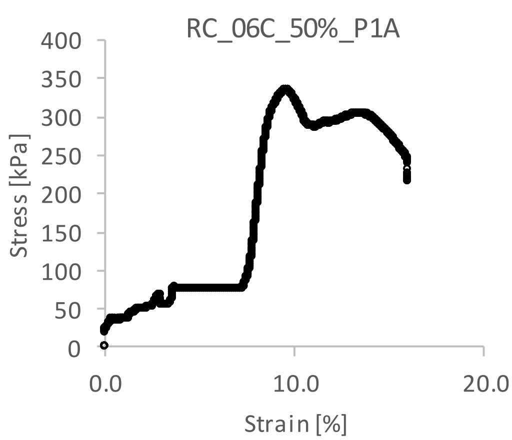
RC_06C_50%_P1A
Stress [kPa]
400
350
300
250
200
150
100
50
0
0.0
10.0
20.0
Strain [%]

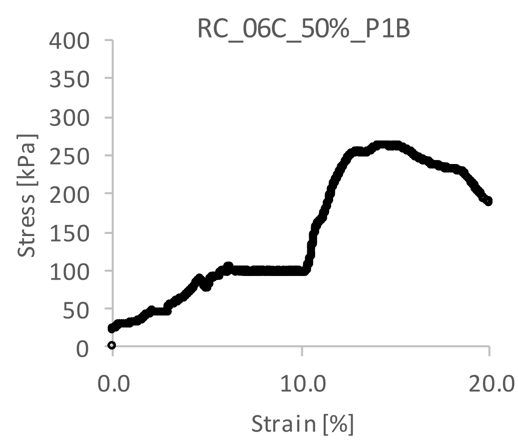
RC_06C_50%_P1B
Stress [kPa]
400
350
300
250
200
150
100
50
0
0.0
10.0
20.0
Strain [%]

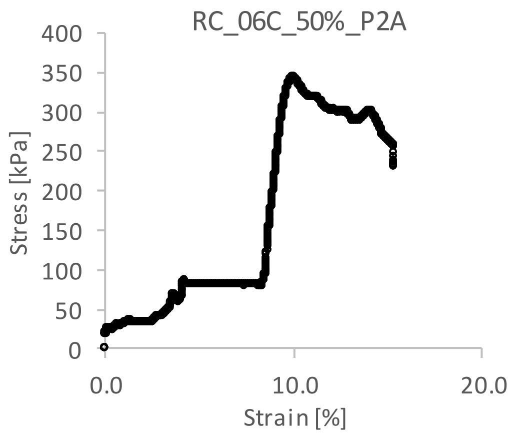
RC_06C_50%_P2A
Stress [kPa]
Strain [%]

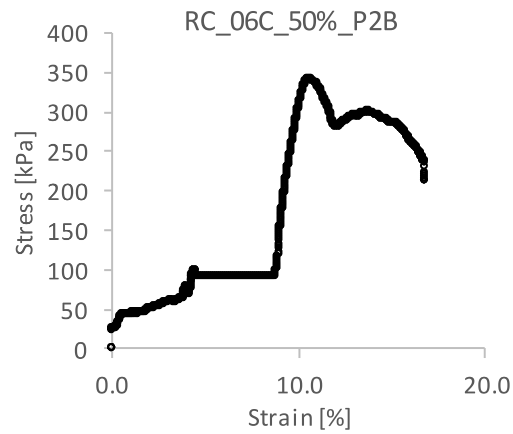
RC_06C_50%_P2B
Stress [kPa]
Strain [%]

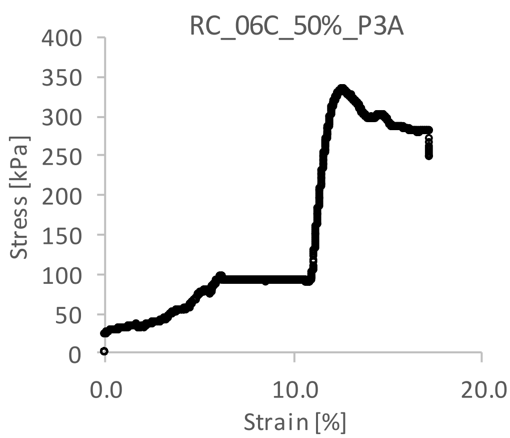
RC_06C_50%_P3A
Stress [kPa]
Strain [%]

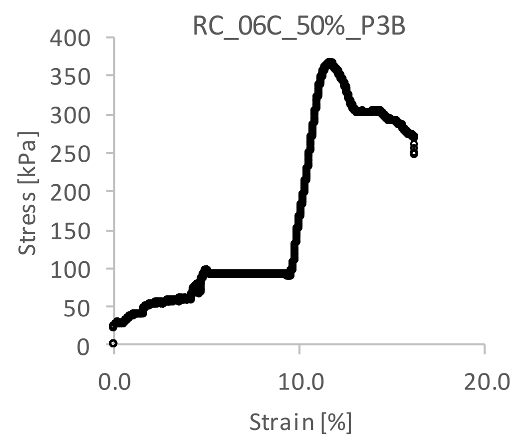
RC_06C_50%_P3B
Stress [kPa]
Strain [%]

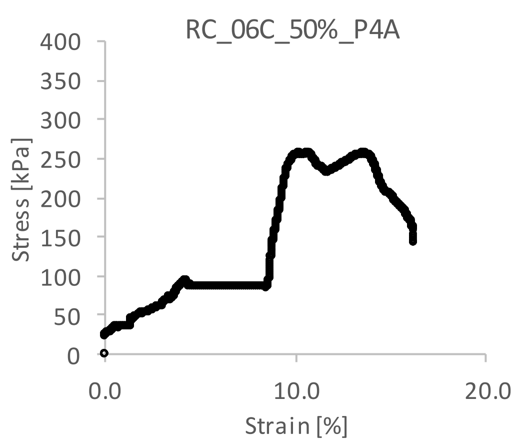
RC_06C_50%_P4A
Stress [kPa]
Strain [%]

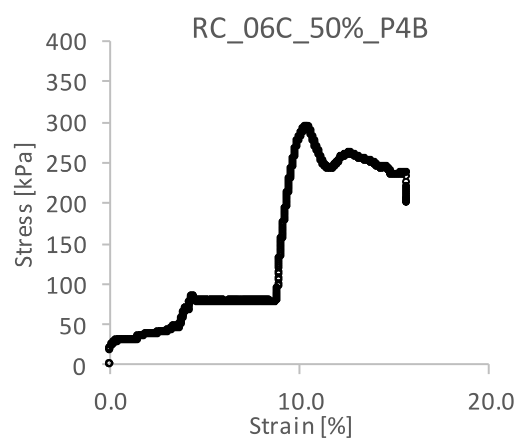
RC_06C_50%_P4B
Stress [kPa]
Strain [%]

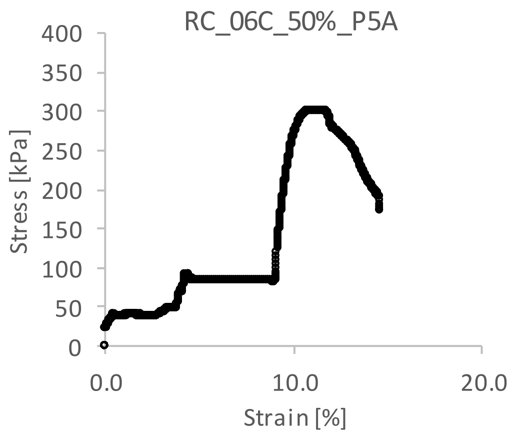
RC_06C_50%_P5A
Stress [kPa]
Strain [%]
0
50
100
150
200
250
300
350
400
0.0
10.0
20.0

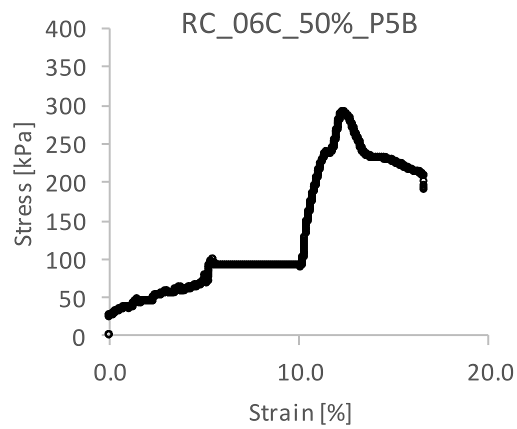
RC_06C_50%_P5B
Stress [kPa]
Strain [%]
0
50
100
150
200
250
300
350
400
0.0
10.0
20.0

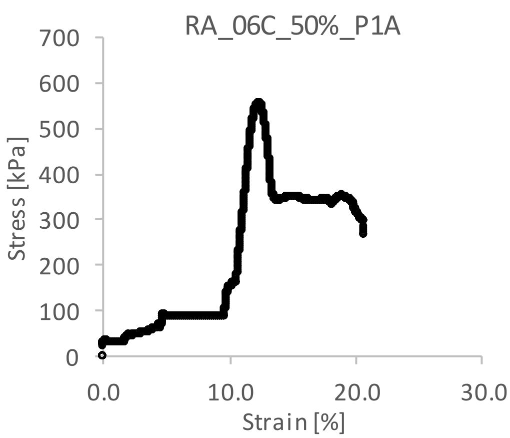
RA_06C_50%_P1A
Stress [kPa]
Strain [%]
0
100
200
300
400
500
600
700
0.0
10.0
20.0
30.0

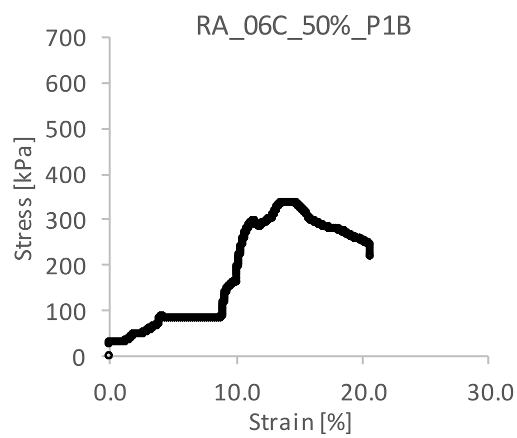
RA_06C_50%_P1B
Stress [kPa]
Strain [%]
0
100
200
300
400
500
600
700
0.0
10.0
20.0
30.0

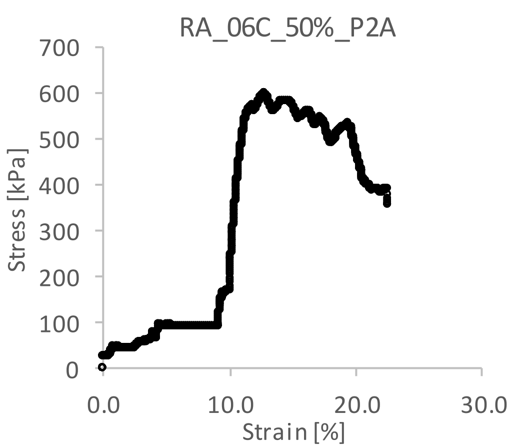
RA_06C_50%_P2A
Stress [kPa]
Strain [%]
0
100
200
300
400
500
600
700
0.0
10.0
20.0
30.0

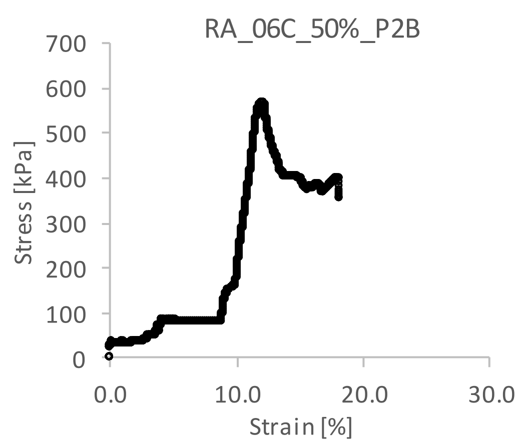
RA_06C_50%_P2B
Stress [kPa]
Strain [%]
0
100
200
300
400
500
600
700
0.0
10.0
20.0
30.0

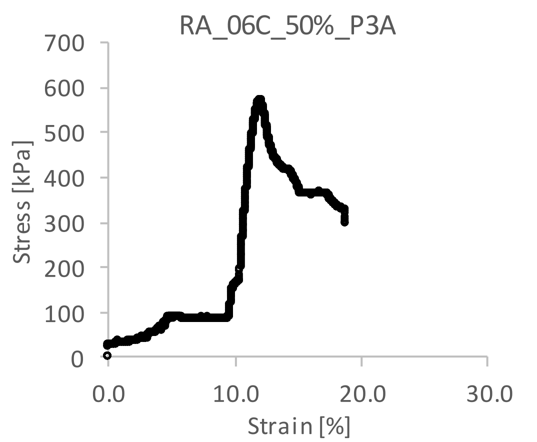
RA_06C_50%_P3A
Stress [kPa]
Strain [%]
0
100
200
300
400
500
600
700
0.0
10.0
20.0
30.0

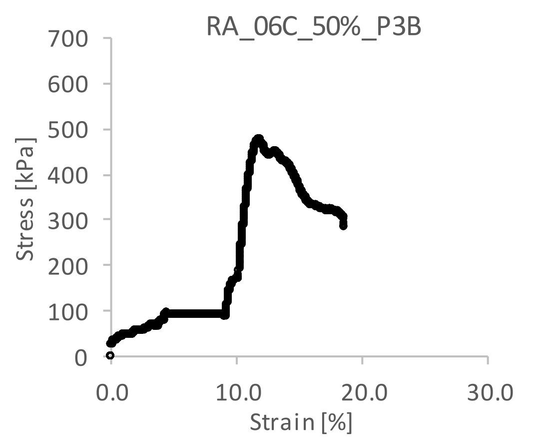
RA_06C_50%_P3B
Stress [kPa]
Strain [%]
0
100
200
300
400
500
600
700
0.0
10.0
20.0
30.0

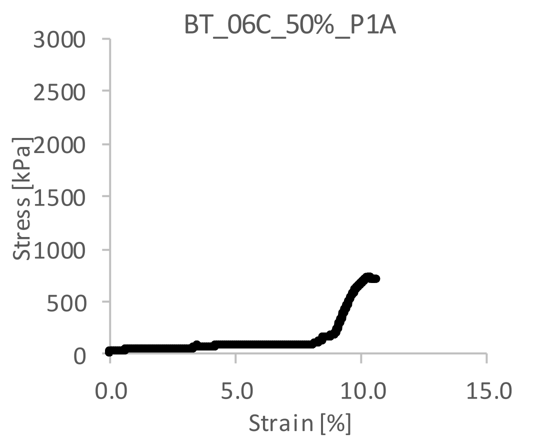
BT_06C_50%_P1A
Stress [kPa]
Strain [%]
0
500
1000
1500
2000
2500
3000
0.0
5.0
10.0
15.0

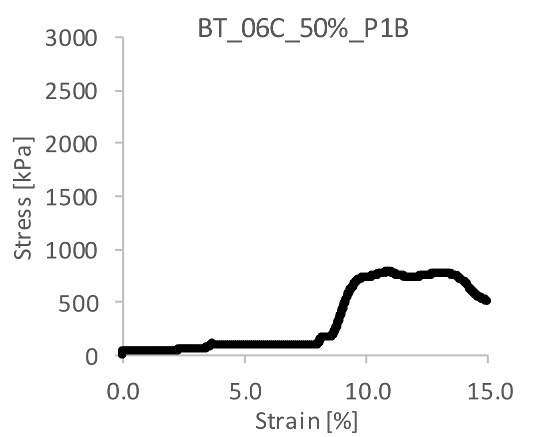
BT_06C_50%_P1B
Stress [kPa]
Strain [%]
0
500
1000
1500
2000
2500
3000
0.0
5.0
10.0
15.0

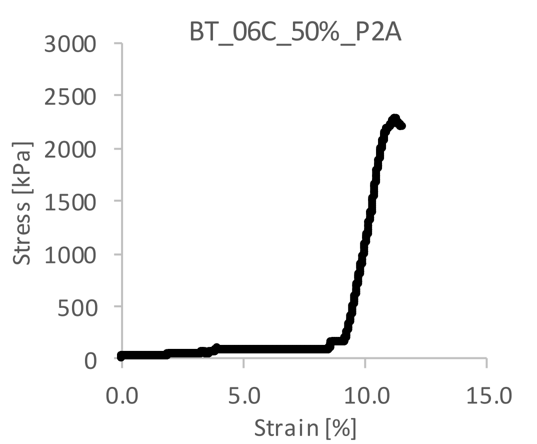
BT_06C_50%_P2A
Stress [kPa]
Strain [%]
0
500
1000
1500
2000
2500
3000
0.0
5.0
10.0
15.0

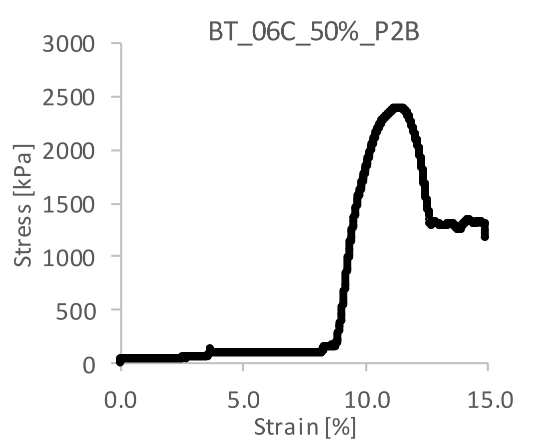
BT_06C_50%_P2B
Stress [kPa]
Strain [%]
0
500
1000
1500
2000
2500
3000
0.0
5.0
10.0
15.0

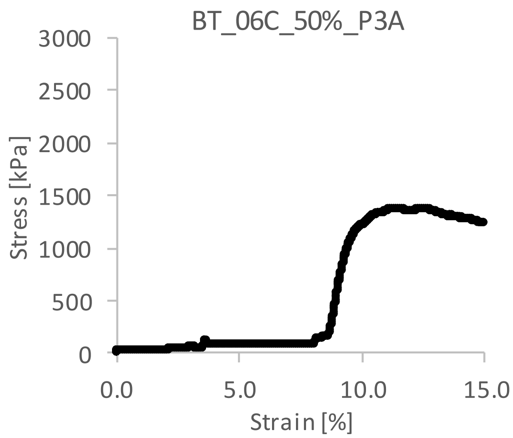
BT_06C_50%_P3A
Stress [kPa]
Strain [%]

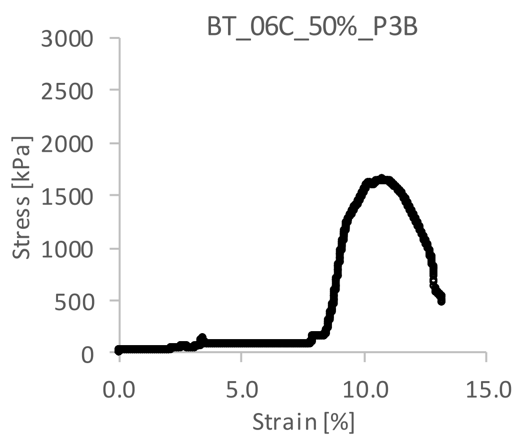
BT_06C_50%_P3B
Stress [kPa]
Strain [%]

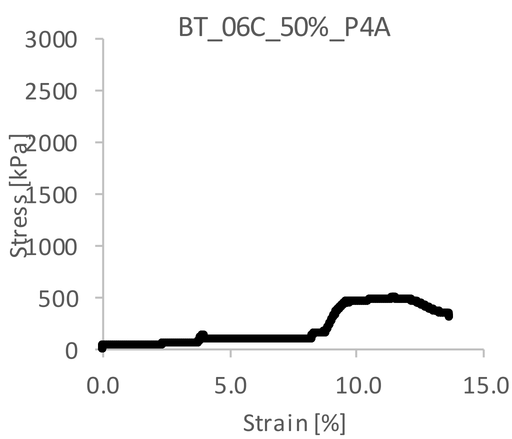
BT_06C_50%_P4A
Stress [kPa]
Strain [%]

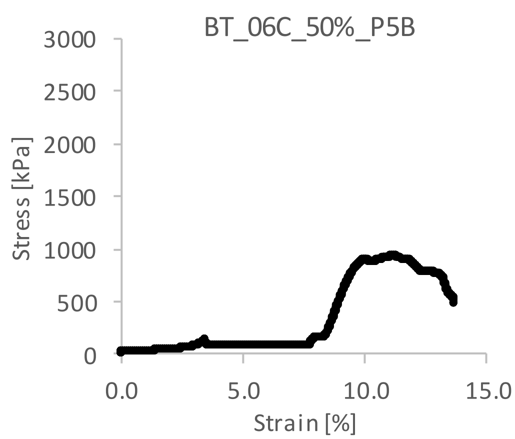
BT_06C_50%_P5B
Stress [kPa]
Strain [%]

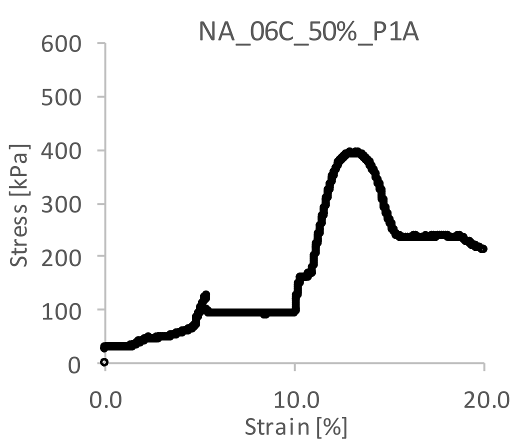
NA_06C_50%_P1A
Stress [kPa]
Strain [%]

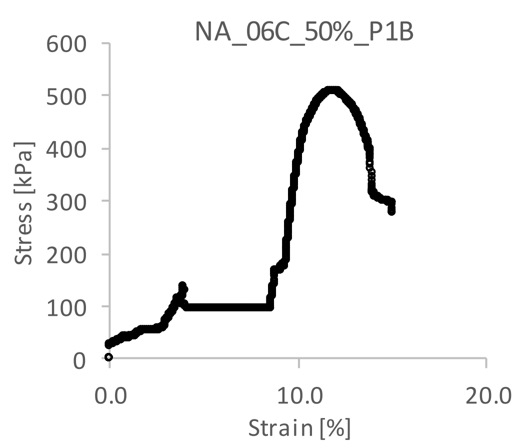
NA_06C_50%_P1B
Stress [kPa]
Strain [%]

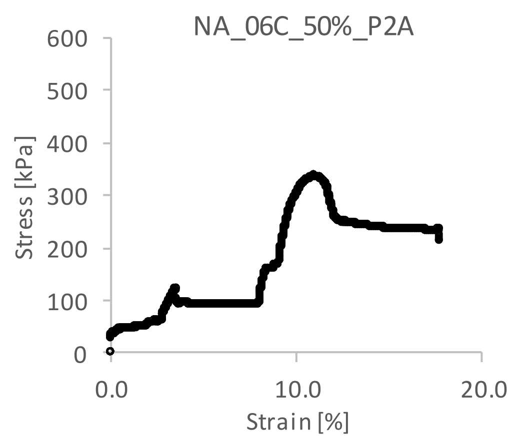
NA_06C_50%_P2A
Stress [kPa]
0
100
200
300
400
500
600
Strain [%]
0.0
10.0
20.0

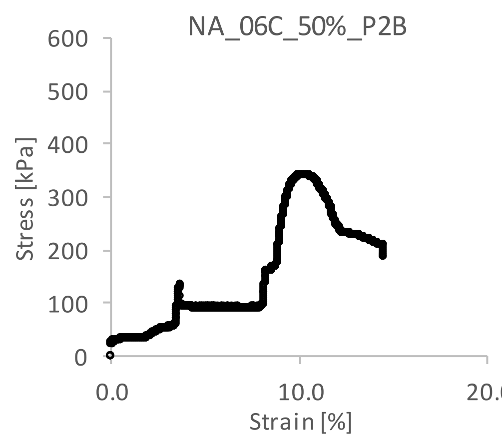
NA_06C_50%_P2B
Stress [kPa]
0
100
200
300
400
500
600
Strain [%]
0.0
10.0
20.0

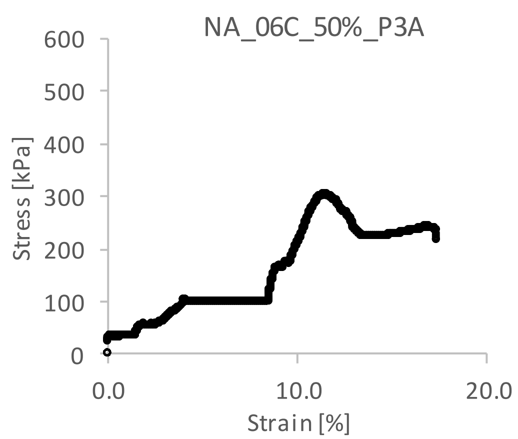
NA_06C_50%_P3A
Stress [kPa]
0
100
200
300
400
500
600
Strain [%]
0.0
10.0
20.0

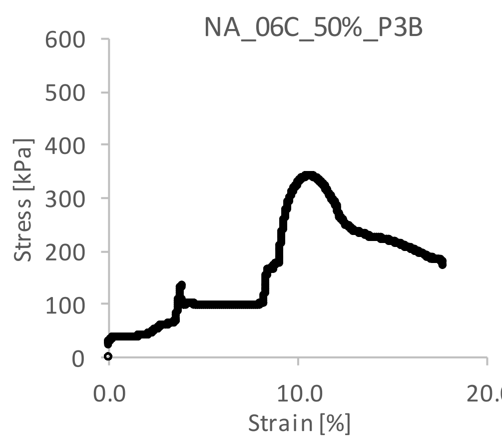
NA_06C_50%_P3B
Stress [kPa]
0
100
200
300
400
500
600
Strain [%]
0.0
10.0
20.0

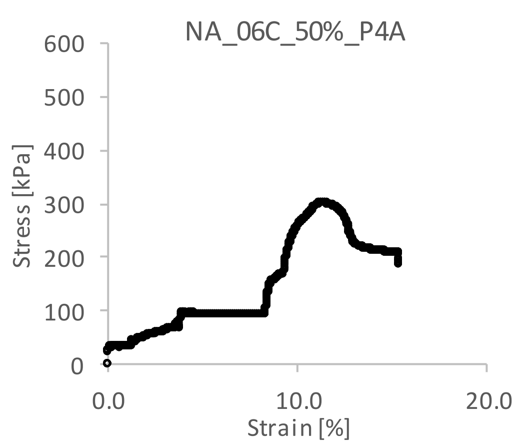
NA_06C_50%_P4A
Stress [kPa]
0
100
200
300
400
500
600
Strain [%]
0.0
10.0
20.0

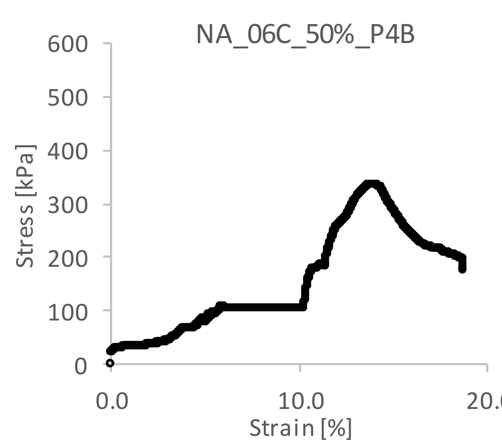
NA_06C_50%_P4B
Stress [kPa]
0
100
200
300
400
500
600
Strain [%]
0.0
10.0
20.0

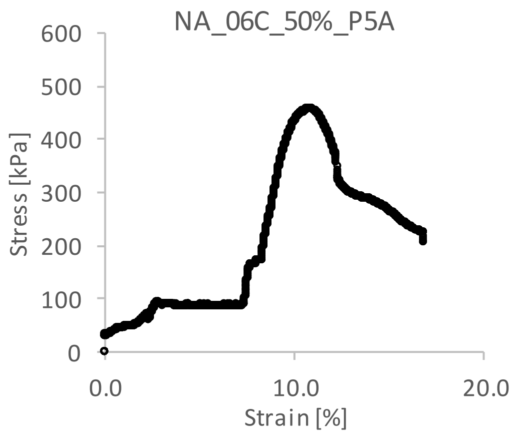
NA_06C_50%_P5A
Stress [kPa]
0
100
200
300
400
500
600
0.0
10.0
20.0
Strain [%]

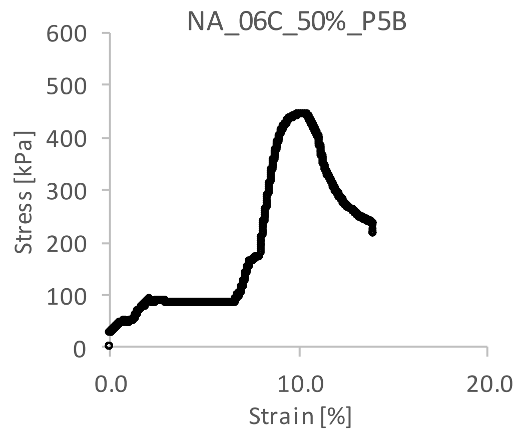
NA_06C_50%_P5B
Stress [kPa]
0
100
200
300
400
500
600
0.0
10.0
20.0
Strain [%]

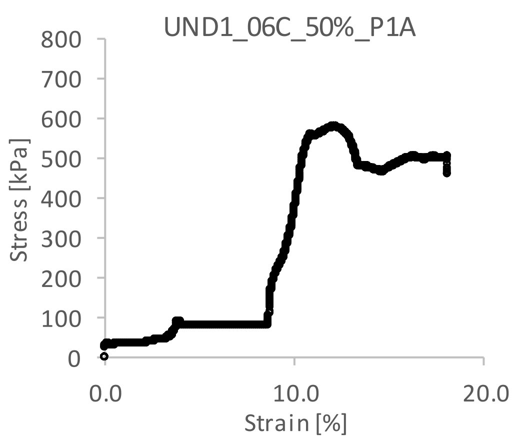
UND1_06C_50%_P1A
Stress [kPa]
0
100
200
300
400
500
600
700
800
0.0
10.0
20.0
Strain [%]

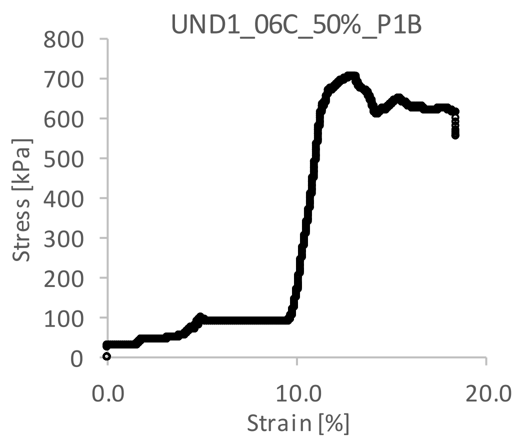
UND1_06C_50%_P1B
Stress [kPa]
0
100
200
300
400
500
600
700
800
0.0
10.0
20.0
Strain [%]

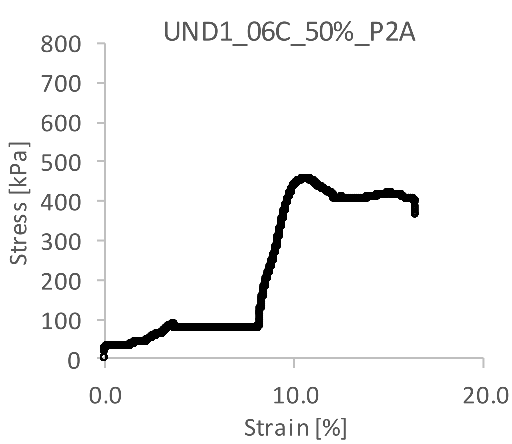
UND1_06C_50%_P2A
Stress [kPa]
0
100
200
300
400
500
600
700
800
0.0
10.0
20.0
Strain [%]

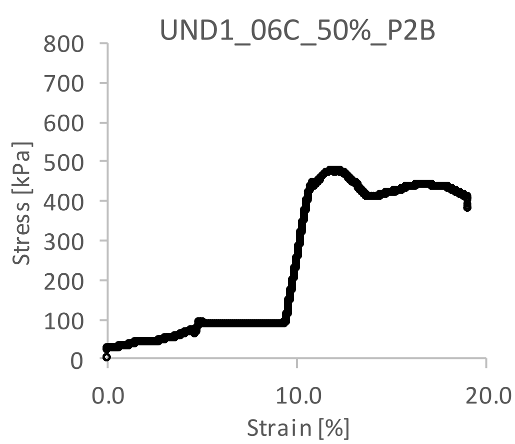
UND1_06C_50%_P2B
Stress [kPa]
0
100
200
300
400
500
600
700
800
0.0
10.0
20.0
Strain [%]

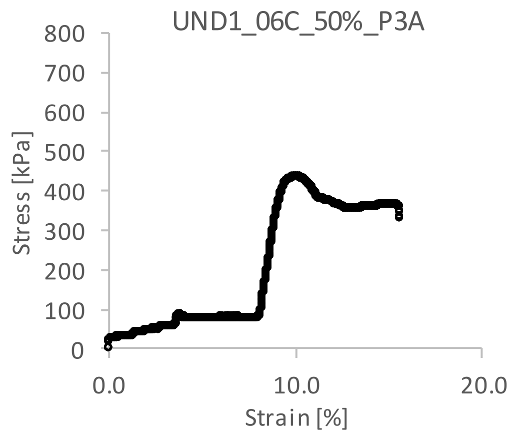
UND1_06C_50%_P3A
Stress [kPa]
Strain [%]
0
100
200
300
400
500
600
700
800
0.0
10.0
20.0

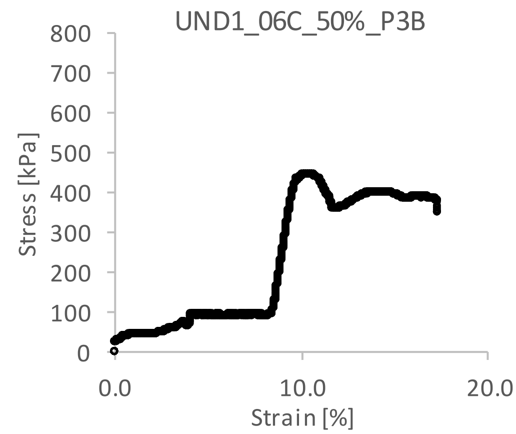
UND1_06C_50%_P3B
Stress [kPa]
Strain [%]
0
100
200
300
400
500
600
700
800
0.0
10.0
20.0

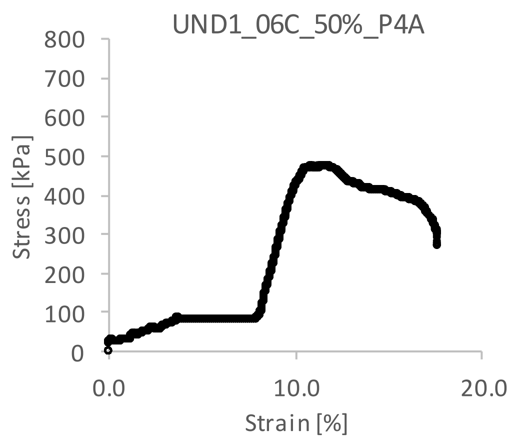
UND1_06C_50%_P4A
Stress [kPa]
Strain [%]
0
100
200
300
400
500
600
700
800
0.0
10.0
20.0

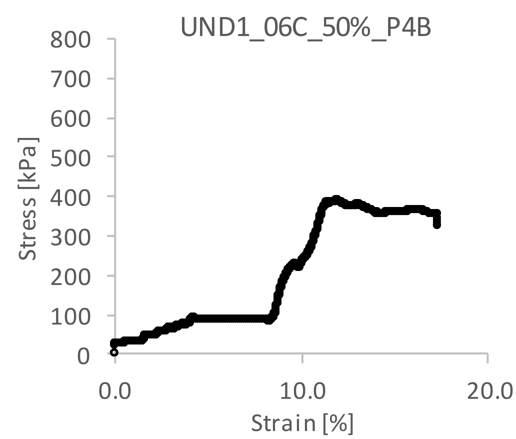
UND1_06C_50%_P4B
Stress [kPa]
Strain [%]
0
100
200
300
400
500
600
700
800
0.0
10.0
20.0

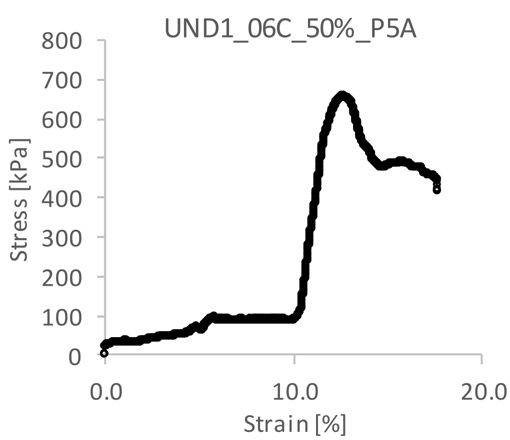
UND1_06C_50%_P5A
Stress [kPa]
Strain [%]
0
100
200
300
400
500
600
700
800
0.0
10.0
20.0

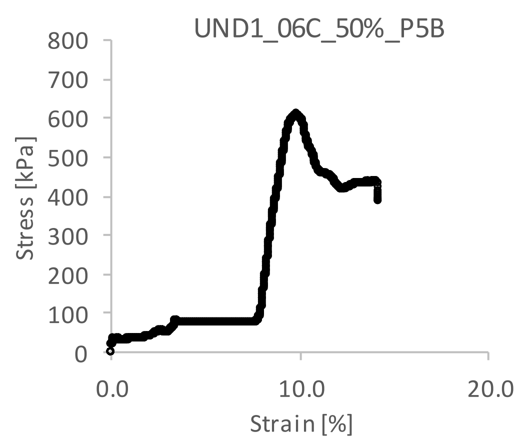
UND1_06C_50%_P5B
Stress [kPa]
Strain [%]
0
100
200
300
400
500
600
700
800
0.0
10.0
20.0

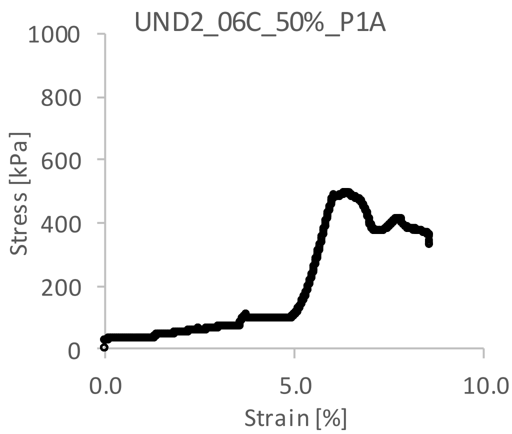
UND2_06C_50%_P1A
Stress [kPa]
Strain [%]

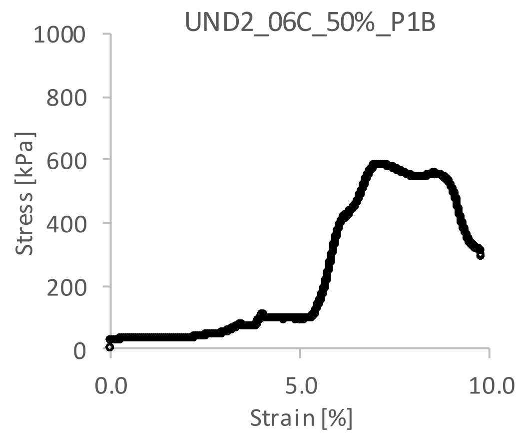
UND2_06C_50%_P1B
Stress [kPa]
Strain [%]

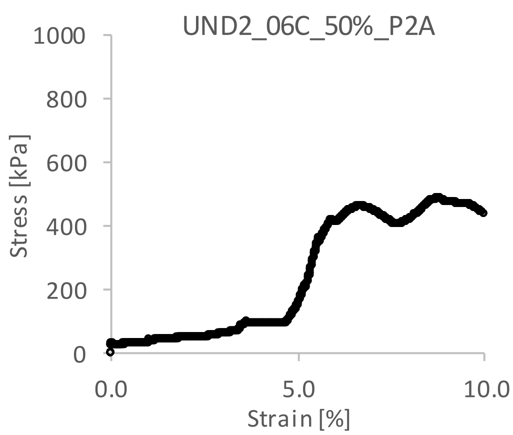
UND2_06C_50%_P2A
Stress [kPa]
Strain [%]

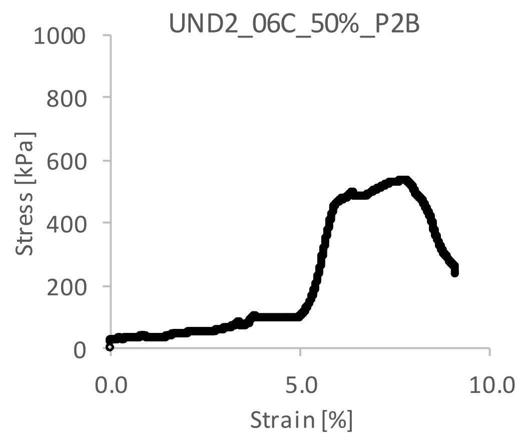
UND2_06C_50%_P2B
Stress [kPa]
Strain [%]

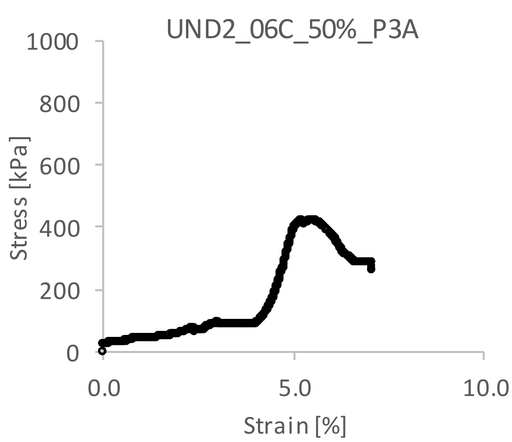
UND2_06C_50%_P3A
Stress [kPa]
Strain [%]

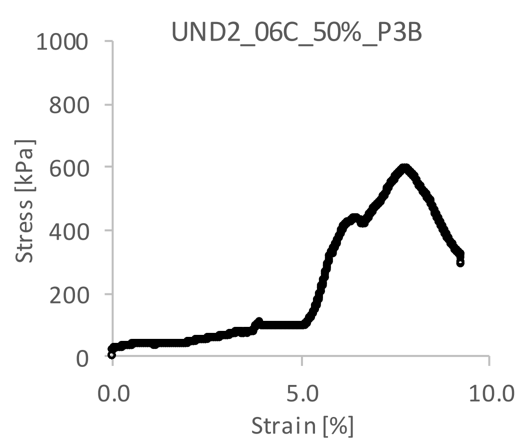
UND2_06C_50%_P3B
Stress [kPa]
Strain [%]

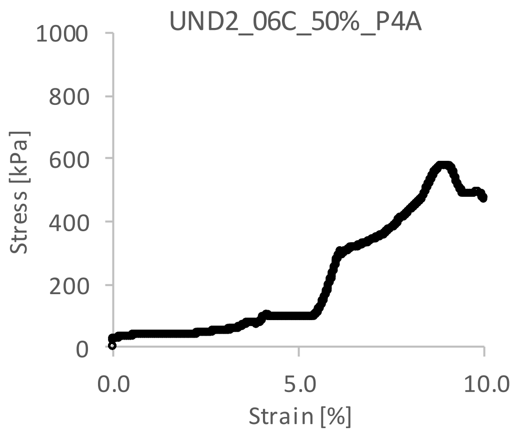

UND2_06C_50%_P4A
Stress [kPa]
1000
800
600
400
200
0
0.0
5.0
10.0
Strain [%]

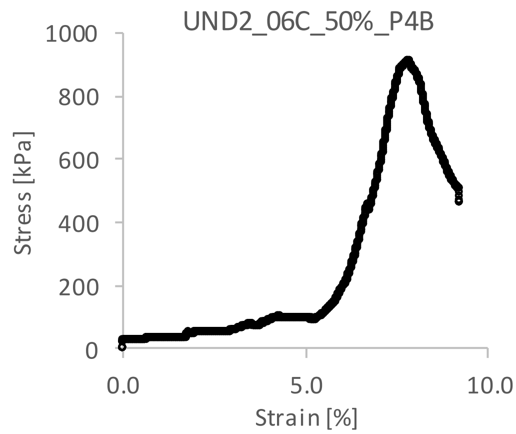

UND2_06C_50%_P4B
Stress [kPa]
1000
800
600
400
200
0
0.0
5.0
10.0
Strain [%]

Stress-Strain curves for l/s = 0.5

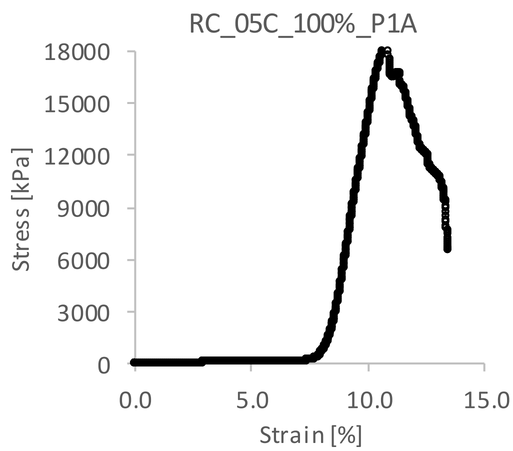

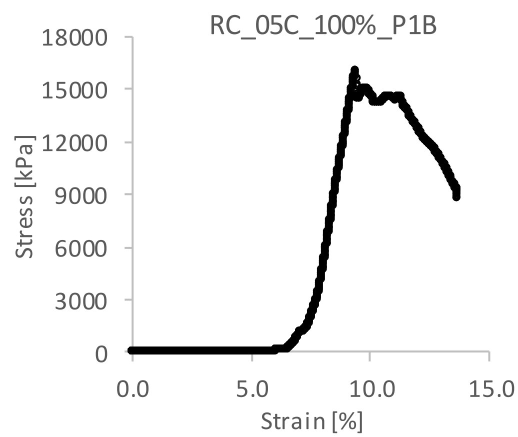

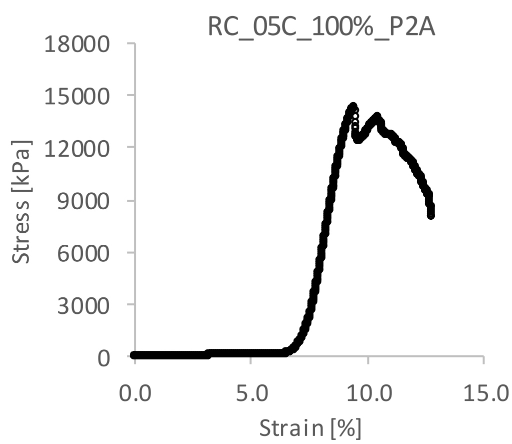

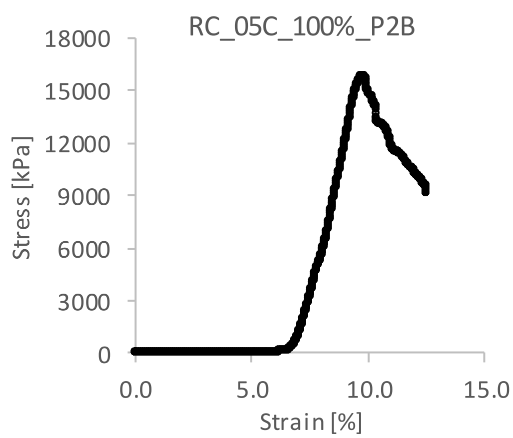

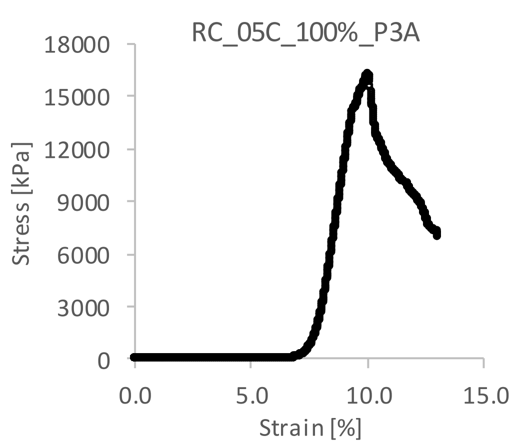

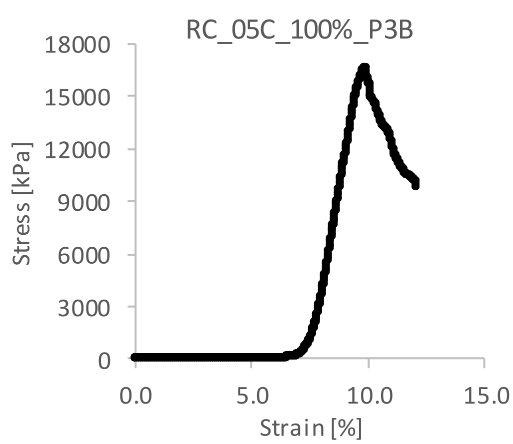

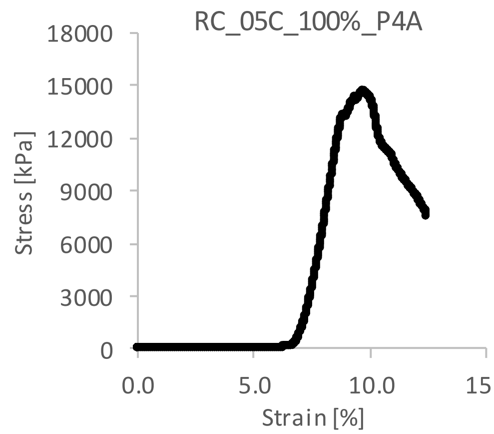
RC_05C_100%_P4A
Stress [kPa]
Strain [%]
0
3000
6000
9000
12000
15000
18000
0.0
5.0
10.0
15.0

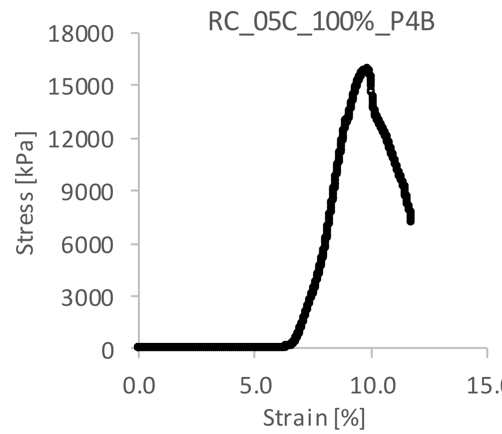
RC_05C_100%_P4B
Stress [kPa]
Strain [%]
0
3000
6000
9000
12000
15000
18000
0.0
5.0
10.0
15.0

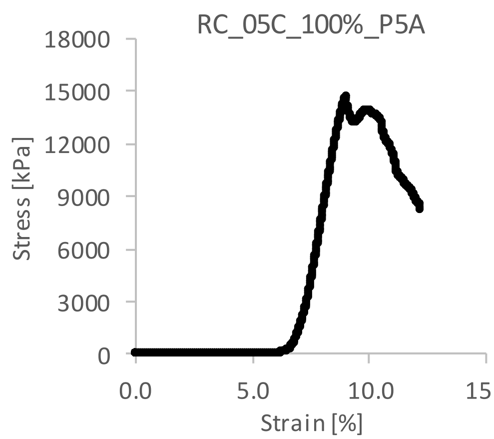
RC_05C_100%_P5A
Stress [kPa]
Strain [%]
0
3000
6000
9000
12000
15000
18000
0.0
5.0
10.0
15.0

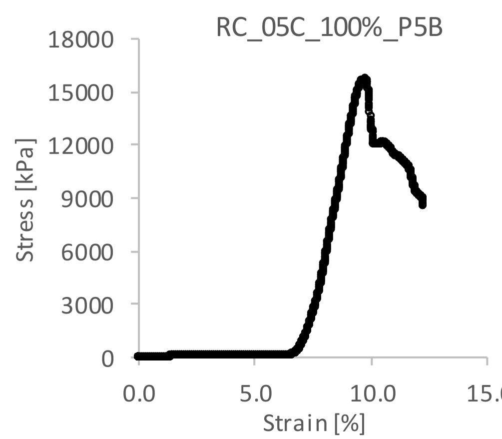
RC_05C_100%_P5B
Stress [kPa]
Strain [%]
0
3000
6000
9000
12000
15000
18000
0.0
5.0
10.0
15.0

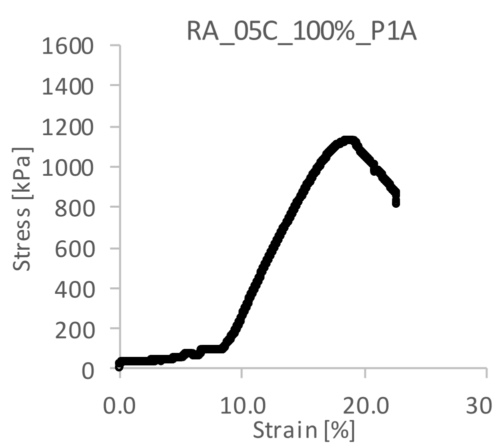
RA_05C_100%_P1A
Stress [kPa]
Strain [%]
0
200
400
600
800
1000
1200
1400
1600
0.0
10.0
20.0
30.0

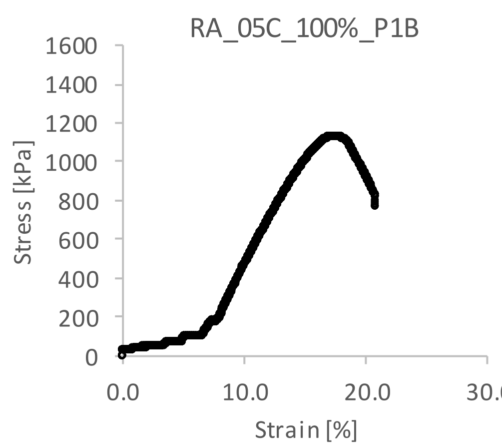
RA_05C_100%_P1B
Stress [kPa]
Strain [%]
0
200
400
600
800
1000
1200
1400
1600
0.0
10.0
20.0
30.0

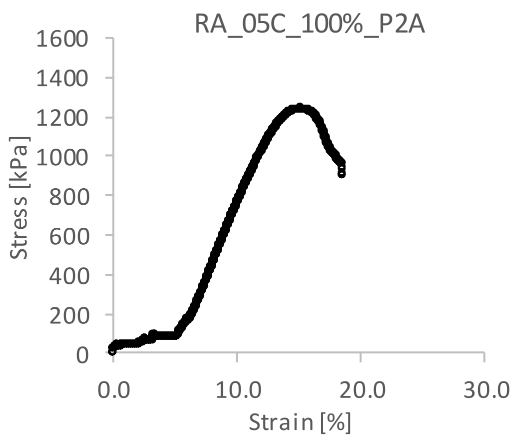
RA_05C_100%_P2A
Stress [kPa]
Strain [%]

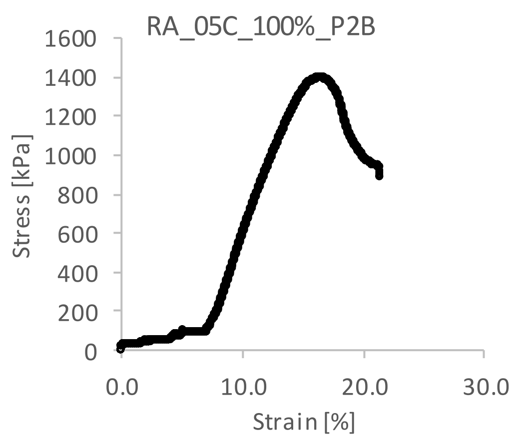
RA_05C_100%_P2B
Stress [kPa]
Strain [%]

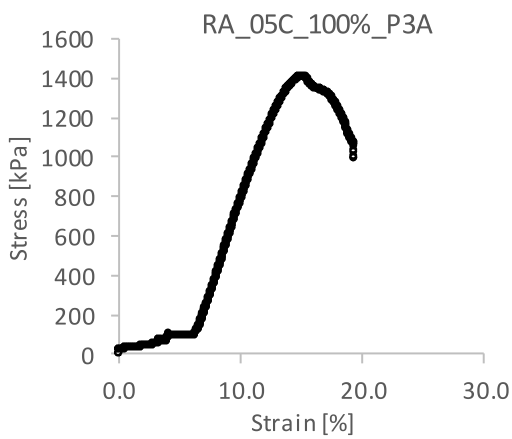
RA_05C_100%_P3A
Stress [kPa]
Strain [%]

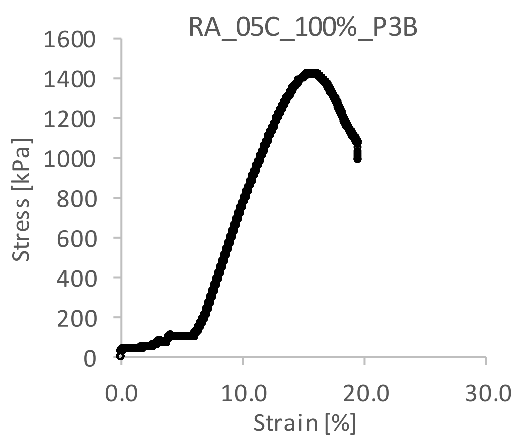
RA_05C_100%_P3B
Stress [kPa]
Strain [%]

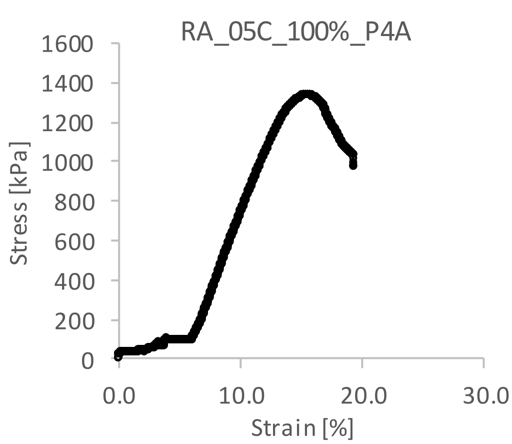
RA_05C_100%_P4A
Stress [kPa]
Strain [%]

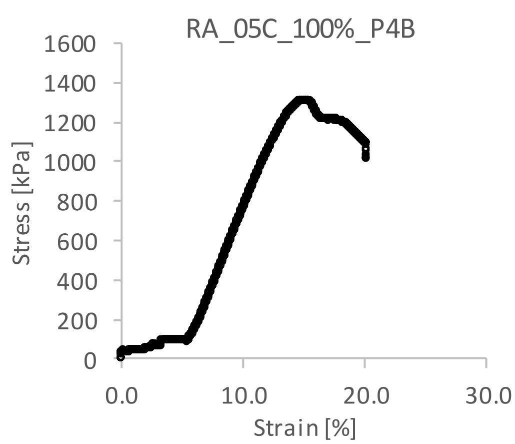
RA_05C_100%_P4B
Stress [kPa]
Strain [%]

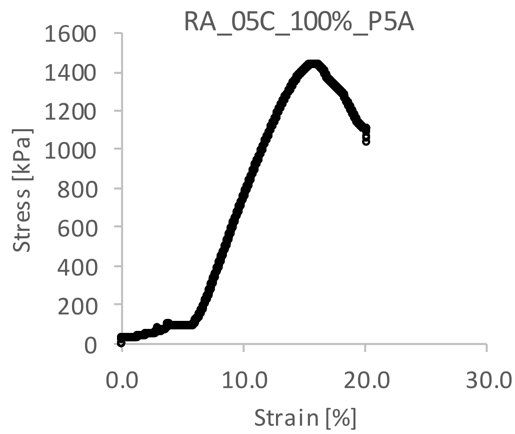
RA_05C_100%_P5A
Stress [kPa]
Strain [%]
1600
1400
1200
1000
800
600
400
200
0
0.0
10.0
20.0
30.0

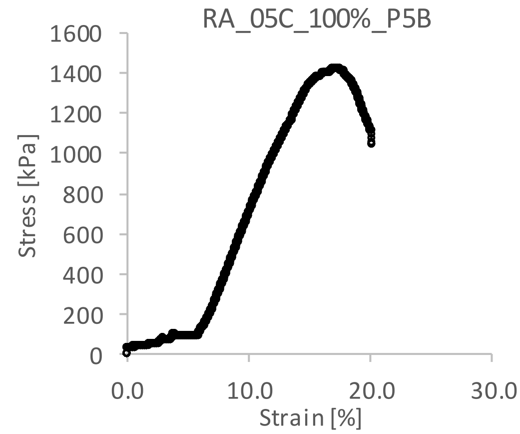
RA_05C_100%_P5B
Stress [kPa]
Strain [%]
1600
1400
1200
1000
800
600
400
200
0
0.0
10.0
20.0
30.0

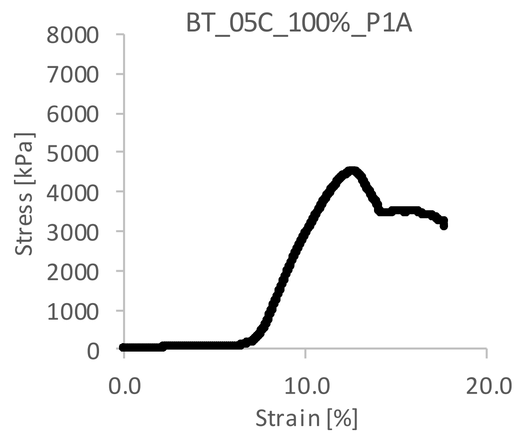
BT_05C_100%_P1A
Stress [kPa]
Strain [%]
8000
7000
6000
5000
4000
3000
2000
1000
0
0.0
10.0
20.0

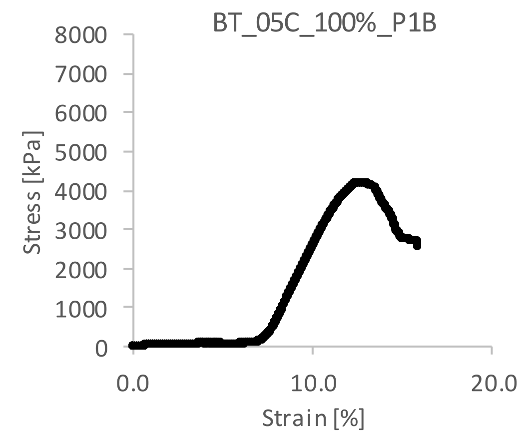
BT_05C_100%_P1B
Stress [kPa]
Strain [%]
8000
7000
6000
5000
4000
3000
2000
1000
0
0.0
10.0
20.0

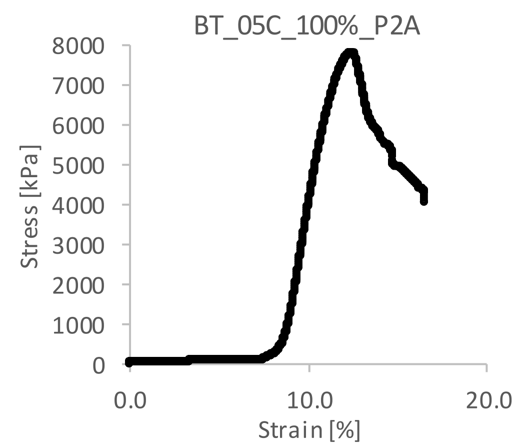
BT_05C_100%_P2A
Stress [kPa]
Strain [%]
8000
7000
6000
5000
4000
3000
2000
1000
0
0.0
10.0
20.0

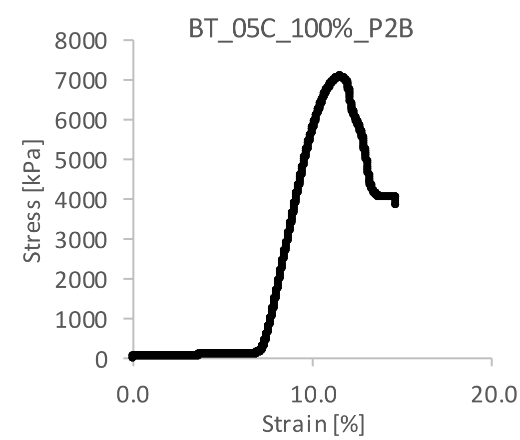
BT_05C_100%_P2B
Stress [kPa]
Strain [%]
8000
7000
6000
5000
4000
3000
2000
1000
0
0.0
10.0
20.0

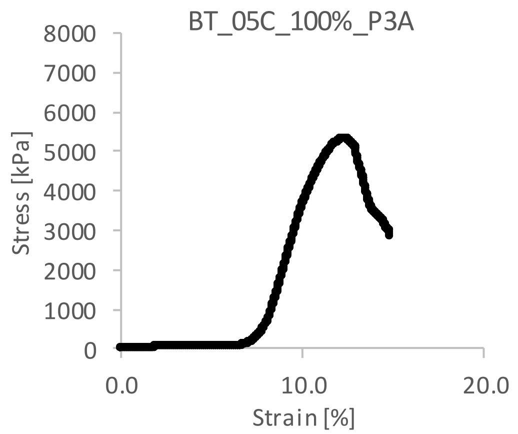
BT_05C_100%_P3A
8000
7000
6000
5000
4000
3000
2000
1000
0
Stress [kPa]
0.0
10.0
20.0
Strain [%]

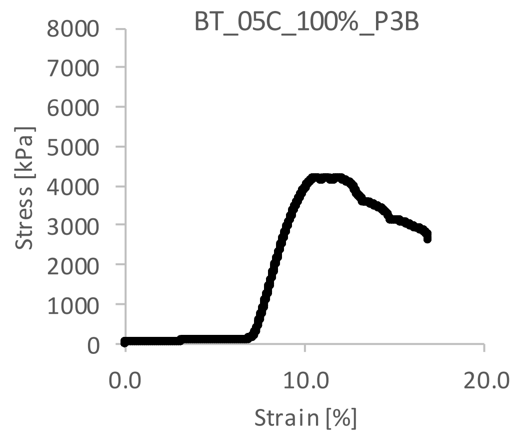
BT_05C_100%_P3B
8000
7000
6000
5000
4000
3000
2000
1000
0
Stress [kPa]
0.0
10.0
20.0
Strain [%]

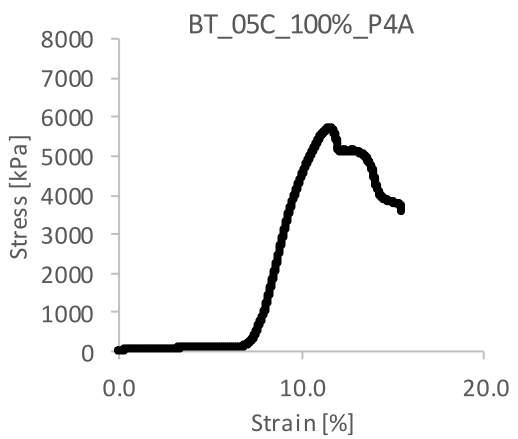
BT_05C_100%_P4A
8000
7000
6000
5000
4000
3000
2000
1000
0
Stress [kPa]
0.0
10.0
20.0
Strain [%]

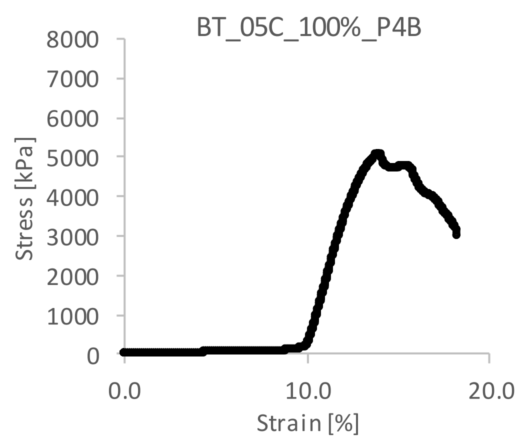
BT_05C_100%_P4B
8000
7000
6000
5000
4000
3000
2000
1000
0
Stress [kPa]
0.0
10.0
20.0
Strain [%]

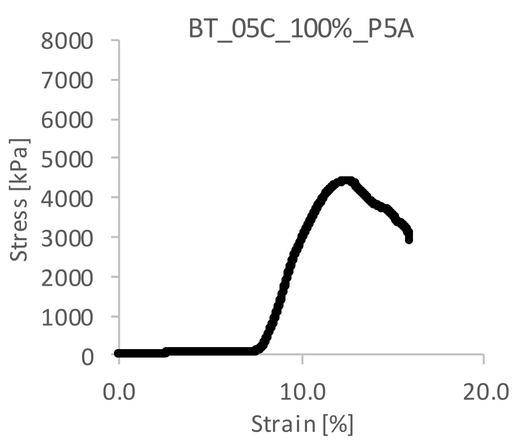
BT_05C_100%_P5A
8000
7000
6000
5000
4000
3000
2000
1000
0
Stress [kPa]
0.0
10.0
20.0
Strain [%]

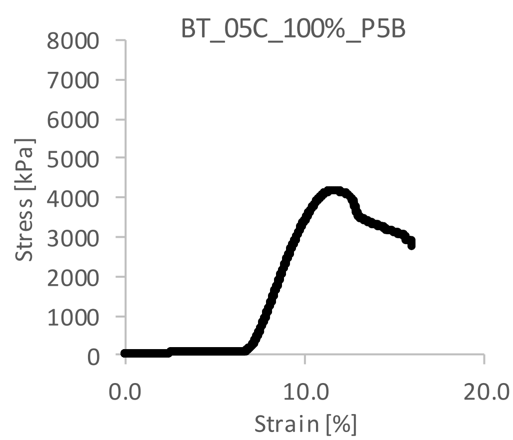
BT_05C_100%_P5B
8000
7000
6000
5000
4000
3000
2000
1000
0
Stress [kPa]
0.0
10.0
20.0
Strain [%]

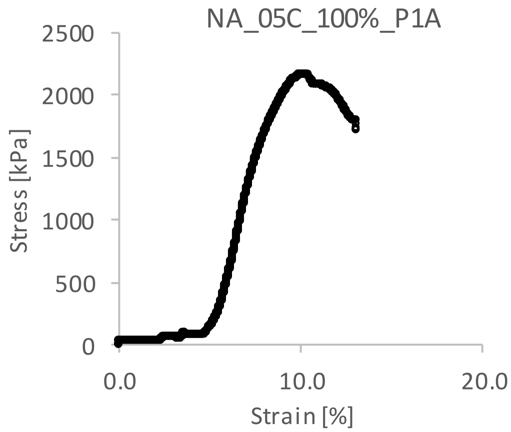
NA_05C_100%_P1A
Stress [kPa]
Strain [%]

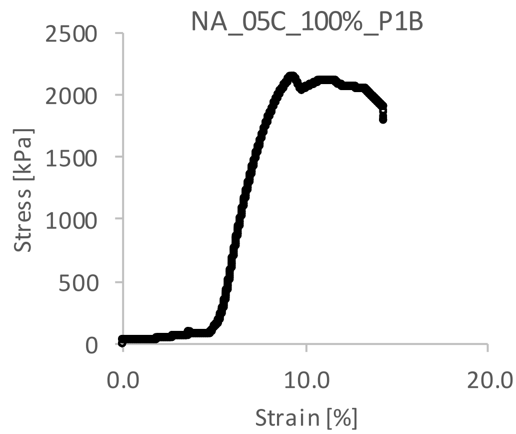
NA_05C_100%_P1B
Stress [kPa]
Strain [%]

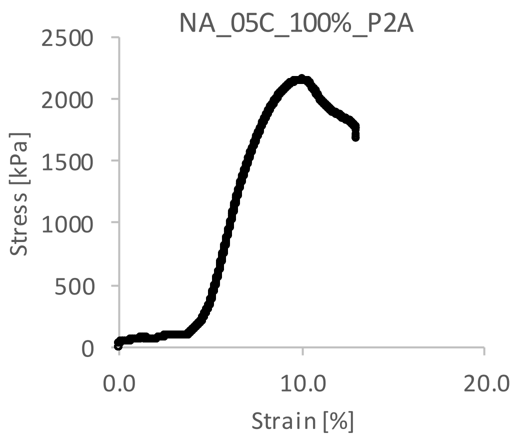
NA_05C_100%_P2A
Stress [kPa]
Strain [%]

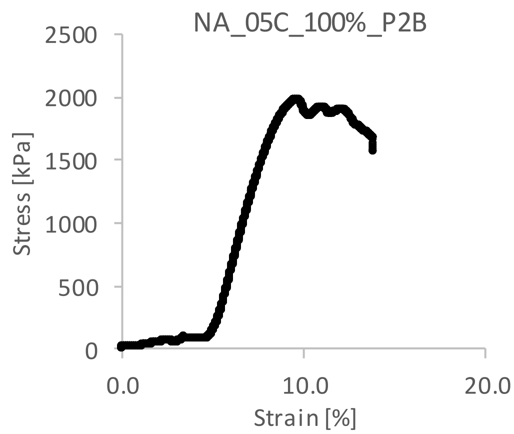
NA_05C_100%_P2B
Stress [kPa]
Strain [%]

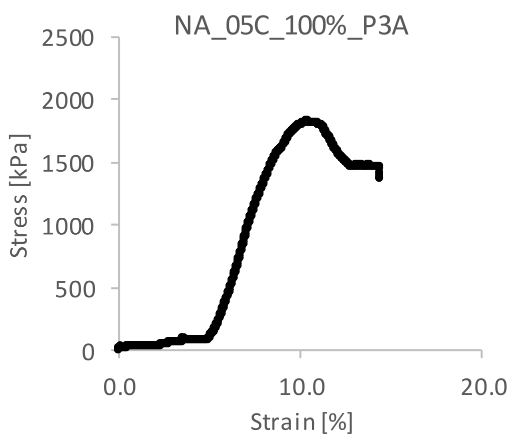
NA_05C_100%_P3A
Stress [kPa]
Strain [%]

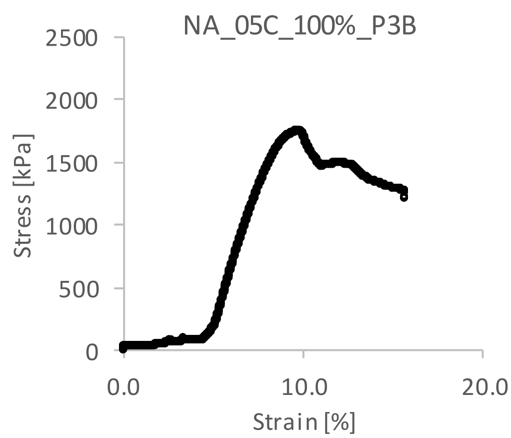
NA_05C_100%_P3B
Stress [kPa]
Strain [%]

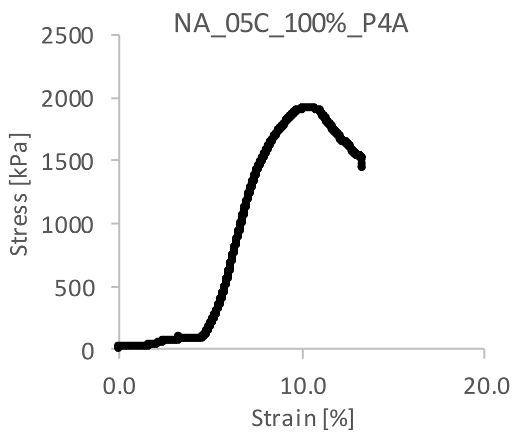
NA_05C_100%_P4A
Stress [kPa]
2500
2000
1500
1000
500
0
0.0
10.0
20.0
Strain [%]

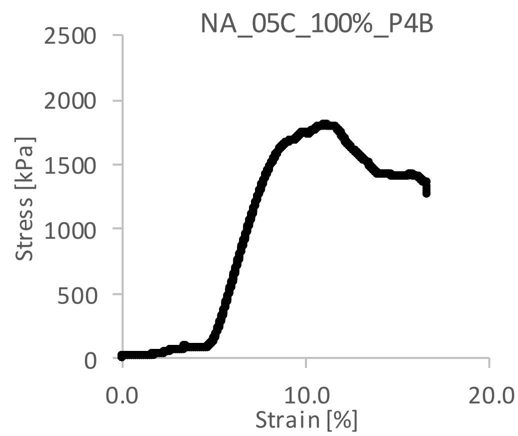
NA_05C_100%_P4B
Stress [kPa]
2500
2000
1500
1000
500
0
0.0
10.0
20.0
Strain [%]

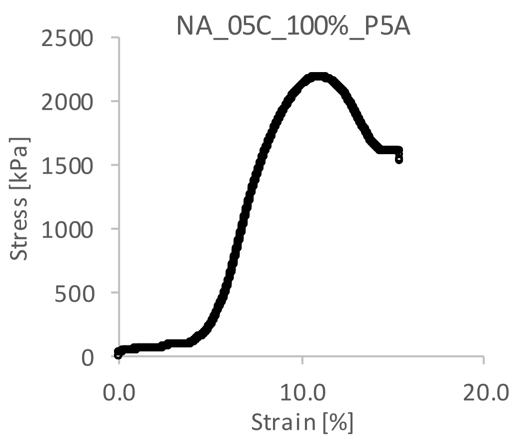
NA_05C_100%_P5A
Stress [kPa]
2500
2000
1500
1000
500
0
0.0
10.0
20.0
Strain [%]

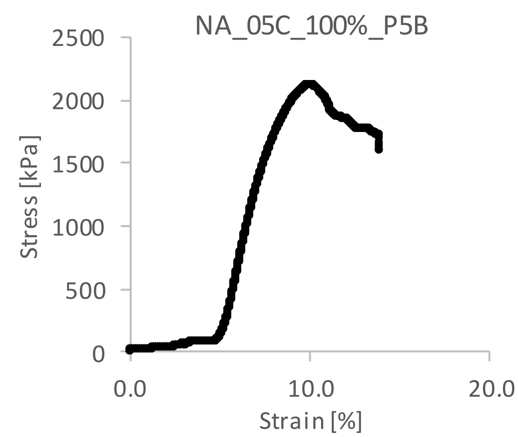
NA_05C_100%_P5B
Stress [kPa]
2500
2000
1500
1000
500
0
0.0
10.0
20.0
Strain [%]

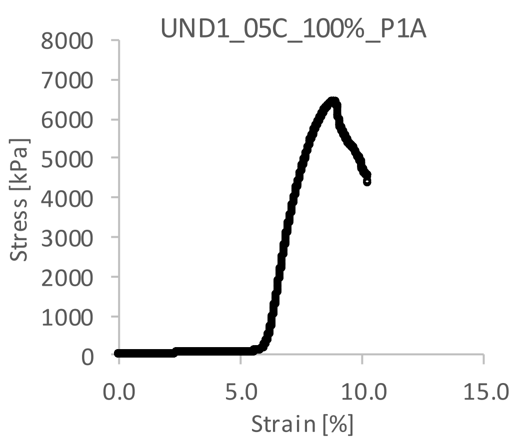
UND1_05C_100%_P1A
Stress [kPa]
8000
7000
6000
5000
4000
3000
2000
1000
0
0.0
5.0
10.0
15.0
Strain [%]

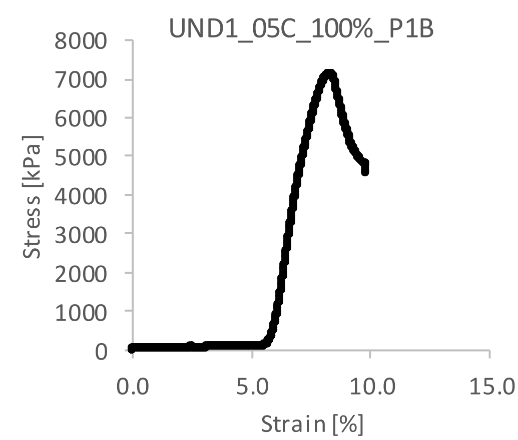
UND1_05C_100%_P1B
Stress [kPa]
8000
7000
6000
5000
4000
3000
2000
1000
0
0.0
5.0
10.0
15.0
Strain [%]

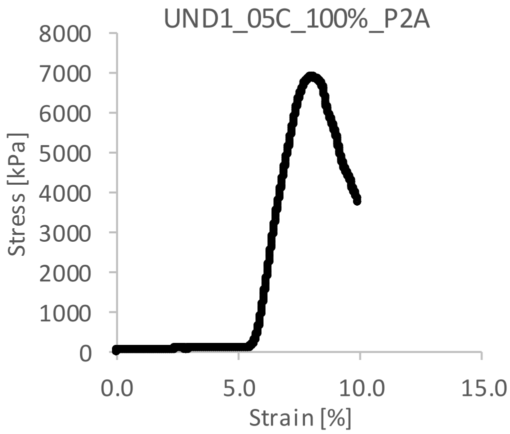
UND1_05C_100%_P2A
Stress [kPa]
Strain [%]
0
1000
2000
3000
4000
5000
6000
7000
8000
0.0
5.0
10.0
15.0

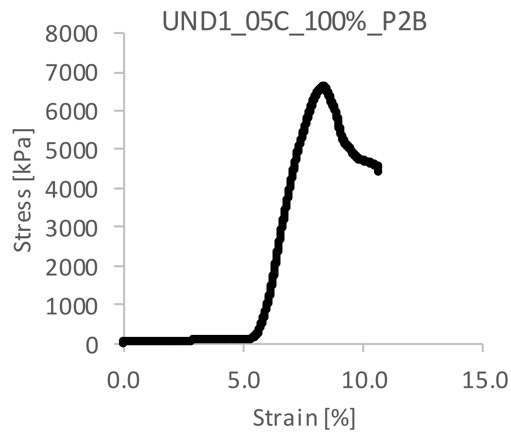
UND1_05C_100%_P2B
Stress [kPa]
Strain [%]
0
1000
2000
3000
4000
5000
6000
7000
8000
0.0
5.0
10.0
15.0

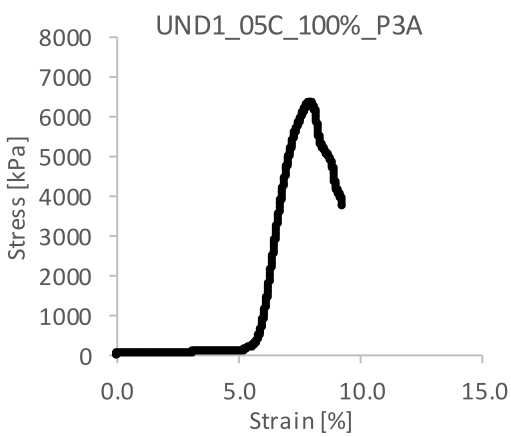
UND1_05C_100%_P3A
Stress [kPa]
Strain [%]
0
1000
2000
3000
4000
5000
6000
7000
8000
0.0
5.0
10.0
15.0

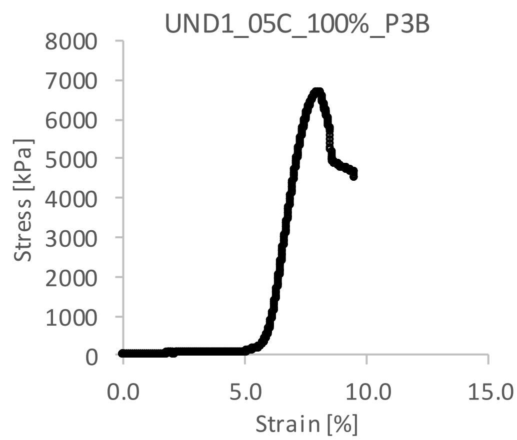
UND1_05C_100%_P3B
Stress [kPa]
Strain [%]
0
1000
2000
3000
4000
5000
6000
7000
8000
0.0
5.0
10.0
15.0

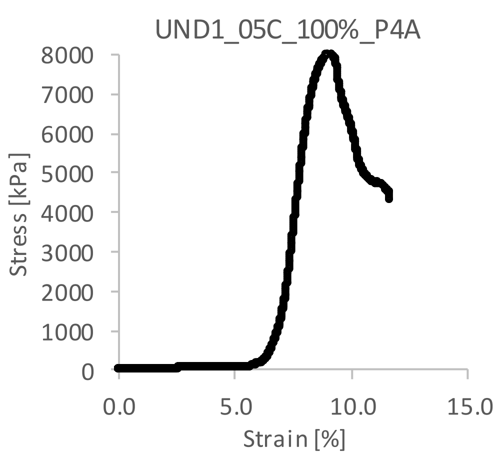
UND1_05C_100%_P4A
Stress [kPa]
Strain [%]
0
1000
2000
3000
4000
5000
6000
7000
8000
0.0
5.0
10.0
15.0

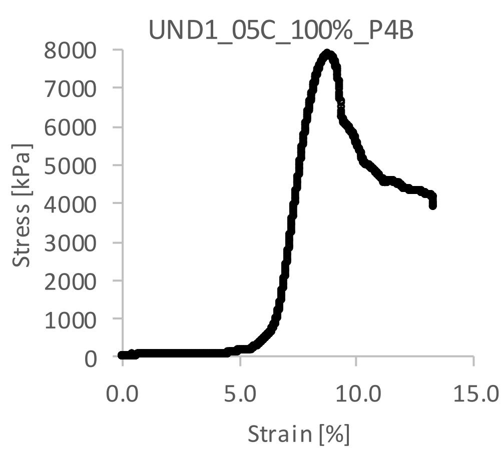
UND1_05C_100%_P4B
Stress [kPa]
Strain [%]
0
1000
2000
3000
4000
5000
6000
7000
8000
0.0
5.0
10.0
15.0

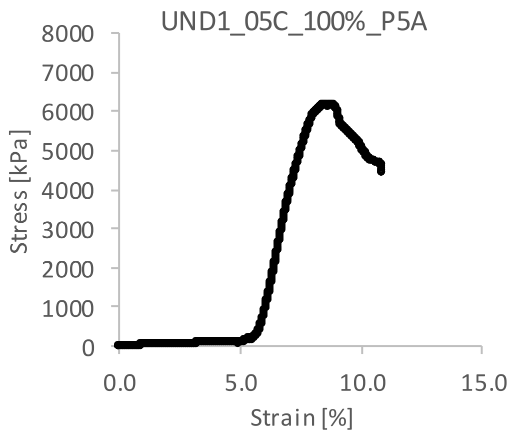
UND1_05C_100%_P5A
Stress [kPa]
0
1000
2000
3000
4000
5000
6000
7000
8000
Strain [%]
0.0
5.0
10.0
15.0

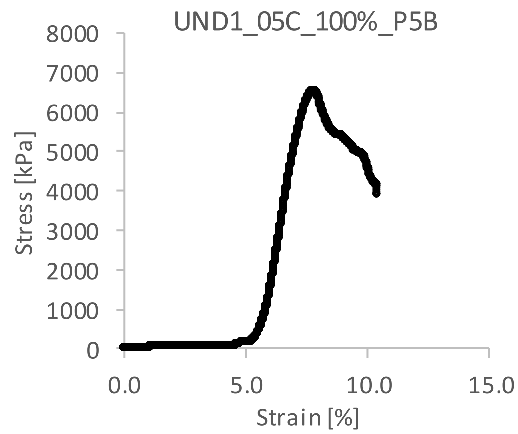
UND1_05C_100%_P5B
Stress [kPa]
0
1000
2000
3000
4000
5000
6000
7000
8000
Strain [%]
0.0
5.0
10.0
15.0

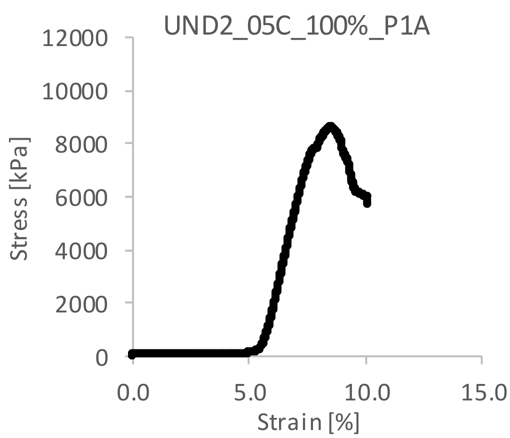
UND2_05C_100%_P1A
Stress [kPa]
0
2000
4000
6000
8000
10000
12000
Strain [%]
0.0
5.0
10.0
15.0

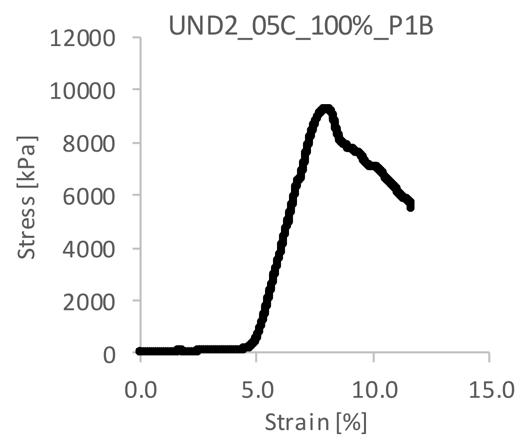
UND2_05C_100%_P1B
Stress [kPa]
0
2000
4000
6000
8000
10000
12000
Strain [%]
0.0
5.0
10.0
15.0

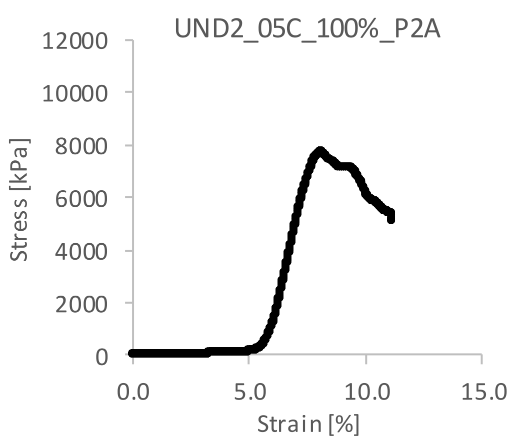
UND2_05C_100%_P2A
Stress [kPa]
0
2000
4000
6000
8000
10000
12000
Strain [%]
0.0
5.0
10.0
15.0

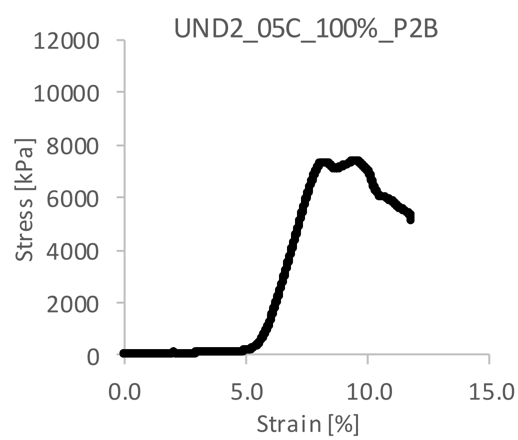
UND2_05C_100%_P2B
Stress [kPa]
0
2000
4000
6000
8000
10000
12000
Strain [%]
0.0
5.0
10.0
15.0

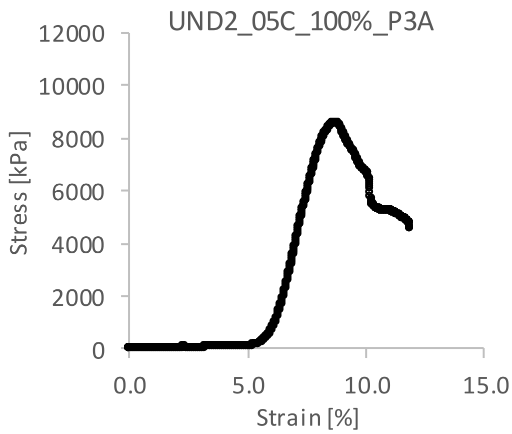
UND2_05C_100%_P3A
Stress [kPa]
Strain [%]

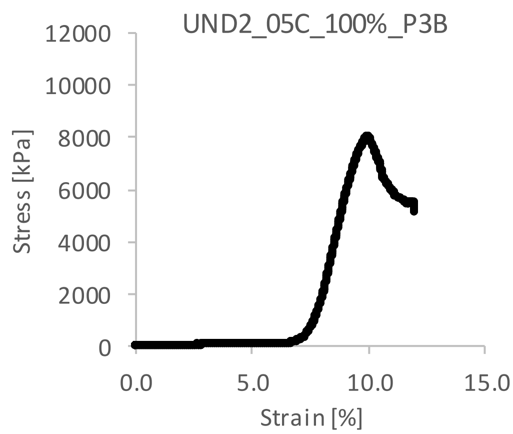
UND2_05C_100%_P3B
Stress [kPa]
Strain [%]

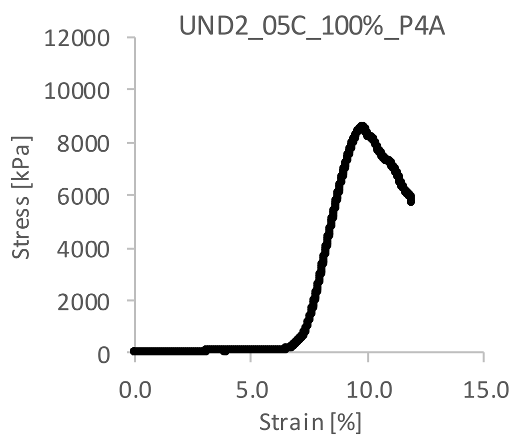
UND2_05C_100%_P4A
Stress [kPa]
Strain [%]

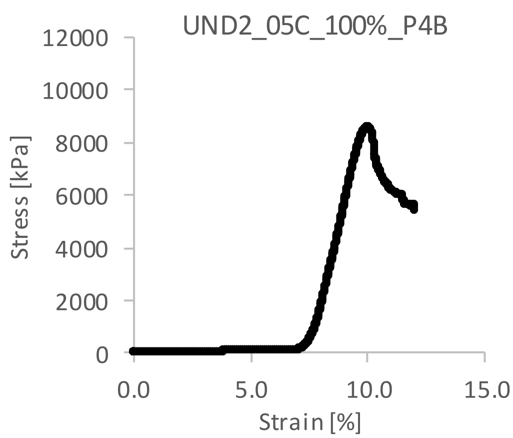
UND2_05C_100%_P4B
Stress [kPa]
Strain [%]

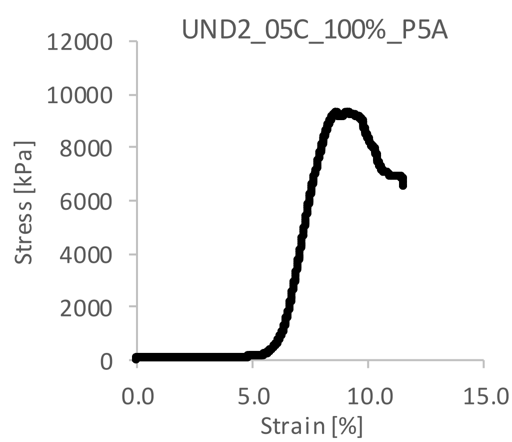
UND2_05C_100%_P5A
Stress [kPa]
Strain [%]

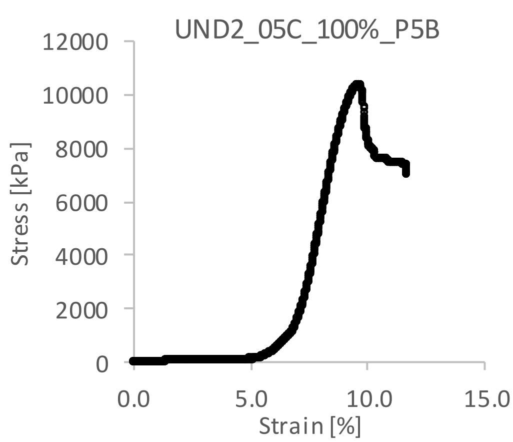
UND2_05C_100%_P5B
Stress [kPa]
Strain [%]

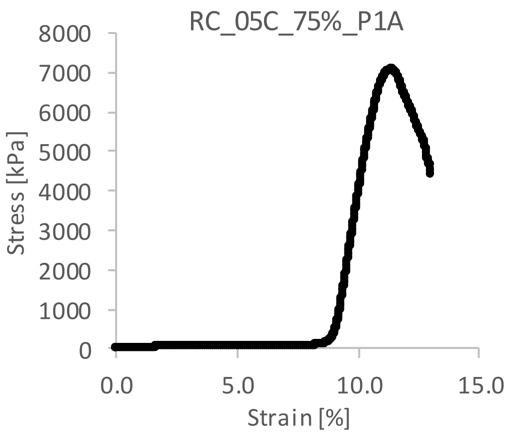
RC_05C_75%_P1A
Stress [kPa]
8000
7000
6000
5000
4000
3000
2000
1000
0
0.0
5.0
10.0
15.0
Strain [%]

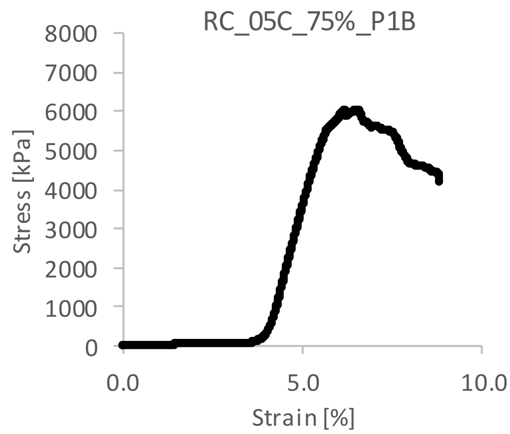
RC_05C_75%_P1B
Stress [kPa]
8000
7000
6000
5000
4000
3000
2000
1000
0
0.0
5.0
10.0
Strain [%]

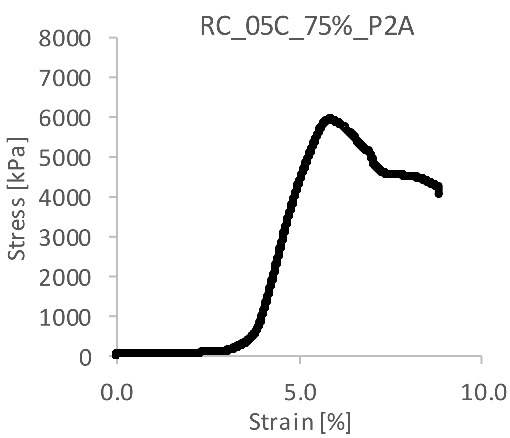
RC_05C_75%_P2A
Stress [kPa]
8000
7000
6000
5000
4000
3000
2000
1000
0
0.0
5.0
10.0
Strain [%]

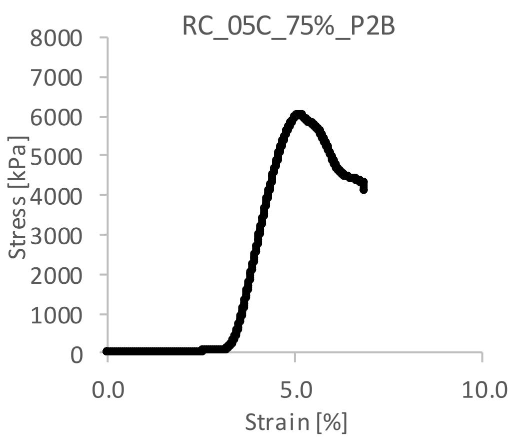
RC_05C_75%_P2B
Stress [kPa]
8000
7000
6000
5000
4000
3000
2000
1000
0
0.0
5.0
10.0
Strain [%]

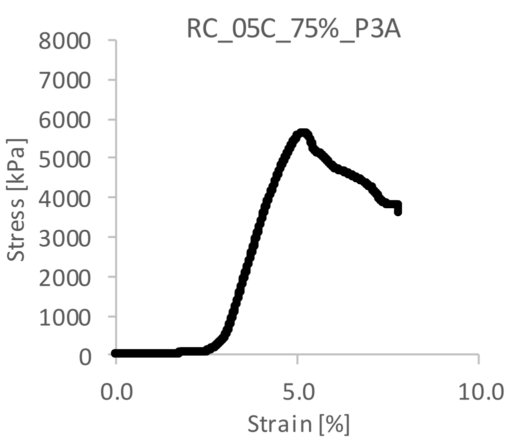
RC_05C_75%_P3A
Stress [kPa]
8000
7000
6000
5000
4000
3000
2000
1000
0
0.0
5.0
10.0
Strain [%]

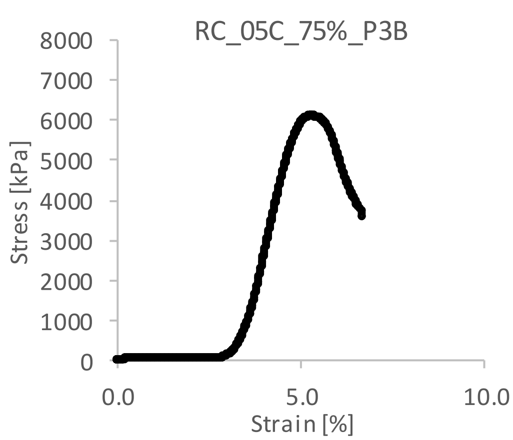
RC_05C_75%_P3B
Stress [kPa]
8000
7000
6000
5000
4000
3000
2000
1000
0
0.0
5.0
10.0
Strain [%]

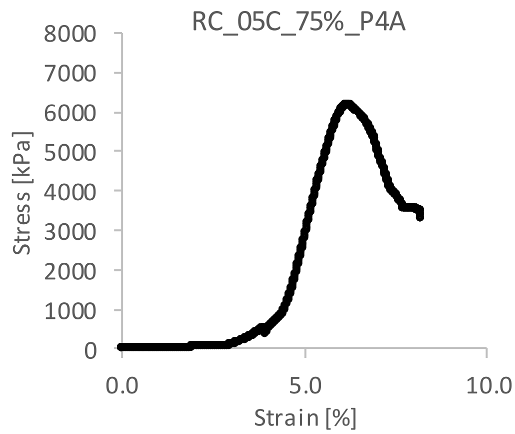
RC_05C_75%_P4A
Stress [kPa]
8000
7000
6000
5000
4000
3000
2000
1000
0
0.0
5.0
10.0
Strain [%]

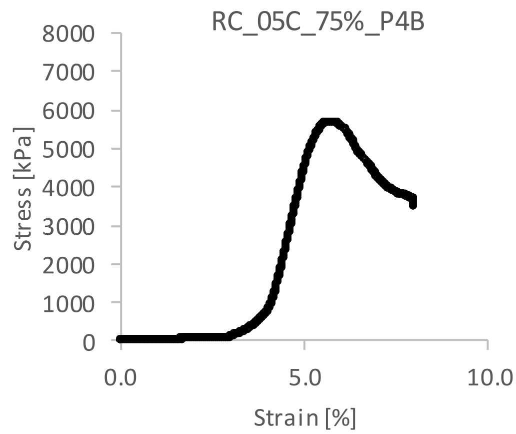
RC_05C_75%_P4B
Stress [kPa]
8000
7000
6000
5000
4000
3000
2000
1000
0
0.0
5.0
10.0
Strain [%]

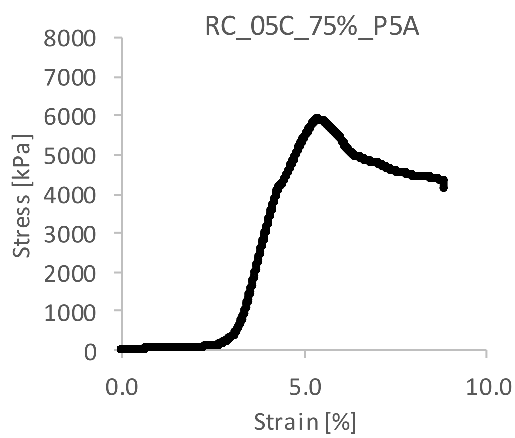
RC_05C_75%_P5A
Stress [kPa]
8000
7000
6000
5000
4000
3000
2000
1000
0
0.0
5.0
10.0
Strain [%]

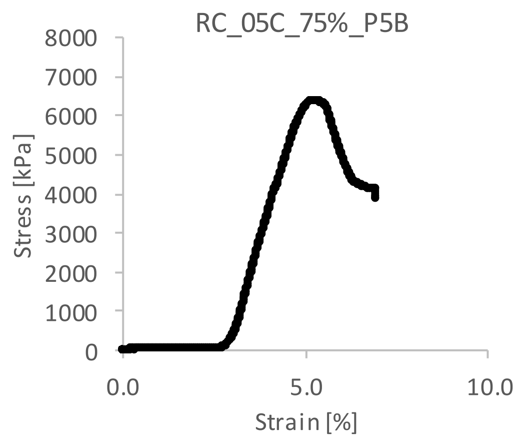
RC_05C_75%_P5B
Stress [kPa]
8000
7000
6000
5000
4000
3000
2000
1000
0
0.0
5.0
10.0
Strain [%]

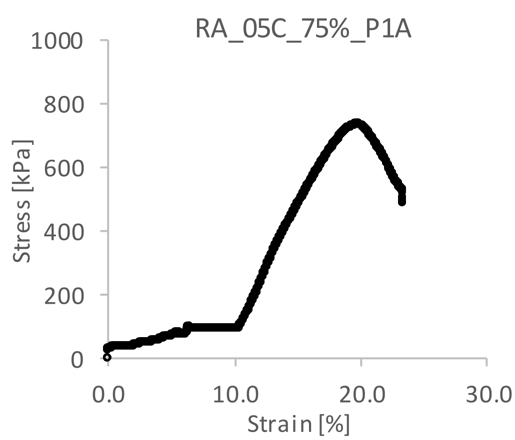
RA_05C_75%_P1A
Stress [kPa]
1000
800
600
400
200
0
0.0
10.0
20.0
30.0
Strain [%]

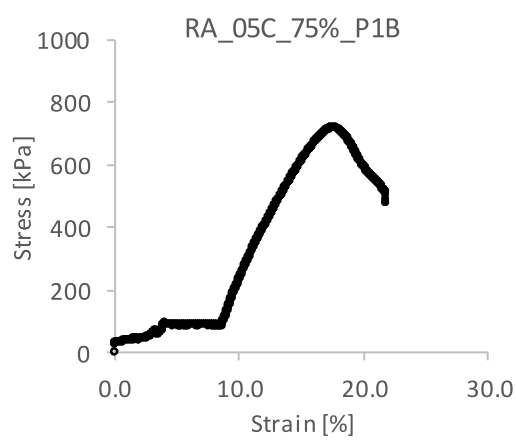
RA_05C_75%_P1B
Stress [kPa]
1000
800
600
400
200
0
0.0
10.0
20.0
30.0
Strain [%]

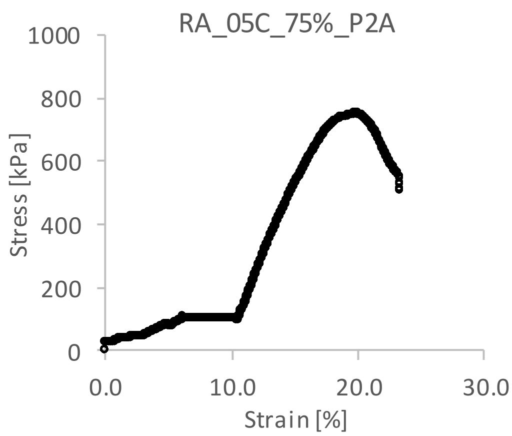
RA_05C_75%_P2A
Stress [kPa]
Strain [%]
0
200
400
600
800
1000
0.0
10.0
20.0
30.0

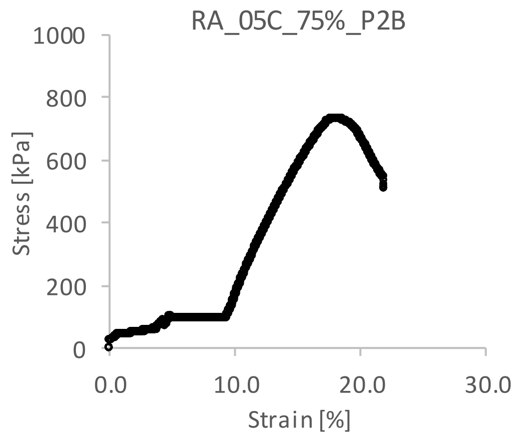
RA_05C_75%_P2B
Stress [kPa]
Strain [%]
0
200
400
600
800
1000
0.0
10.0
20.0
30.0

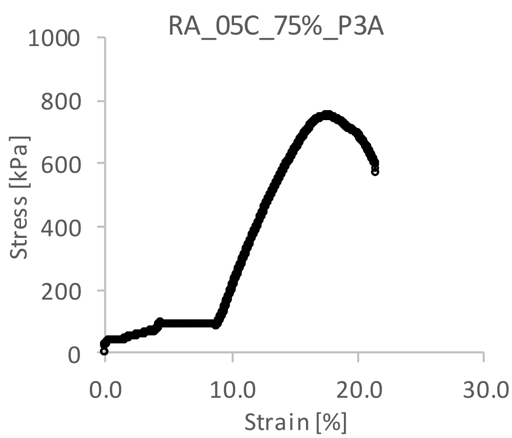
RA_05C_75%_P3A
Stress [kPa]
Strain [%]
0
200
400
600
800
1000
0.0
10.0
20.0
30.0

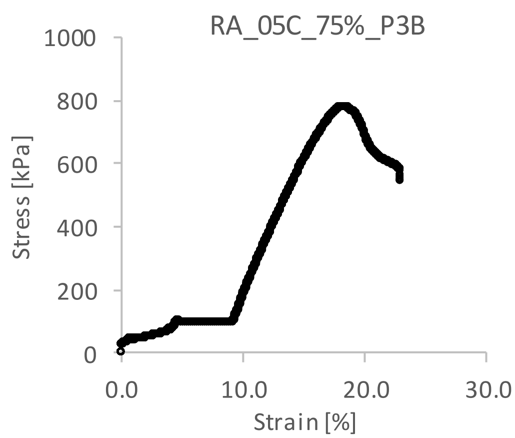
RA_05C_75%_P3B
Stress [kPa]
Strain [%]
0
200
400
600
800
1000
0.0
10.0
20.0
30.0

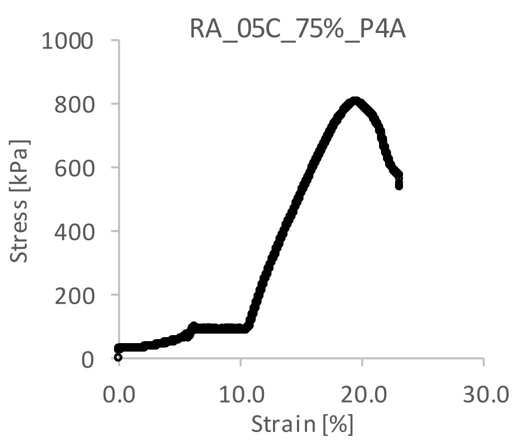
RA_05C_75%_P4A
Stress [kPa]
Strain [%]
0
200
400
600
800
1000
0.0
10.0
20.0
30.0

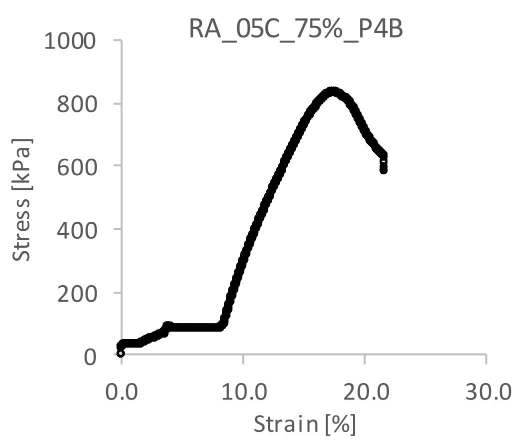
RA_05C_75%_P4B
Stress [kPa]
Strain [%]
0
200
400
600
800
1000
0.0
10.0
20.0
30.0

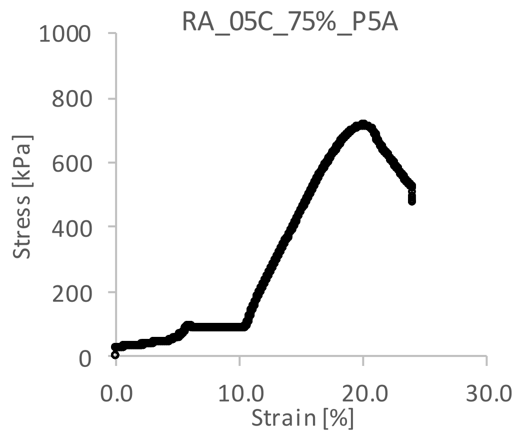
RA_05C_75%_P5A
Stress [kPa]
0
200
400
600
800
1000
Strain [%]
0.0
10.0
20.0
30.0

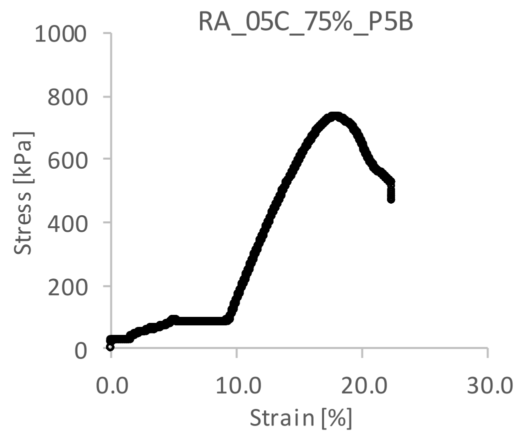
RA_05C_75%_P5B
Stress [kPa]
0
200
400
600
800
1000
Strain [%]
0.0
10.0
20.0
30.0

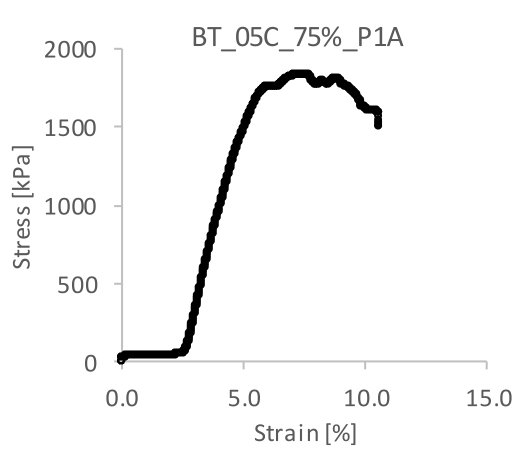
BT_05C_75%_P1A
Stress [kPa]
0
500
1000
1500
2000
Strain [%]
0.0
5.0
10.0
15.0

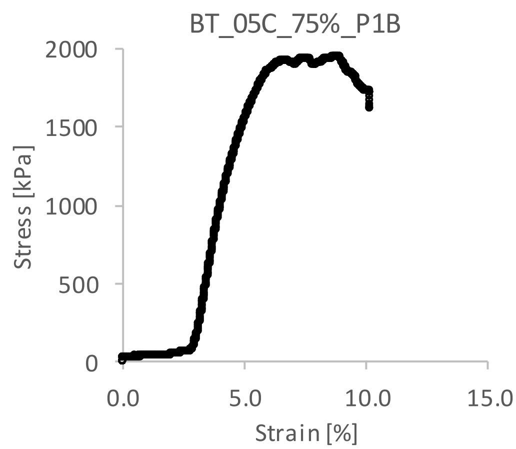
BT_05C_75%_P1B
Stress [kPa]
0
500
1000
1500
2000
Strain [%]
0.0
5.0
10.0
15.0

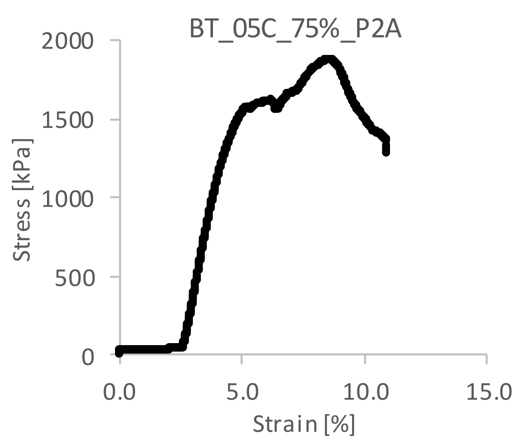
BT_05C_75%_P2A
Stress [kPa]
0
500
1000
1500
2000
Strain [%]
0.0
5.0
10.0
15.0

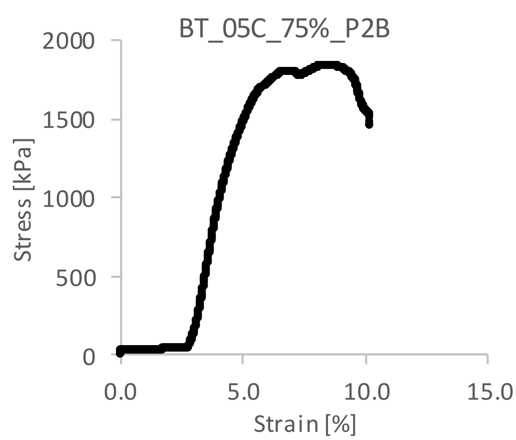
BT_05C_75%_P2B
Stress [kPa]
0
500
1000
1500
2000
Strain [%]
0.0
5.0
10.0
15.0

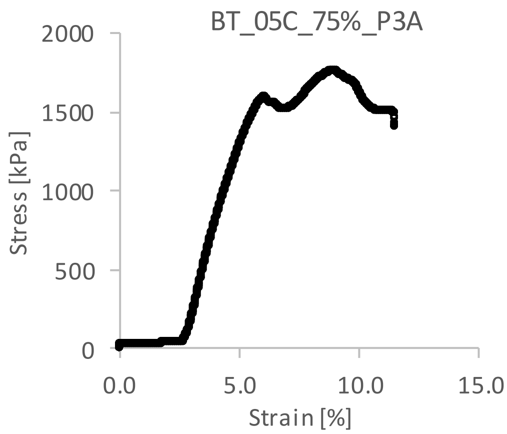
BT_05C_75%_P3A
Stress [kPa]
Strain [%]
0
500
1000
1500
2000
0.0
5.0
10.0
15.0

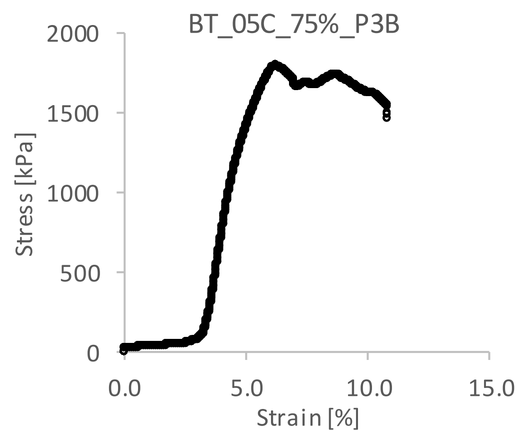
BT_05C_75%_P3B
Stress [kPa]
Strain [%]
0
500
1000
1500
2000
0.0
5.0
10.0
15.0

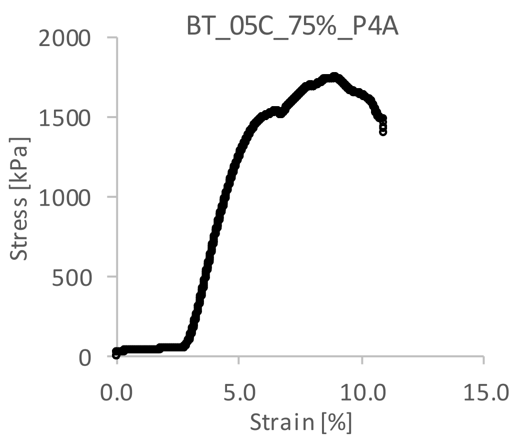
BT_05C_75%_P4A
Stress [kPa]
Strain [%]
0
500
1000
1500
2000
0.0
5.0
10.0
15.0

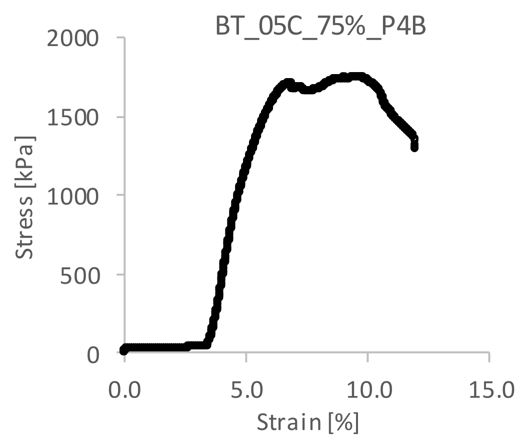
BT_05C_75%_P4B
Stress [kPa]
Strain [%]
0
500
1000
1500
2000
0.0
5.0
10.0
15.0

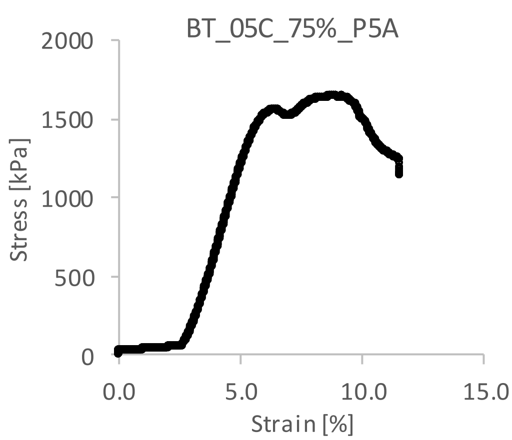
BT_05C_75%_P5A
Stress [kPa]
Strain [%]
0
500
1000
1500
2000
0.0
5.0
10.0
15.0

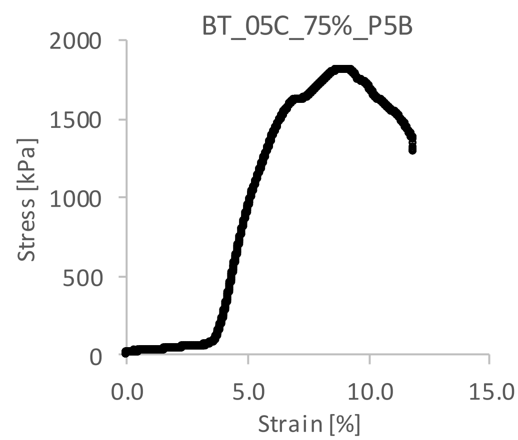
BT_05C_75%_P5B
Stress [kPa]
Strain [%]
0
500
1000
1500
2000
0.0
5.0
10.0
15.0

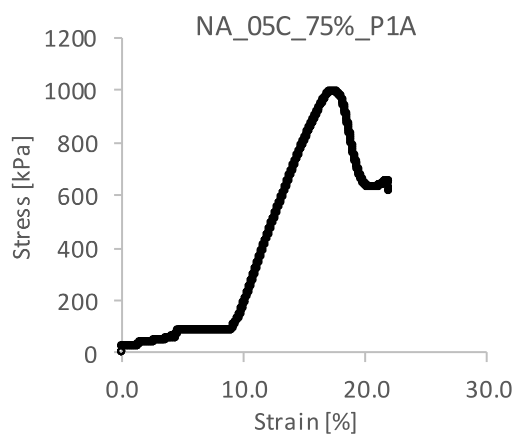
NA_05C_75%_P1A
Stress [kPa]
Strain [%]
0
200
400
600
800
1000
1200
0.0
10.0
20.0
30.0

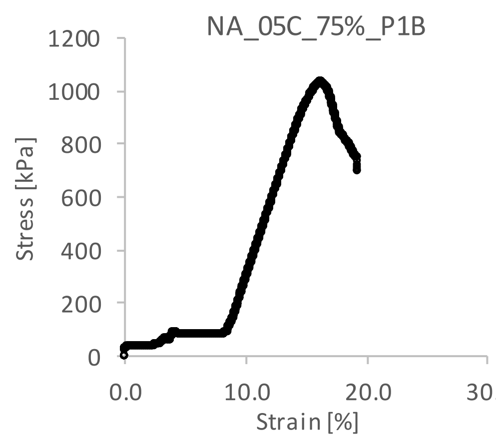
NA_05C_75%_P1B
Stress [kPa]
Strain [%]
0
200
400
600
800
1000
1200
0.0
10.0
20.0
30.0

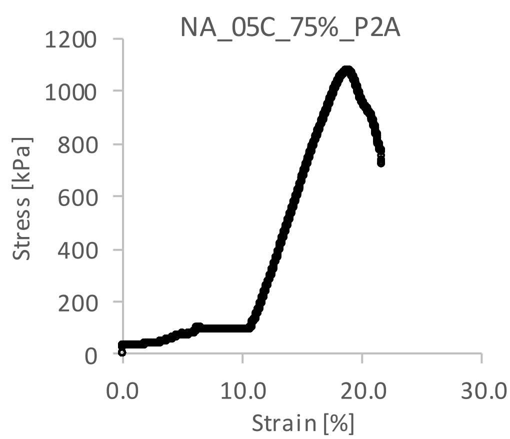
NA_05C_75%_P2A
Stress [kPa]
Strain [%]
0
200
400
600
800
1000
1200
0.0
10.0
20.0
30.0

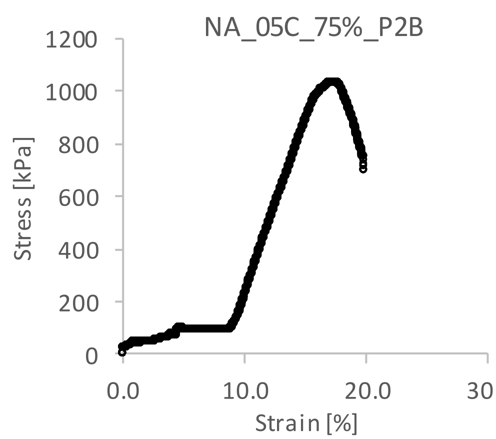
NA_05C_75%_P2B
Stress [kPa]
Strain [%]
0
200
400
600
800
1000
1200
0.0
10.0
20.0
30.0

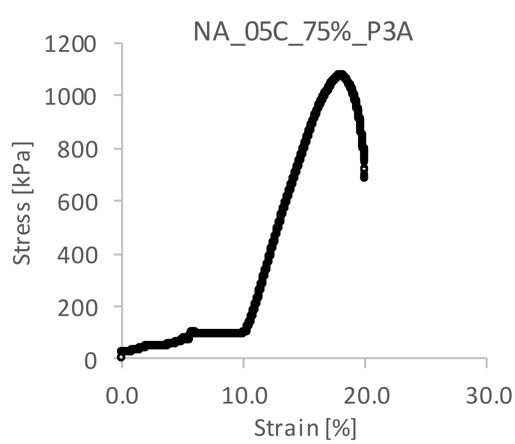
NA_05C_75%_P3A
Stress [kPa]
Strain [%]
0
200
400
600
800
1000
1200
0.0
10.0
20.0
30.0

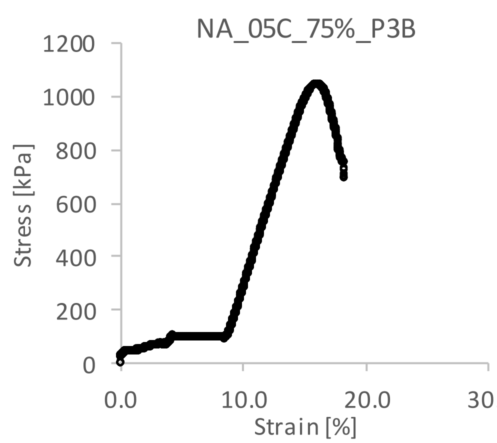
NA_05C_75%_P3B
Stress [kPa]
Strain [%]
0
200
400
600
800
1000
1200
0.0
10.0
20.0
30.0

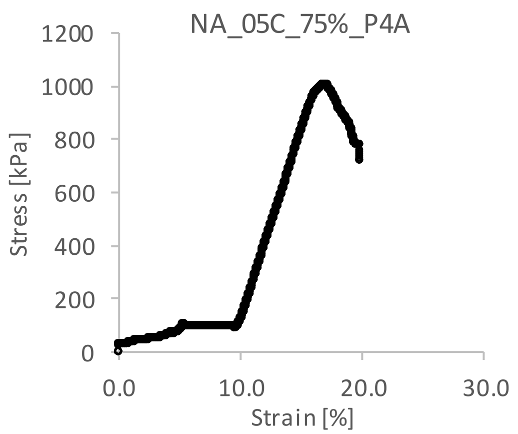
NA_05C_75%_P4A
Stress [kPa]
1200
1000
800
600
400
200
0
0.0
10.0
20.0
30.0
Strain [%]

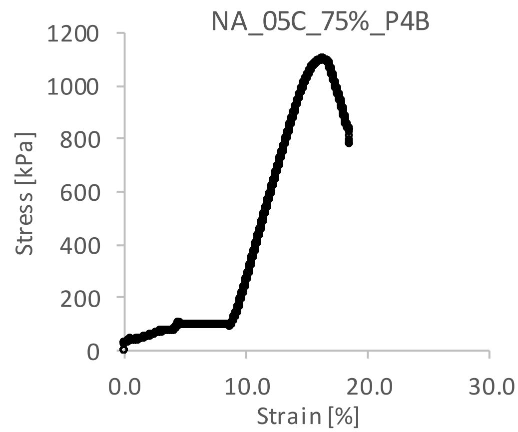
NA_05C_75%_P4B
Stress [kPa]
1200
1000
800
600
400
200
0
0.0
10.0
20.0
30.0
Strain [%]

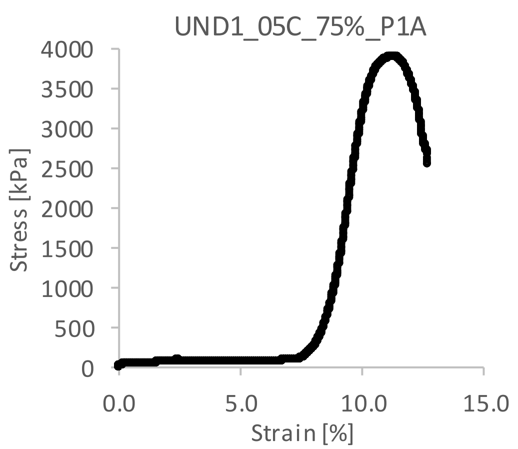
UND1_05C_75%_P1A
Stress [kPa]
4000
3500
3000
2500
2000
1500
1000
500
0
0.0
5.0
10.0
15.0
Strain [%]

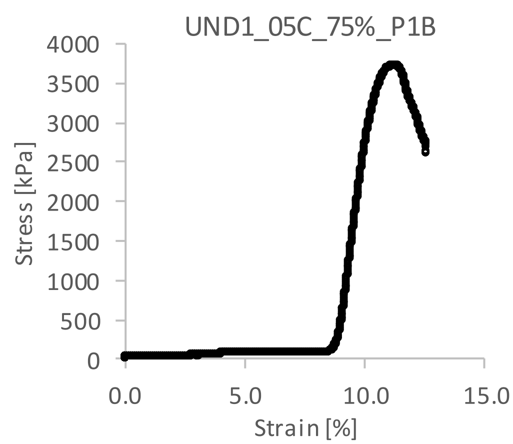
UND1_05C_75%_P1B
Stress [kPa]
4000
3500
3000
2500
2000
1500
1000
500
0
0.0
5.0
10.0
15.0
Strain [%]

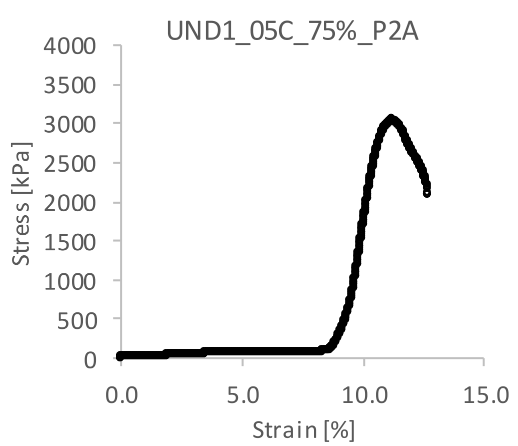
UND1_05C_75%_P2A
Stress [kPa]
4000
3500
3000
2500
2000
1500
1000
500
0
0.0
5.0
10.0
15.0
Strain [%]

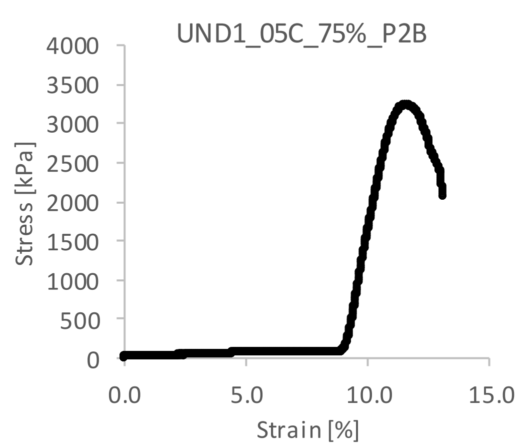
UND1_05C_75%_P2B
Stress [kPa]
4000
3500
3000
2500
2000
1500
1000
500
0
0.0
5.0
10.0
15.0
Strain [%]

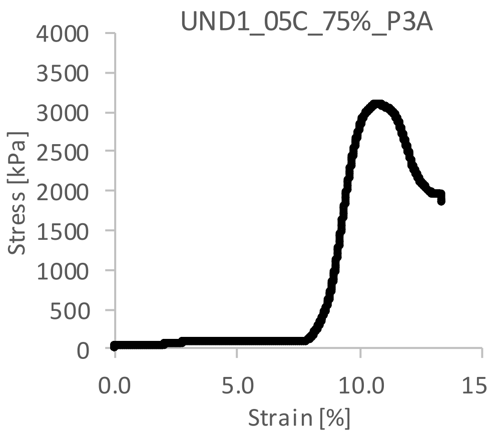
UND1_05C_75%_P3A
Stress [kPa]
Strain [%]
0
500
1000
1500
2000
2500
3000
3500
4000
0.0
5.0
10.0
15.0

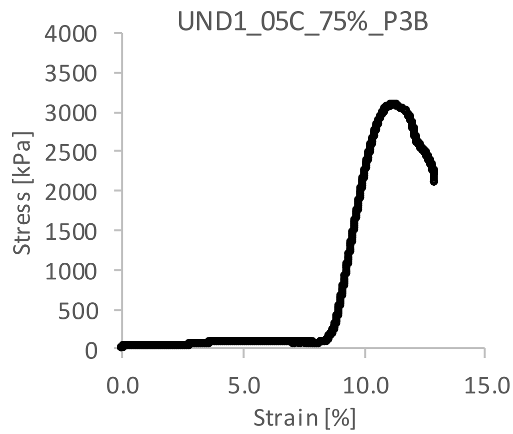
UND1_05C_75%_P3B
Stress [kPa]
Strain [%]
0
500
1000
1500
2000
2500
3000
3500
4000
0.0
5.0
10.0
15.0

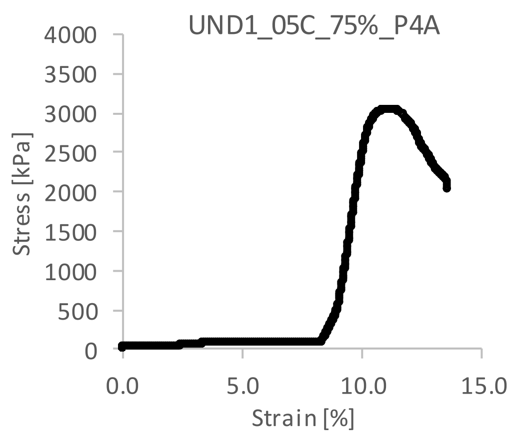
UND1_05C_75%_P4A
Stress [kPa]
Strain [%]
0
500
1000
1500
2000
2500
3000
3500
4000
0.0
5.0
10.0
15.0

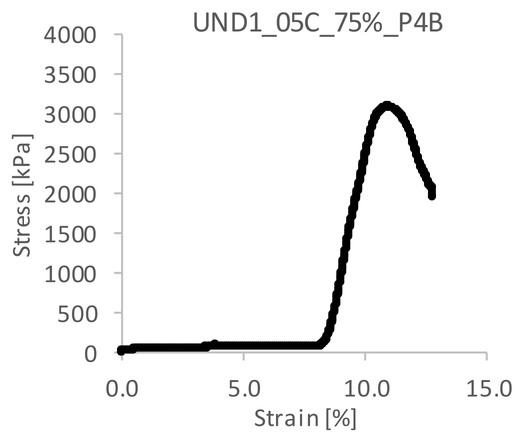
UND1_05C_75%_P4B
Stress [kPa]
Strain [%]
0
500
1000
1500
2000
2500
3000
3500
4000
0.0
5.0
10.0
15.0

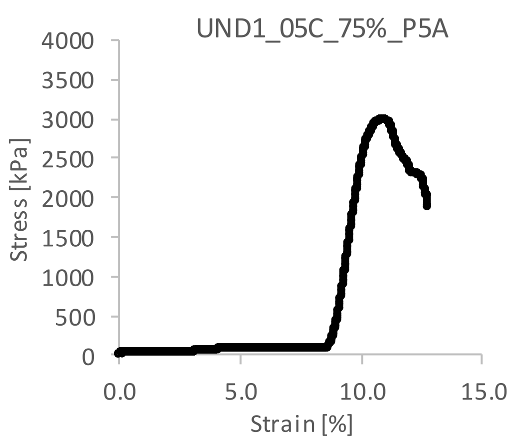
UND1_05C_75%_P5A
Stress [kPa]
Strain [%]
0
500
1000
1500
2000
2500
3000
3500
4000
0.0
5.0
10.0
15.0

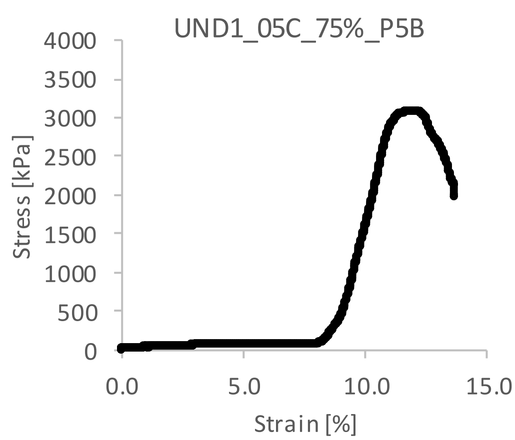
UND1_05C_75%_P5B
Stress [kPa]
Strain [%]
0
500
1000
1500
2000
2500
3000
3500
4000
0.0
5.0
10.0
15.0

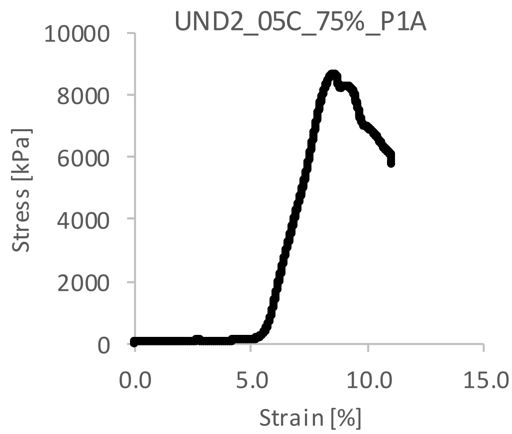
UND2_05C_75%_P1A
Stress [kPa]
10000
8000
6000
4000
2000
0
0.0
5.0
10.0
15.0
Strain [%]

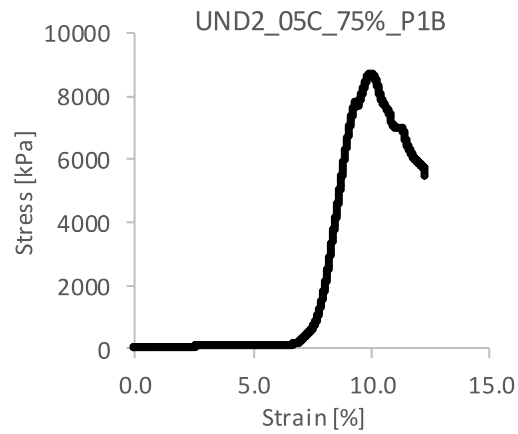
UND2_05C_75%_P1B
Stress [kPa]
10000
8000
6000
4000
2000
0
0.0
5.0
10.0
15.0
Strain [%]

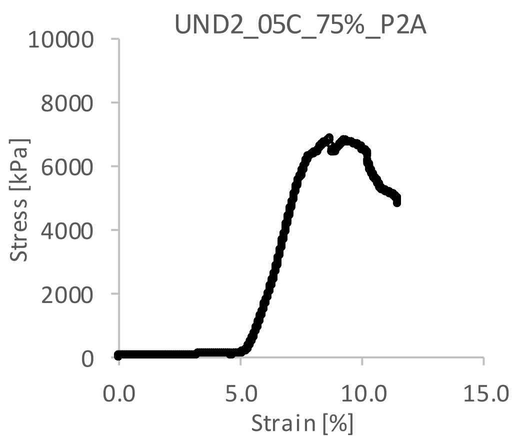
UND2_05C_75%_P2A
Stress [kPa]
10000
8000
6000
4000
2000
0
0.0
5.0
10.0
15.0
Strain [%]

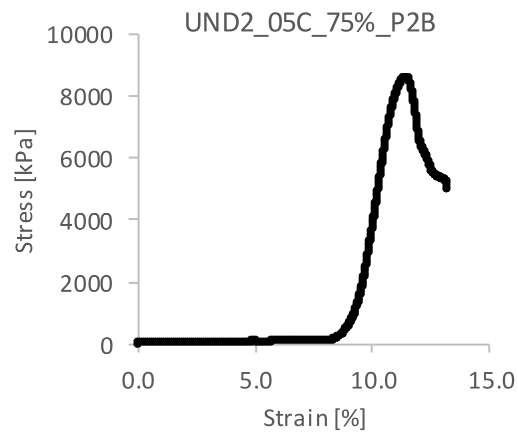
UND2_05C_75%_P2B
Stress [kPa]
10000
8000
6000
4000
2000
0
0.0
5.0
10.0
15.0
Strain [%]

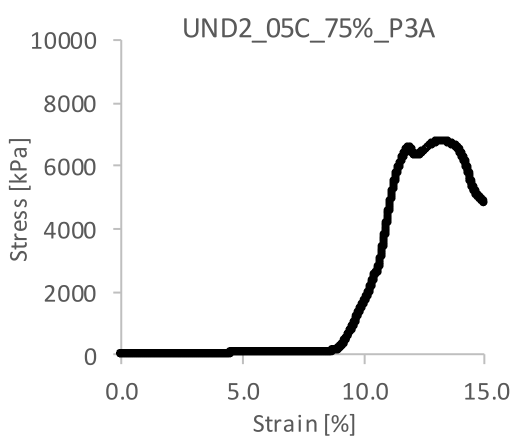
UND2_05C_75%_P3A
Stress [kPa]
10000
8000
6000
4000
2000
0
0.0
5.0
10.0
15.0
Strain [%]

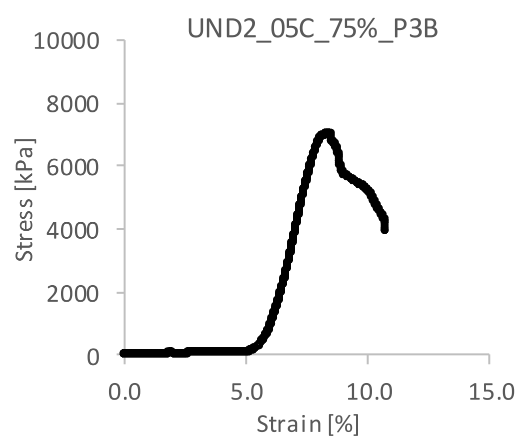
UND2_05C_75%_P3B
Stress [kPa]
10000
8000
6000
4000
2000
0
0.0
5.0
10.0
15.0
Strain [%]

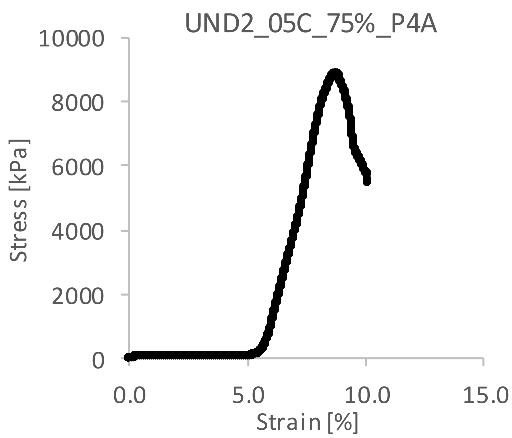
UND2_05C_75%_P4A
10000
8000
6000
4000
2000
0
Stress [kPa]
0.0
5.0
10.0
15.0
Strain [%]

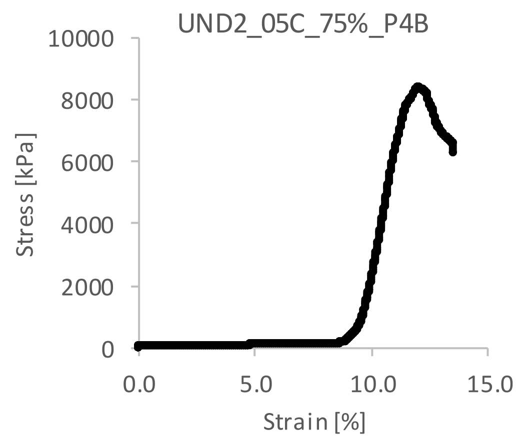
UND2_05C_75%_P4B
10000
8000
6000
4000
2000
0
Stress [kPa]
0.0
5.0
10.0
15.0
Strain [%]

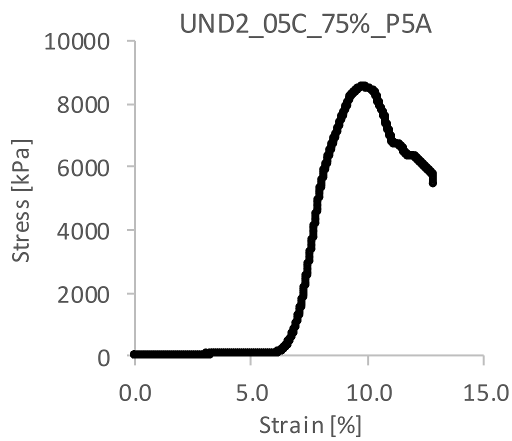
UND2_05C_75%_P5A
10000
8000
6000
4000
2000
0
Stress [kPa]
0.0
5.0
10.0
15.0
Strain [%]

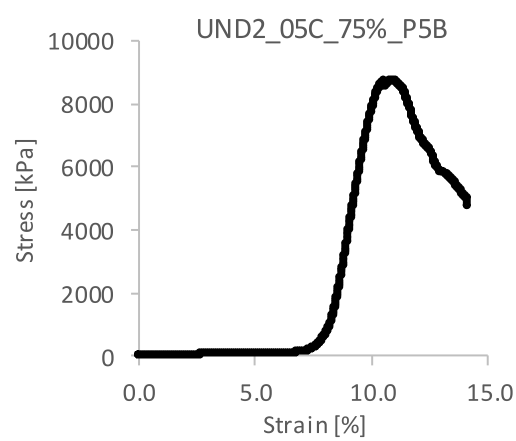
UND2_05C_75%_P5B
10000
8000
6000
4000
2000
0
Stress [kPa]
0.0
5.0
10.0
15.0
Strain [%]

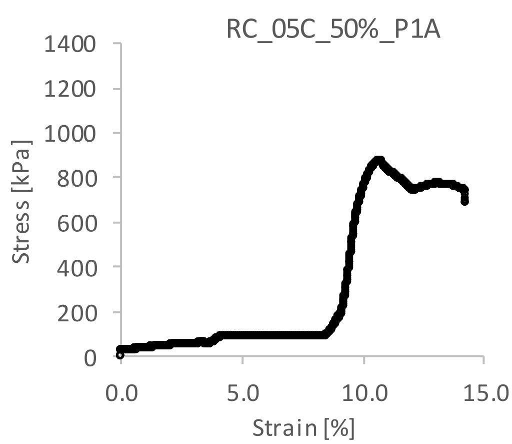
RC_05C_50%_P1A
1400
1200
1000
800
600
400
200
0
Stress [kPa]
0.0
5.0
10.0
15.0
Strain [%]

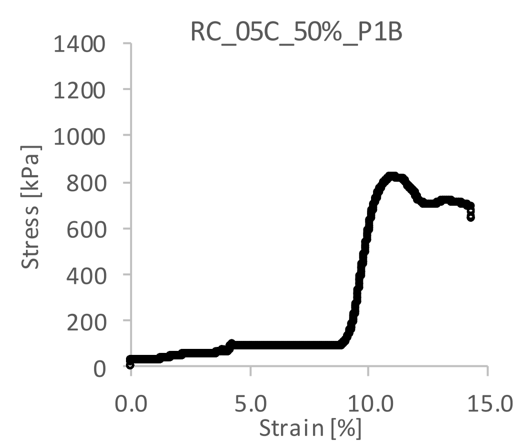
RC_05C_50%_P1B
1400
1200
1000
800
600
400
200
0
Stress [kPa]
0.0
5.0
10.0
15.0
Strain [%]

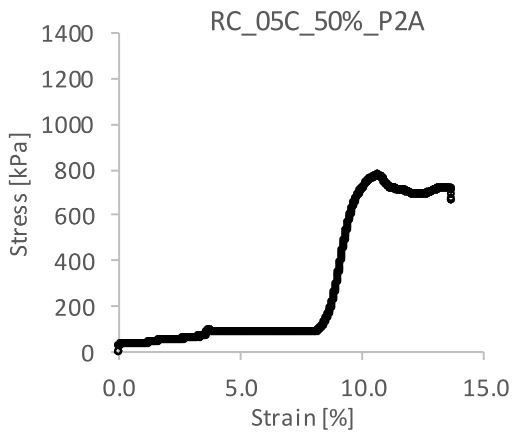
RC_05C_50%_P2A
Stress [kPa]
0
200
400
600
800
1000
1200
1400
Strain [%]
0.0
5.0
10.0
15.0

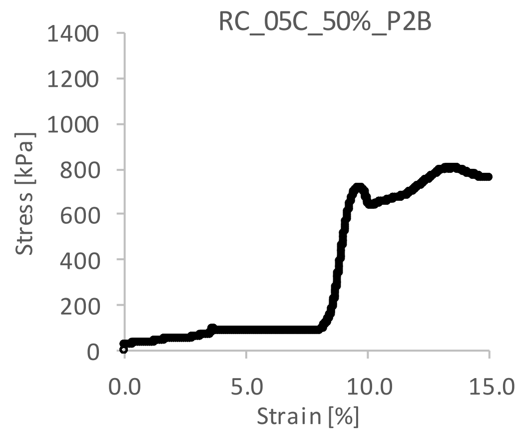
RC_05C_50%_P2B
Stress [kPa]
0
200
400
600
800
1000
1200
1400
Strain [%]
0.0
5.0
10.0
15.0

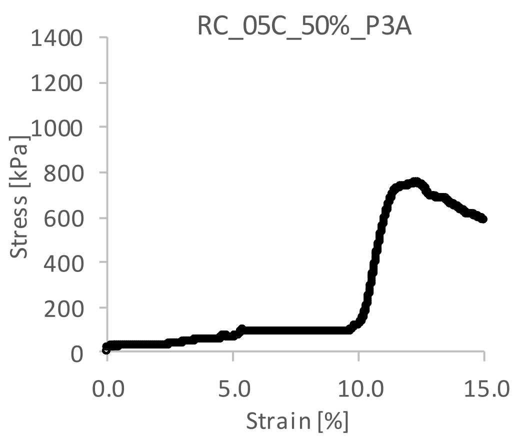
RC_05C_50%_P3A
Stress [kPa]
0
200
400
600
800
1000
1200
1400
Strain [%]
0.0
5.0
10.0
15.0

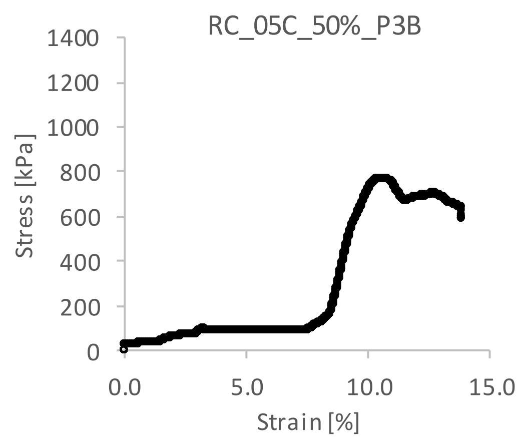
RC_05C_50%_P3B
Stress [kPa]
0
200
400
600
800
1000
1200
1400
Strain [%]
0.0
5.0
10.0
15.0

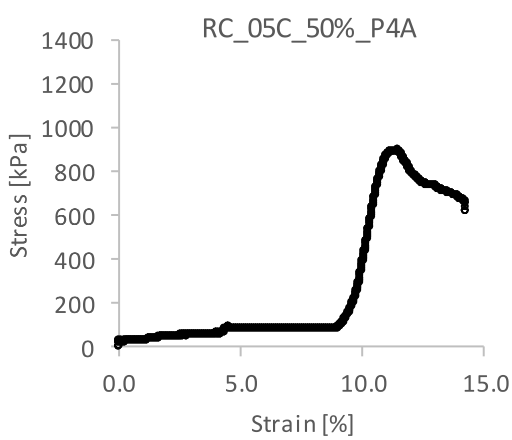
RC_05C_50%_P4A
Stress [kPa]
0
200
400
600
800
1000
1200
1400
Strain [%]
0.0
5.0
10.0
15.0

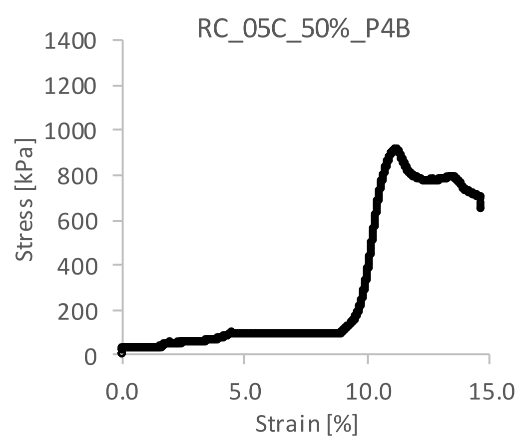
RC_05C_50%_P4B
Stress [kPa]
0
200
400
600
800
1000
1200
1400
Strain [%]
0.0
5.0
10.0
15.0

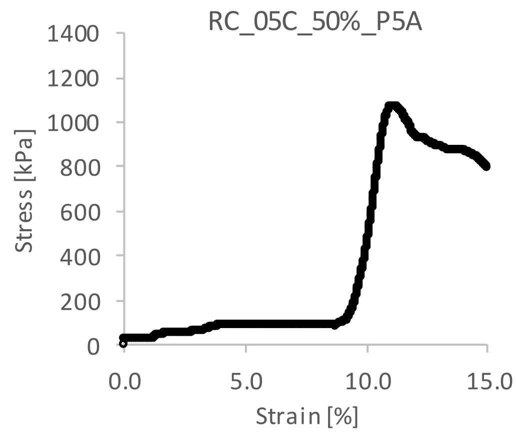
RC_05C_50%_P5A
1400
1200
1000
800
600
400
200
0
Stress [kPa]
0.0
5.0
10.0
15.0
Strain [%]

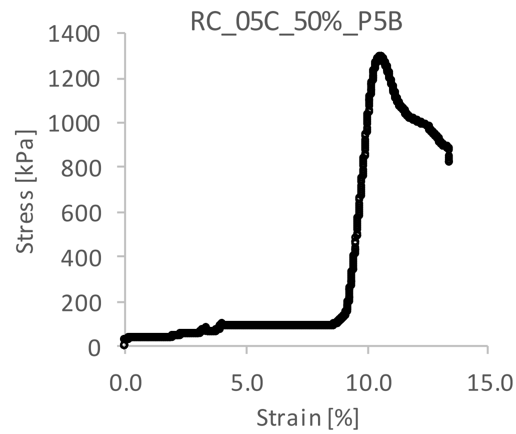
RC_05C_50%_P5B
1400
1200
1000
800
600
400
200
0
Stress [kPa]
0.0
5.0
10.0
15.0
Strain [%]

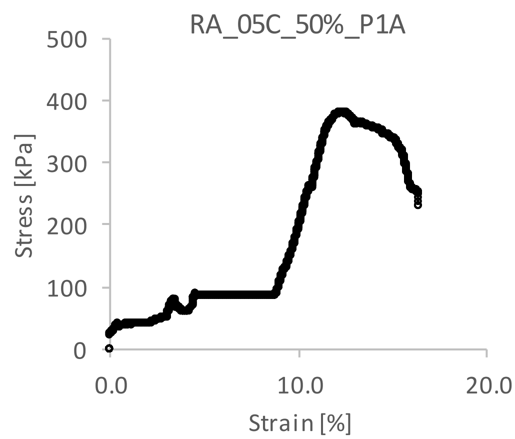
RA_05C_50%_P1A
500
400
300
200
100
0
Stress [kPa]
0.0
10.0
20.0
Strain [%]

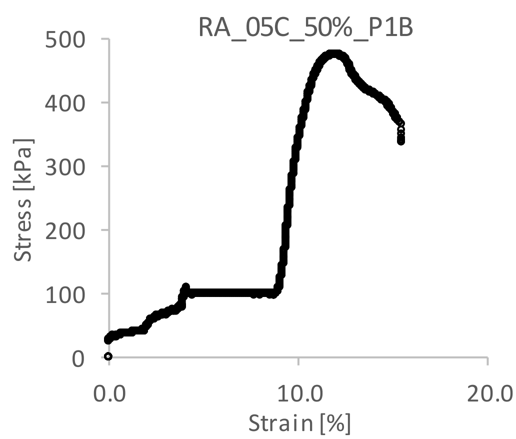
RA_05C_50%_P1B
500
400
300
200
100
0
Stress [kPa]
0.0
10.0
20.0
Strain [%]

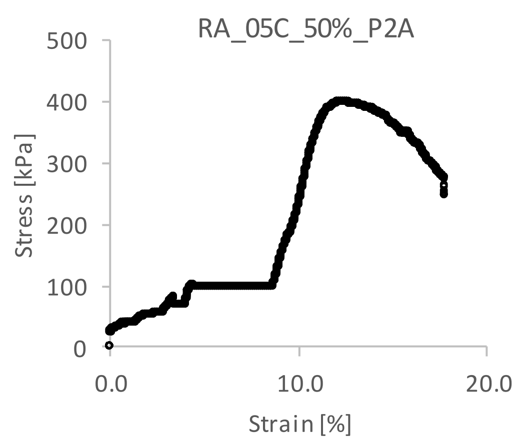
RA_05C_50%_P2A
500
400
300
200
100
0
Stress [kPa]
0.0
10.0
20.0
Strain [%]

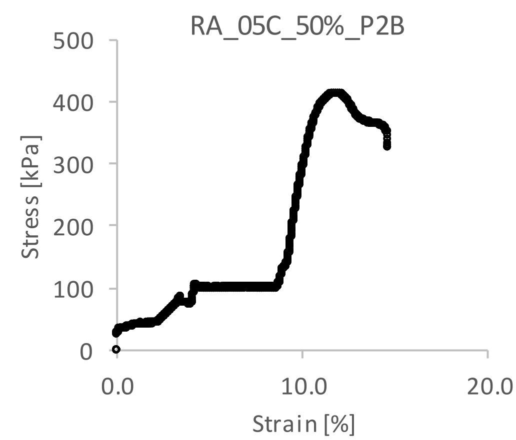
RA_05C_50%_P2B
500
400
300
200
100
0
Stress [kPa]
0.0
10.0
20.0
Strain [%]

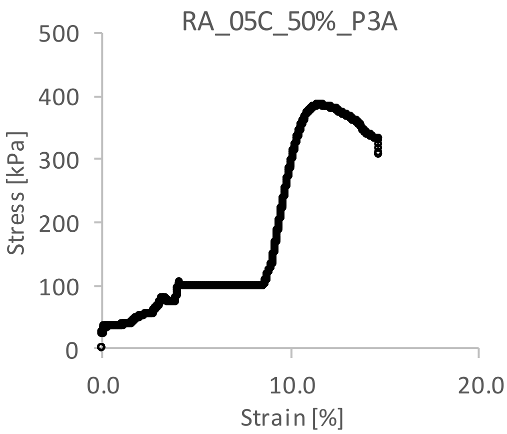
RA_05C_50%_P3A
Stress [kPa]
500
400
300
200
100
0
0.0
10.0
20.0
Strain [%]

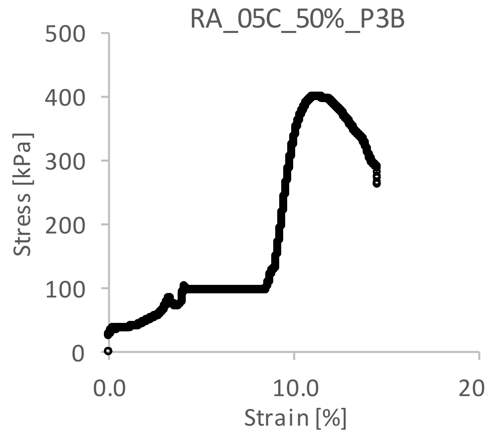
RA_05C_50%_P3B
Stress [kPa]
500
400
300
200
100
0
0.0
10.0
20.0
Strain [%]

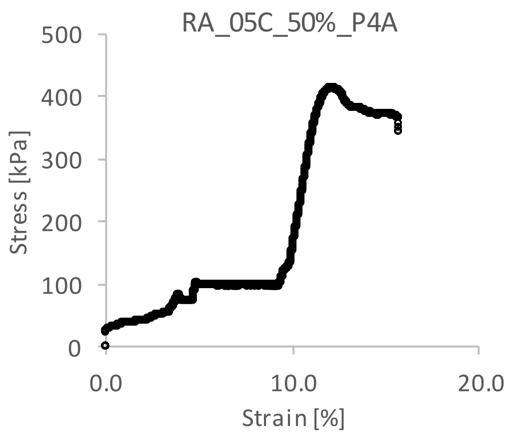
RA_05C_50%_P4A
Stress [kPa]
500
400
300
200
100
0
0.0
10.0
20.0
Strain [%]

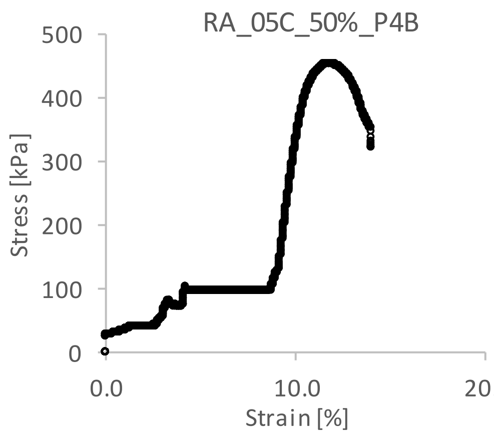
RA_05C_50%_P4B
Stress [kPa]
500
400
300
200
100
0
0.0
10.0
20.0
Strain [%]

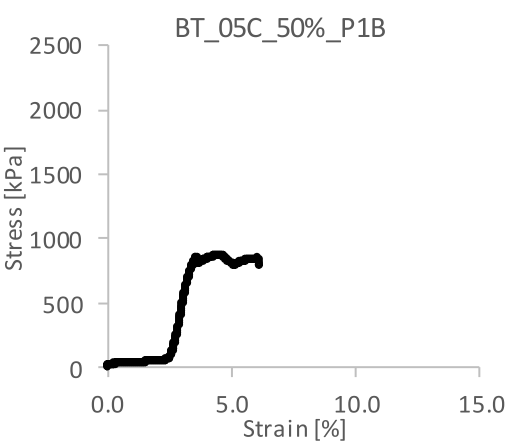
BT_05C_50%_P1B
Stress [kPa]
2500
2000
1500
1000
500
0
0.0
5.0
10.0
15.0
Strain [%]

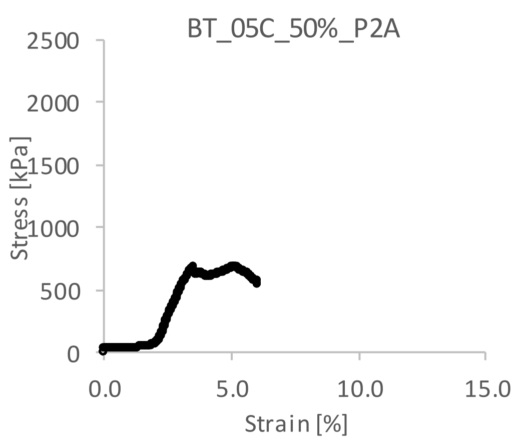
BT_05C_50%_P2A
Stress [kPa]
2500
2000
1500
1000
500
0
0.0
5.0
10.0
15.0
Strain [%]

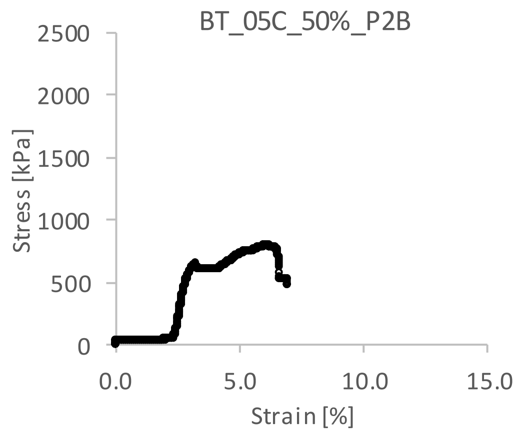
BT_05C_50%_P2B
Stress [kPa]
Strain [%]

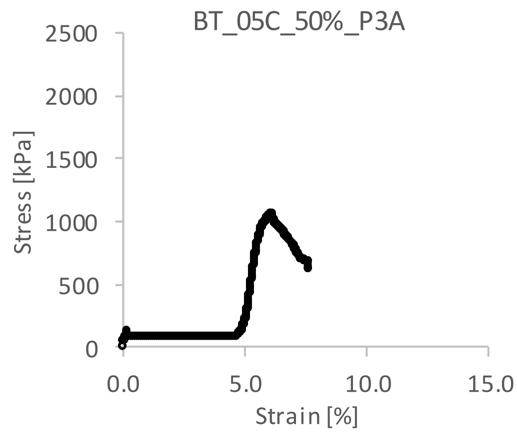
BT_05C_50%_P3A
Stress [kPa]
Strain [%]

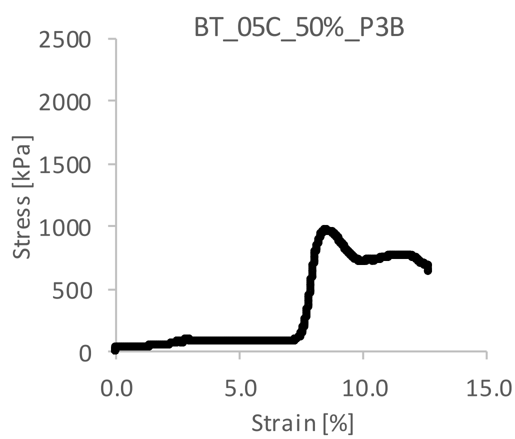
BT_05C_50%_P3B
Stress [kPa]
Strain [%]

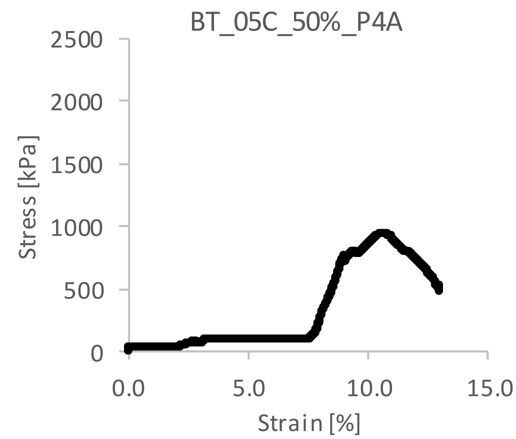
BT_05C_50%_P4A
Stress [kPa]
Strain [%]

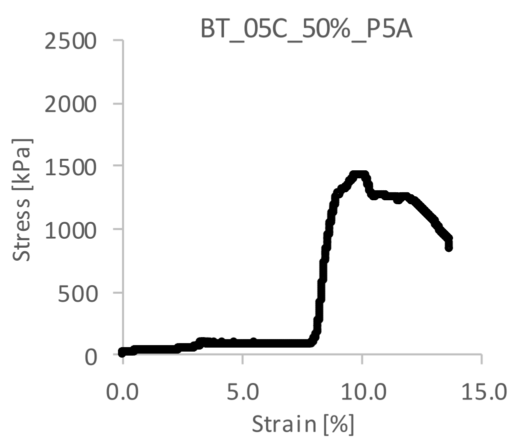
BT_05C_50%_P5A
Stress [kPa]
Strain [%]

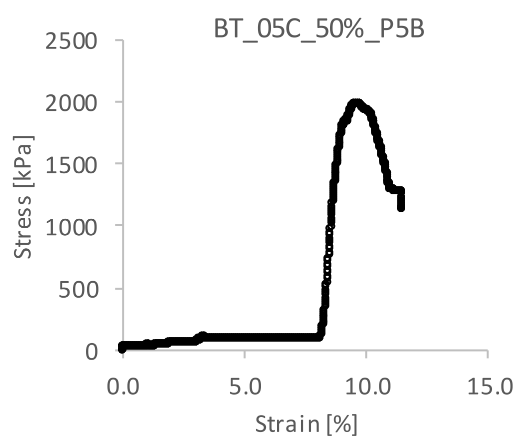
BT_05C_50%_P5B
Stress [kPa]
Strain [%]

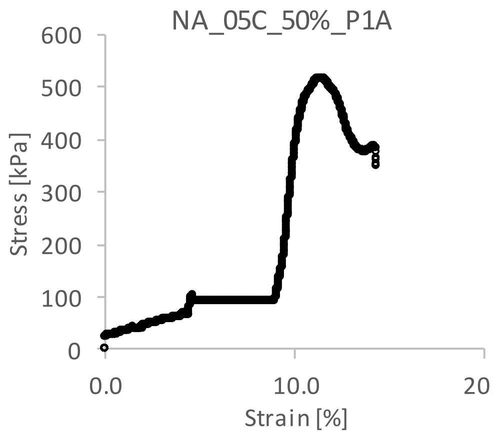
NA_05C_50%_P1A
Stress [kPa]
0
100
200
300
400
500
600
0.0
10.0
20.0
Strain [%]

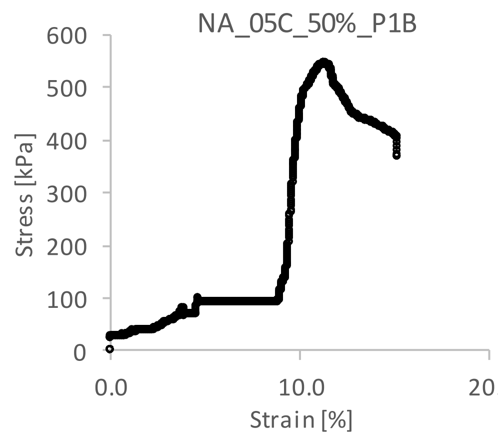
NA_05C_50%_P1B
Stress [kPa]
0
100
200
300
400
500
600
0.0
10.0
20.0
Strain [%]

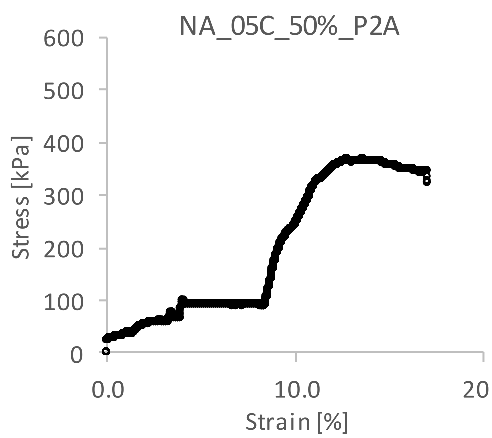
NA_05C_50%_P2A
Stress [kPa]
0
100
200
300
400
500
600
0.0
10.0
20.0
Strain [%]

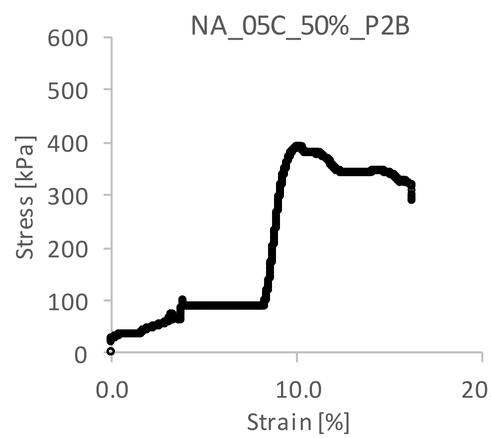
NA_05C_50%_P2B
Stress [kPa]
0
100
200
300
400
500
600
0.0
10.0
20.0
Strain [%]

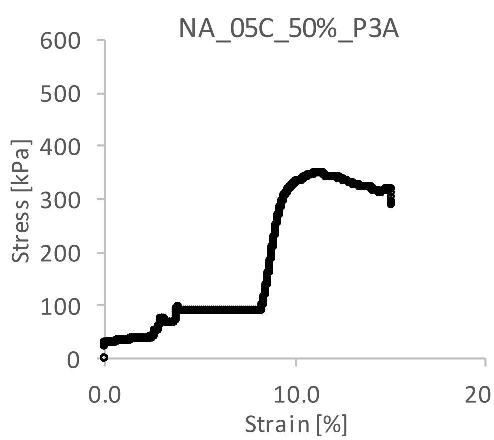
NA_05C_50%_P3A
Stress [kPa]
0
100
200
300
400
500
600
0.0
10.0
20.0
Strain [%]

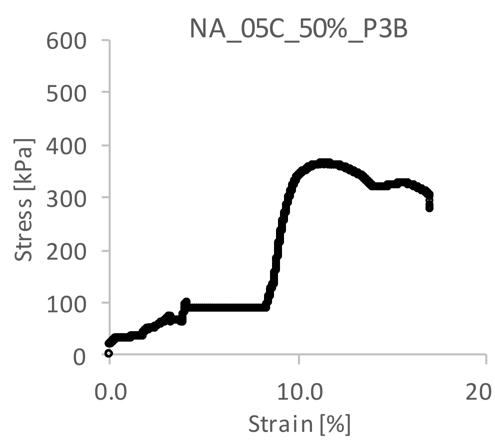
NA_05C_50%_P3B
Stress [kPa]
0
100
200
300
400
500
600
0.0
10.0
20.0
Strain [%]

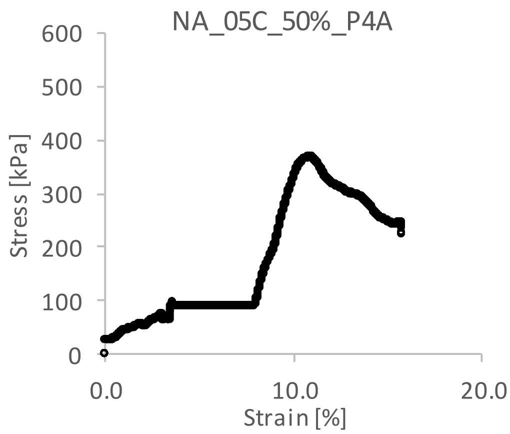
NA_05C_50%_P4A
Stress [kPa]
Strain [%]
0
100
200
300
400
500
600
0.0
10.0
20.0

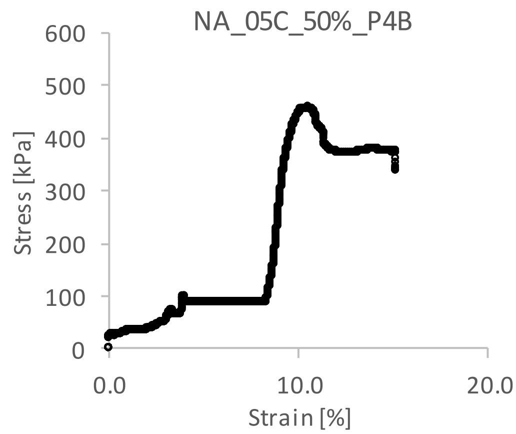
NA_05C_50%_P4B
Stress [kPa]
Strain [%]
0
100
200
300
400
500
600
0.0
10.0
20.0

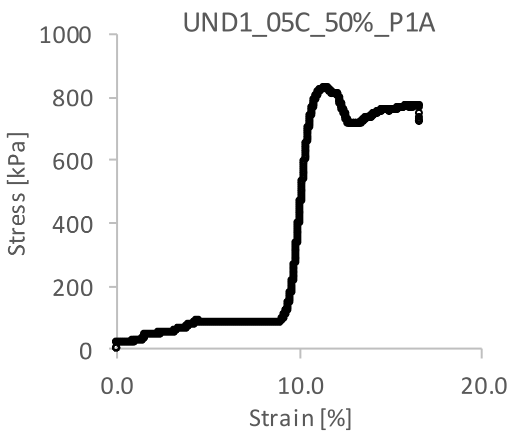
UND1_05C_50%_P1A
Stress [kPa]
Strain [%]
0
200
400
600
800
1000
0.0
10.0
20.0

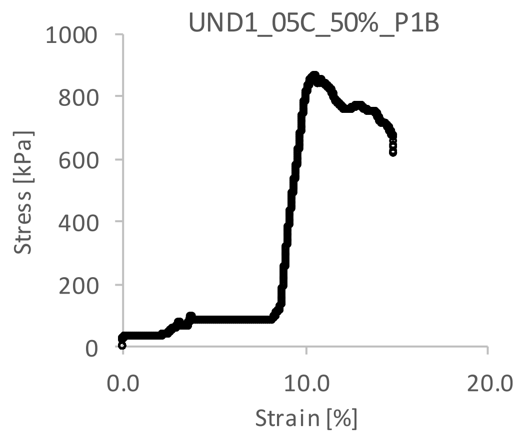
UND1_05C_50%_P1B
Stress [kPa]
Strain [%]
0
200
400
600
800
1000
0.0
10.0
20.0

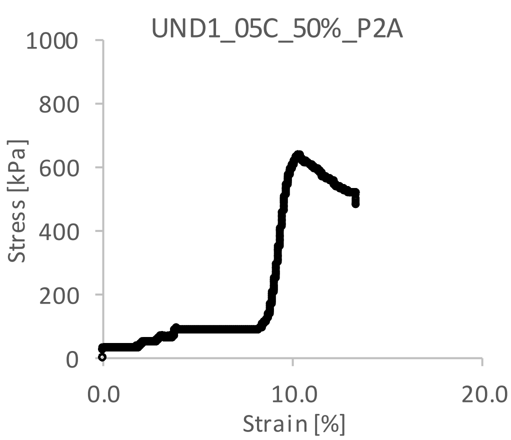
UND1_05C_50%_P2A
Stress [kPa]
Strain [%]
0
200
400
600
800
1000
0.0
10.0
20.0

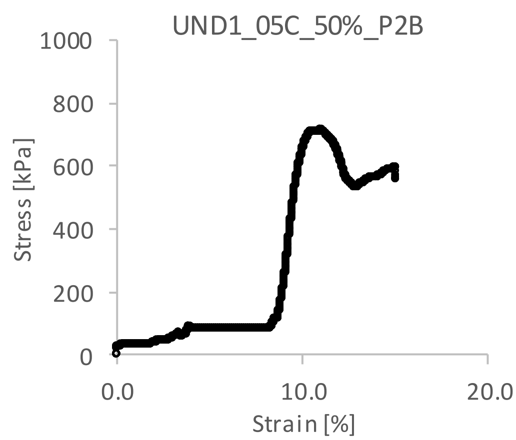
UND1_05C_50%_P2B
Stress [kPa]
Strain [%]
0
200
400
600
800
1000
0.0
10.0
20.0

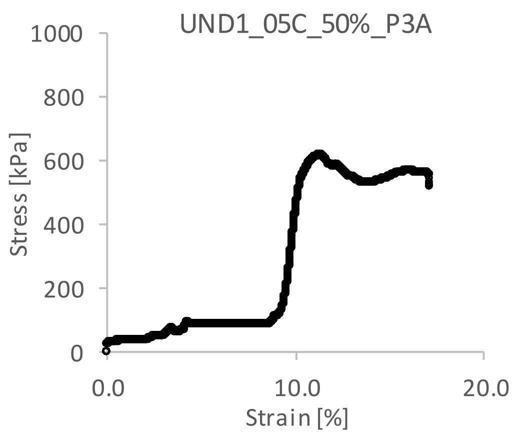
UND1_05C_50%_P3A
Stress [kPa]
Strain [%]
1000
800
600
400
200
0
0.0
10.0
20.0

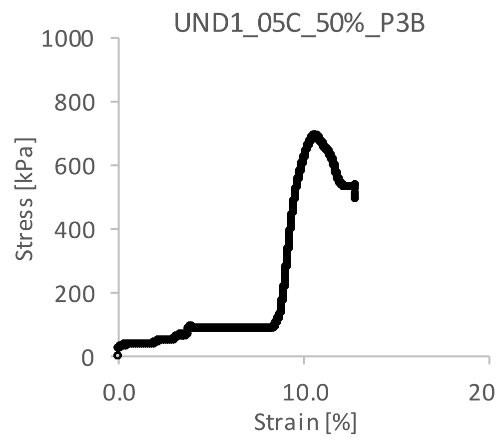
UND1_05C_50%_P3B
Stress [kPa]
Strain [%]
1000
800
600
400
200
0
0.0
10.0
20.0

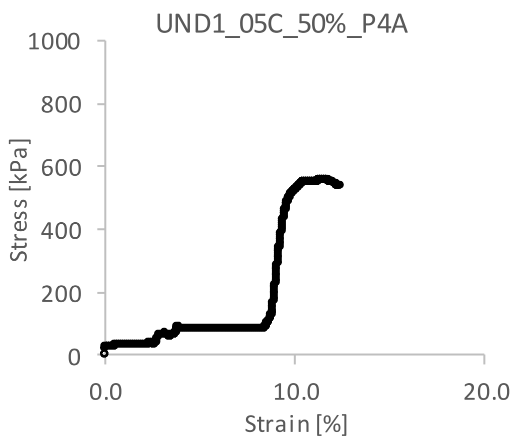
UND1_05C_50%_P4A
Stress [kPa]
Strain [%]
1000
800
600
400
200
0
0.0
10.0
20.0

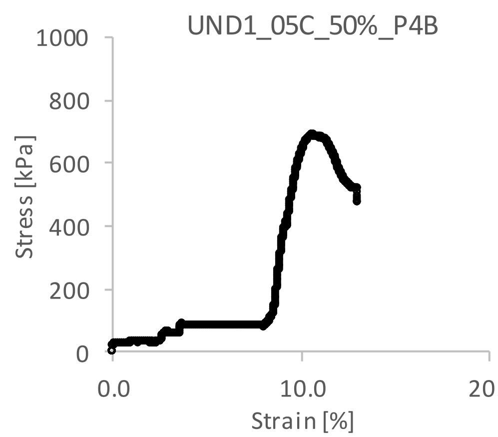
UND1_05C_50%_P4B
Stress [kPa]
Strain [%]
1000
800
600
400
200
0
0.0
10.0
20.0

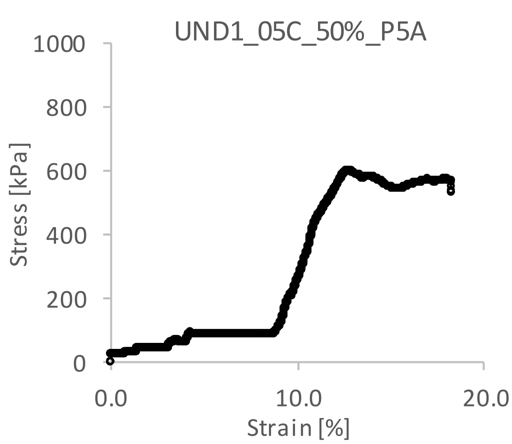
UND1_05C_50%_P5A
Stress [kPa]
Strain [%]
1000
800
600
400
200
0
0.0
10.0
20.0

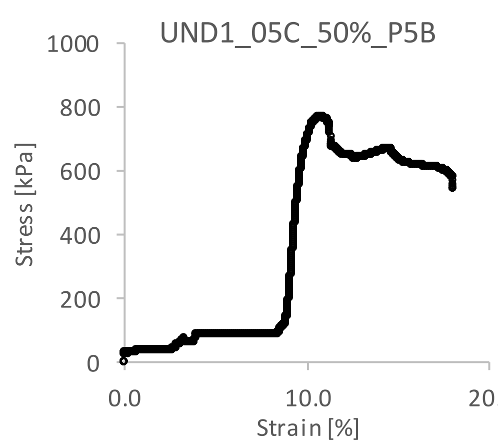
UND1_05C_50%_P5B
Stress [kPa]
Strain [%]
1000
800
600
400
200
0
0.0
10.0
20.0

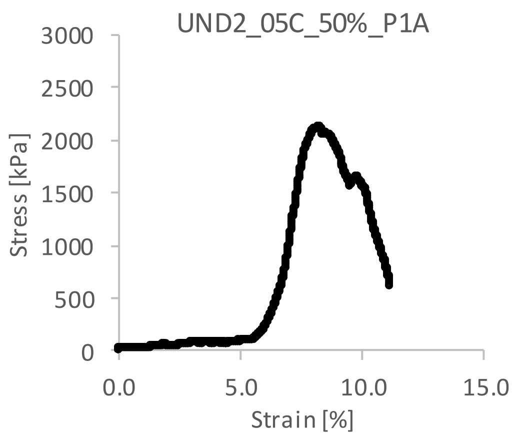
UND2_05C_50%_P1A
Stress [kPa]
Strain [%]
0
500
1000
1500
2000
2500
3000
0.0
5.0
10.0
15.0

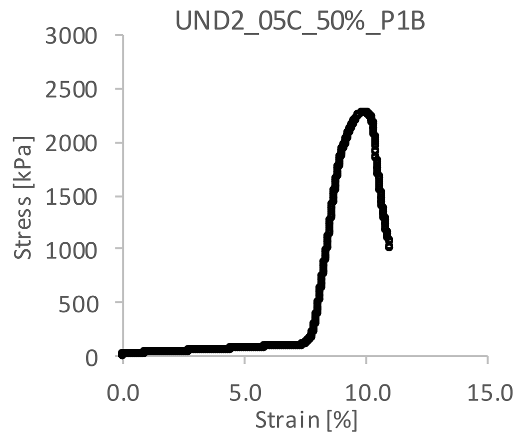
UND2_05C_50%_P1B
Stress [kPa]
Strain [%]
0
500
1000
1500
2000
2500
3000
0.0
5.0
10.0
15.0

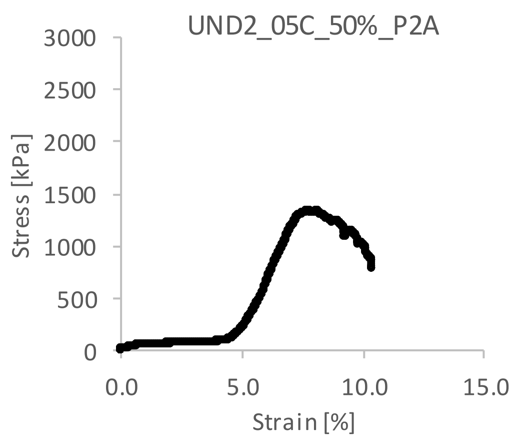
UND2_05C_50%_P2A
Stress [kPa]
Strain [%]
0
500
1000
1500
2000
2500
3000
0.0
5.0
10.0
15.0

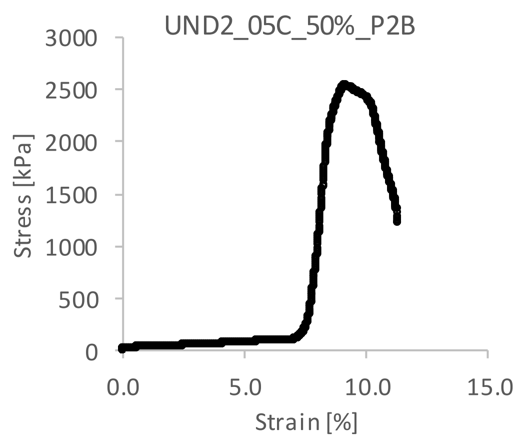
UND2_05C_50%_P2B
Stress [kPa]
Strain [%]
0
500
1000
1500
2000
2500
3000
0.0
5.0
10.0
15.0

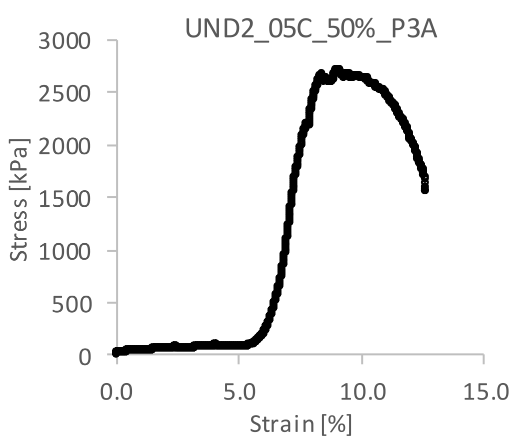
UND2_05C_50%_P3A
Stress [kPa]
Strain [%]
0
500
1000
1500
2000
2500
3000
0.0
5.0
10.0
15.0

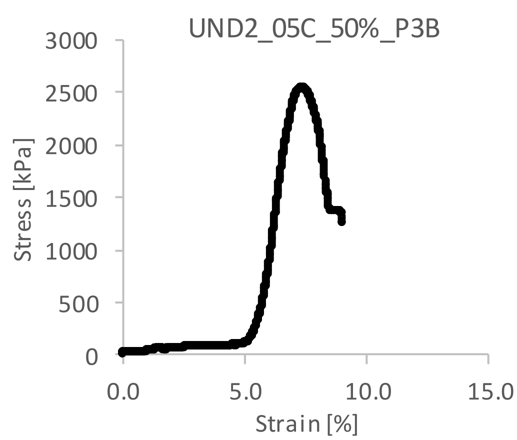
UND2_05C_50%_P3B
Stress [kPa]
Strain [%]
0
500
1000
1500
2000
2500
3000
0.0
5.0
10.0
15.0

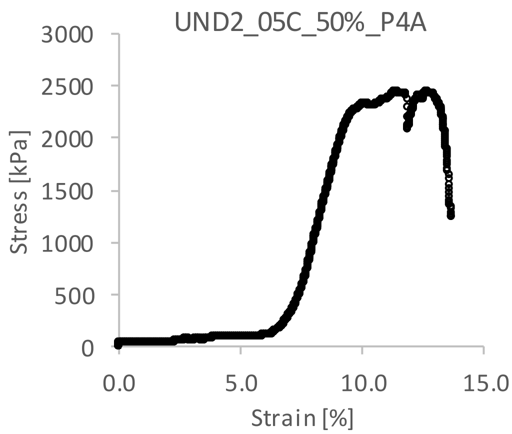
UND2_05C_50%_P4A
Stress [kPa]
3000
2500
2000
1500
1000
500
0
0.0
5.0
10.0
15.0
Strain [%]

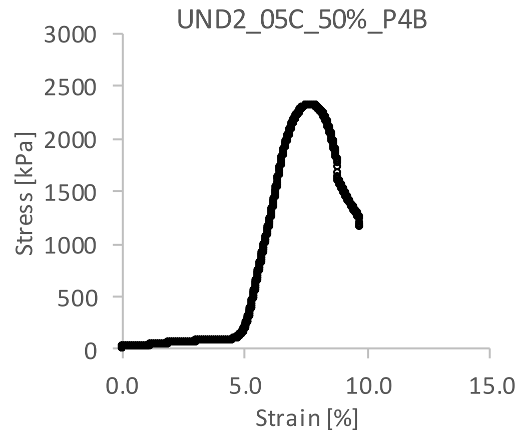
UND2_05C_50%_P4B
Stress [kPa]
3000
2500
2000
1500
1000
500
0
0.0
5.0
10.0
15.0
Strain [%]

Stress-Strain curves for l/s = 0.4

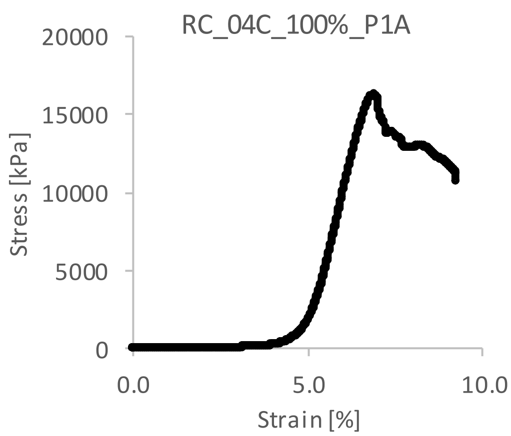

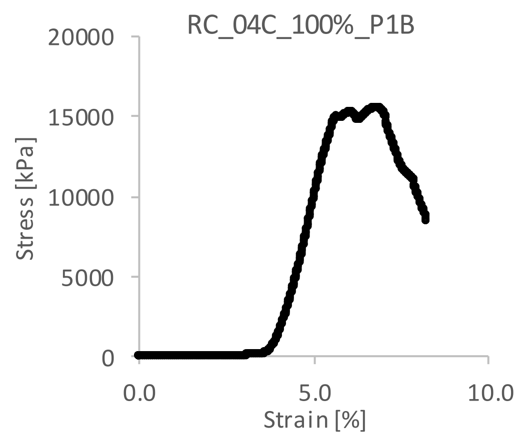

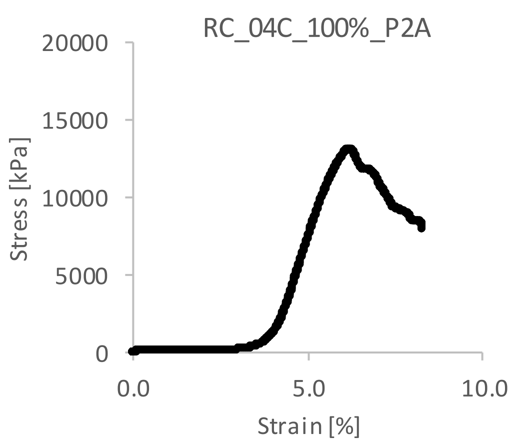

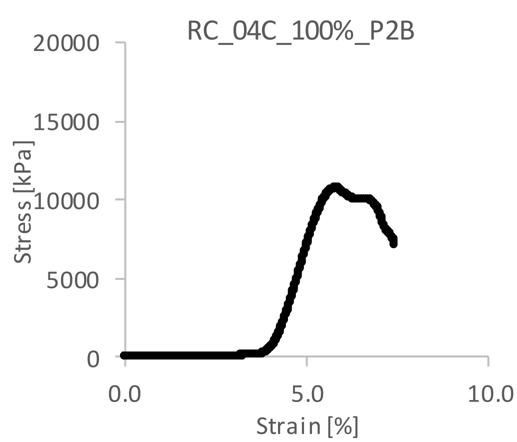

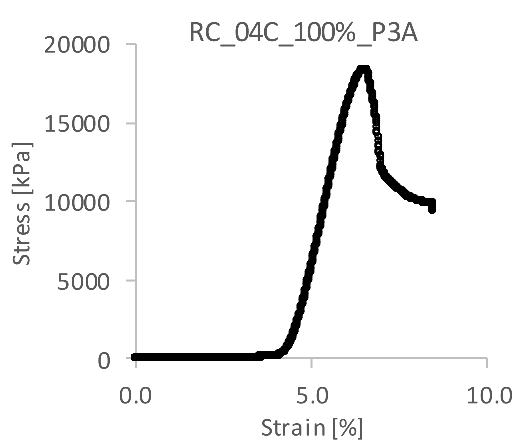

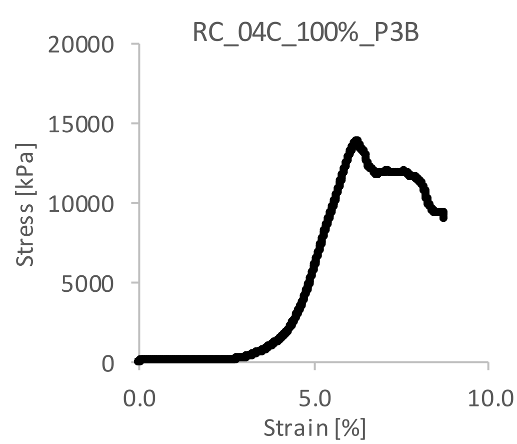

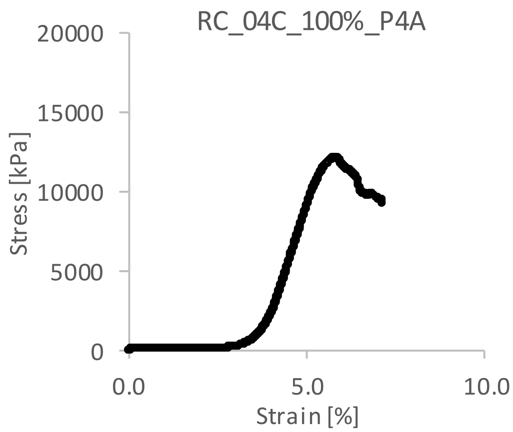
RC_04C_100%_P4A
Stress [kPa]
20000
15000
10000
5000
0
0.0
5.0
10.0
Strain [%]

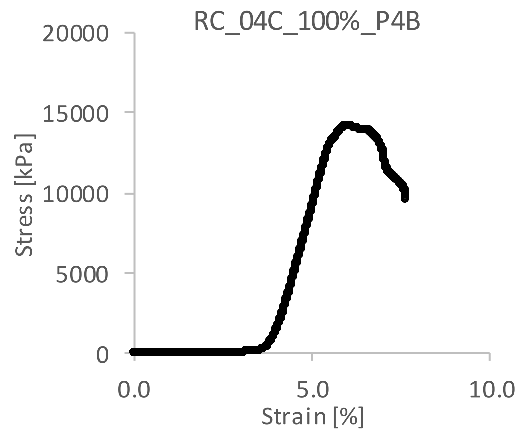
RC_04C_100%_P4B
Stress [kPa]
20000
15000
10000
5000
0
0.0
5.0
10.0
Strain [%]

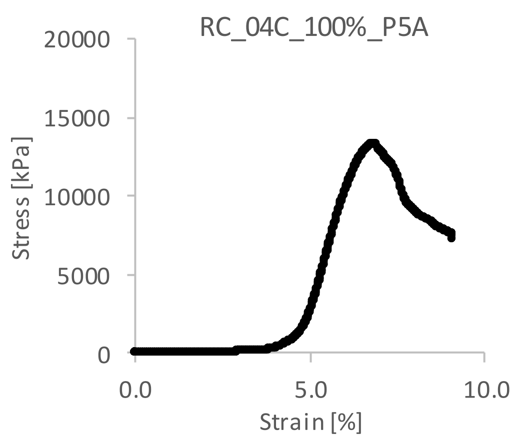
RC_04C_100%_P5A
Stress [kPa]
20000
15000
10000
5000
0
0.0
5.0
10.0
Strain [%]

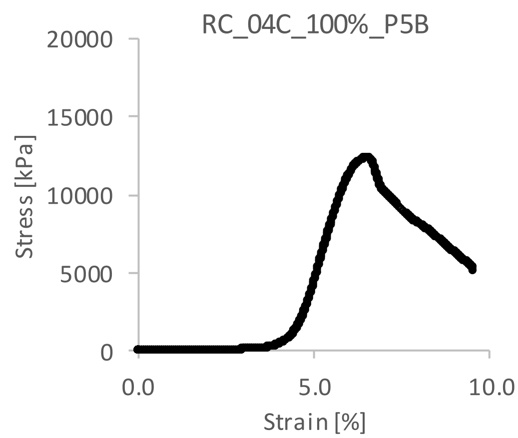
RC_04C_100%_P5B
Stress [kPa]
20000
15000
10000
5000
0
0.0
5.0
10.0
Strain [%]

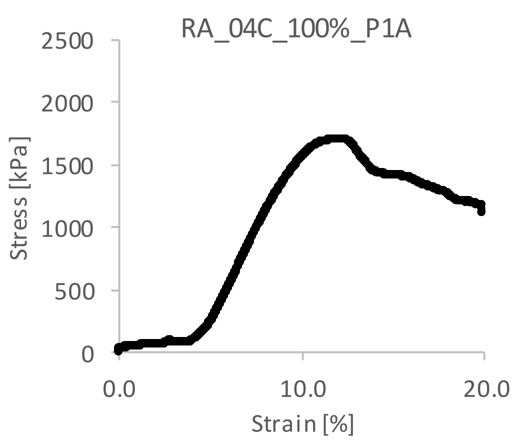
RA_04C_100%_P1A
Stress [kPa]
2500
2000
1500
1000
500
0
0.0
10.0
20.0
Strain [%]

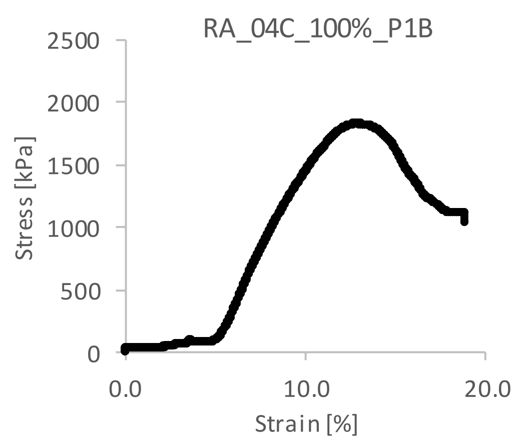
RA_04C_100%_P1B
Stress [kPa]
2500
2000
1500
1000
500
0
0.0
10.0
20.0
Strain [%]

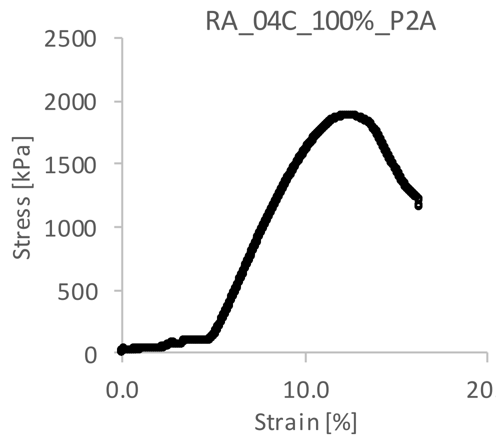
RA_04C_100%_P2A
Stress [kPa]
2500
2000
1500
1000
500
0
0.0
10.0
20.0
Strain [%]

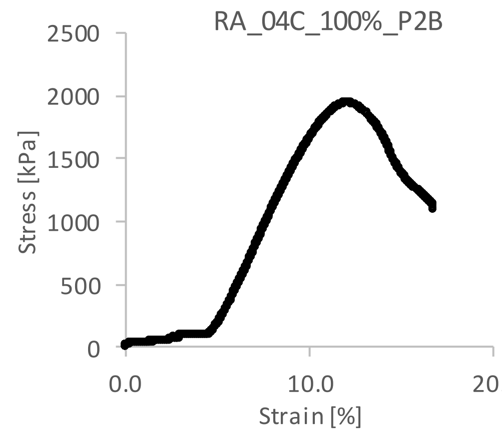
RA_04C_100%_P2B
Stress [kPa]
2500
2000
1500
1000
500
0
0.0
10.0
20.0
Strain [%]

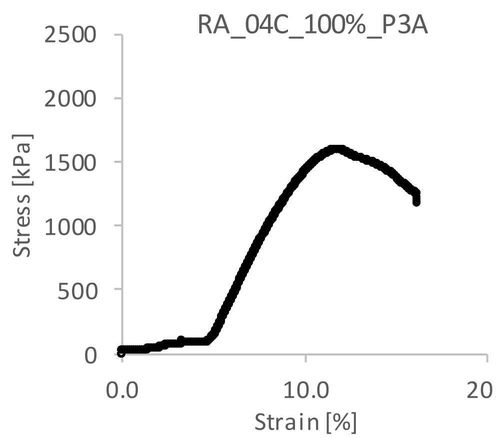
RA_04C_100%_P3A
Stress [kPa]
2500
2000
1500
1000
500
0
0.0
10.0
20.0
Strain [%]

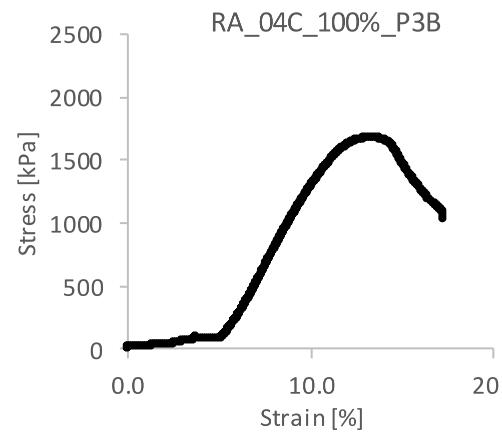
RA_04C_100%_P3B
Stress [kPa]
2500
2000
1500
1000
500
0
0.0
10.0
20.0
Strain [%]

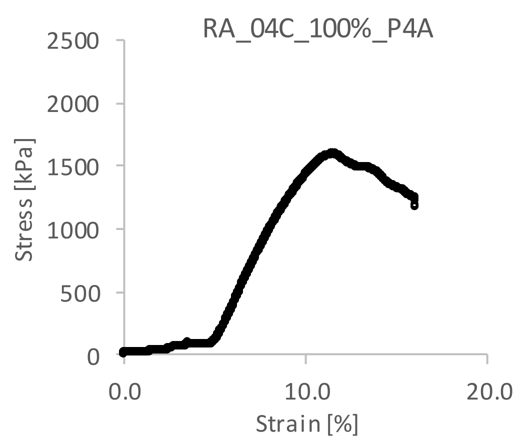
RA_04C_100%_P4A
Stress [kPa]
2500
2000
1500
1000
500
0
0.0
10.0
20.0
Strain [%]

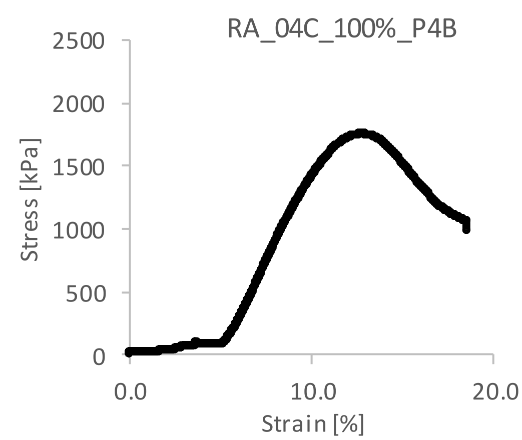
RA_04C_100%_P4B
Stress [kPa]
2500
2000
1500
1000
500
0
0.0
10.0
20.0
Strain [%]

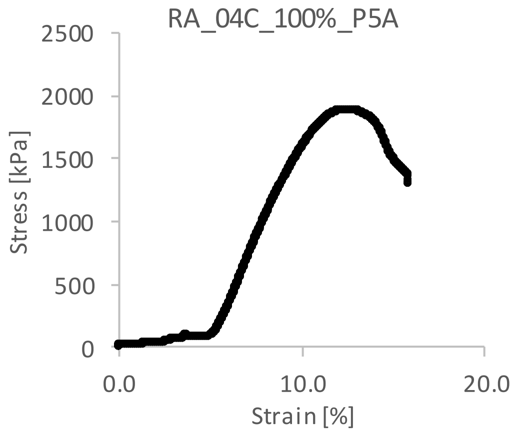
RA_04C_100%_P5A
Stress [kPa]
2500
2000
1500
1000
500
0
0.0
10.0
20.0
Strain [%]

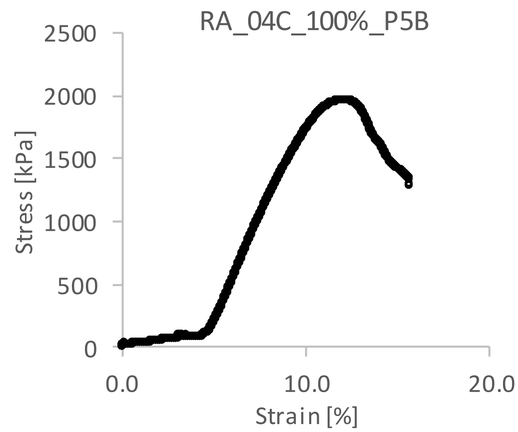
RA_04C_100%_P5B
Stress [kPa]
2500
2000
1500
1000
500
0
0.0
10.0
20.0
Strain [%]

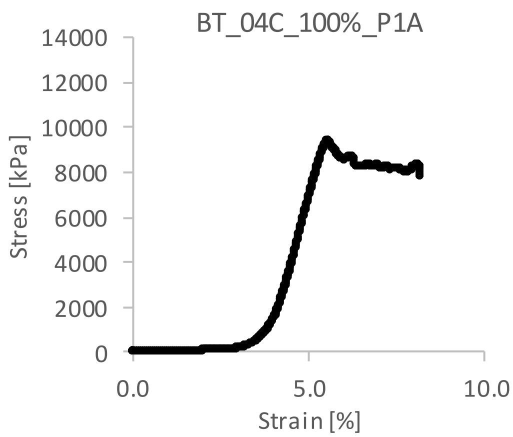
BT_04C_100%_P1A
Stress [kPa]
14000
12000
10000
8000
6000
4000
2000
0
0.0
5.0
10.0
Strain [%]

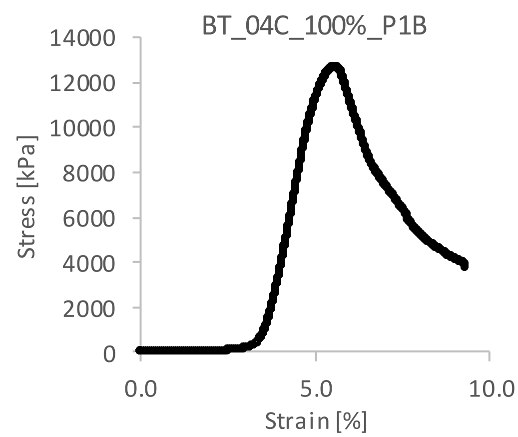
BT_04C_100%_P1B
Stress [kPa]
14000
12000
10000
8000
6000
4000
2000
0
0.0
5.0
10.0
Strain [%]

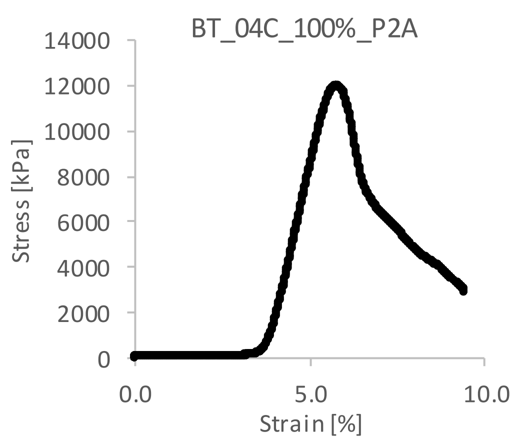
BT_04C_100%_P2A
Stress [kPa]
14000
12000
10000
8000
6000
4000
2000
0
0.0
5.0
10.0
Strain [%]

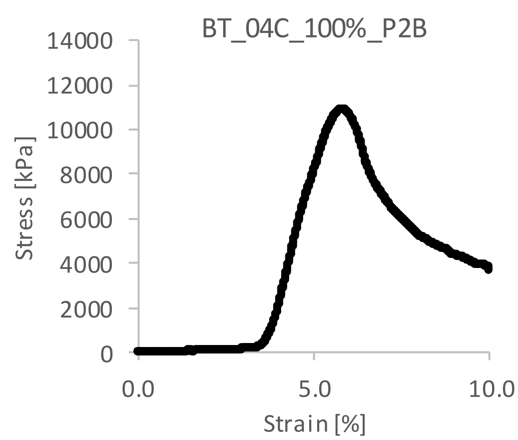
BT_04C_100%_P2B
Stress [kPa]
14000
12000
10000
8000
6000
4000
2000
0
0.0
5.0
10.0
Strain [%]

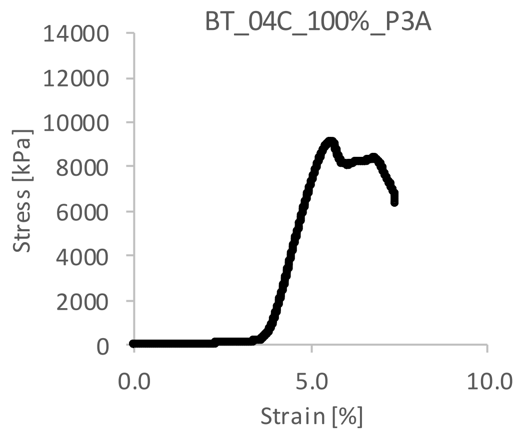
BT_04C_100%_P3A
14000
12000
10000
8000
6000
4000
2000
0
Stress [kPa]
0.0
5.0
10.0
Strain [%]

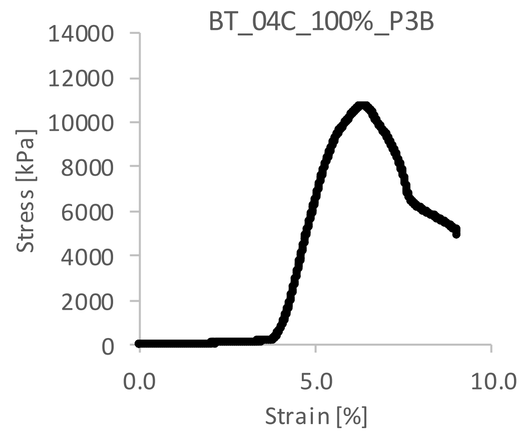
BT_04C_100%_P3B
14000
12000
10000
8000
6000
4000
2000
0
Stress [kPa]
0.0
5.0
10.0
Strain [%]

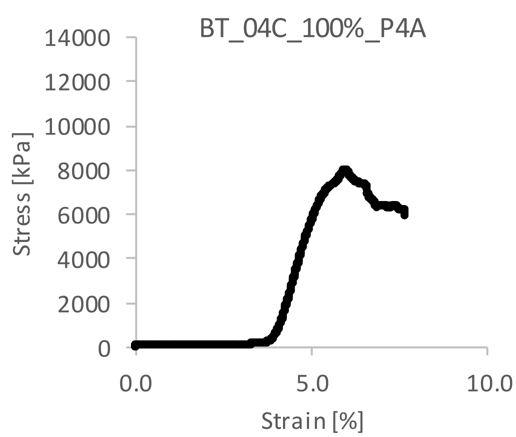
BT_04C_100%_P4A
14000
12000
10000
8000
6000
4000
2000
0
Stress [kPa]
0.0
5.0
10.0
Strain [%]

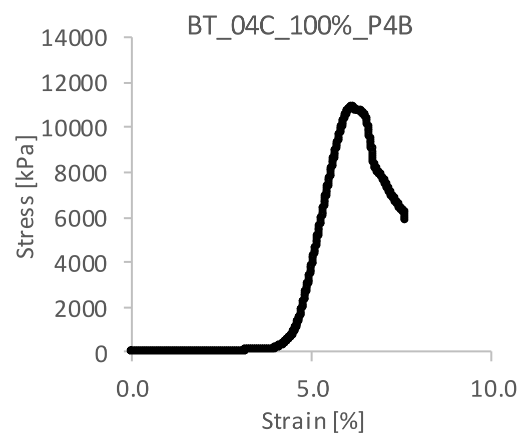
BT_04C_100%_P4B
14000
12000
10000
8000
6000
4000
2000
0
Stress [kPa]
0.0
5.0
10.0
Strain [%]

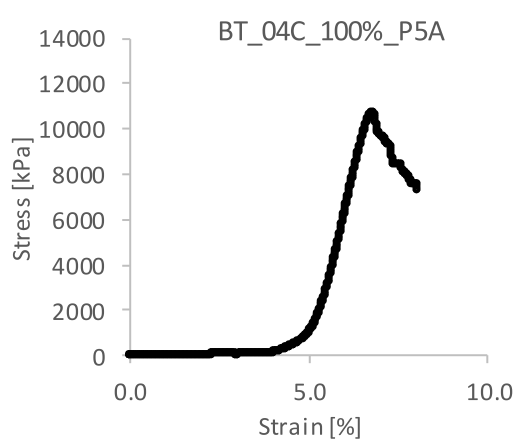
BT_04C_100%_P5A
14000
12000
10000
8000
6000
4000
2000
0
Stress [kPa]
0.0
5.0
10.0
Strain [%]

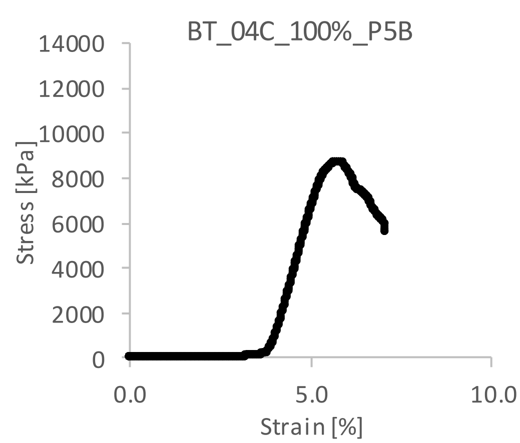
BT_04C_100%_P5B
14000
12000
10000
8000
6000
4000
2000
0
Stress [kPa]
0.0
5.0
10.0
Strain [%]

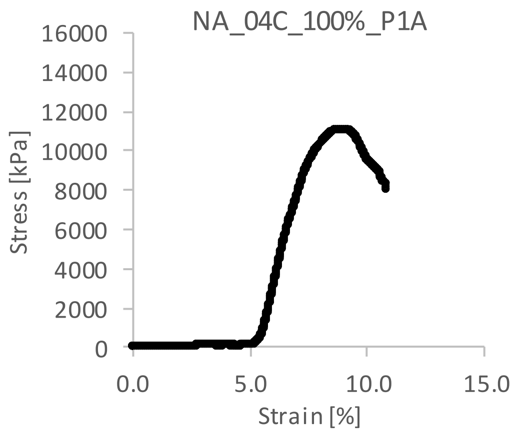
NA_04C_100%_P1A
Stress [kPa]
Strain [%]
0
2000
4000
6000
8000
10000
12000
14000
16000
0.0
5.0
10.0
15.0

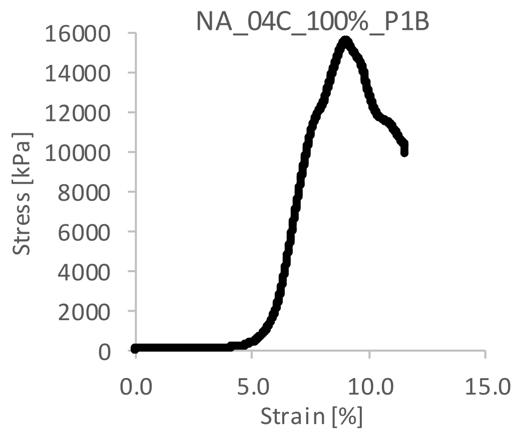
NA_04C_100%_P1B
Stress [kPa]
Strain [%]
0
2000
4000
6000
8000
10000
12000
14000
16000
0.0
5.0
10.0
15.0

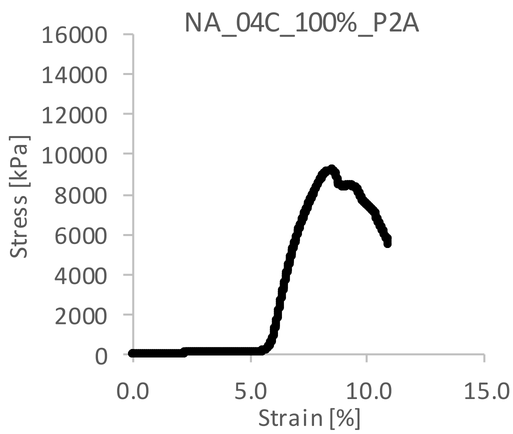
NA_04C_100%_P2A
Stress [kPa]
Strain [%]
0
2000
4000
6000
8000
10000
12000
14000
16000
0.0
5.0
10.0
15.0

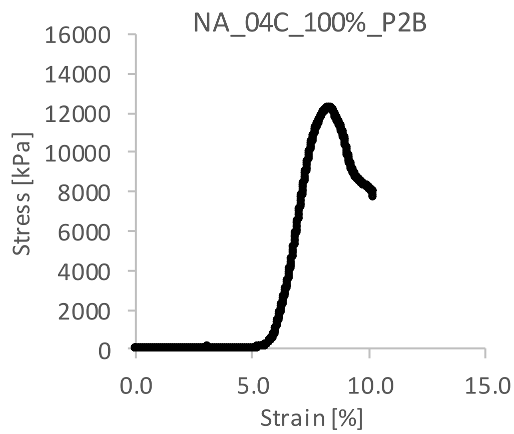
NA_04C_100%_P2B
Stress [kPa]
Strain [%]
0
2000
4000
6000
8000
10000
12000
14000
16000
0.0
5.0
10.0
15.0

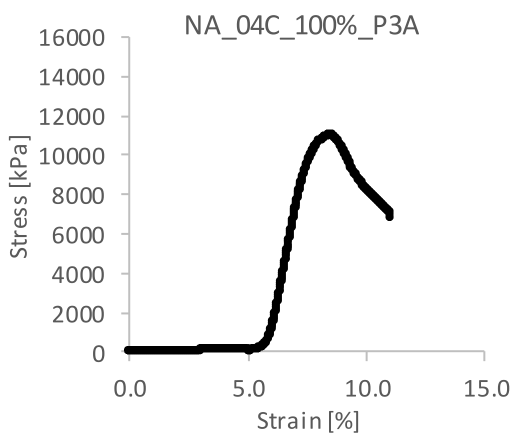
NA_04C_100%_P3A
Stress [kPa]
Strain [%]
0
2000
4000
6000
8000
10000
12000
14000
16000
0.0
5.0
10.0
15.0

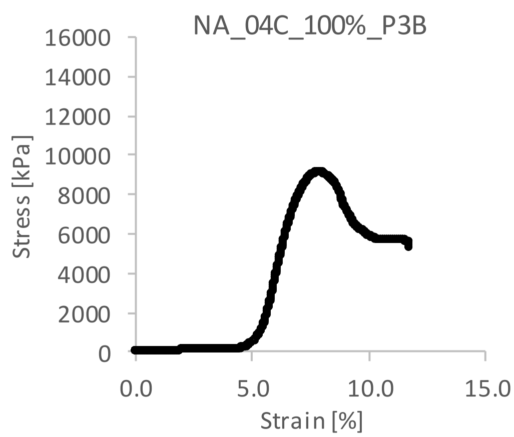
NA_04C_100%_P3B
Stress [kPa]
Strain [%]
0
2000
4000
6000
8000
10000
12000
14000
16000
0.0
5.0
10.0
15.0

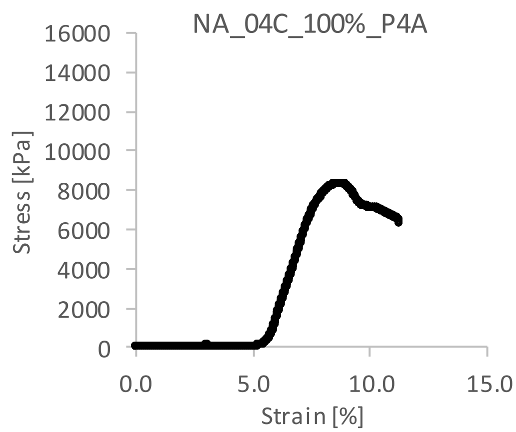
NA_04C_100%_P4A
Stress [kPa]
Strain [%]

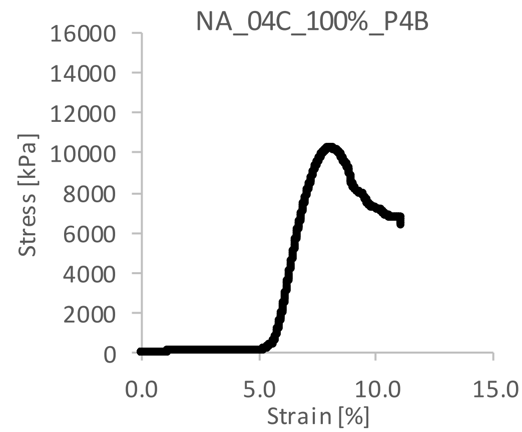
NA_04C_100%_P4B
Stress [kPa]
Strain [%]

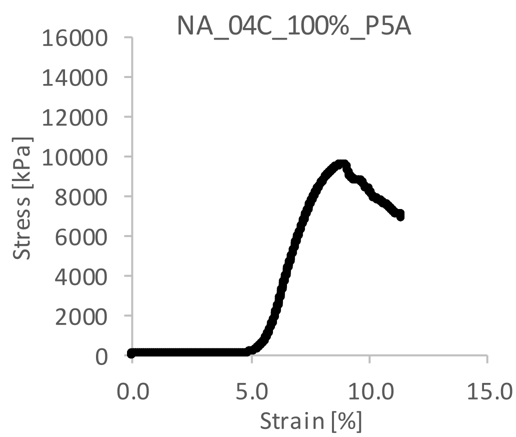
NA_04C_100%_P5A
Stress [kPa]
Strain [%]

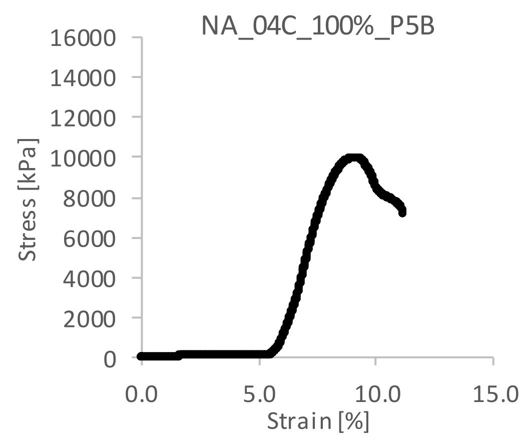
NA_04C_100%_P5B
Stress [kPa]
Strain [%]

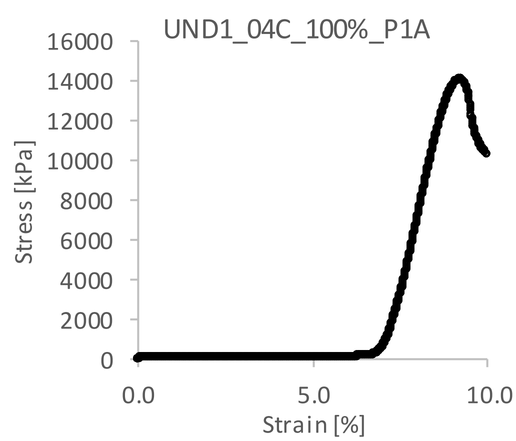
UND1_04C_100%_P1A
Stress [kPa]
Strain [%]

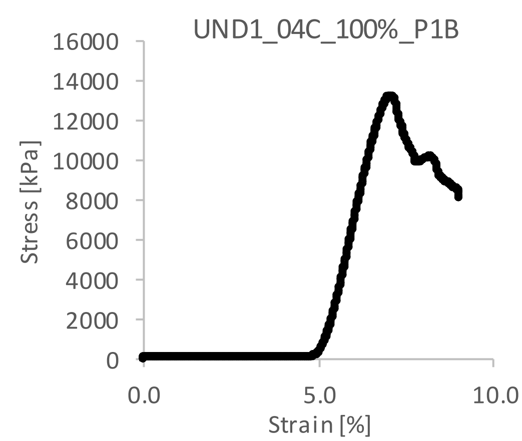
UND1_04C_100%_P1B
Stress [kPa]
Strain [%]

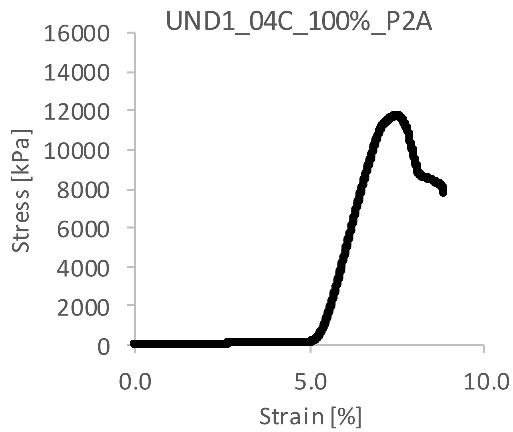
UND1_04C_100%_P2A
Stress [kPa]
Strain [%]

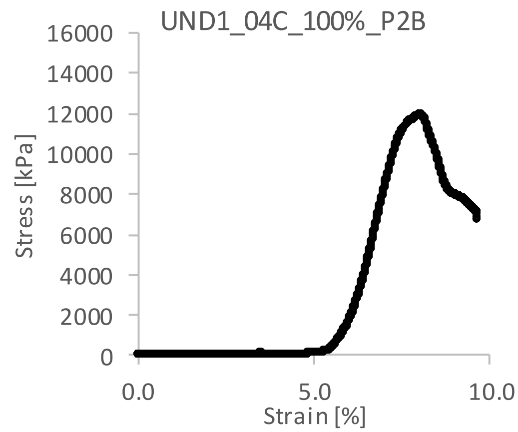
UND1_04C_100%_P2B
Stress [kPa]
Strain [%]

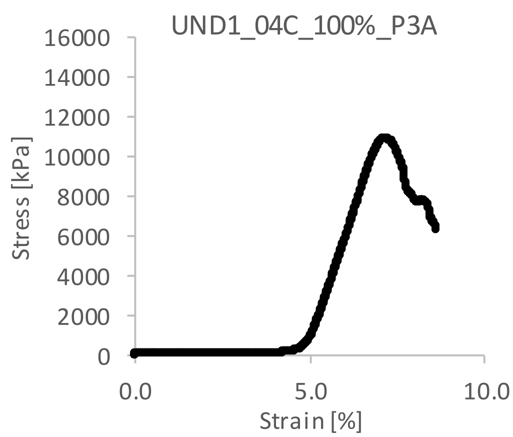
UND1_04C_100%_P3A
Stress [kPa]
Strain [%]

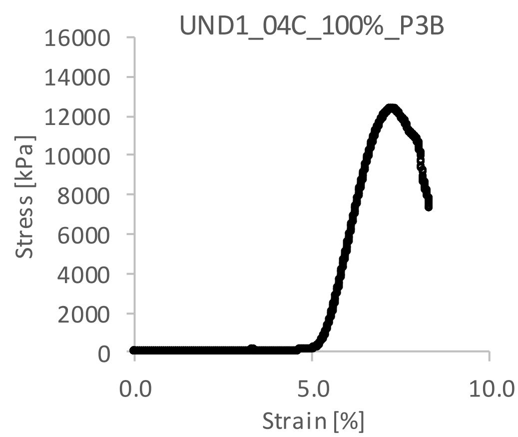
UND1_04C_100%_P3B
Stress [kPa]
Strain [%]

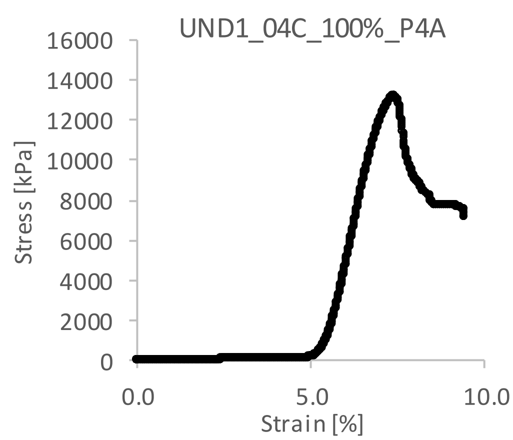
UND1_04C_100%_P4A
Stress [kPa]
Strain [%]

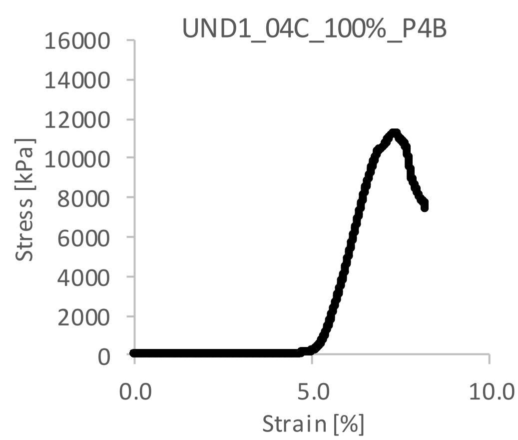
UND1_04C_100%_P4B
Stress [kPa]
Strain [%]

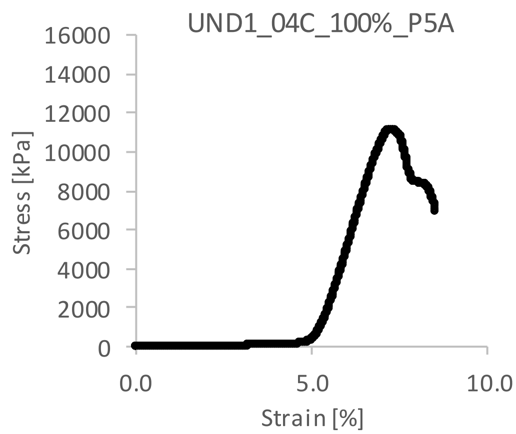
UND1_04C_100%_P5A
16000
14000
12000
10000
8000
6000
4000
2000
0
Stress [kPa]
0.0
5.0
10.0
Strain [%]

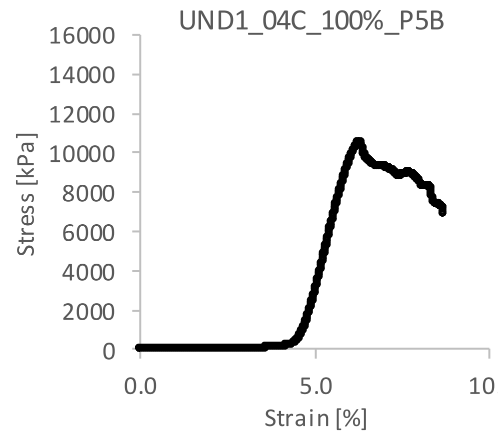
UND1_04C_100%_P5B
16000
14000
12000
10000
8000
6000
4000
2000
0
Stress [kPa]
0.0
5.0
10.0
Strain [%]

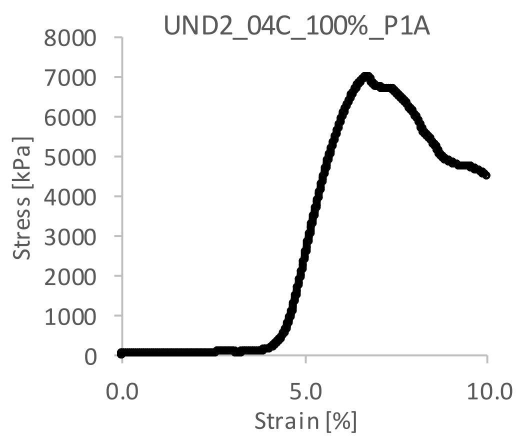
UND2_04C_100%_P1A
8000
7000
6000
5000
4000
3000
2000
1000
0
Stress [kPa]
0.0
5.0
10.0
Strain [%]

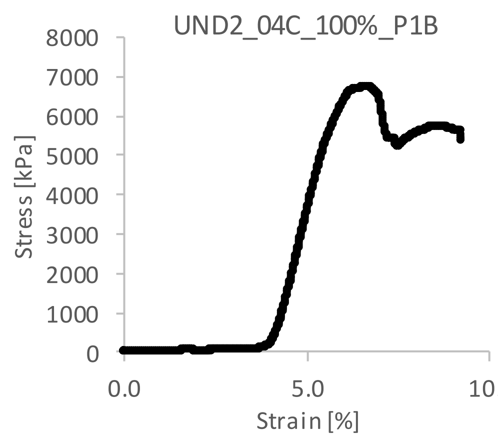
UND2_04C_100%_P1B
8000
7000
6000
5000
4000
3000
2000
1000
0
Stress [kPa]
0.0
5.0
10.0
Strain [%]

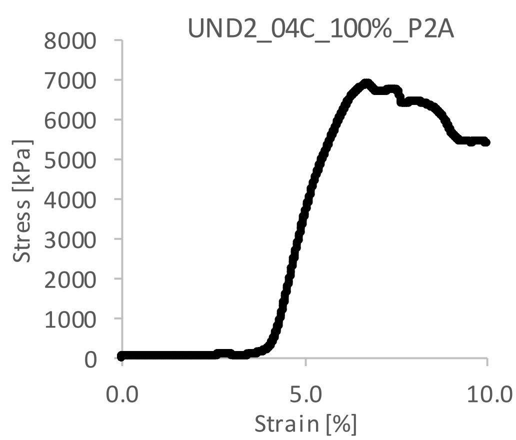
UND2_04C_100%_P2A
8000
7000
6000
5000
4000
3000
2000
1000
0
Stress [kPa]
0.0
5.0
10.0
Strain [%]

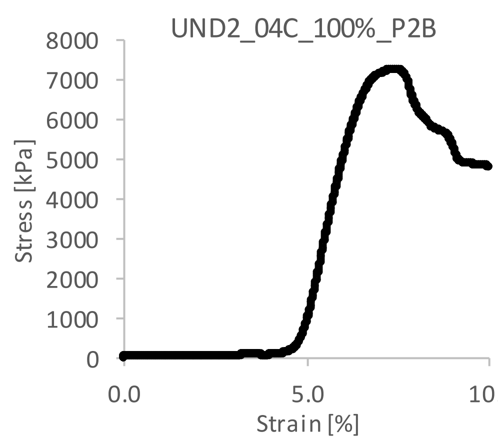
UND2_04C_100%_P2B
8000
7000
6000
5000
4000
3000
2000
1000
0
Stress [kPa]
0.0
5.0
10.0
Strain [%]

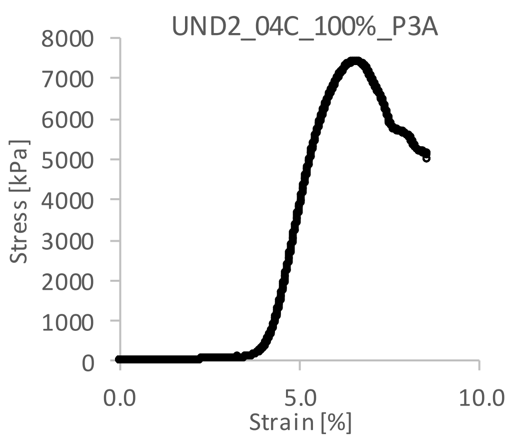
UND2_04C_100%_P3A
Stress [kPa]
8000
7000
6000
5000
4000
3000
2000
1000
0
0.0
5.0
10.0
Strain [%]

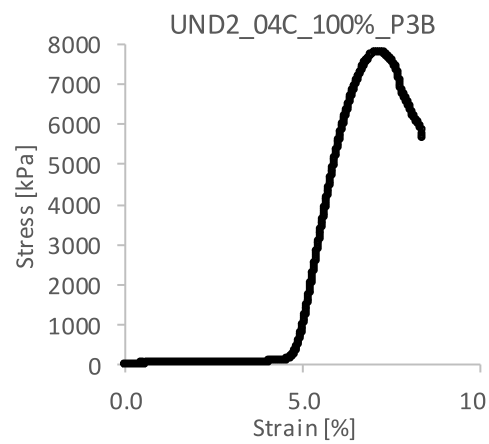
UND2_04C_100%_P3B
Stress [kPa]
8000
7000
6000
5000
4000
3000
2000
1000
0
0.0
5.0
10.0
Strain [%]

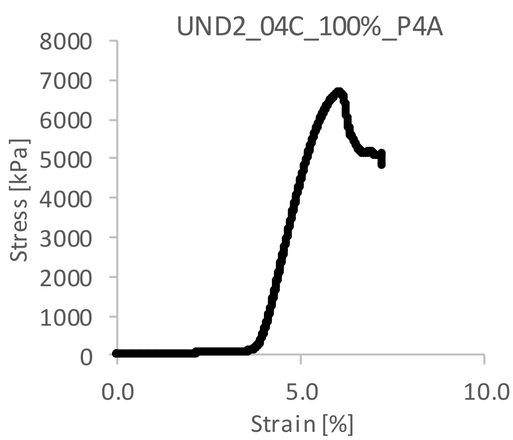
UND2_04C_100%_P4A
Stress [kPa]
8000
7000
6000
5000
4000
3000
2000
1000
0
0.0
5.0
10.0
Strain [%]

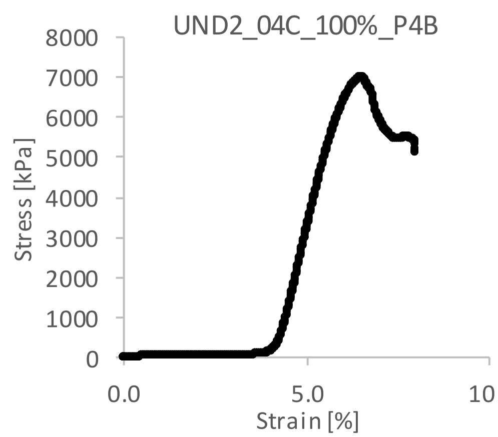
UND2_04C_100%_P4B
Stress [kPa]
8000
7000
6000
5000
4000
3000
2000
1000
0
0.0
5.0
10.0
Strain [%]

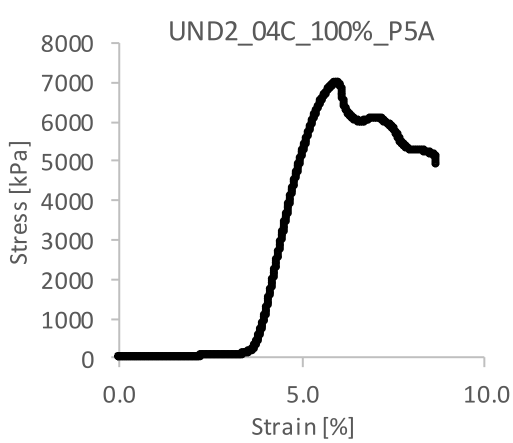
UND2_04C_100%_P5A
Stress [kPa]
8000
7000
6000
5000
4000
3000
2000
1000
0
0.0
5.0
10.0
Strain [%]

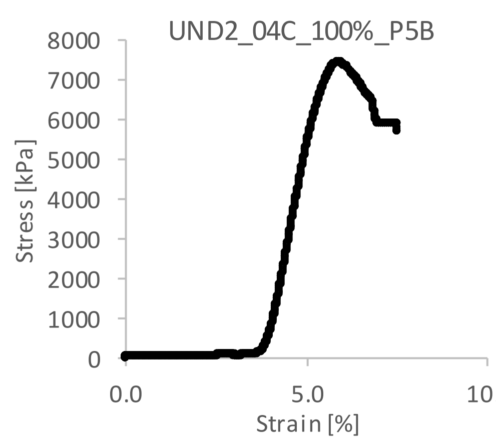
UND2_04C_100%_P5B
Stress [kPa]
8000
7000
6000
5000
4000
3000
2000
1000
0
0.0
5.0
10.0
Strain [%]

APPENDIX 2: flexural test results

Sample ID	Material	l/s	AS	F_{max} [N]	σ_{max} [kPa]	σ_{max} [MPa]	$\varepsilon_{(\sigma max)}$ [mm/mm]	$\varepsilon_{(\sigma max)}$ [%]	E_{sec} [kPa]	E_{sec} [MPa]	E_{tan} [kPa]	E_{tan} [MPa]	T [kPa*mm/mm]	ρ [kg/m^3]
RC_06_100%_P1	RC	0.6	100%	114.7	1265.5	1.3	0.003	0.330	383899.2	383.9	388827.1	388.8	2.104	1932
RC_06_100%_P2	RC	0.6	100%	126.6	1417.7	1.4	0.005	0.540	262460.8	262.5	263461.0	263.5	3.849	1897
RC_06_100%_P3	RC	0.6	100%	99.1	1067.7	1.1	0.005	0.520	205411.1	205.4	209140.0	209.1	2.821	1905
RC_06_100%_P4	RC	0.6	100%	101.0	1029.9	1.0	0.006	0.611	168417.3	168.4	170273.7	170.3	3.175	1886
RC_06_100%_P5	RC	0.6	100%	108.3	1154.3	1.2	0.008	0.820	140793.4	140.8	141290.8	141.3	4.754	1922
RA_06_100%_P1	RA	0.6	100%	40.4	460.2	0.5	0.066	6.590	6982.8	7.0	7133.9	7.1	15.514	1839
RA_06_100%_P2	RA	0.6	100%	35.7	459.6	0.5	0.027	2.741	16768.2	16.8	18917.0	18.9	6.918	1848
RA_06_100%_P3	RA	0.6	100%	31.6	380.3	0.4	0.054	5.371	7081.0	7.1	7427.7	7.4	10.761	1858
RA_06_100%_P4	RA	0.6	100%	31.4	421.5	0.4	0.023	2.314	18219.2	18.2	18935.6	18.9	5.047	1887
RA_06_100%_P5	RA	0.6	100%	30.9	410.2	0.4	0.023	2.337	17556.2	17.6	20763.7	20.8	5.262	1935
BT_06_100%_P1	BT	0.6	100%	110.3	1260.0	1.3	0.023	2.302	54728.9	54.7	54784.4	54.8	14.532	2000
BT_06_100%_P2	BT	0.6	100%	124.7	1348.3	1.3	0.030	2.969	45418.8	45.4	45431.0	45.4	20.003	1925
BT_06_100%_P3	BT	0.6	100%	122.3	1440.0	1.4	0.012	1.211	118870.8	118.9	134077.4	134.1	9.488	2003
BT_06_100%_P4	BT	0.6	100%	139.3	1599.3	1.6	0.009	0.941	169978.7	170.0	195981.0	196.0	8.161	1981
BT_06_100%_P5	BT	0.6	100%	130.7	1470.4	1.5	0.018	1.810	81253.6	81.3	82290.9	82.3	13.439	1955
NA_06_100%_P1	NA	0.6	100%	160.9	2079.5	2.1	0.017	1.671	124469.2	124.5	126012.6	126.0	17.609	2021
NA_06_100%_P2	NA	0.6	100%	114.8	1609.3	1.6	0.021	2.116	76062.1	76.1	96028.4	96.0	19.829	2178
NA_06_100%_P3	NA	0.6	100%	121.0	1752.5	1.8	0.006	0.552	317523.9	317.5	348748.4	348.7	5.208	1999
NA_06_100%_P4	NA	0.6	100%	166.0	2222.1	2.2	0.010	0.966	230136.7	230.1	248827.6	248.8	11.375	1963
NA_06_100%_P5	NA	0.6	100%	158.2	2226.7	2.2	0.022	2.168	102728.4	102.7	108681.5	108.7	25.367	1904
UND_06_100%_P1	UND	0.6	100%	25.1	240.0	0.2	0.007	0.711	33772.6	33.8	38089.6	38.1	0.953	1913
UND_06_100%_P2	UND	0.6	100%	32.1	327.4	0.3	0.008	0.846	38711.5	38.7	39907.2	39.9	1.426	1952
UND_06_100%_P3	UND	0.6	100%	27.9	273.8	0.3	0.010	0.967	28322.4	28.3	28709.1	28.7	1.339	1917
UND_06_100%_P4	UND	0.6	100%	30.1	294.1	0.3	0.009	0.868	33873.3	33.9	35635.2	35.6	1.349	1923
UND_06_100%_P5	UND	0.6	100%	35.1	357.7	0.4	0.007	0.749	47762.1	47.8	52948.1	52.9	1.463	1965
UND2_06_100%_P1	UND2	0.6	100%	29.8	308.6	0.3	0.015	1.502	20547.4	20.5	22539.2	22.5	2.507	1926
UND2_06_100%_P2	UND2	0.6	100%	31.7	356.5	0.4	0.012	1.244	28646.1	28.6	29894.9	29.9	2.301	1911
UND2_06_100%_P3	UND2	0.6	100%	37.6	377.9	0.4	0.013	1.303	28990.9	29.0	30233.3	30.2	2.610	1933
UND2_06_100%_P4	UND2	0.6	100%	42.0	440.6	0.4	0.013	1.296	34002.9	34.0	34006.1	34.0	2.859	1948
UND2_06_100%_P5	UND2	0.6	100%	41.7	440.1	0.4	0.016	1.565	28112.1	28.1	28508.1	28.5	3.490	1910

Sample ID	Material	l/s	AS	F_{max} [N]	σ_{max} [kPa]	σ_{max} [MPa]	$\varepsilon_{(\sigma max)}$ [mm/mm]	$\varepsilon_{(\sigma max)}$ [%]	E_{sec} [kPa]	E_{sec} [MPa]	E_{tan} [kPa]	E_{tan} [MPa]	T [kPa*mm/mm]	ρ [kg/m^3]
RC_06_75%_P1	RC	0.6	75%	217.7	2593.1	2.6	0.006	0.564	460122.0	460.1	461042.4	461.0	7.323	1755
RC_06_75%_P2	RC	0.6	75%	179.5	2092.9	2.1	0.006	0.624	335177.7	335.2	335601.3	335.6	6.552	1778
RC_06_75%_P3	RC	0.6	75%	188.6	2111.5	2.1	0.010	1.020	206978.3	207.0	179553.2	179.6	67.879	1772
RC_06_75%_P4	RC	0.6	75%	200.3	2253.7	2.3	0.007	0.714	315740.0	315.7	315798.2	315.8	8.050	1768
RC_06_75%_P5	RC	0.6	75%	-	-	-	-	-	-	-	-	-	-	-
RA_06_75%_P1	RA	0.6	75%	97.1	1337.9	1.3	0.011	1.068	125281.4	125.3	155821.0	155.8	8.211	1855
RA_06_75%_P2	RA	0.6	75%	65.5	867.5	0.9	0.014	1.443	60138.6	60.1	82607.3	82.6	7.548	1866
RA_06_75%_P3	RA	0.6	75%	66.7	1007.9	1.0	0.017	1.683	59885.6	59.9	65288.3	65.3	9.118	1849
RA_06_75%_P4	RA	0.6	75%	83.0	1067.2	1.1	0.015	1.544	69102.9	69.1	102873.9	102.9	10.212	1824
RA_06_75%_P5	RA	0.6	75%	58.9	844.8	0.8	0.011	1.138	74210.0	74.2	84571.9	84.6	5.341	1910
BT_06_75%_P1	BT	0.6	75%	79.1	962.5	1.0	0.013	1.255	76712.5	76.7	82390.5	82.4	6.424	1864
BT_06_75%_P2	BT	0.6	75%	49.5	535.8	0.5	0.018	1.784	30024.1	30.0	32039.7	32.0	5.028	1900
BT_06_75%_P3	BT	0.6	75%	76.8	966.9	1.0	0.013	1.308	73912.9	73.9	76519.4	76.5	6.510	1986
BT_06_75%_P4	BT	0.6	75%	46.3	634.6	0.6	0.008	0.846	75028.7	75.0	83057.1	83.1	2.887	1935
BT_06_75%_P5	BT	0.6	75%	62.6	790.8	0.8	0.013	1.277	61917.2	61.9	63269.2	63.3	5.145	2047
NA_06_75%_P1	NA	0.6	75%	95.3	1253.8	1.3	0.011	1.118	112160.5	112.2	117255.7	117.3	7.466	2002
NA_06_75%_P2	NA	0.6	75%	67.3	906.5	0.9	0.012	1.167	77688.0	77.7	84314.0	84.3	5.620	2016
NA_06_75%_P3	NA	0.6	75%	60.1	937.2	0.9	0.006	0.631	148556.3	148.6	154384.2	154.4	3.061	1971
NA_06_75%_P4	NA	0.6	75%	182.8	2344.5	2.3	0.013	1.318	177861.3	177.9	185947.3	185.9	16.077	1941
NA_06_75%_P5	NA	0.6	75%	58.2	897.6	0.9	0.010	1.012	88720.5	88.7	93598.5	93.6	4.863	1976
UND_06_75%_P1	UND	0.6	75%	221.0	2614.6	2.6	0.017	1.675	156135.5	156.1	156155.8	156.2	21.873	1846
UND_06_75%_P2	UND	0.6	75%	223.6	2659.4	2.7	0.010	1.045	254604.8	254.6	254733.9	254.7	13.905	1838
UND_06_75%_P3	UND	0.6	75%	158.8	1947.2	1.9	0.013	1.307	149010.2	149.0	169570.0	169.6	13.970	1835
UND_06_75%_P4	UND	0.6	75%	191.0	2138.9	2.1	0.010	1.039	205859.4	205.9	207414.9	207.4	11.216	1821
UND_06_75%_P5	UND	0.6	75%	244.5	3078.7	3.1	0.011	1.137	270690.2	270.7	271954.5	272.0	17.546	1823
UND2_06_75%_P1	UND2	0.6	75%	108.0	1389.5	1.4	0.009	0.927	149823.5	149.8	150272.1	150.3	6.472	1860
UND2_06_75%_P2	UND2	0.6	75%	106.0	1314.9	1.3	0.009	0.925	142083.3	142.1	142602.3	142.6	6.105	1909
UND2_06_75%_P3	UND2	0.6	75%	93.8	1084.9	1.1	0.015	1.525	71147.0	71.1	71154.9	71.2	8.278	1885
UND2_06_75%_P4	UND2	0.6	75%	107.6	1340.8	1.3	0.009	0.855	156896.2	156.9	159171.3	159.2	5.789	1907
UND2_06_75%_P5	UND2	0.6	75%	98.4	1347.3	1.3	0.009	0.895	150523.3	150.5	151890.2	151.9	6.061	1898

Sample ID	Material	l/s	AS	F_{max} [N]	σ_{max} [kPa]	σ_{max} [MPa]	$\varepsilon_{(\sigma max)}$ [mm/mm]	$\varepsilon_{(\sigma max)}$ [%]	E_{sec} [kPa]	E_{sec} [MPa]	E_{tan} [kPa]	E_{tan} [MPa]	T [kPa*mm/mm]	ρ [kg/m^3]
RC_06_50%_P1	RC	0.6	50%	15.2	167.5	0.2	0.008	0.804	20832.9	20.8	20868.9	20.9	0.674	1532
RC_06_50%_P2	RC	0.6	50%	14.1	165.3	0.2	0.006	0.643	25701.7	25.7	25714.2	25.7	0.531	1546
RC_06_50%_P3	RC	0.6	50%	13.6	148.5	0.1	0.011	1.142	12999.2	13.0	13015.0	13.0	0.847	1429
RC_06_50%_P4	RC	0.6	50%	13.8	149.6	0.1	0.009	0.943	15864.7	15.9	13669.3	13.7	0.614	1474
RC_06_50%_P5	RC	0.6	50%	13.7	169.6	0.2	0.008	0.768	22086.3	22.1	22115.2	22.1	0.651	1459
RA_06_50%_P1	RA	0.6	50%	6.5	78.2	0.1	0.007	0.744	10510.2	10.5	10515.0	10.5	0.309	1695
RA_06_50%_P2	RA	0.6	50%	8.5	94.8	0.1	0.004	0.437	21681.7	21.7	23779.5	23.8	0.244	1630
RA_06_50%_P3	RA	0.6	50%	11.2	135.4	0.1	0.006	0.555	24406.8	24.4	26715.1	26.7	0.398	1713
RA_06_50%_P4	RA	0.6	50%	-	-	-	-	-	-	-	-	-	-	-
RA_06_50%_P5	RA	0.6	50%	-	-	-	-	-	-	-	-	-	-	-
BT_06_50%_P1	BT	0.6	50%	66.3	759.4	0.8	0.009	0.880	86310.0	86.3	135067.8	135.1	4.252	1593
BT_06_50%_P2	BT	0.6	50%	123.9	1600.4	1.6	0.007	0.726	220347.4	220.3	343199.3	343.2	7.151	1594
BT_06_50%_P3	BT	0.6	50%	125.1	1505.0	1.5	0.008	0.760	197928.3	197.9	267897.1	267.9	6.970	1586
BT_06_50%_P4	BT	0.6	50%	51.8	576.2	0.6	0.009	0.873	66015.4	66.0	97853.6	97.9	3.197	1624
BT_06_50%_P5	BT	0.6	50%	66.0	762.5	0.8	0.011	1.085	70243.7	70.2	103318.1	103.3	5.348	1610
NA_06_50%_P1	NA	0.6	50%	8.5	115.8	0.1	0.008	0.808	14336.4	14.3	14357.0	14.4	0.465	1724
NA_06_50%_P2	NA	0.6	50%	9.3	112.6	0.1	0.008	0.848	13283.3	13.3	13300.0	13.3	0.478	1701
NA_06_50%_P3	NA	0.6	50%	9.5	114.2	0.1	0.011	1.052	10858.3	10.9	10873.1	10.9	0.602	1730
NA_06_50%_P4	NA	0.6	50%	9.6	112.3	0.1	0.010	1.030	10907.2	10.9	10907.5	10.9	0.580	1720
NA_06_50%_P5	NA	0.6	50%	9.5	118.6	0.1	0.007	0.744	15947.4	15.9	15971.2	16.0	0.445	1675
UND_06_50%_P1	UND	0.6	50%	57.5	742.9	0.7	0.008	0.816	91051.8	91.1	95865.5	95.9	3.165	1607
UND_06_50%_P2	UND	0.6	50%	23.5	273.0	0.3	0.006	0.611	44671.1	44.7	45189.0	45.2	0.843	1622
UND_06_50%_P3	UND	0.6	50%	31.1	348.3	0.3	0.010	0.990	35168.7	35.2	45980.8	46.0	1.978	1616
UND_06_50%_P4	UND	0.6	50%	35.6	417.7	0.4	0.011	1.068	39126.4	39.1	58793.7	58.8	2.831	1620
UND_06_50%_P5	UND	0.6	50%	44.8	522.4	0.5	0.010	1.017	51350.0	51.4	65888.6	65.9	2.844	1579
UND2_06_50%_P1	UND2	0.6	50%	36.4	500.8	0.5	0.004	0.415	120739.2	120.7	121759.6	121.8	1.045	1537
UND2_06_50%_P2	UND2	0.6	50%	35.6	443.3	0.4	0.010	0.958	46293.7	46.3	52292.9	52.3	2.316	1556
UND2_06_50%_P3	UND2	0.6	50%	44.8	525.2	0.5	0.007	0.746	70443.1	70.4	76171.1	76.2	2.052	1525
UND2_06_50%_P4	UND2	0.6	50%	53.8	639.8	0.6	0.005	0.484	132209.5	132.2	133872.2	133.9	1.562	1498
UND2_06_50%_P5	UND2	0.6	50%	-	-	-	-	-	-	-	-	-	-	-

Sample ID	Material	l/s	AS	F_{max} [N]	σ_{max} [kPa]	σ_{max} [MPa]	$\varepsilon_{(\sigma max)}$ [mm/mm]	$\varepsilon_{(\sigma max)}$ [%]	E_{sec} [kPa]	E_{sec} [MPa]	E_{tan} [kPa]	E_{tan} [MPa]	T [kPa*mm/mm]	ρ [kg/m^3]
RC_05_100%_P1	RC	0.5	100%	612.2	6622.3	6.6	0.005	0.535	1237438.0	1237.4	1239622.4	1239.6	17.737	1898
RC_05_100%_P2	RC	0.5	100%	472.5	4832.2	4.8	0.011	1.146	421730.2	421.7	382981.9	383.0	24.959	1901
RC_05_100%_P3	RC	0.5	100%	549.0	5754.6	5.8	0.005	0.540	1065691.7	1065.7	1071952.8	1072.0	15.622	1903
RC_05_100%_P4	RC	0.5	100%	542.0	5645.9	5.6	0.006	0.551	1024052.5	1024.1	1028737.4	1028.7	15.560	1905
RC_05_100%_P5	RC	0.5	100%	509.4	5209.8	5.2	0.005	0.537	970719.0	970.7	975579.8	975.6	14.054	1894
RA_05_100%_P1	RA	0.5	100%	28.4	299.6	0.3	0.086	8.563	3498.7	3.5	3762.5	3.8	13.689	1946
RA_05_100%_P2	RA	0.5	100%	32.6	334.0	0.3	0.066	6.637	5032.1	5.0	5257.2	5.3	11.598	1890
RA_05_100%_P3	RA	0.5	100%	31.7	364.9	0.4	0.060	5.981	6101.2	6.1	6512.6	6.5	11.530	1938
RA_05_100%_P4	RA	0.5	100%	31.7	347.8	0.3	0.083	8.325	4178.4	4.2	4565.7	4.6	15.616	1953
RA_05_100%_P5	RA	0.5	100%	21.2	253.5	0.3	0.058	5.755	4403.9	4.4	5217.5	5.2	8.286	1966
BT_05_100%_P1	BT	0.5	100%	126.3	1258.0	1.3	0.011	1.138	110504.1	110.5	125067.6	125.1	15.232	1862
BT_05_100%_P2	BT	0.5	100%	288.2	2968.2	3.0	0.010	1.027	288959.8	289.0	292838.8	292.8	15.438	1861
BT_05_100%_P3	BT	0.5	100%	178.9	1806.4	1.8	0.010	0.995	181537.6	181.5	190181.0	190.2	12.447	1860
BT_05_100%_P4	BT	0.5	100%	209.2	2092.5	2.1	0.026	2.563	81650.4	81.7	66511.6	66.5	22.315	1856
BT_05_100%_P5	BT	0.5	100%	124.9	1286.2	1.3	0.011	1.057	121711.4	121.7	126054.3	126.1	7.023	1904
NA_05_100%_P1	NA	0.5	100%	39.8	479.0	0.5	0.011	1.146	41809.0	41.8	49112.7	49.1	3.123	2035
NA_05_100%_P2	NA	0.5	100%	37.4	427.5	0.4	0.015	1.461	29264.9	29.3	35435.8	35.4	3.478	2017
NA_05_100%_P3	NA	0.5	100%	37.3	401.0	0.4	0.016	1.563	25661.0	25.7	30725.8	30.7	3.579	1999
NA_05_100%_P4	NA	0.5	100%	42.8	453.4	0.5	0.013	1.313	34544.3	34.5	41154.5	41.2	3.361	2024
NA_05_100%_P5	NA	0.5	100%	42.7	481.5	0.5	0.012	1.212	39723.8	39.7	46584.5	46.6	3.320	2007
UND_05_100%_P1	UND	0.5	100%	141.6	1596.9	1.6	0.004	0.410	389366.3	389.4	415359.9	415.4	3.454	1921
UND_05_100%_P2	UND	0.5	100%	213.8	2381.2	2.4	0.006	0.561	424422.9	424.4	429002.7	429.0	6.746	1942
UND_05_100%_P3	UND	0.5	100%	155.1	1728.4	1.7	0.004	0.403	429228.9	429.2	434444.1	434.4	3.519	1900
UND_05_100%_P4	UND	0.5	100%	144.3	1763.6	1.8	0.007	0.678	260061.2	260.1	260242.5	260.2	5.998	1916
UND_05_100%_P5	UND	0.5	100%	149.8	1688.9	1.7	0.004	0.408	414302.5	414.3	431181.2	431.2	3.599	1902
UND2_05_100%_P1	UND2	0.5	100%	293.7	3207.2	3.2	0.007	0.672	477396.4	477.4	487467.8	487.5	10.976	1864
UND2_05_100%_P2	UND2	0.5	100%	278.2	3148.4	3.1	0.008	0.758	415274.5	415.3	417437.5	417.4	14.424	1867
UND2_05_100%_P3	UND2	0.5	100%	264.7	2977.8	3.0	0.006	0.565	527438.4	527.4	533225.4	533.2	8.515	1934
UND2_05_100%_P4	UND2	0.5	100%	246.6	2888.8	2.9	0.005	0.454	636690.0	636.7	649391.8	649.4	6.684	1923
UND2_05_100%_P5	UND2	0.5	100%	257.4	3261.2	3.3	0.006	0.573	568956.6	569.0	574367.7	574.4	9.426	1951

Sample ID	Material	l/s	AS	F_{max} [N]	σ_{max} [kPa]	σ_{max} [MPa]	$\varepsilon_{(\sigma max)}$ [mm/mm]	$\varepsilon_{(\sigma max)}$ [%]	E_{sec} [kPa]	E_{sec} [MPa]	E_{tan} [kPa]	E_{tan} [MPa]	T [kPa*mm/mm]	ρ [kg/m^3]
RC_05_75%_P1	RC	0.5	75%	277.0	3042.6	3.0	0.005	0.539	564536.2	564.5	565260.3	565.3	8.208	1920
RC_05_75%_P2	RC	0.5	75%	239.3	2541.8	2.5	0.005	0.530	479497.8	479.5	480365.0	480.4	6.757	1902
RC_05_75%_P3	RC	0.5	75%	199.3	2177.4	2.2	0.005	0.468	464784.3	464.8	466852.7	466.9	5.125	1921
RC_05_75%_P4	RC	0.5	75%	227.0	2456.5	2.5	0.005	0.514	477756.5	477.8	477951.4	478.0	6.318	1899
RC_05_75%_P5	RC	0.5	75%	256.5	2696.3	2.7	0.006	0.585	461121.5	461.1	461546.5	461.5	7.883	1879
RA_05_75%_P1	RA	0.5	75%	14.8	181.4	0.2	0.053	5.276	3438.2	3.4	3994.6	4.0	5.267	1920
RA_05_75%_P2	RA	0.5	75%	10.2	126.0	0.1	0.026	2.643	4766.2	4.8	4853.8	4.9	1.750	1948
RA_05_75%_P3	RA	0.5	75%	10.9	142.4	0.1	0.035	3.547	4013.1	4.0	4310.2	4.3	2.906	1947
RA_05_75%_P4	RA	0.5	75%	-	-	-	-	-	-	-	-	-	-	-
RA_05_75%_P5	RA	0.5	75%	10.8	138.9	0.1	0.047	4.711	2947.8	2.9	2948.5	2.9	3.268	1957
BT_05_75%_P1	BT	0.5	75%	38.0	423.0	0.4	0.007	0.672	62939.4	62.9	65392.2	65.4	1.475	1914
BT_05_75%_P2	BT	0.5	75%	33.9	365.3	0.4	0.008	0.758	48177.3	48.2	49219.7	49.2	1.416	1937
BT_05_75%_P3	BT	0.5	75%	36.2	399.5	0.4	0.007	0.705	56706.6	56.7	58663.6	58.7	1.445	1935
BT_05_75%_P4	BT	0.5	75%	35.7	393.5	0.4	0.006	0.572	68785.9	68.8	71618.1	71.6	1.172	1923
BT_05_75%_P5	BT	0.5	75%	32.2	358.9	0.4	0.006	0.561	63959.1	64.0	69234.3	69.2	1.077	1948
NA_05_75%_P1	NA	0.5	75%	13.8	163.3	0.2	0.037	3.674	4445.1	4.4	4645.1	4.6	3.118	2104
NA_05_75%_P2	NA	0.5	75%	10.7	127.1	0.1	0.029	2.897	4388.9	4.4	5715.5	5.7	2.178	2090
NA_05_75%_P3	NA	0.5	75%	10.0	116.7	0.1	0.021	2.112	5525.8	5.5	5528.4	5.5	1.234	2096
NA_05_75%_P4	NA	0.5	75%	9.6	112.3	0.1	0.025	2.542	4415.4	4.4	5316.9	5.3	1.633	2048
NA_05_75%_P5	NA	0.5	75%	-	-	-	-	-	-	-	-	-	-	-
UND_05_75%_P1	UND	0.5	75%	153.6	1677.4	1.7	0.007	0.715	234541.0	234.5	236095.3	236.1	6.039	1954
UND_05_75%_P2	UND	0.5	75%	106.5	1119.9	1.1	0.005	0.546	205206.0	205.2	211853.2	211.9	3.168	1946
UND_05_75%_P3	UND	0.5	75%	114.4	1197.0	1.2	0.007	0.668	179205.3	179.2	180042.4	180.0	4.014	1956
UND_05_75%_P4	UND	0.5	75%	107.9	1112.3	1.1	0.007	0.678	163982.3	164.0	164818.0	164.8	3.787	1947
UND_05_75%_P5	UND	0.5	75%	126.7	1314.2	1.3	0.007	0.743	176783.8	176.8	177334.7	177.3	4.899	1951
UND2_05_75%_P1	UND2	0.5	75%	407.1	4605.3	4.6	0.013	1.312	351124.8	351.1	352927.6	352.9	30.381	1718
UND2_05_75%_P2	UND2	0.5	75%	292.5	3357.3	3.4	0.010	1.008	332985.2	333.0	334696.7	334.7	17.027	1729
UND2_05_75%_P3	UND2	0.5	75%	337.4	3724.4	3.7	0.013	1.266	294110.6	294.1	301477.3	301.5	24.149	1745
UND2_05_75%_P4	UND2	0.5	75%	299.4	3597.2	3.6	0.009	0.887	405528.8	405.5	405742.0	405.7	15.963	1739
UND2_05_75%_P5	UND2	0.5	75%	259.8	3253.3	3.3	0.007	0.720	451943.8	451.9	452841.9	452.8	11.739	1753

Sample ID	Material	l/s	AS	F_{max} [N]	σ_{max} [kPa]	σ_{max} [MPa]	$\varepsilon_{(\sigma max)}$ [mm/mm]	$\varepsilon_{(\sigma max)}$ [%]	E_{sec} [kPa]	E_{sec} [MPa]	E_{tan} [kPa]	E_{tan} [MPa]	T [kPa*mm/mm]	ρ [kg/m^3]
RC_05_50%_P1	RC	0.5	50%	28.1	336.2	0.3	0.003	0.316	106421.9	106.4	106785.4	106.8	0.534	1632
RC_05_50%_P2	RC	0.5	50%	29.3	316.9	0.3	0.008	0.793	39941.1	39.9	40109.7	40.1	1.257	1587
RC_05_50%_P3	RC	0.5	50%	26.7	290.1	0.3	0.015	1.476	19650.9	19.7	35292.4	35.3	2.436	1593
RC_05_50%_P4	RC	0.5	50%	36.4	405.1	0.4	0.010	0.988	41009.4	41.0	41123.0	41.1	4.699	1544
RC_05_50%_P5	RC	0.5	50%	35.3	453.2	0.5	0.006	0.589	77005.3	77.0	77327.9	77.3	1.341	1606
RA_05_50%_P1	RA	0.5	50%	10.3	130.3	0.1	0.006	0.571	22806.0	22.8	22846.1	22.8	0.373	1742
RA_05_50%_P2	RA	0.5	50%	8.3	104.4	0.1	0.005	0.498	20942.2	20.9	20987.6	21.0	0.264	1734
RA_05_50%_P3	RA	0.5	50%	10.3	127.8	0.1	0.009	0.901	14184.4	14.2	14193.2	14.2	0.577	1753
RA_05_50%_P4	RA	0.5	50%	9.9	118.5	0.1	0.011	1.125	10537.7	10.5	10539.1	10.5	0.669	1721
RA_05_50%_P5	RA	0.5	50%	-	-	-	-	-	-	-	-	-	-	-
BT_05_50%_P1	BT	0.5	50%	59.8	689.0	0.7	0.015	1.462	47122.4	47.1	47246.2	47.2	5.047	1743
BT_05_50%_P2	BT	0.5	50%	49.9	574.9	0.6	0.006	0.561	102485.5	102.5	113270.5	113.3	1.709	1723
BT_05_50%_P3	BT	0.5	50%	83.0	941.1	0.9	0.007	0.737	127768.8	127.8	131347.9	131.3	3.545	1741
BT_05_50%_P4	BT	0.5	50%	61.7	701.0	0.7	0.009	0.902	77707.0	77.7	125294.7	125.3	3.911	1730
BT_05_50%_P5	BT	0.5	50%	185.9	2062.7	2.1	0.010	0.977	211195.4	211.2	214148.2	214.1	10.207	1663
NA_05_50%_P1	NA	0.5	50%	21.1	243.8	0.2	0.009	0.883	27601.4	27.6	27918.5	27.9	1.090	1871
NA_05_50%_P2	NA	0.5	50%	15.0	174.4	0.2	0.007	0.692	25192.4	25.2	25584.6	25.6	0.623	1911
NA_05_50%_P3	NA	0.5	50%	12.4	142.6	0.1	0.007	0.706	20202.2	20.2	20254.8	20.3	0.502	1898
NA_05_50%_P4	NA	0.5	50%	14.3	162.3	0.2	0.004	0.380	42729.2	42.7	43069.3	43.1	0.311	1896
NA_05_50%_P5	NA	0.5	50%	-	-	-	-	-	-	-	-	-	-	-
UND_05_50%_P1	UND	0.5	50%	65.6	768.5	0.8	0.007	0.698	110153.5	110.2	117543.7	117.5	2.811	1786
UND_05_50%_P2	UND	0.5	50%	27.4	310.1	0.3	0.005	0.481	64436.5	64.4	64577.8	64.6	0.747	1809
UND_05_50%_P3	UND	0.5	50%	28.7	329.0	0.3	0.010	0.987	33332.7	33.3	33397.2	33.4	1.627	1831
UND_05_50%_P4	UND	0.5	50%	30.0	351.7	0.4	0.004	0.440	79918.1	79.9	80034.1	80.0	0.775	1839
UND_05_50%_P5	UND	0.5	50%	32.6	376.3	0.4	0.009	0.932	40358.8	40.4	40379.8	40.4	1.756	1824
UND2_05_50%_P1	UND2	0.5	50%	69.4	743.5	0.7	0.010	1.012	73478.5	73.5	73630.2	73.6	3.769	1549
UND2_05_50%_P2	UND2	0.5	50%	85.8	923.8	0.9	0.010	0.962	95978.4	96.0	97246.8	97.2	4.493	1511
UND2_05_50%_P3	UND2	0.5	50%	77.5	917.3	0.9	0.007	0.748	122694.3	122.7	123802.8	123.8	3.466	1558
UND2_05_50%_P4	UND2	0.5	50%	86.0	982.8	1.0	0.005	0.501	196046.9	196.0	196417.8	196.4	2.467	1557
UND2_05_50%_P5	UND2	0.5	50%	-	-	-	-	-	-	-	-	-	-	-

Sample ID	Material	l/s	AS	F_{max} [N]	σ_{max} [kPa]	σ_{max} [MPa]	$\varepsilon_{(\sigma max)}$ [mm/mm]	$\varepsilon_{(\sigma max)}$ [%]	E_{sec} [kPa]	E_{sec} [MPa]	E_{tan} [kPa]	E_{tan} [MPa]	T [kPa*mm/mm]	ρ [kg/m^3]
RC_04_100%_P1	RC	0.4	100%	466.8	4903.1	4.9	0.003	0.323	1515980.0	1516.0	1523275.6	1523.3	7.988	1897
RC_04_100%_P2	RC	0.4	100%	252.6	2759.4	2.8	0.004	0.352	783336.1	783.3	808503.7	808.5	4.988	1850
RC_04_100%_P3	RC	0.4	100%	465.4	5087.5	5.1	0.005	0.468	1086627.8	1086.6	1093640.7	1093.6	11.934	1854
RC_04_100%_P4	RC	0.4	100%	308.0	3217.3	3.2	0.003	0.299	1076407.8	1076.4	1103146.9	1103.1	4.888	1877
RC_04_100%_P5	RC	0.4	100%	213.9	2600.7	2.6	0.003	0.332	783521.8	783.5	797527.7	797.5	4.401	1777
RA_04_100%_P1	RA	0.4	100%	37.7	407.9	0.4	0.037	3.688	11058.7	11.1	12025.6	12.0	8.040	1989
RA_04_100%_P2	RA	0.4	100%	45.7	509.8	0.5	0.046	4.629	11013.9	11.0	11603.8	11.6	12.343	1935
RA_04_100%_P3	RA	0.4	100%	41.1	440.4	0.4	0.047	4.719	9332.6	9.3	11305.7	11.3	11.738	1966
RA_04_100%_P4	RA	0.4	100%	45.5	491.7	0.5	0.048	4.796	10251.5	10.3	11105.7	11.1	12.550	1983
RA_04_100%_P5	RA	0.4	100%	46.4	523.2	0.5	0.042	4.230	12369.0	12.4	13685.0	13.7	12.096	2004
BT_04_100%_P1	BT	0.4	100%	278.0	3483.1	3.5	0.005	0.524	664968.9	665.0	676688.9	676.7	9.249	1512
BT_04_100%_P2	BT	0.4	100%	230.1	2601.2	2.6	0.004	0.423	615174.4	615.2	623915.2	623.9	5.571	1522
BT_04_100%_P3	BT	0.4	100%	347.2	3644.5	3.6	0.005	0.523	696241.5	696.2	707079.0	707.1	9.632	1556
BT_04_100%_P4	BT	0.4	100%	256.9	2778.8	2.8	0.004	0.413	672468.2	672.5	685649.3	685.6	5.815	1571
BT_04_100%_P5	BT	0.4	100%	178.5	2102.4	2.1	0.003	0.327	643158.7	643.2	664029.6	664.0	3.532	1520
NA_04_100%_P1	NA	0.4	100%	509.6	6281.5	6.3	0.006	0.556	1128892.9	1128.9	1147858.6	1147.9	17.808	1943
NA_04_100%_P2	NA	0.4	100%	391.5	4953.5	5.0	0.006	0.554	894436.3	894.4	905063.2	905.1	13.922	2036
NA_04_100%_P3	NA	0.4	100%	394.9	4802.6	4.8	0.005	0.531	904569.5	904.6	927554.1	927.6	13.005	2014
NA_04_100%_P4	NA	0.4	100%	334.3	4058.1	4.1	0.008	0.811	500379.5	500.4	503273.9	503.3	16.545	1967
NA_04_100%_P5	NA	0.4	100%	298.7	4179.8	4.2	0.009	0.855	488801.3	488.8	494174.9	494.2	18.039	2009
UND_04_100%_P1	UND	0.4	100%	324.6	3725.8	3.7	0.004	0.358	1040871.6	1040.9	1046218.3	1046.2	6.712	2007
UND_04_100%_P2	UND	0.4	100%	382.5	4306.3	4.3	0.005	0.510	843970.5	844.0	845120.9	845.1	11.002	1981
UND_04_100%_P3	UND	0.4	100%	413.6	4606.6	4.6	0.006	0.601	766852.8	766.9	774217.8	774.2	14.006	1977
UND_04_100%_P4	UND	0.4	100%	353.3	4254.7	4.3	0.004	0.370	1150467.4	1150.5	1160126.8	1160.1	7.942	1935
UND_04_100%_P5	UND	0.4	100%	349.4	4036.6	4.0	0.004	0.375	1076222.3	1076.2	1080618.8	1080.6	7.630	1972
UND2_04_100%_P1	UND2	0.4	100%	162.2	1738.9	1.7	0.004	0.390	446195.8	446.2	452259.7	452.3	3.423	1939
UND2_04_100%_P2	UND2	0.4	100%	61.4	734.9	0.7	0.003	0.279	263724.5	263.7	276389.3	276.4	1.076	1961
UND2_04_100%_P3	UND2	0.4	100%	173.9	2057.5	2.1	0.005	0.460	446896.0	446.9	450290.8	450.3	4.775	1963
UND2_04_100%_P4	UND2	0.4	100%	164.2	1802.5	1.8	0.004	0.358	503946.0	503.9	508555.6	508.6	3.253	1980
UND2_04_100%_P5	UND2	0.4	100%	179.6	1905.0	1.9	0.004	0.372	511416.4	511.4	518461.6	518.5	3.595	1966

Stress-Strain curves for l/s = 0.6

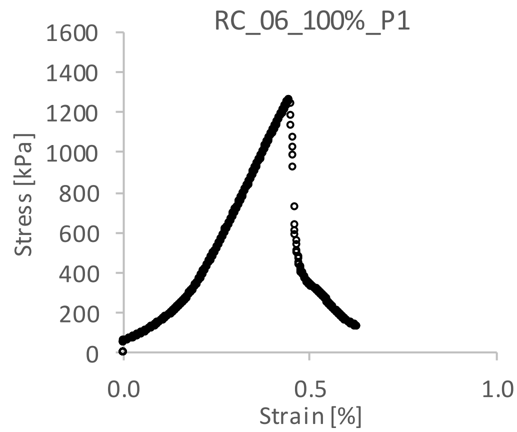

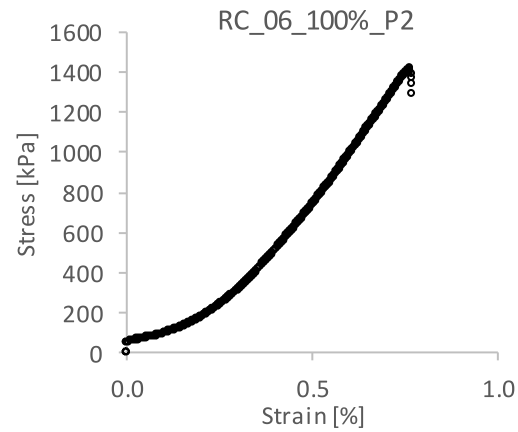

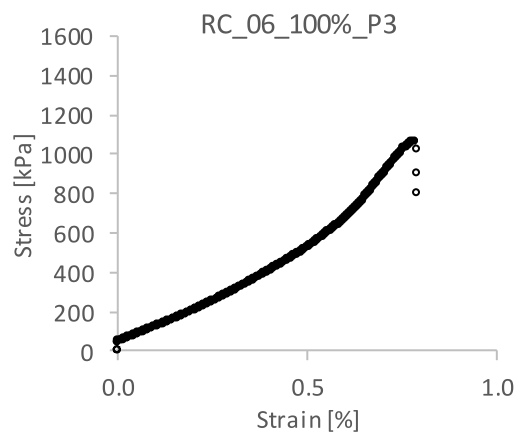

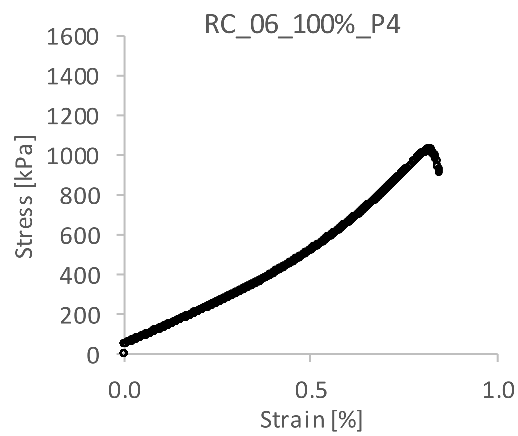

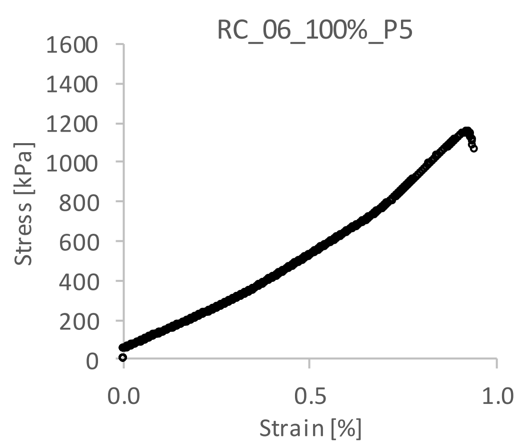

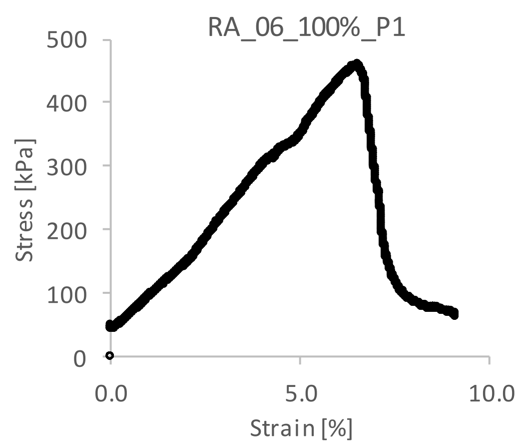

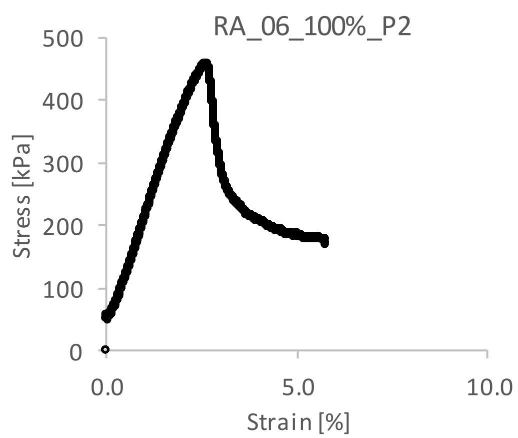
RA_06_100%_P2
Stress [kPa]
500
400
300
200
100
0
0.0
5.0
10.0
Strain [%]

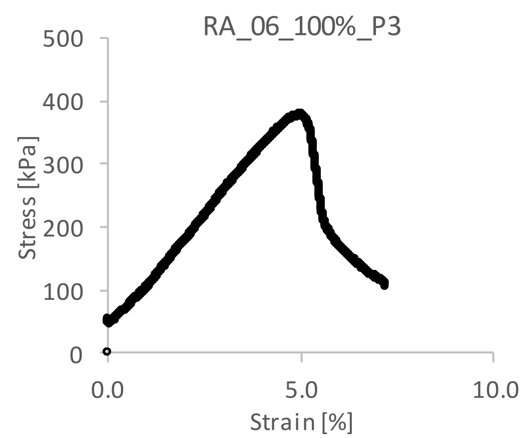
RA_06_100%_P3
Stress [kPa]
500
400
300
200
100
0
0.0
5.0
10.0
Strain [%]

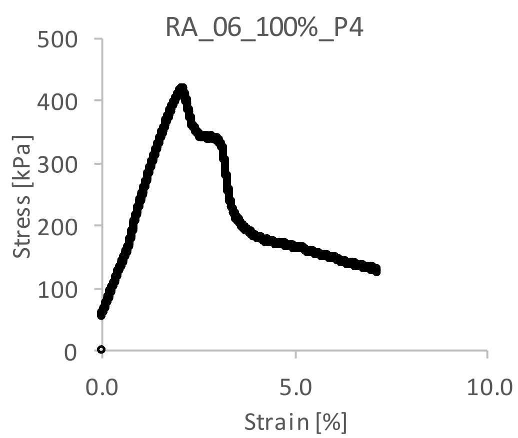
RA_06_100%_P4
Stress [kPa]
500
400
300
200
100
0
0.0
5.0
10.0
Strain [%]

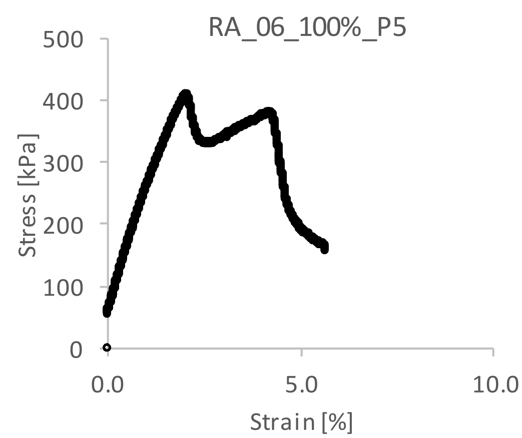
RA_06_100%_P5
Stress [kPa]
500
400
300
200
100
0
0.0
5.0
10.0
Strain [%]

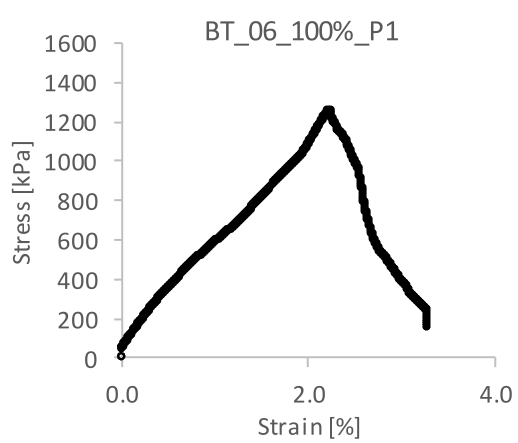
BT_06_100%_P1
Stress [kPa]
1600
1400
1200
1000
800
600
400
200
0
0.0
2.0
4.0
Strain [%]

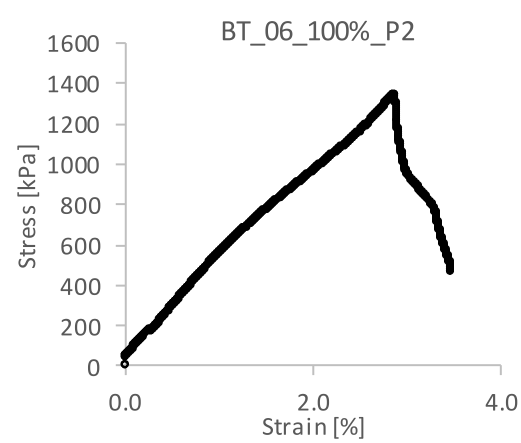
BT_06_100%_P2
Stress [kPa]
1600
1400
1200
1000
800
600
400
200
0
0.0
2.0
4.0
Strain [%]

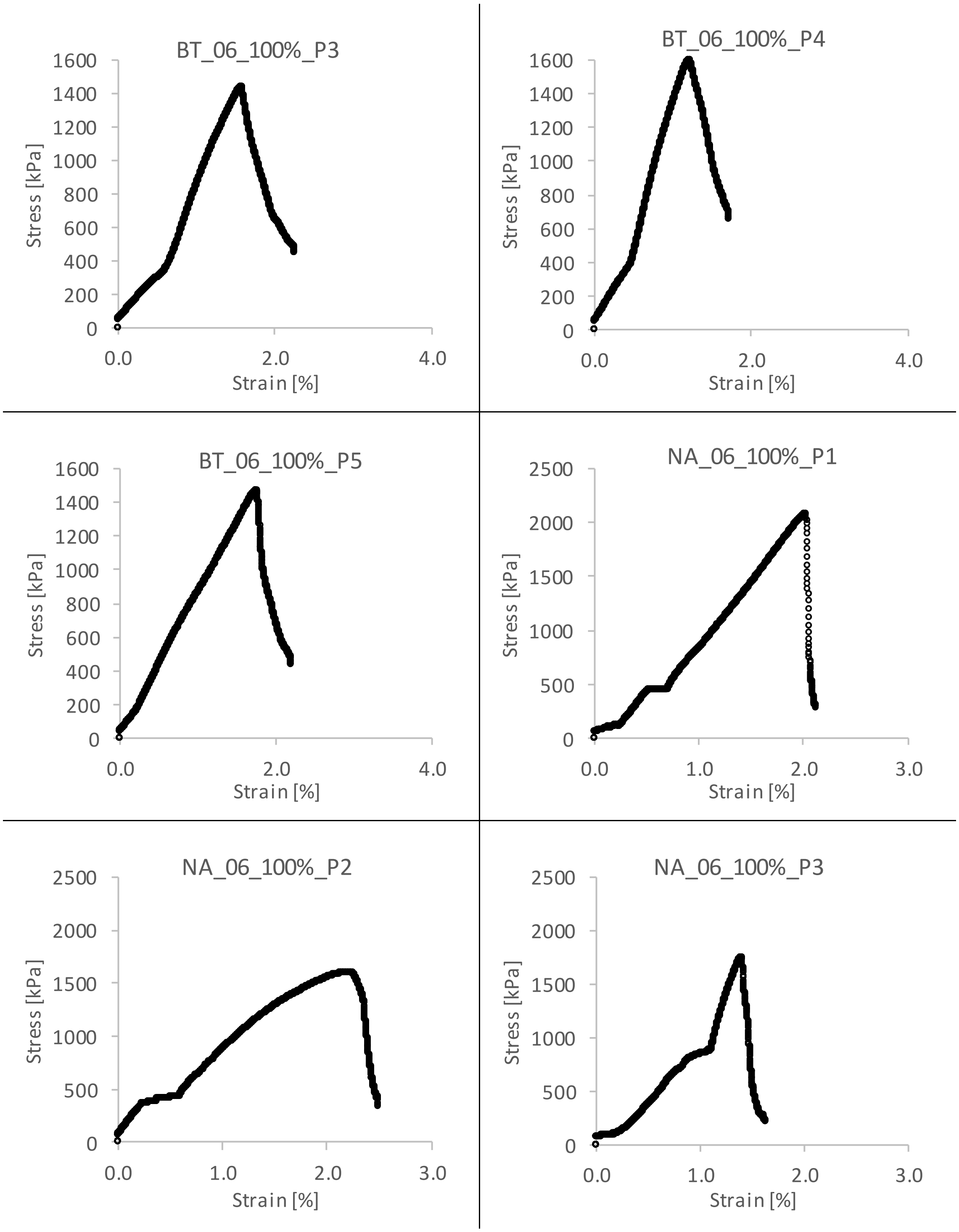
BT_06_100%_P3
Stress [kPa]
Strain [%]
BT_06_100%_P4
Stress [kPa]
Strain [%]
BT_06_100%_P5
Stress [kPa]
Strain [%]
NA_06_100%_P1
Stress [kPa]
Strain [%]
NA_06_100%_P2
Stress [kPa]
Strain [%]
NA_06_100%_P3
Stress [kPa]
Strain [%]

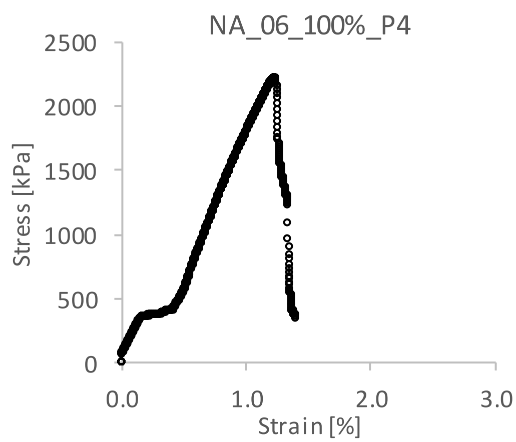
NA_06_100%_P4
Stress [kPa]
2500
2000
1500
1000
500
0
0.0
1.0
2.0
3.0
Strain [%]

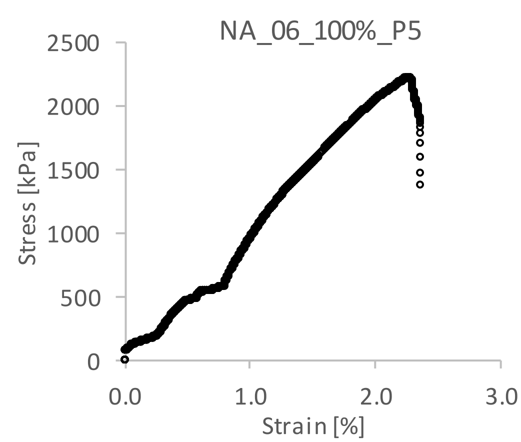
NA_06_100%_P5
Stress [kPa]
2500
2000
1500
1000
500
0
0.0
1.0
2.0
3.0
Strain [%]

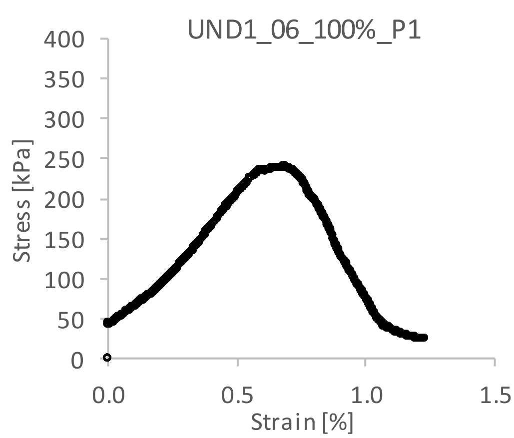
UND1_06_100%_P1
Stress [kPa]
400
350
300
250
200
150
100
50
0
0.0
0.5
1.0
1.5
Strain [%]

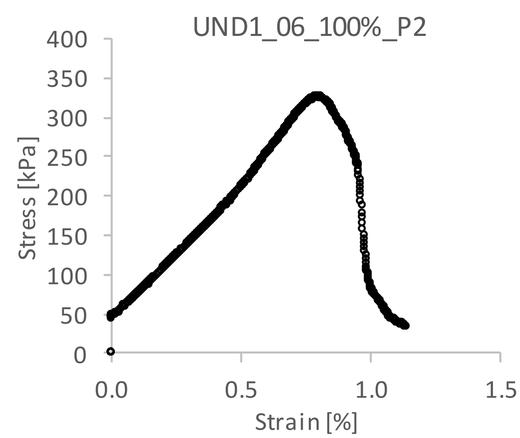
UND1_06_100%_P2
Stress [kPa]
400
350
300
250
200
150
100
50
0
0.0
0.5
1.0
1.5
Strain [%]

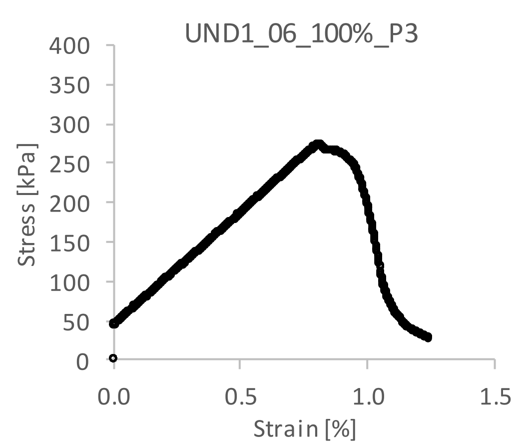
UND1_06_100%_P3
Stress [kPa]
400
350
300
250
200
150
100
50
0
0.0
0.5
1.0
1.5
Strain [%]

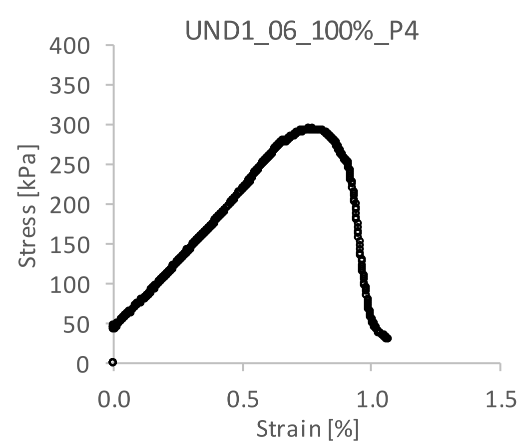
UND1_06_100%_P4
Stress [kPa]
400
350
300
250
200
150
100
50
0
0.0
0.5
1.0
1.5
Strain [%]

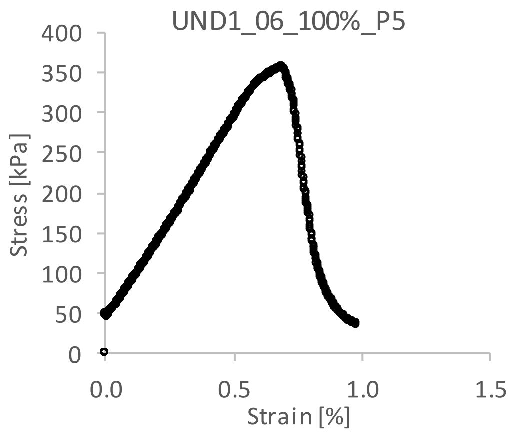
UND1_06_100%_P5
Stress [kPa]
0
50
100
150
200
250
300
350
400
0.0
0.5
1.0
1.5
Strain [%]

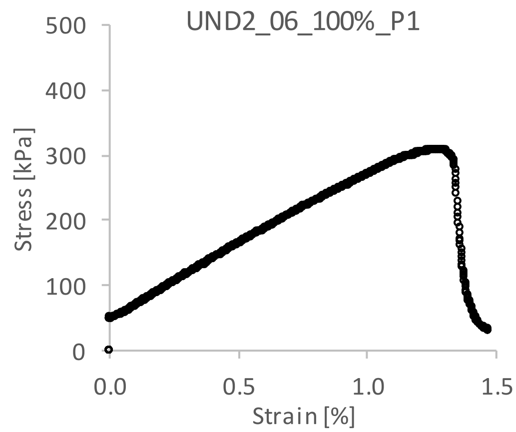
UND2_06_100%_P1
Stress [kPa]
0
100
200
300
400
500
0.0
0.5
1.0
1.5
Strain [%]

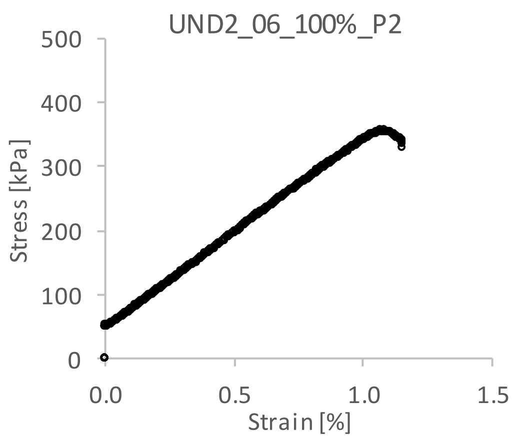
UND2_06_100%_P2
Stress [kPa]
0
100
200
300
400
500
0.0
0.5
1.0
1.5
Strain [%]

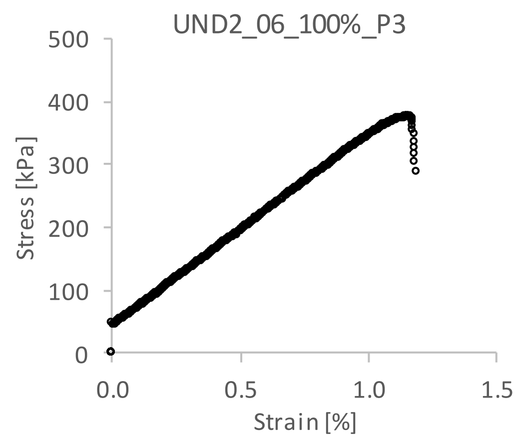
UND2_06_100%_P3
Stress [kPa]
0
100
200
300
400
500
0.0
0.5
1.0
1.5
Strain [%]

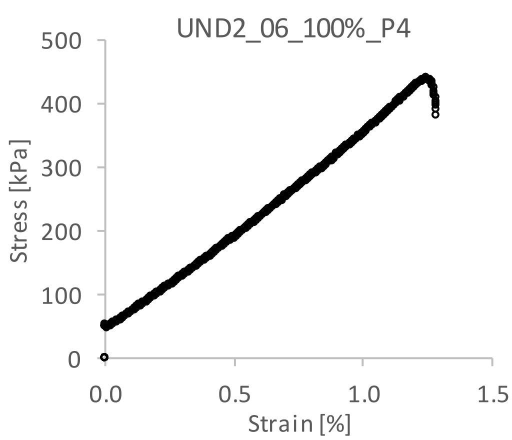
UND2_06_100%_P4
Stress [kPa]
0
100
200
300
400
500
0.0
0.5
1.0
1.5
Strain [%]

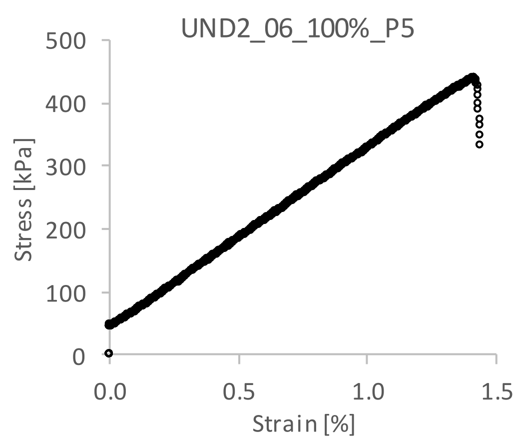
UND2_06_100%_P5
Stress [kPa]
0
100
200
300
400
500
0.0
0.5
1.0
1.5
Strain [%]

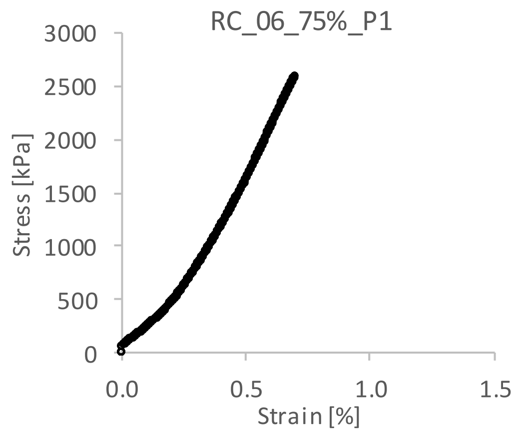
RC_06_75%_P1
Stress [kPa]
Strain [%]
3000
2500
2000
1500
1000
500
0
0.0
0.5
1.0
1.5

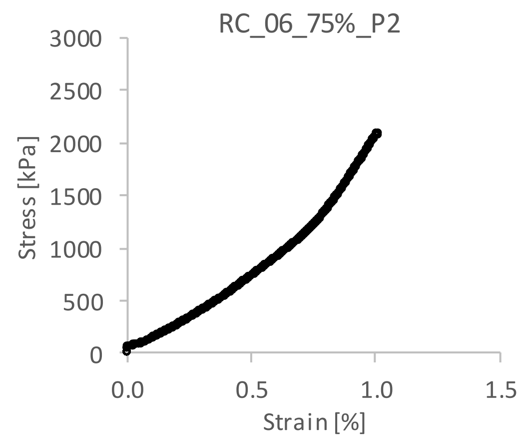
RC_06_75%_P2
Stress [kPa]
Strain [%]
3000
2500
2000
1500
1000
500
0
0.0
0.5
1.0
1.5

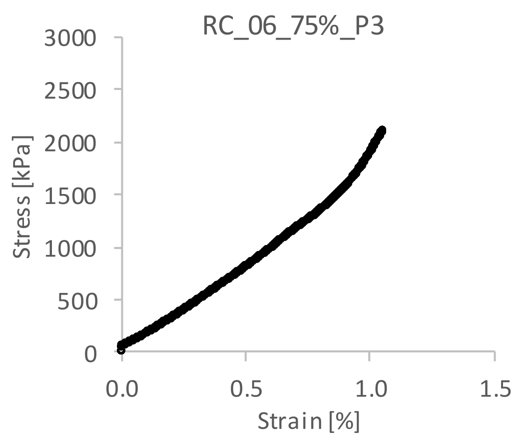
RC_06_75%_P3
Stress [kPa]
Strain [%]
3000
2500
2000
1500
1000
500
0
0.0
0.5
1.0
1.5

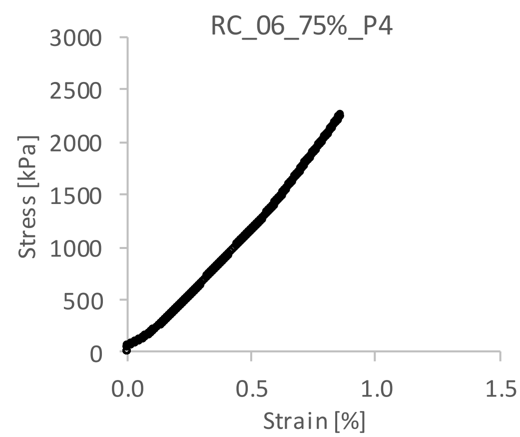
RC_06_75%_P4
Stress [kPa]
Strain [%]
3000
2500
2000
1500
1000
500
0
0.0
0.5
1.0
1.5

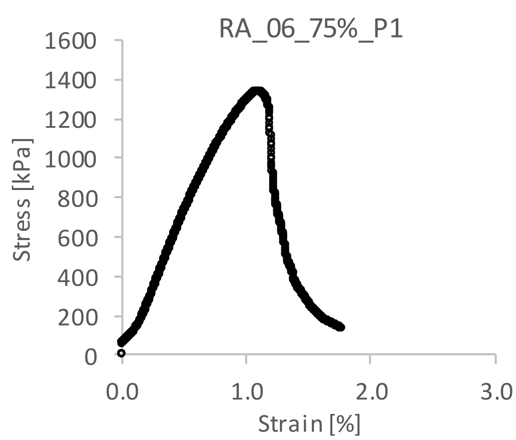
RA_06_75%_P1
Stress [kPa]
Strain [%]
1600
1400
1200
1000
800
600
400
200
0
0.0
1.0
2.0
3.0

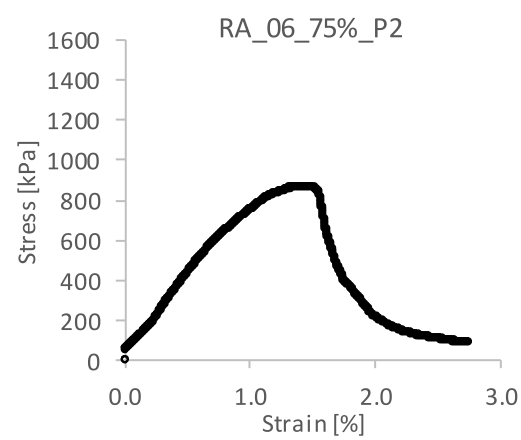
RA_06_75%_P2
Stress [kPa]
Strain [%]
1600
1400
1200
1000
800
600
400
200
0
0.0
1.0
2.0
3.0

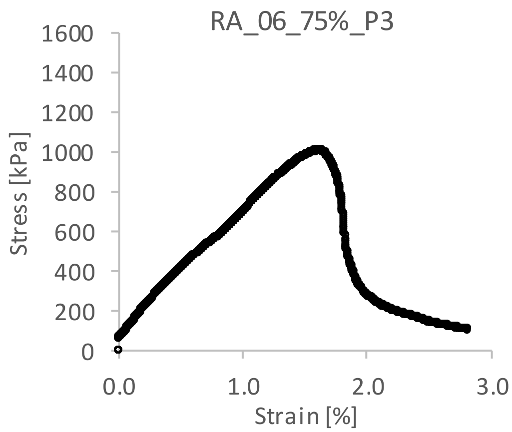
RA_06_75%_P3
Stress [kPa]
1600
1400
1200
1000
800
600
400
200
0
0.0
1.0
2.0
3.0
Strain [%]

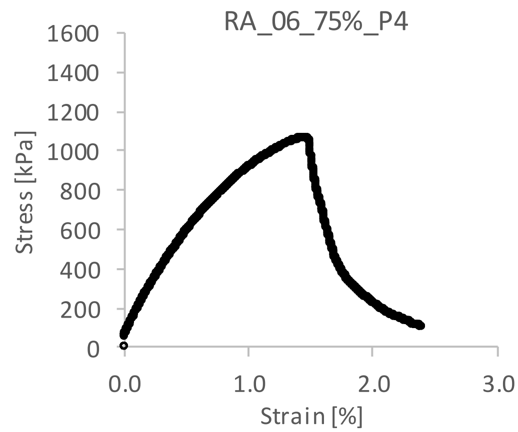
RA_06_75%_P4
Stress [kPa]
1600
1400
1200
1000
800
600
400
200
0
0.0
1.0
2.0
3.0
Strain [%]

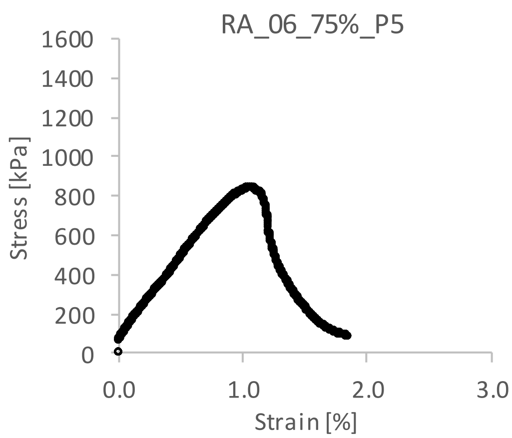
RA_06_75%_P5
Stress [kPa]
1600
1400
1200
1000
800
600
400
200
0
0.0
1.0
2.0
3.0
Strain [%]

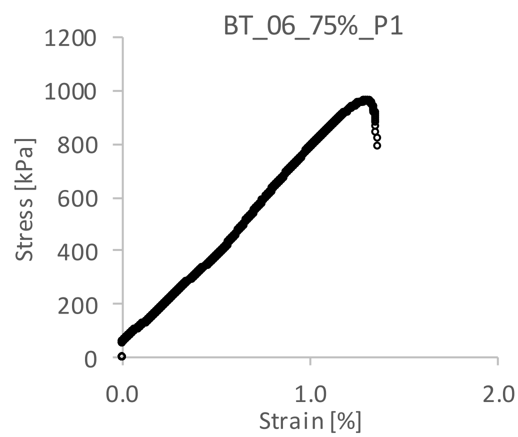
BT_06_75%_P1
Stress [kPa]
1200
1000
800
600
400
200
0
0.0
1.0
2.0
Strain [%]

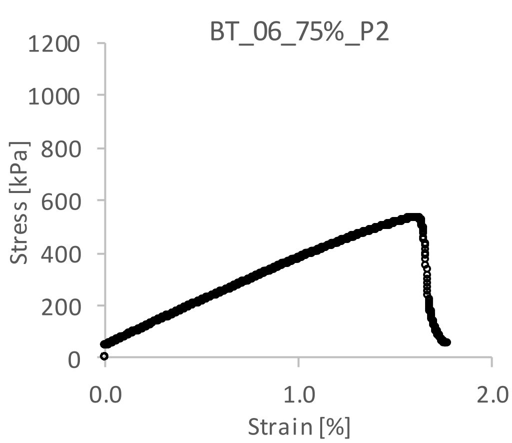
BT_06_75%_P2
Stress [kPa]
1200
1000
800
600
400
200
0
0.0
1.0
2.0
Strain [%]

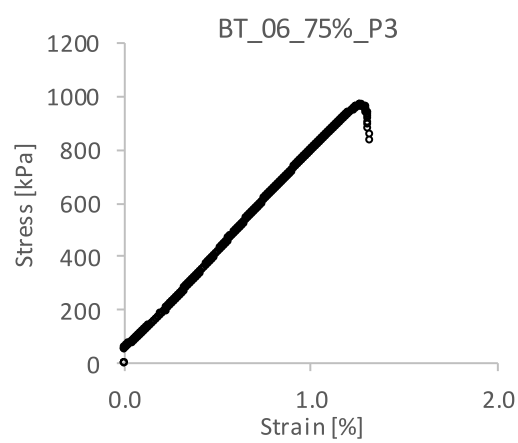
BT_06_75%_P3
Stress [kPa]
1200
1000
800
600
400
200
0
0.0
1.0
2.0
Strain [%]

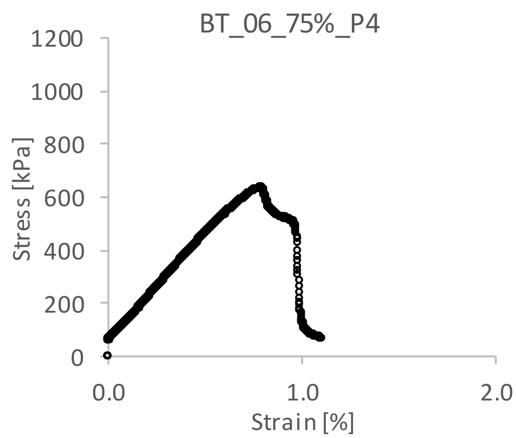
BT_06_75%_P4
1200
1000
800
600
400
200
0
0.0
1.0
2.0
Stress [kPa]
Strain [%]

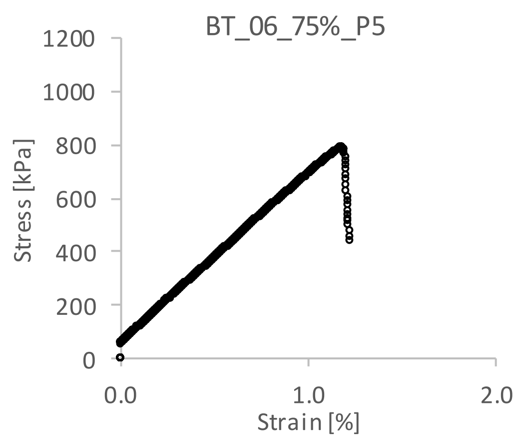
BT_06_75%_P5
1200
1000
800
600
400
200
0
0.0
1.0
2.0
Stress [kPa]
Strain [%]

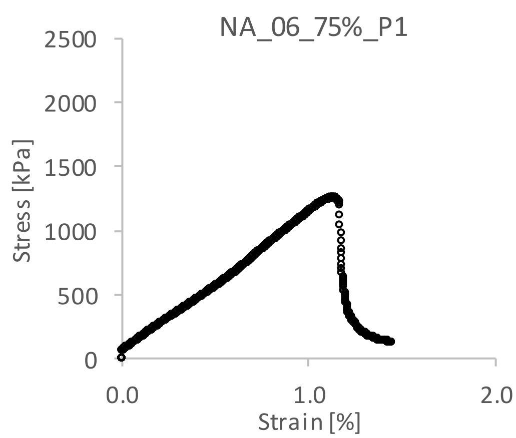
NA_06_75%_P1
2500
2000
1500
1000
500
0
0.0
1.0
2.0
Stress [kPa]
Strain [%]

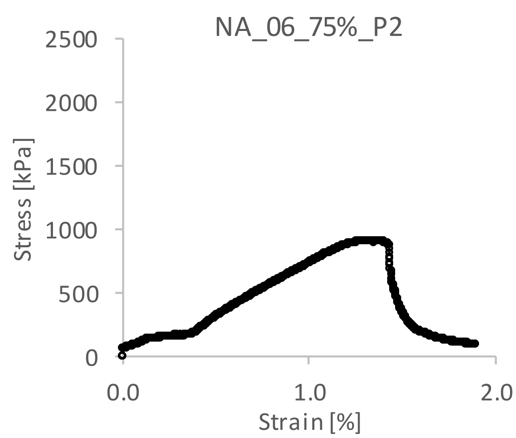
NA_06_75%_P2
2500
2000
1500
1000
500
0
0.0
1.0
2.0
Stress [kPa]
Strain [%]

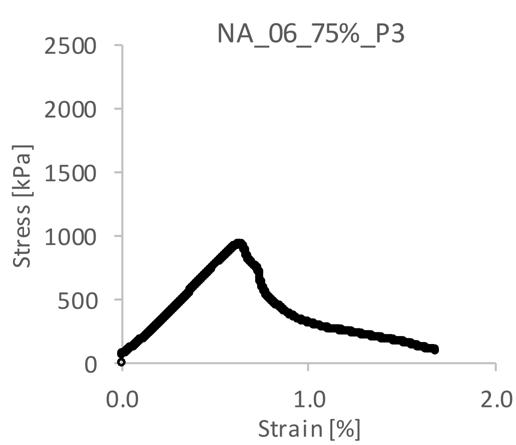
NA_06_75%_P3
2500
2000
1500
1000
500
0
0.0
1.0
2.0
Stress [kPa]
Strain [%]

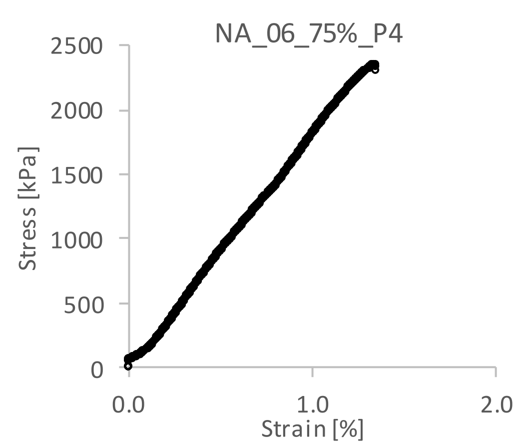
NA_06_75%_P4
2500
2000
1500
1000
500
0
0.0
1.0
2.0
Stress [kPa]
Strain [%]

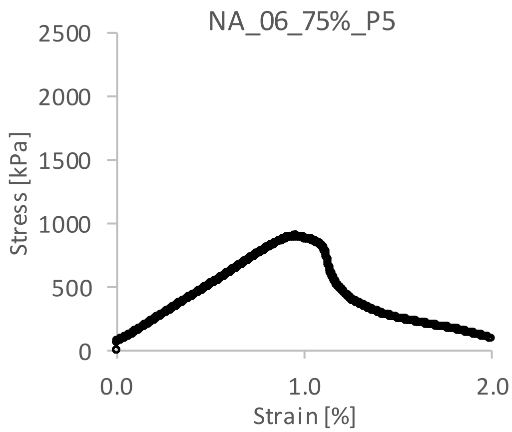
NA_06_75%_P5
Stress [kPa]
2500
2000
1500
1000
500
0
0.0
1.0
2.0
Strain [%]

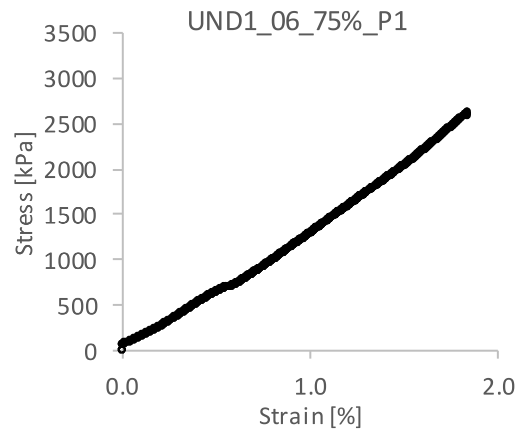
UND1_06_75%_P1
Stress [kPa]
3500
3000
2500
2000
1500
1000
500
0
0.0
1.0
2.0
Strain [%]

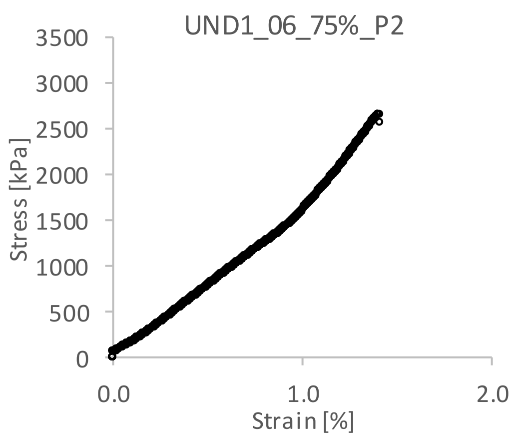
UND1_06_75%_P2
Stress [kPa]
3500
3000
2500
2000
1500
1000
500
0
0.0
1.0
2.0
Strain [%]

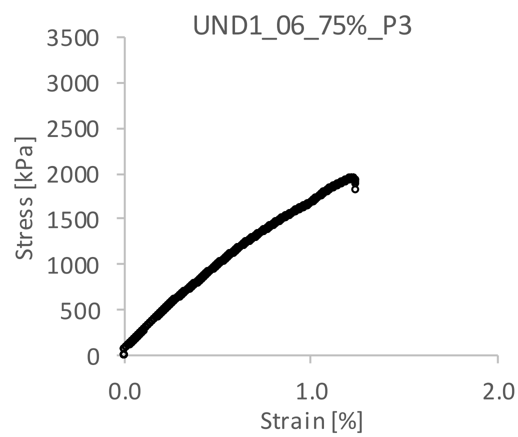
UND1_06_75%_P3
Stress [kPa]
3500
3000
2500
2000
1500
1000
500
0
0.0
1.0
2.0
Strain [%]

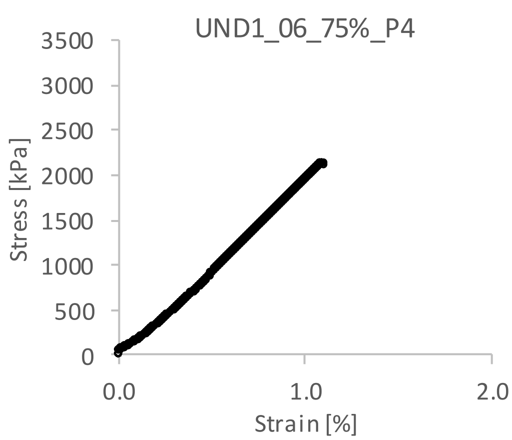
UND1_06_75%_P4
Stress [kPa]
3500
3000
2500
2000
1500
1000
500
0
0.0
1.0
2.0
Strain [%]

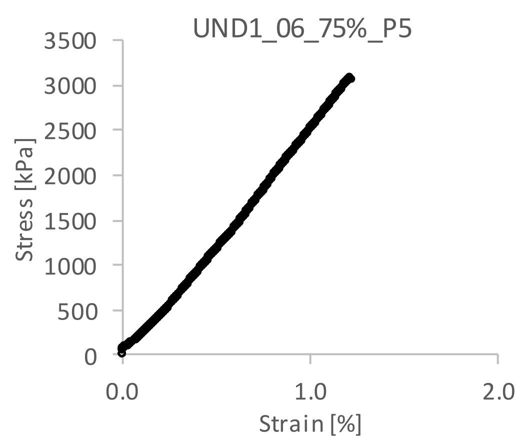
UND1_06_75%_P5
Stress [kPa]
3500
3000
2500
2000
1500
1000
500
0
0.0
1.0
2.0
Strain [%]

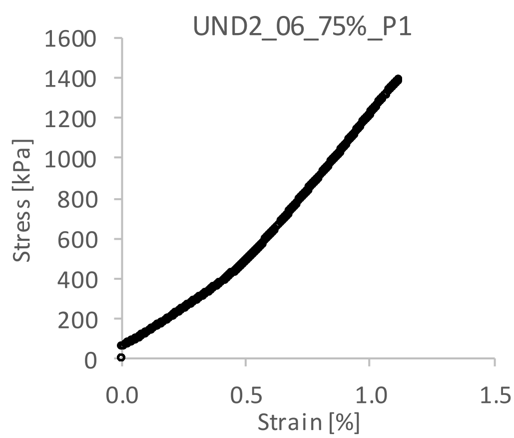
UND2_06_75%_P1
Stress [kPa]
Strain [%]
0
200
400
600
800
1000
1200
1400
1600
0.0
0.5
1.0
1.5

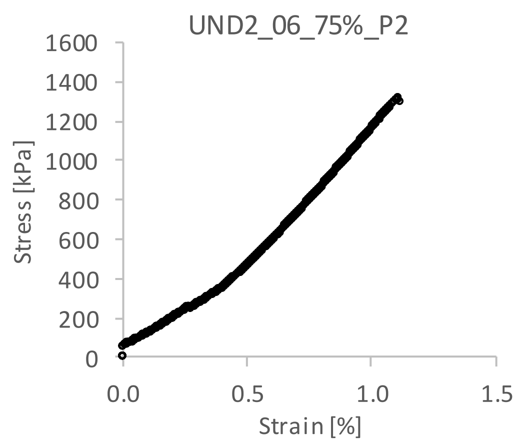
UND2_06_75%_P2
Stress [kPa]
Strain [%]
0
200
400
600
800
1000
1200
1400
1600
0.0
0.5
1.0
1.5

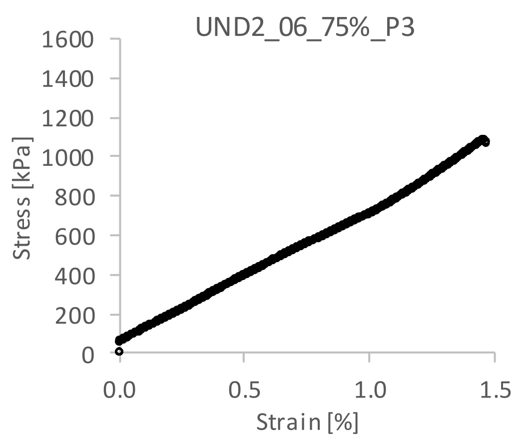
UND2_06_75%_P3
Stress [kPa]
Strain [%]
0
200
400
600
800
1000
1200
1400
1600
0.0
0.5
1.0
1.5

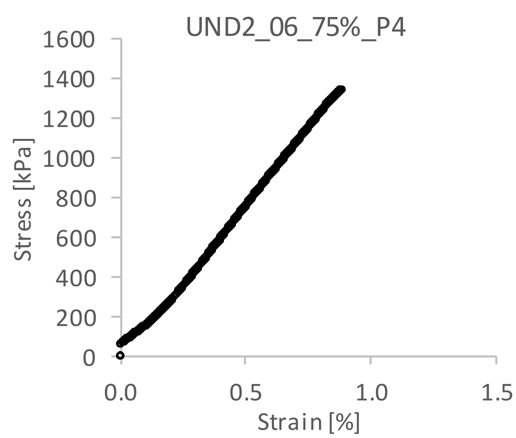
UND2_06_75%_P4
Stress [kPa]
Strain [%]
0
200
400
600
800
1000
1200
1400
1600
0.0
0.5
1.0
1.5

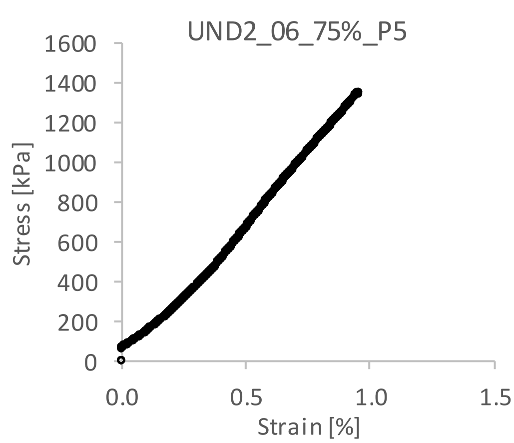
UND2_06_75%_P5
Stress [kPa]
Strain [%]
0
200
400
600
800
1000
1200
1400
1600
0.0
0.5
1.0
1.5

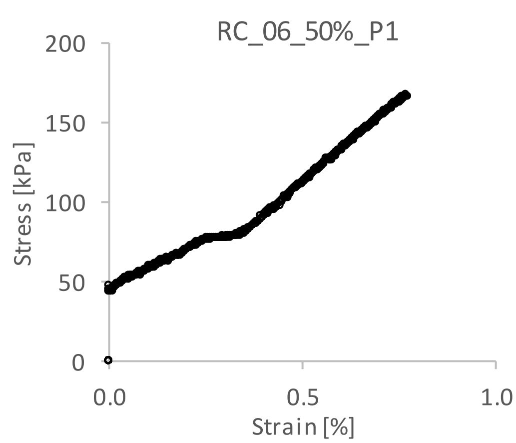
RC_06_50%_P1
Stress [kPa]
Strain [%]
0
50
100
150
200
0.0
0.5
1.0

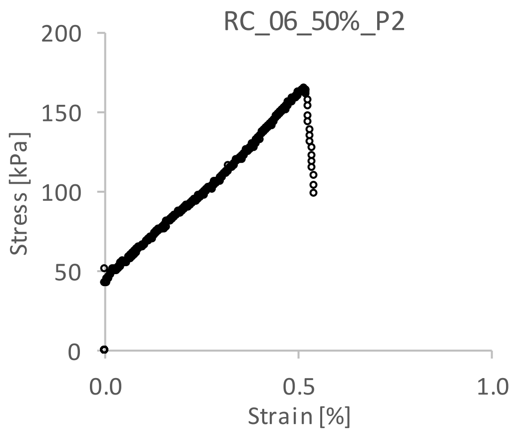
RC_06_50%_P2
Stress [kPa]
Strain [%]

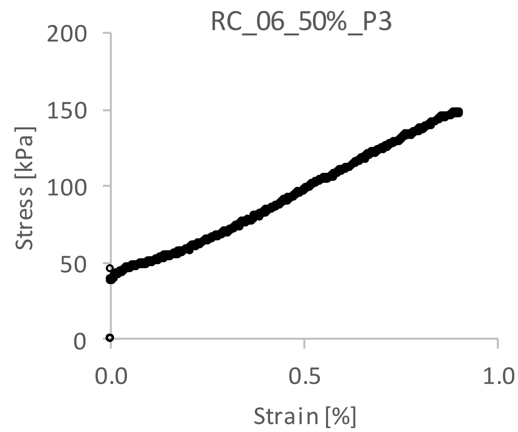
RC_06_50%_P3
Stress [kPa]
Strain [%]

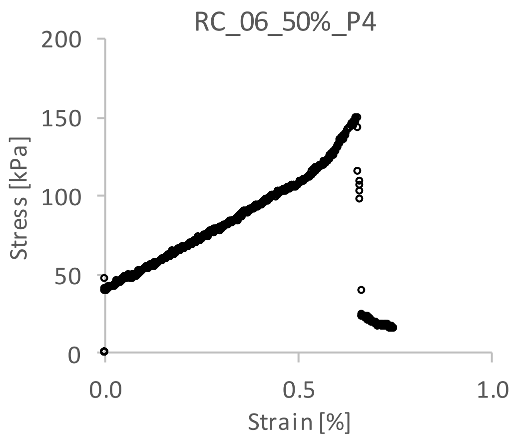
RC_06_50%_P4
Stress [kPa]
Strain [%]

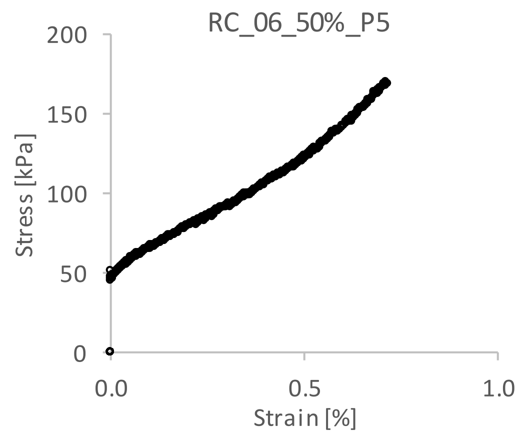
RC_06_50%_P5
Stress [kPa]
Strain [%]

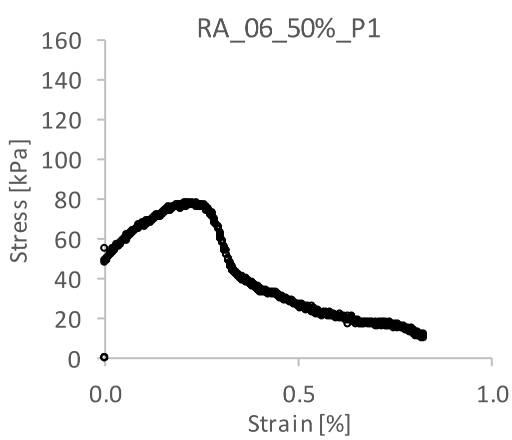
RA_06_50%_P1
Stress [kPa]
Strain [%]

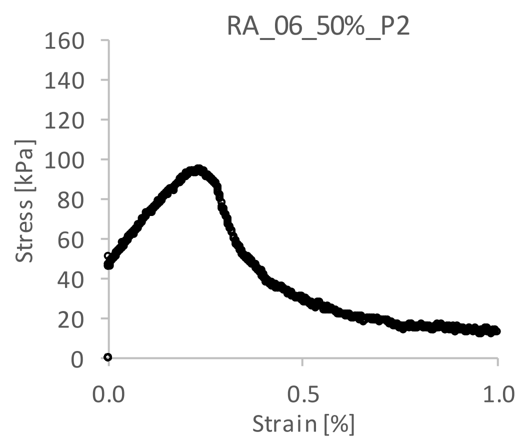
RA_06_50%_P2
Stress [kPa]
Strain [%]

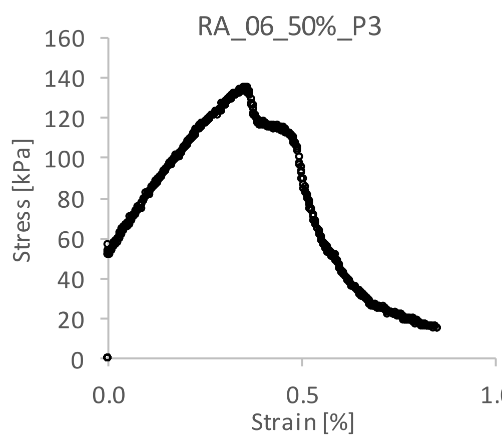
RA_06_50%_P3
Stress [kPa]
160
140
120
100
80
60
40
20
0
0.0
0.5
1.0
Strain [%]

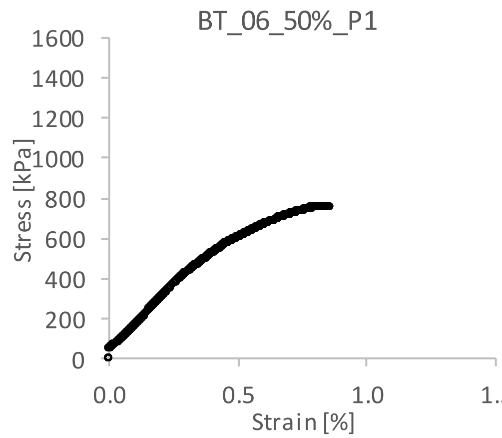
BT_06_50%_P1
Stress [kPa]
1600
1400
1200
1000
800
600
400
200
0
0.0
0.5
1.0
1.5
Strain [%]

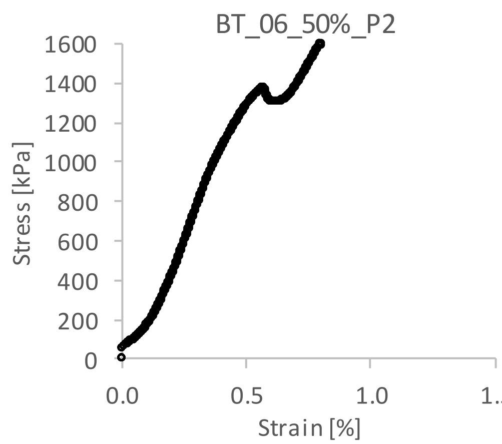
BT_06_50%_P2
Stress [kPa]
1600
1400
1200
1000
800
600
400
200
0
0.0
0.5
1.0
1.5
Strain [%]

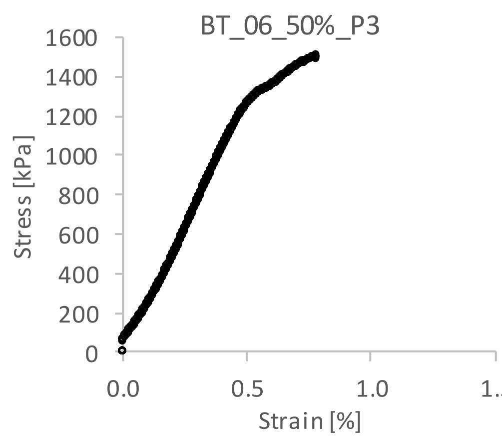
BT_06_50%_P3
Stress [kPa]
1600
1400
1200
1000
800
600
400
200
0
0.0
0.5
1.0
1.5
Strain [%]

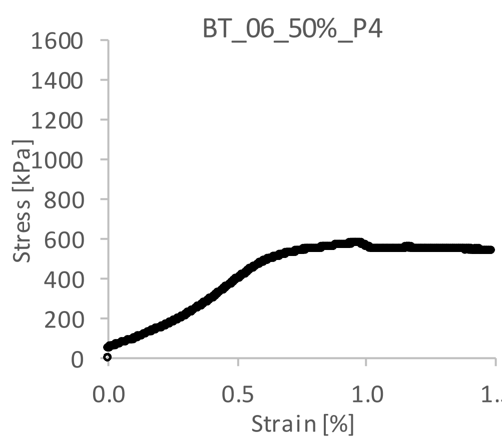
BT_06_50%_P4
Stress [kPa]
1600
1400
1200
1000
800
600
400
200
0
0.0
0.5
1.0
1.5
Strain [%]

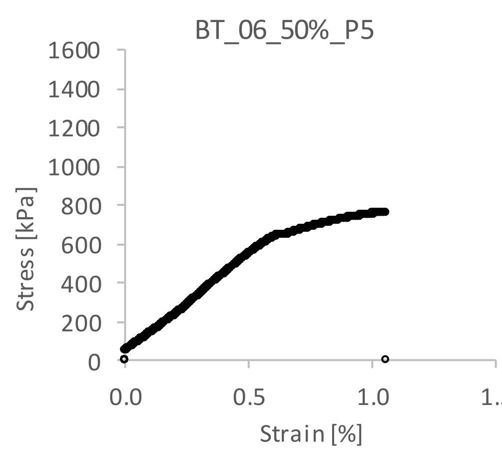
BT_06_50%_P5
Stress [kPa]
1600
1400
1200
1000
800
600
400
200
0
0.0
0.5
1.0
1.5
Strain [%]

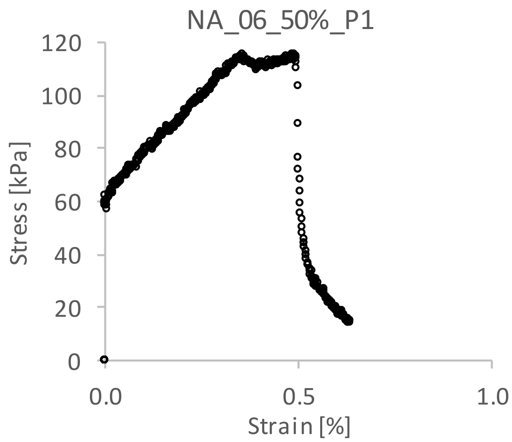
NA_06_50%_P1
Stress [kPa]
120
100
80
60
40
20
0
0.0
0.5
1.0
Strain [%]

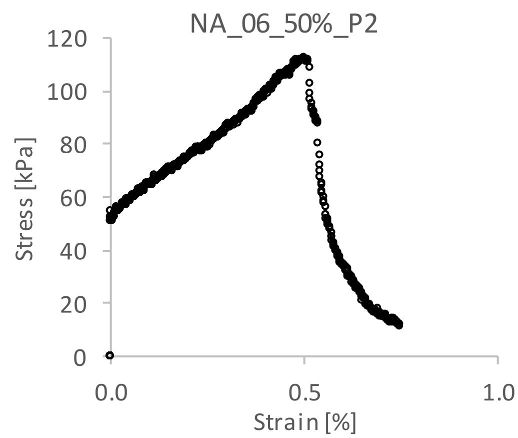
NA_06_50%_P2
Stress [kPa]
120
100
80
60
40
20
0
0.0
0.5
1.0
Strain [%]

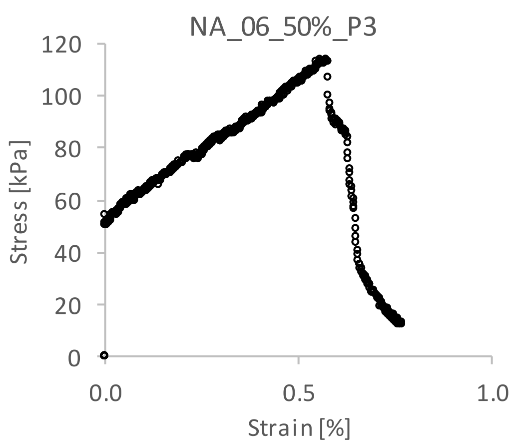
NA_06_50%_P3
Stress [kPa]
120
100
80
60
40
20
0
0.0
0.5
1.0
Strain [%]

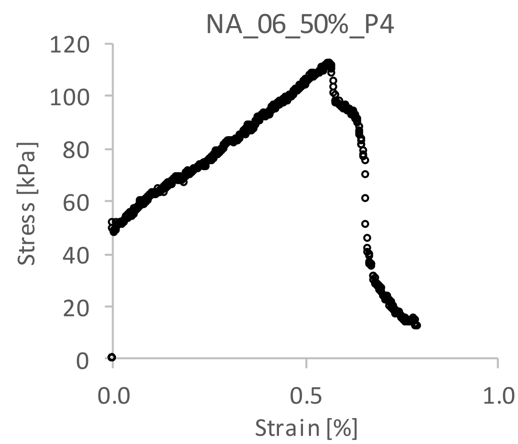
NA_06_50%_P4
Stress [kPa]
120
100
80
60
40
20
0
0.0
0.5
1.0
Strain [%]

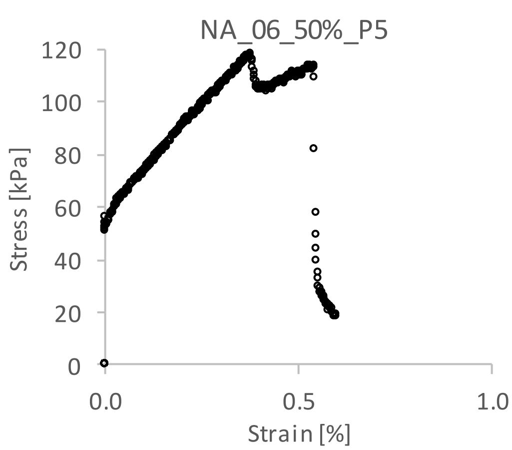
NA_06_50%_P5
Stress [kPa]
120
100
80
60
40
20
0
0.0
0.5
1.0
Strain [%]

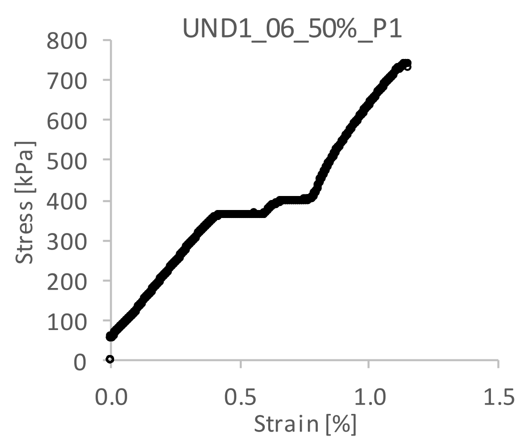
UND1_06_50%_P1
Stress [kPa]
800
700
600
500
400
300
200
100
0
0.0
0.5
1.0
1.5
Strain [%]

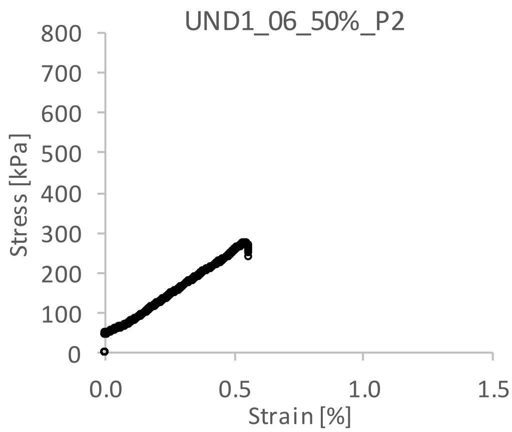
UND1_06_50%_P2
Stress [kPa]
Strain [%]

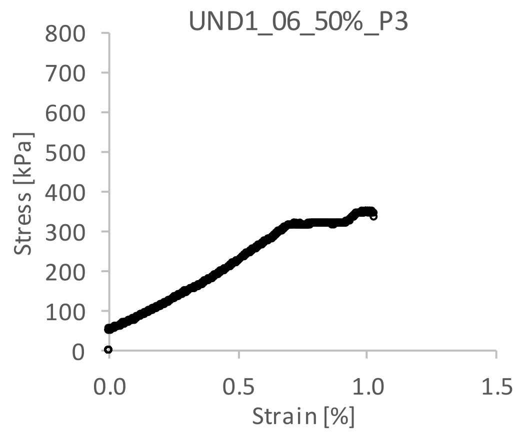
UND1_06_50%_P3
Stress [kPa]
Strain [%]

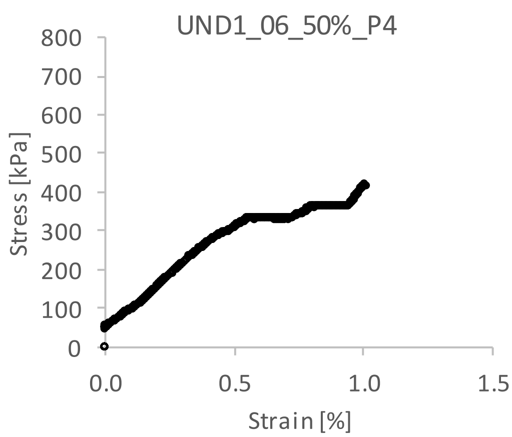
UND1_06_50%_P4
Stress [kPa]
Strain [%]

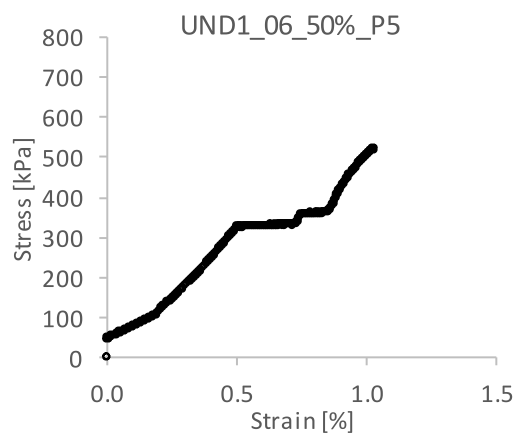
UND1_06_50%_P5
Stress [kPa]
Strain [%]

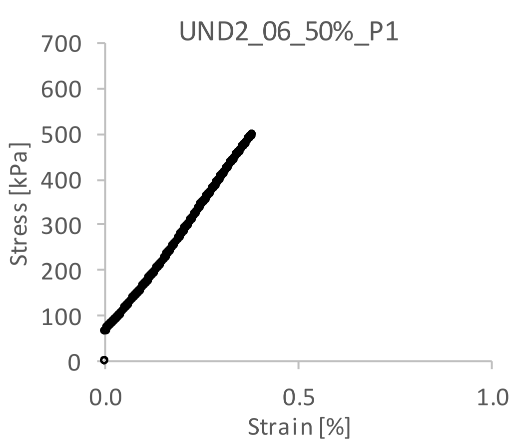
UND2_06_50%_P1
Stress [kPa]
Strain [%]

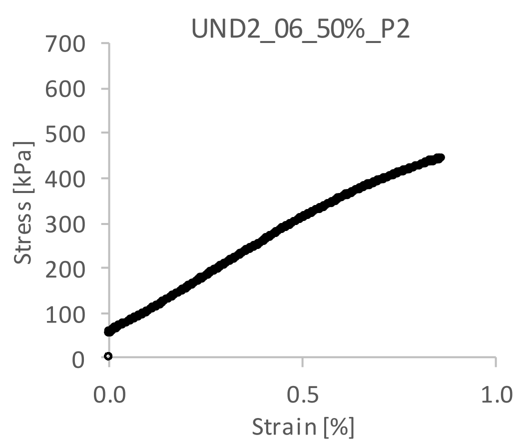
UND2_06_50%_P2
Stress [kPa]
Strain [%]

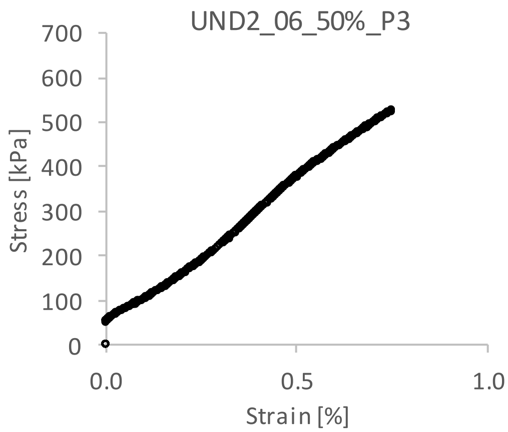

UND2_06_50%_P3
700
600
500
400
300
200
100
0
Stress [kPa]
0.0
0.5
1.0
Strain [%]

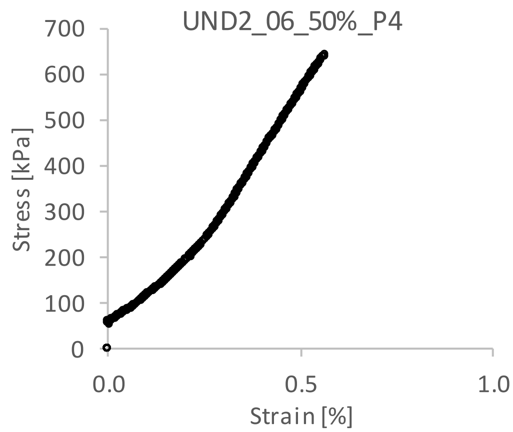

UND2_06_50%_P4
700
600
500
400
300
200
100
0
Stress [kPa]
0.0
0.5
1.0
Strain [%]

Stress-Strain curves for l/s = 0.5

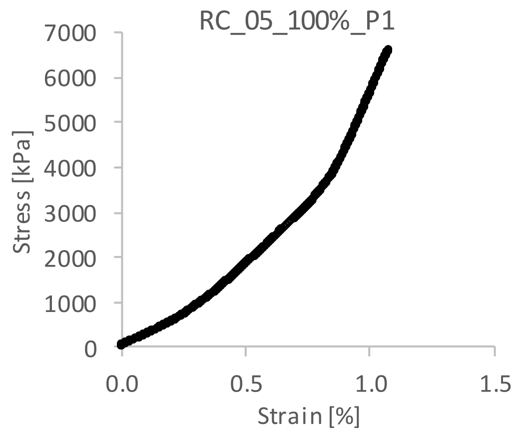

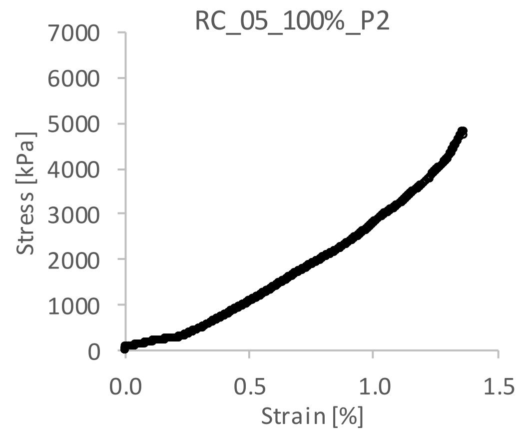

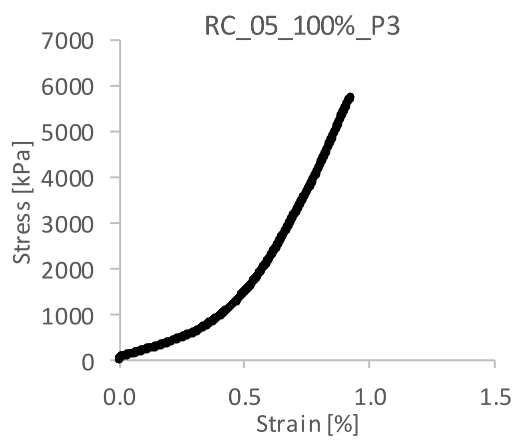

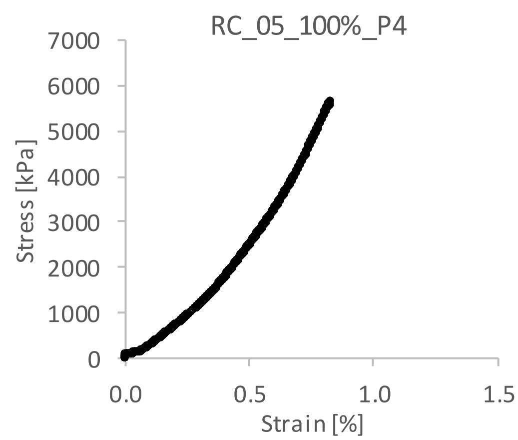

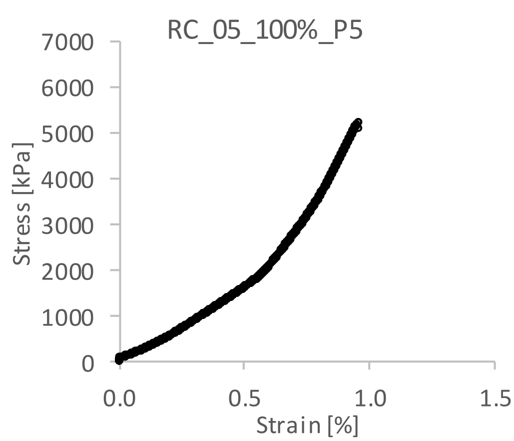

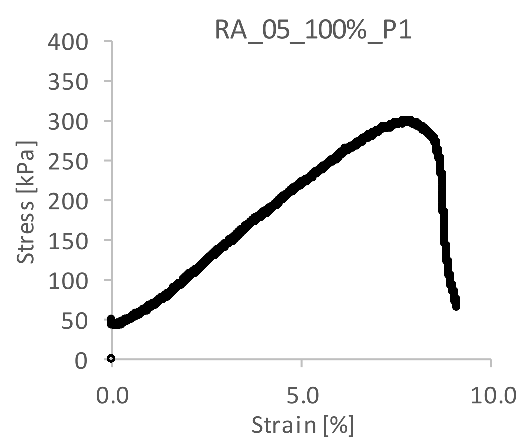

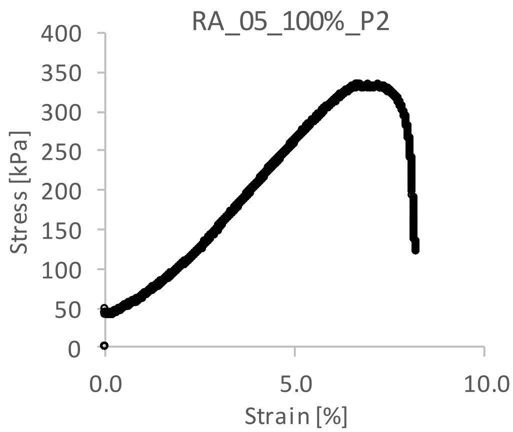
RA_05_100%_P2
400
350
300
250
200
150
100
50
0
0.0
5.0
10.0
Stress [kPa]
Strain [%]

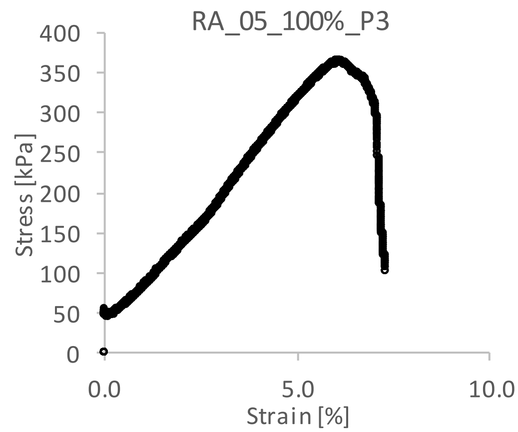
RA_05_100%_P3
400
350
300
250
200
150
100
50
0
0.0
5.0
10.0
Stress [kPa]
Strain [%]

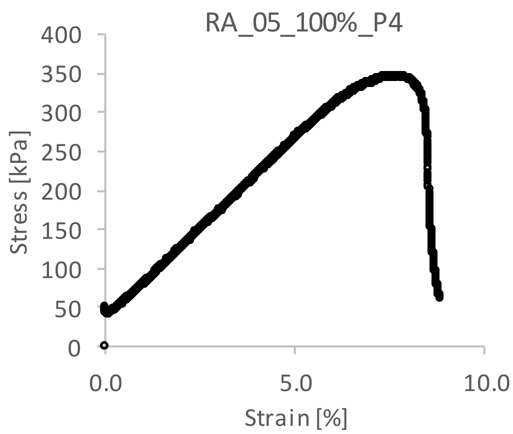
RA_05_100%_P4
400
350
300
250
200
150
100
50
0
0.0
5.0
10.0
Stress [kPa]
Strain [%]

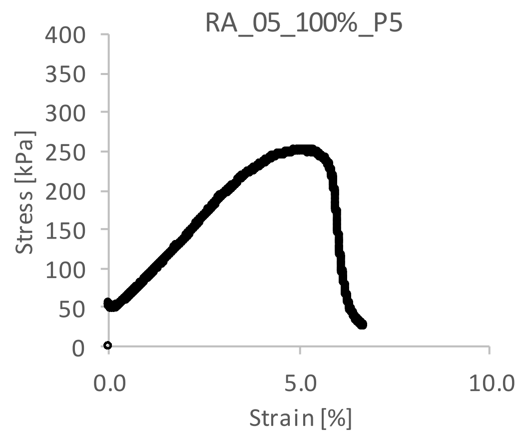
RA_05_100%_P5
400
350
300
250
200
150
100
50
0
0.0
5.0
10.0
Stress [kPa]
Strain [%]

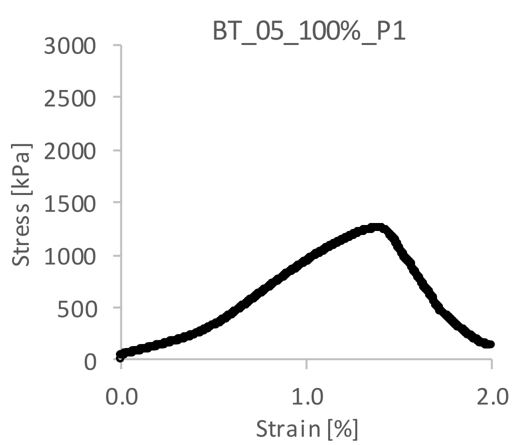
BT_05_100%_P1
3000
2500
2000
1500
1000
500
0
0.0
1.0
2.0
Stress [kPa]
Strain [%]

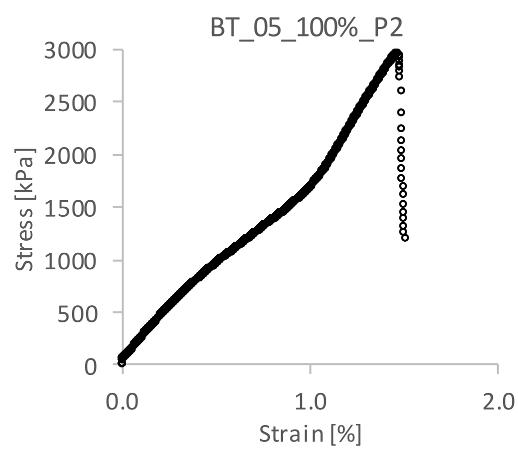
BT_05_100%_P2
3000
2500
2000
1500
1000
500
0
0.0
1.0
2.0
Stress [kPa]
Strain [%]

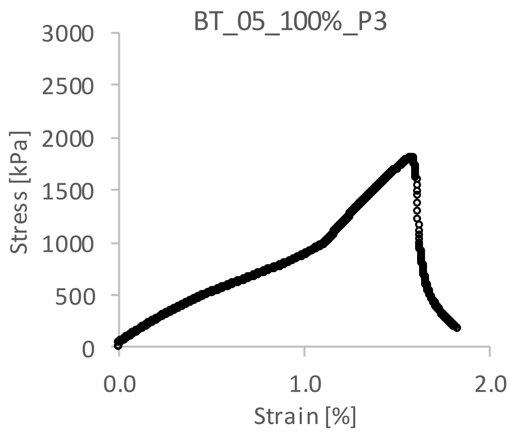
BT_05_100%_P3
Stress [kPa]
3000
2500
2000
1500
1000
500
0
0.0
1.0
2.0
Strain [%]

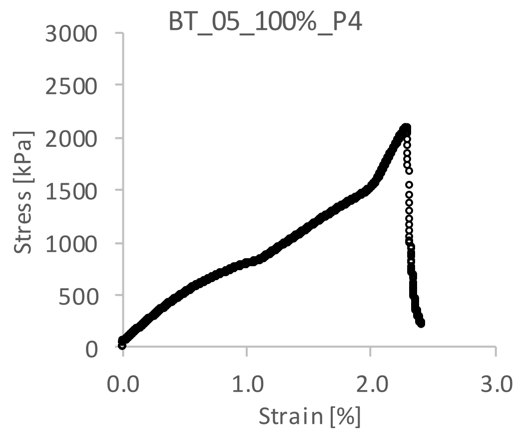
BT_05_100%_P4
Stress [kPa]
3000
2500
2000
1500
1000
500
0
0.0
1.0
2.0
3.0
Strain [%]

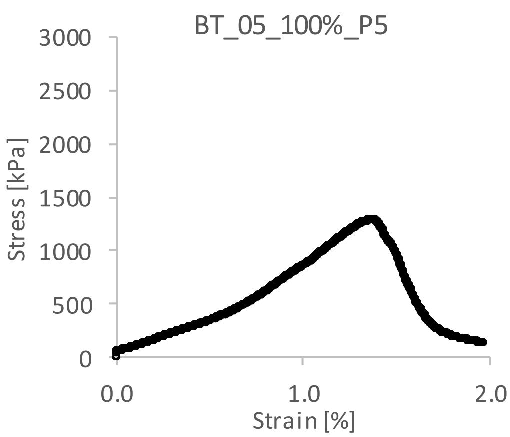
BT_05_100%_P5
Stress [kPa]
3000
2500
2000
1500
1000
500
0
0.0
1.0
2.0
Strain [%]

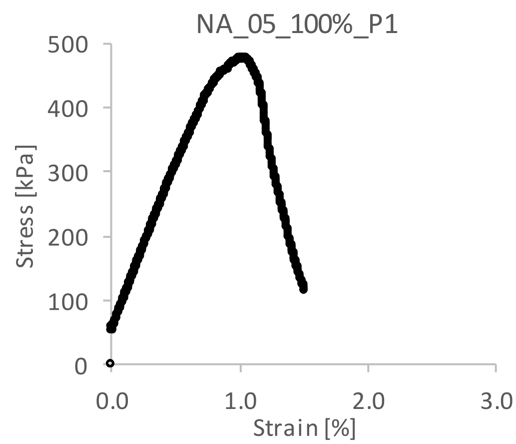
NA_05_100%_P1
Stress [kPa]
500
400
300
200
100
0
0.0
1.0
2.0
3.0
Strain [%]

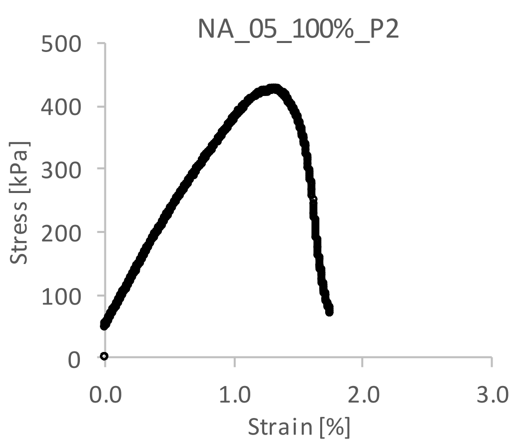
NA_05_100%_P2
Stress [kPa]
500
400
300
200
100
0
0.0
1.0
2.0
3.0
Strain [%]

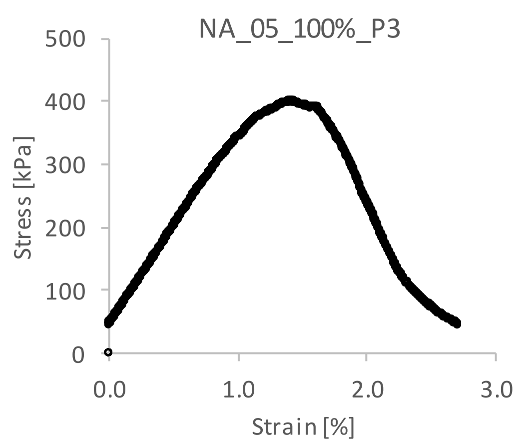
NA_05_100%_P3
Stress [kPa]
500
400
300
200
100
0
0.0
1.0
2.0
3.0
Strain [%]

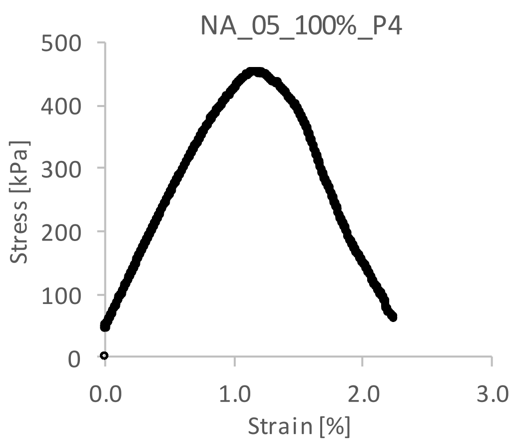
NA_05_100%_P4
Stress [kPa]
500
400
300
200
100
0
0.0
1.0
2.0
3.0
Strain [%]

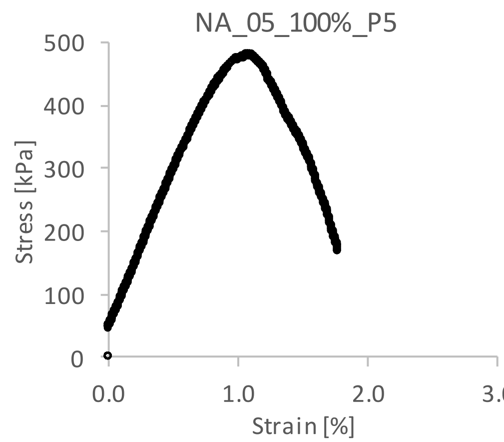
NA_05_100%_P5
Stress [kPa]
500
400
300
200
100
0
0.0
1.0
2.0
3.0
Strain [%]

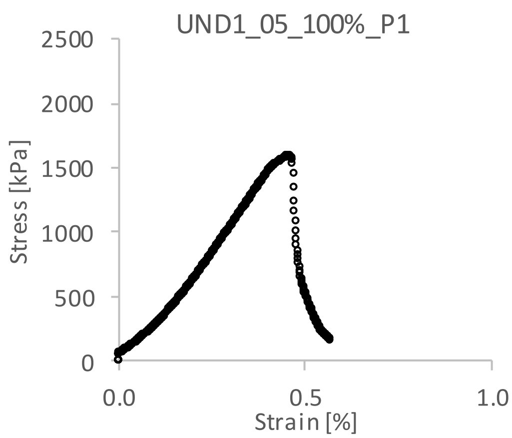
UND1_05_100%_P1
Stress [kPa]
2500
2000
1500
1000
500
0
0.0
0.5
1.0
Strain [%]

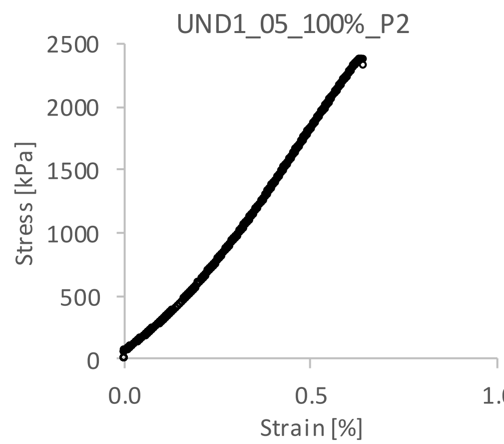
UND1_05_100%_P2
Stress [kPa]
2500
2000
1500
1000
500
0
0.0
0.5
1.0
Strain [%]

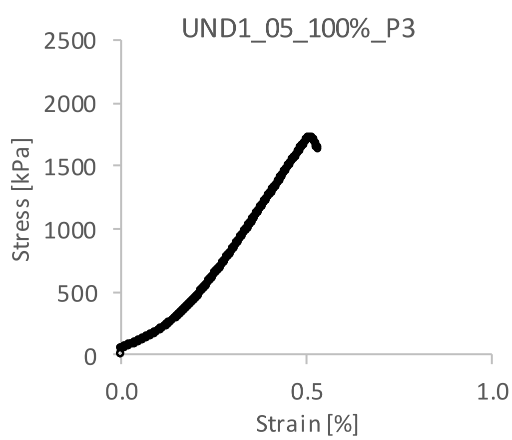
UND1_05_100%_P3
Stress [kPa]
2500
2000
1500
1000
500
0
0.0
0.5
1.0
Strain [%]

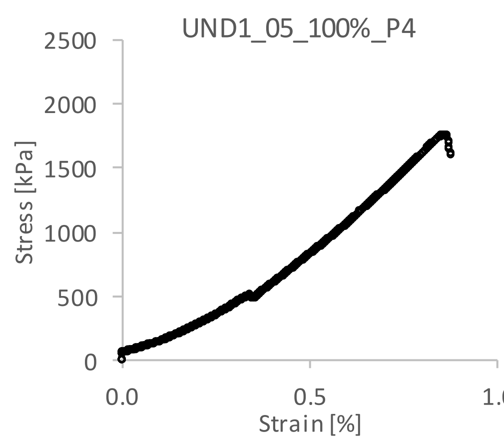
UND1_05_100%_P4
Stress [kPa]
2500
2000
1500
1000
500
0
0.0
0.5
1.0
Strain [%]

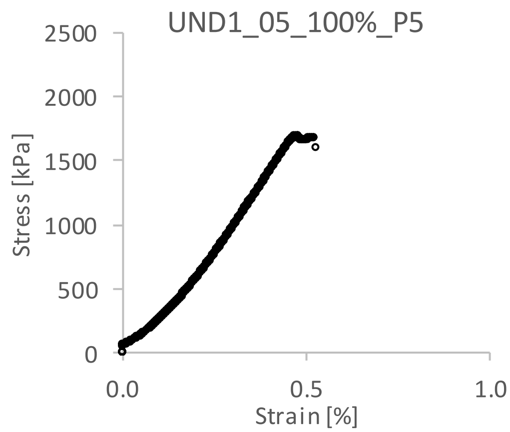
UND1_05_100%_P5
Stress [kPa]
Strain [%]
0
500
1000
1500
2000
2500
0.0
0.5
1.0

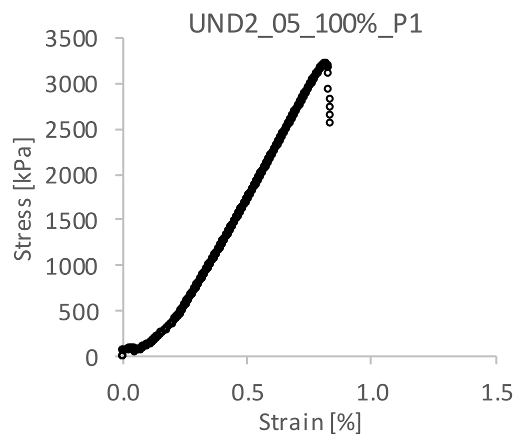
UND2_05_100%_P1
Stress [kPa]
Strain [%]
0
500
1000
1500
2000
2500
3000
3500
0.0
0.5
1.0
1.5

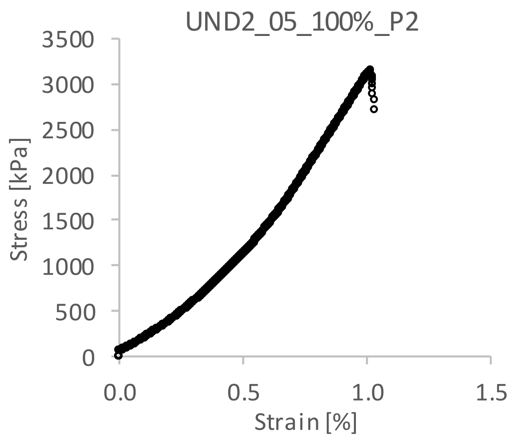
UND2_05_100%_P2
Stress [kPa]
Strain [%]
0
500
1000
1500
2000
2500
3000
3500
0.0
0.5
1.0
1.5

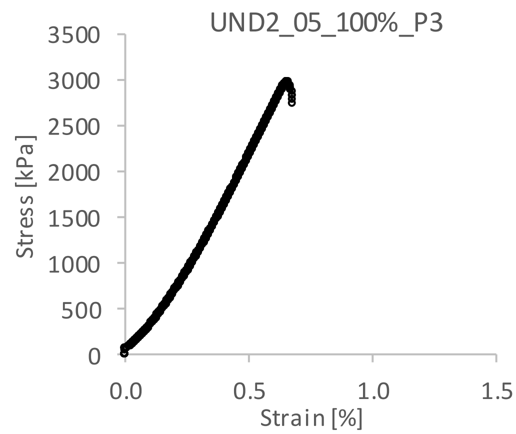
UND2_05_100%_P3
Stress [kPa]
Strain [%]
0
500
1000
1500
2000
2500
3000
3500
0.0
0.5
1.0
1.5

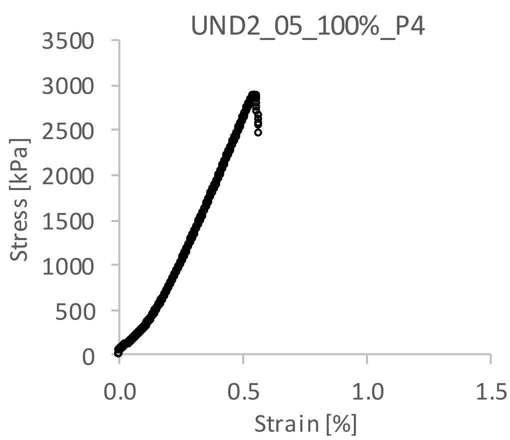
UND2_05_100%_P4
Stress [kPa]
Strain [%]
0
500
1000
1500
2000
2500
3000
3500
0.0
0.5
1.0
1.5

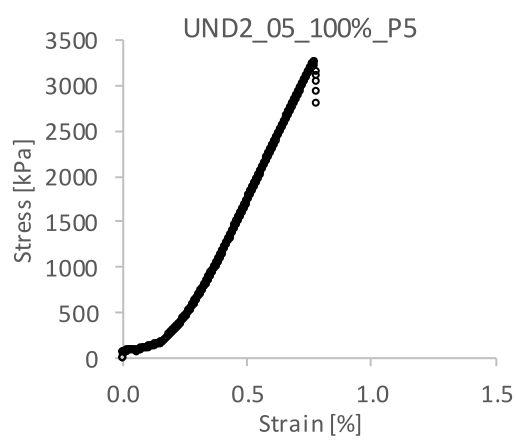
UND2_05_100%_P5
Stress [kPa]
Strain [%]
0
500
1000
1500
2000
2500
3000
3500
0.0
0.5
1.0
1.5

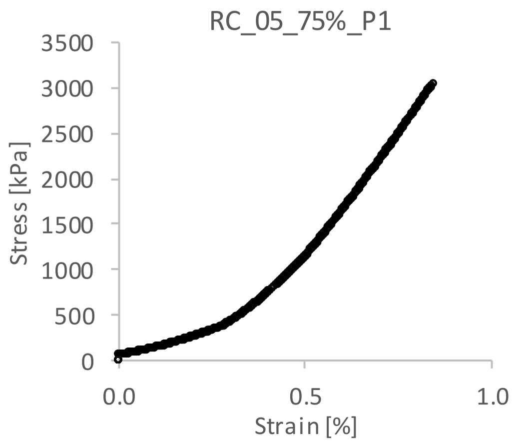
RC_05_75%_P1
Stress [kPa]
0
500
1000
1500
2000
2500
3000
3500
0.0
0.5
1.0
Strain [%]

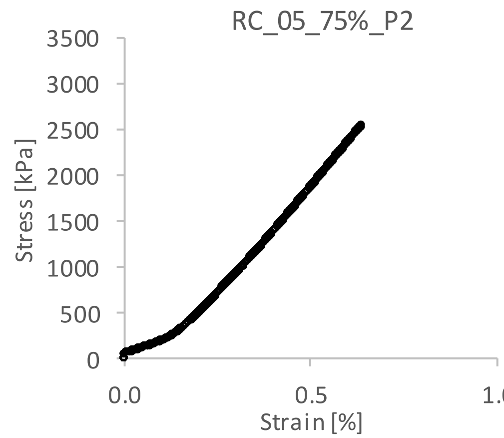
RC_05_75%_P2
Stress [kPa]
0
500
1000
1500
2000
2500
3000
3500
0.0
0.5
1.0
Strain [%]

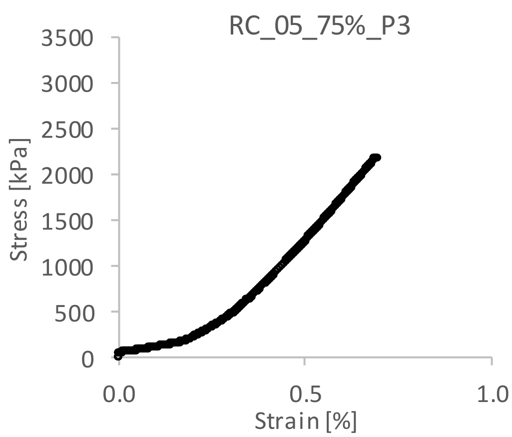
RC_05_75%_P3
Stress [kPa]
0
500
1000
1500
2000
2500
3000
3500
0.0
0.5
1.0
Strain [%]

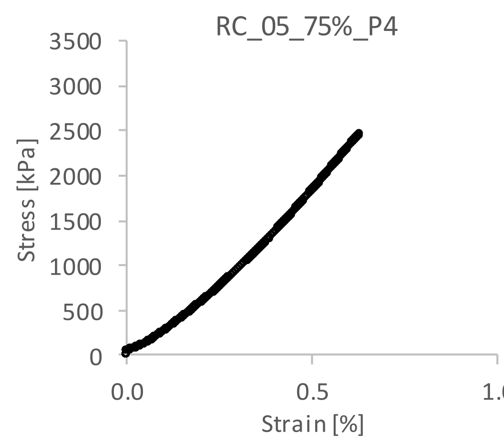
RC_05_75%_P4
Stress [kPa]
0
500
1000
1500
2000
2500
3000
3500
0.0
0.5
1.0
Strain [%]

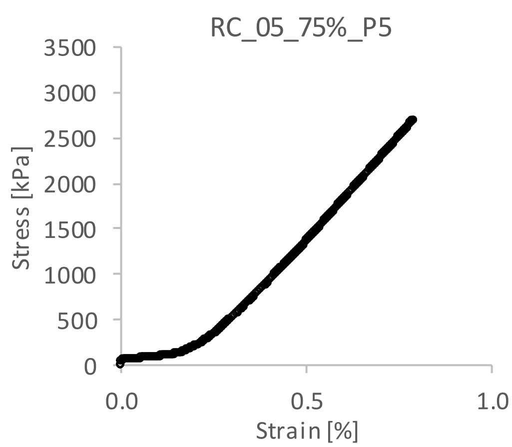
RC_05_75%_P5
Stress [kPa]
0
500
1000
1500
2000
2500
3000
3500
0.0
0.5
1.0
Strain [%]

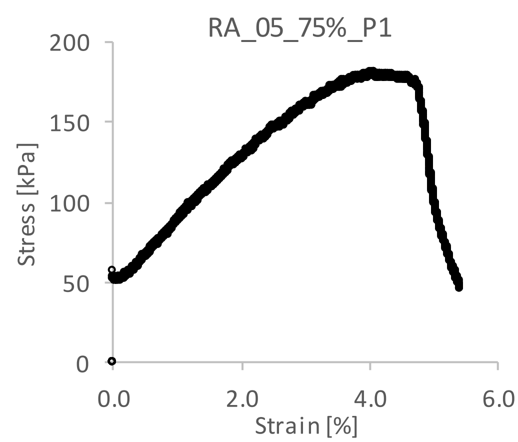
RA_05_75%_P1
Stress [kPa]
0
50
100
150
200
0.0
2.0
4.0
6.0
Strain [%]

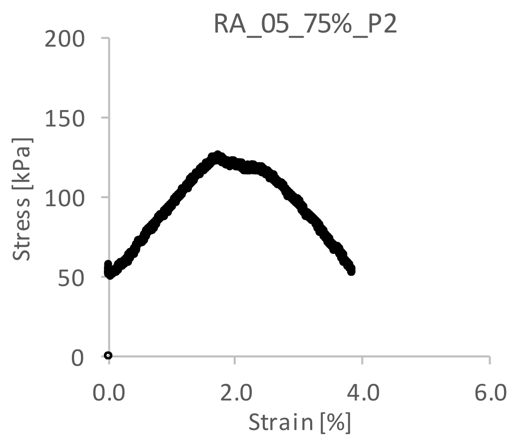
RA_05_75%_P2
Stress [kPa]
Strain [%]
0
50
100
150
200
0.0
2.0
4.0
6.0

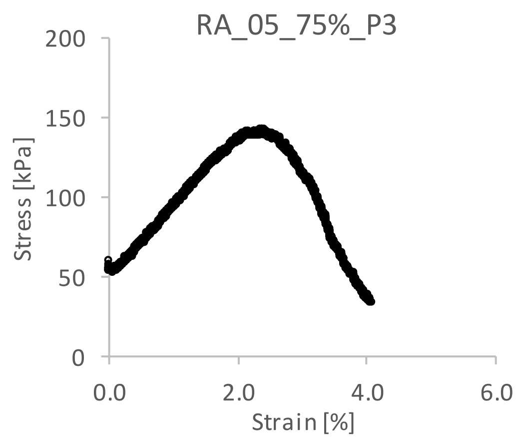
RA_05_75%_P3
Stress [kPa]
Strain [%]
0
50
100
150
200
0.0
2.0
4.0
6.0

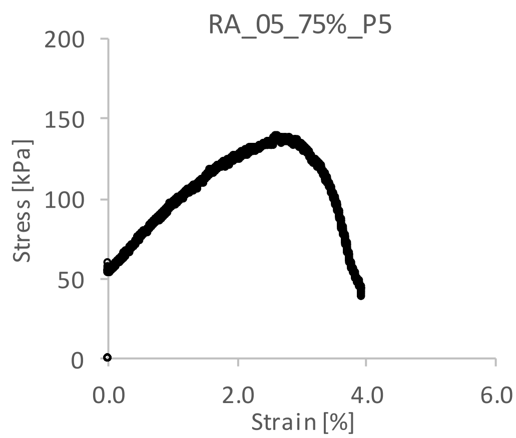
RA_05_75%_P5
Stress [kPa]
Strain [%]
0
50
100
150
200
0.0
2.0
4.0
6.0

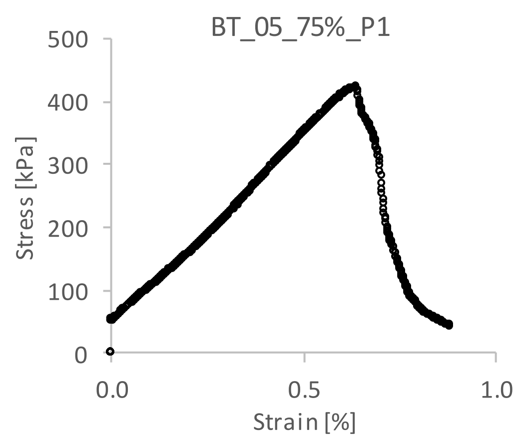
BT_05_75%_P1
Stress [kPa]
Strain [%]
0
100
200
300
400
500
0.0
0.5
1.0

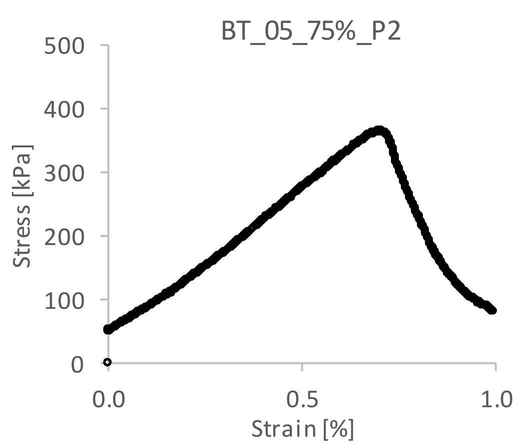
BT_05_75%_P2
Stress [kPa]
Strain [%]
0
100
200
300
400
500
0.0
0.5
1.0

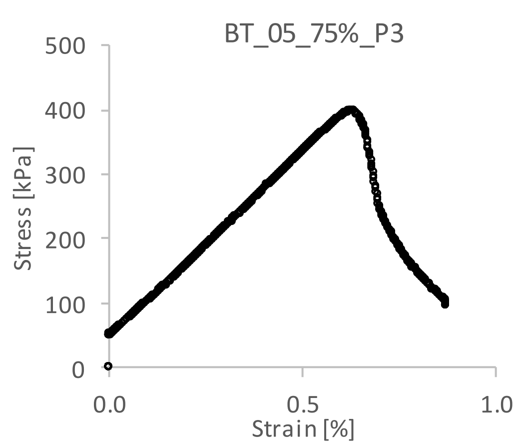
BT_05_75%_P3
Stress [kPa]
Strain [%]
0
100
200
300
400
500
0.0
0.5
1.0

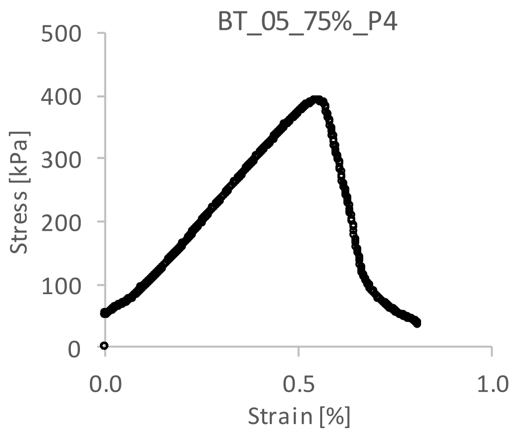
BT_05_75%_P4
Stress [kPa]
Strain [%]
0
100
200
300
400
500
0.0
0.5
1.0

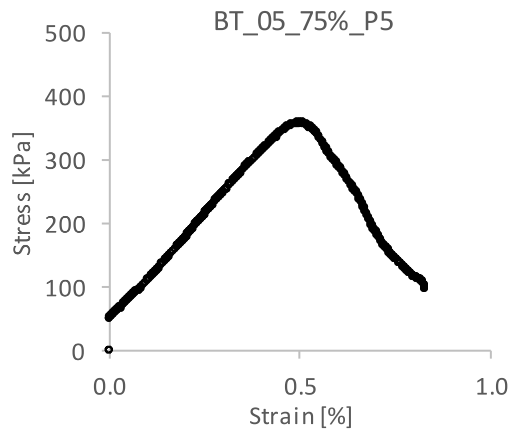
BT_05_75%_P5
Stress [kPa]
Strain [%]
0
100
200
300
400
500
0.0
0.5
1.0

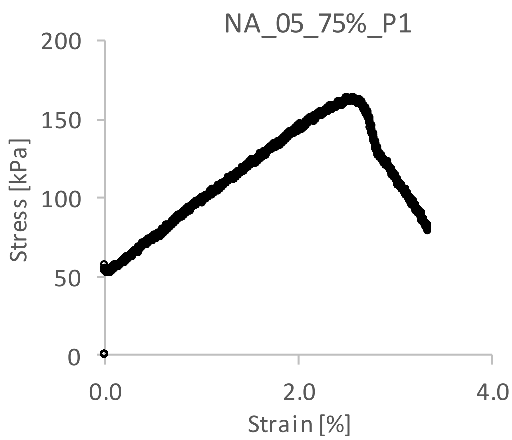
NA_05_75%_P1
Stress [kPa]
Strain [%]
0
50
100
150
200
0.0
2.0
4.0

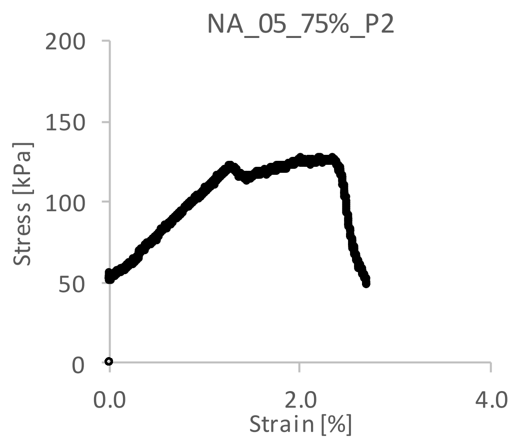
NA_05_75%_P2
Stress [kPa]
Strain [%]
0
50
100
150
200
0.0
2.0
4.0

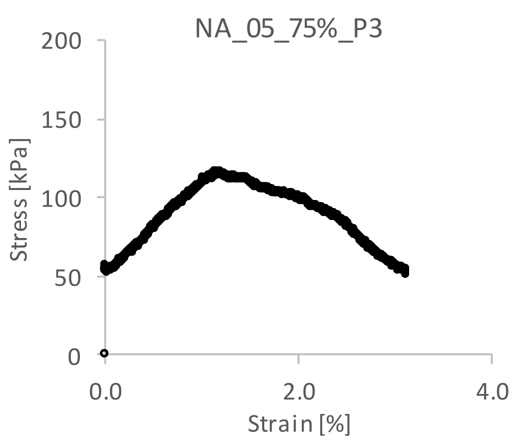
NA_05_75%_P3
Stress [kPa]
Strain [%]
0
50
100
150
200
0.0
2.0
4.0

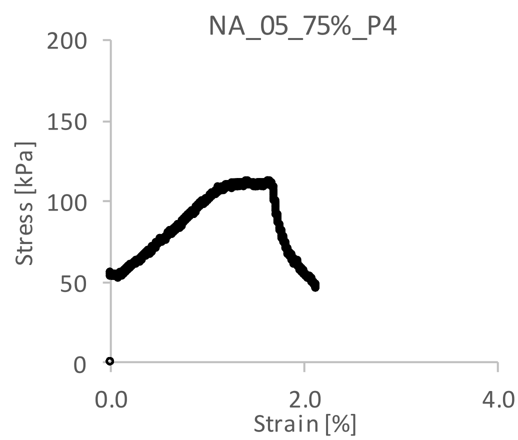
NA_05_75%_P4
Stress [kPa]
Strain [%]
0
50
100
150
200
0.0
2.0
4.0

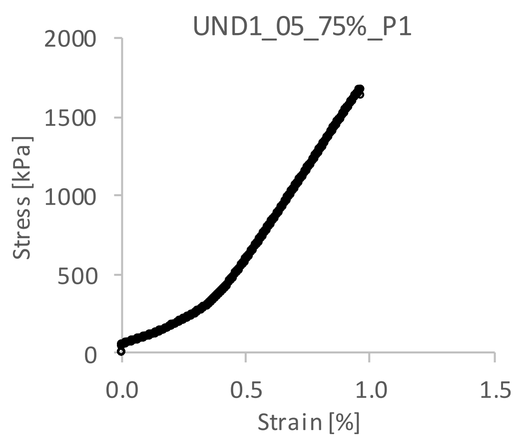
UND1_05_75%_P1
Stress [kPa]
2000
1500
1000
500
0
0.0
0.5
1.0
1.5
Strain [%]

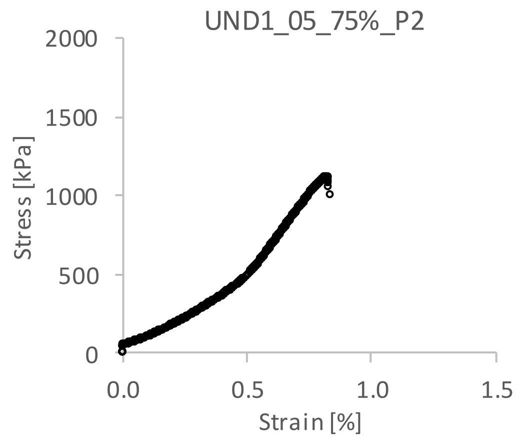
UND1_05_75%_P2
Stress [kPa]
2000
1500
1000
500
0
0.0
0.5
1.0
1.5
Strain [%]

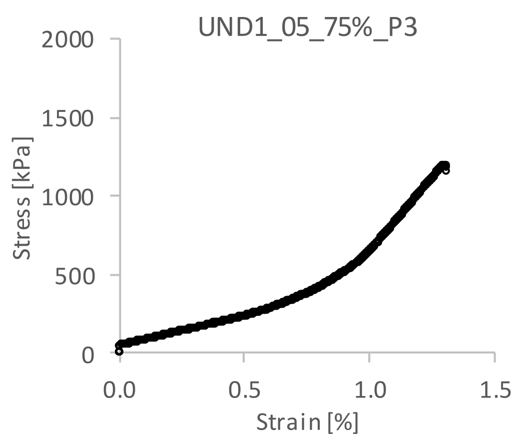
UND1_05_75%_P3
Stress [kPa]
2000
1500
1000
500
0
0.0
0.5
1.0
1.5
Strain [%]

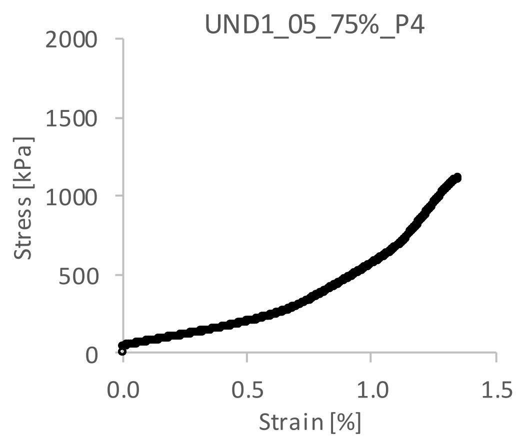
UND1_05_75%_P4
Stress [kPa]
2000
1500
1000
500
0
0.0
0.5
1.0
1.5
Strain [%]

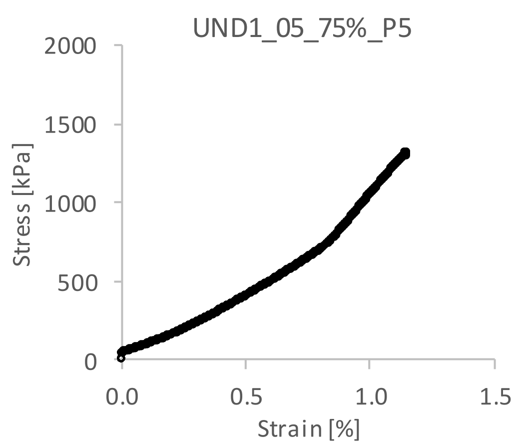
UND1_05_75%_P5
Stress [kPa]
2000
1500
1000
500
0
0.0
0.5
1.0
1.5
Strain [%]

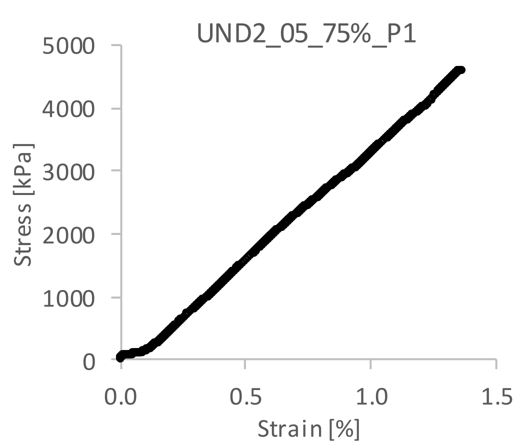
UND2_05_75%_P1
Stress [kPa]
5000
4000
3000
2000
1000
0
0.0
0.5
1.0
1.5
Strain [%]

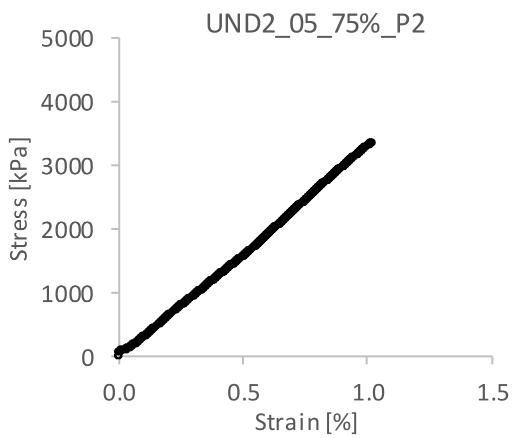
UND2_05_75%_P2
Stress [kPa]
Strain [%]
0
1000
2000
3000
4000
5000
0.0
0.5
1.0
1.5

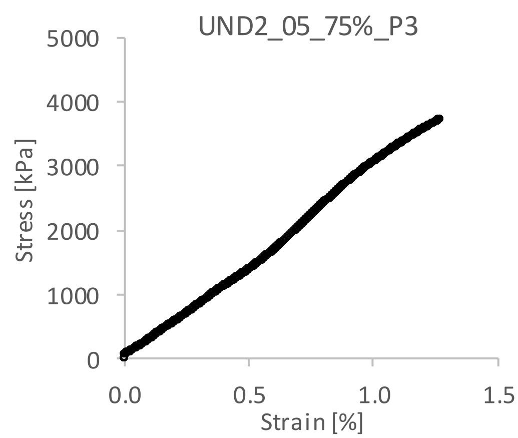
UND2_05_75%_P3
Stress [kPa]
Strain [%]
0
1000
2000
3000
4000
5000
0.0
0.5
1.0
1.5

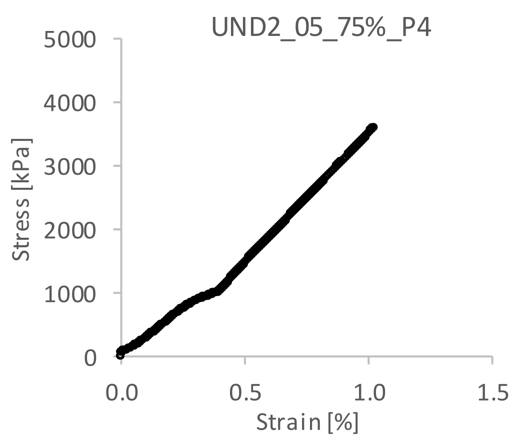
UND2_05_75%_P4
Stress [kPa]
Strain [%]
0
1000
2000
3000
4000
5000
0.0
0.5
1.0
1.5

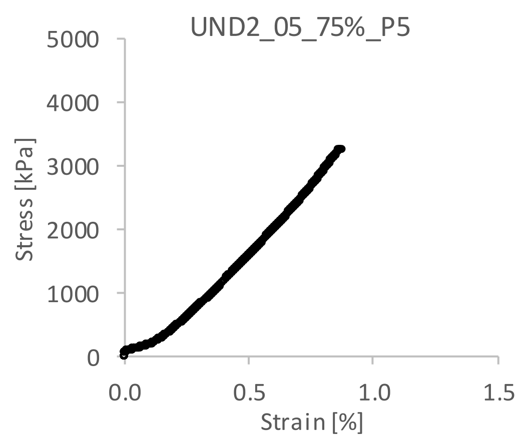
UND2_05_75%_P5
Stress [kPa]
Strain [%]
0
1000
2000
3000
4000
5000
0.0
0.5
1.0
1.5

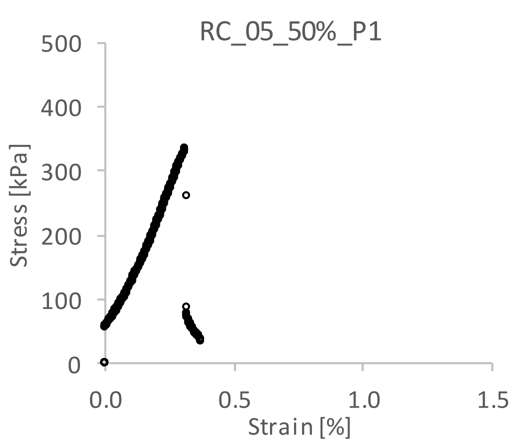
RC_05_50%_P1
Stress [kPa]
Strain [%]
0
100
200
300
400
500
0.0
0.5
1.0
1.5

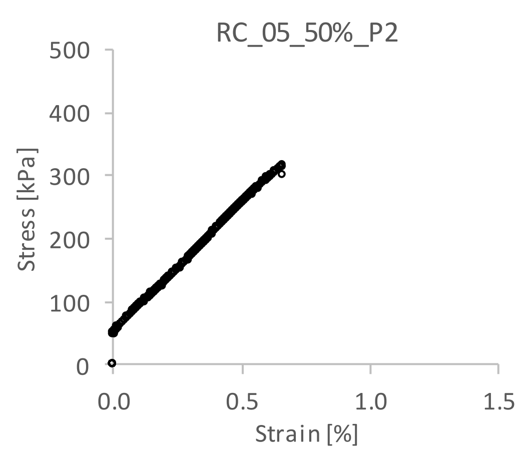
RC_05_50%_P2
Stress [kPa]
Strain [%]
0
100
200
300
400
500
0.0
0.5
1.0
1.5

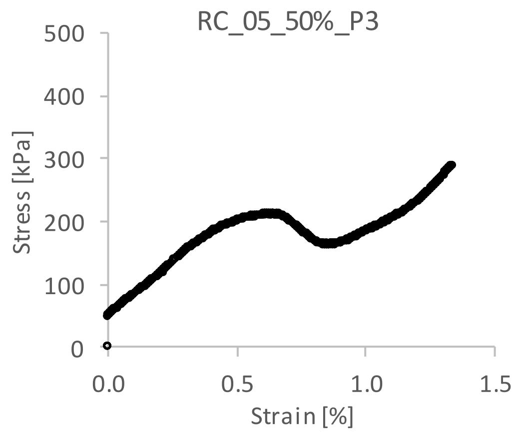
RC_05_50%_P3
Stress [kPa]
Strain [%]
0
100
200
300
400
500
0.0
0.5
1.0
1.5

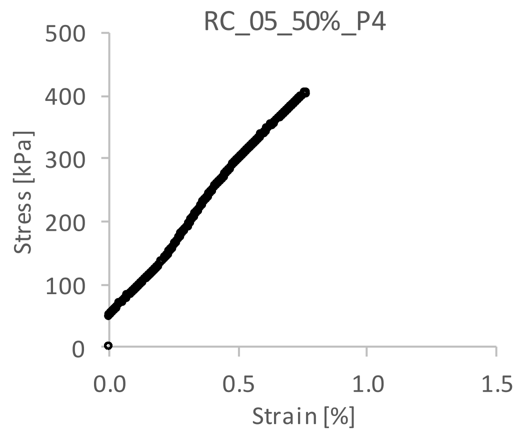
RC_05_50%_P4
Stress [kPa]
Strain [%]
0
100
200
300
400
500
0.0
0.5
1.0
1.5

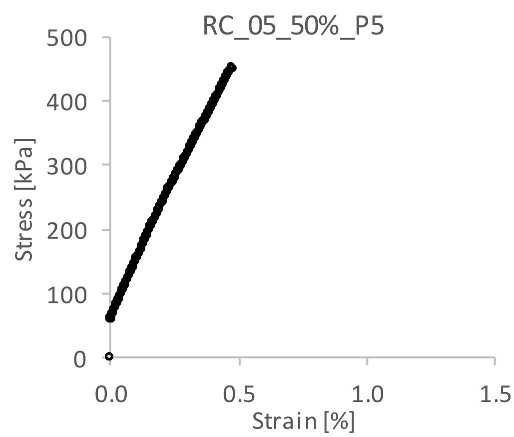
RC_05_50%_P5
Stress [kPa]
Strain [%]
0
100
200
300
400
500
0.0
0.5
1.0
1.5

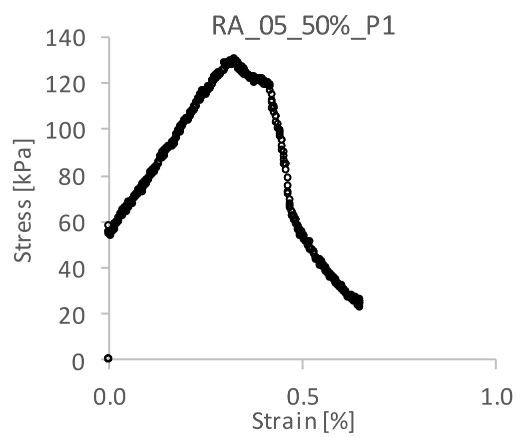
RA_05_50%_P1
Stress [kPa]
Strain [%]
0
20
40
60
80
100
120
140
0.0
0.5
1.0

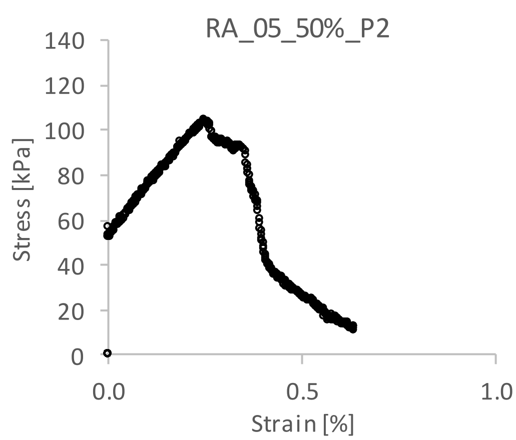
RA_05_50%_P2
Stress [kPa]
Strain [%]
0
20
40
60
80
100
120
140
0.0
0.5
1.0

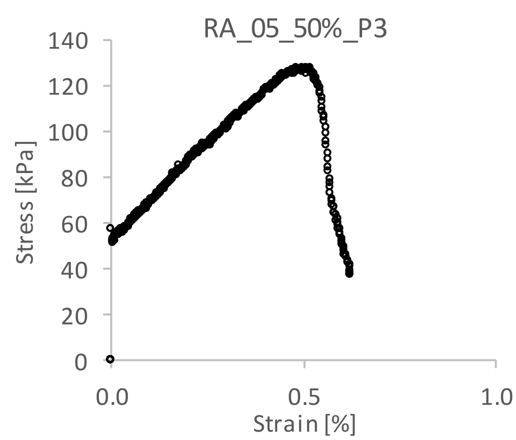
RA_05_50%_P3
Stress [kPa]
Strain [%]
0
20
40
60
80
100
120
140
0.0
0.5
1.0

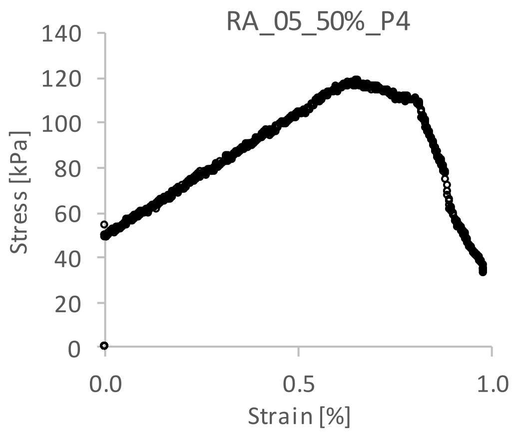
RA_05_50%_P4
Stress [kPa]
Strain [%]
0
20
40
60
80
100
120
140
0.0
0.5
1.0

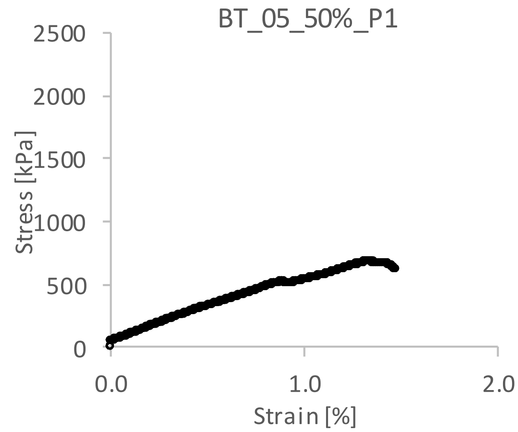
BT_05_50%_P1
Stress [kPa]
Strain [%]
0
500
1000
1500
2000
2500
0.0
1.0
2.0

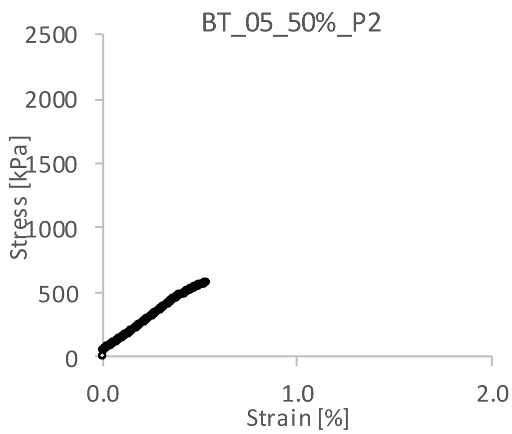
BT_05_50%_P2
Stress [kPa]
Strain [%]
0
500
1000
1500
2000
2500
0.0
1.0
2.0

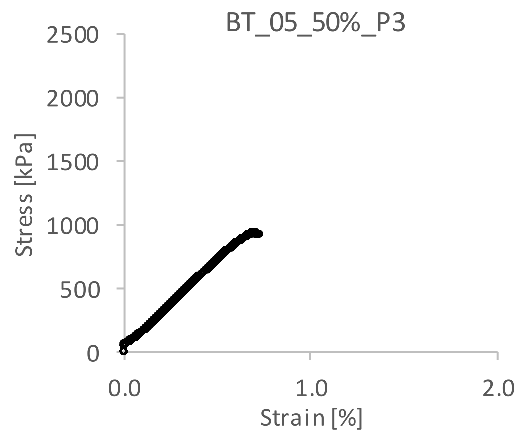
BT_05_50%_P3
Stress [kPa]
Strain [%]
0
500
1000
1500
2000
2500
0.0
1.0
2.0

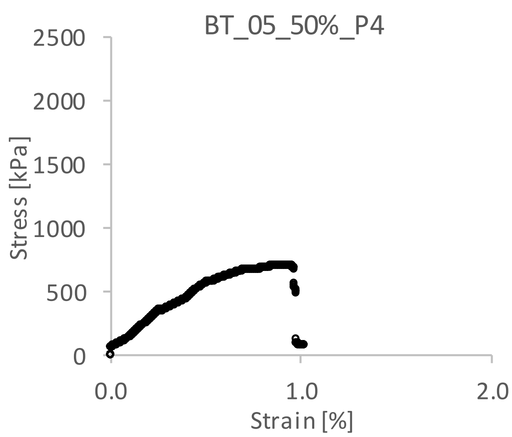
BT_05_50%_P4
Stress [kPa]
Strain [%]
0
500
1000
1500
2000
2500
0.0
1.0
2.0

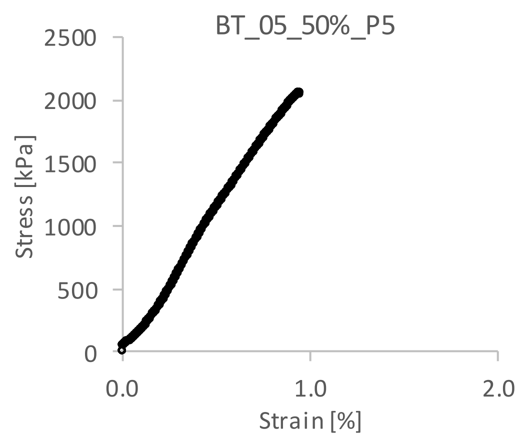
BT_05_50%_P5
Stress [kPa]
Strain [%]
0
500
1000
1500
2000
2500
0.0
1.0
2.0

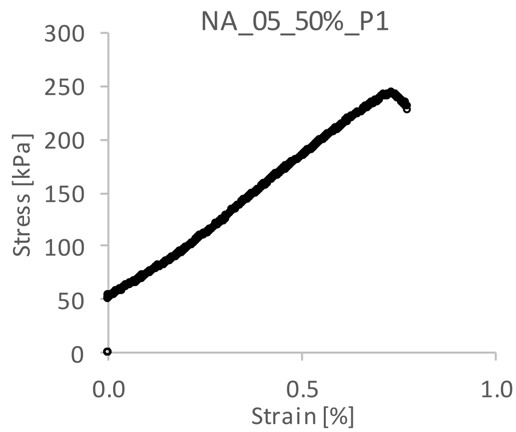
NA_05_50%_P1
Stress [kPa]
Strain [%]

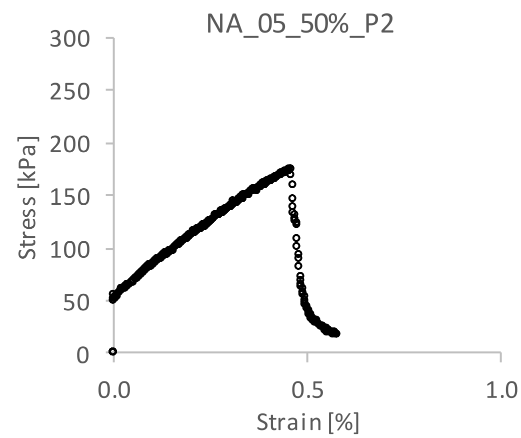
NA_05_50%_P2
Stress [kPa]
Strain [%]

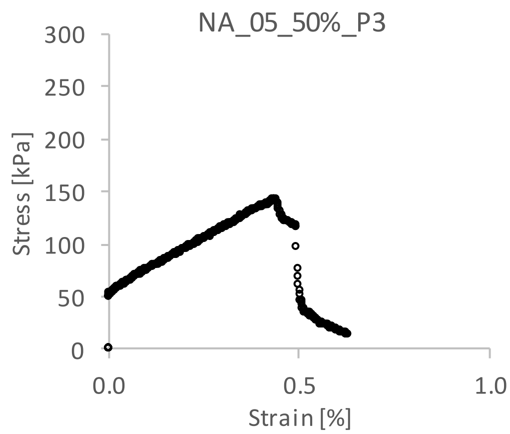
NA_05_50%_P3
Stress [kPa]
Strain [%]

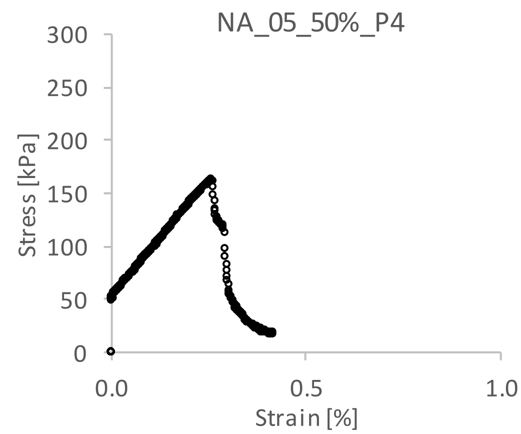
NA_05_50%_P4
Stress [kPa]
Strain [%]

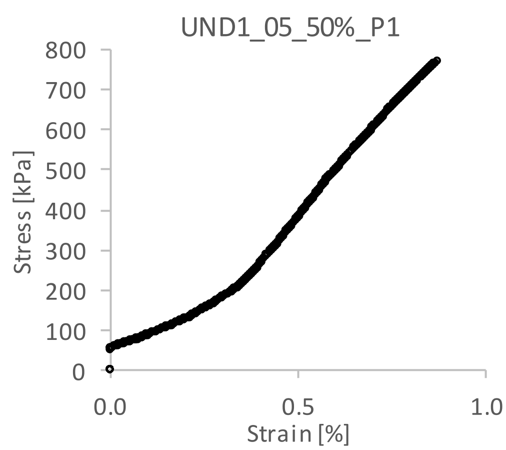
UND1_05_50%_P1
Stress [kPa]
Strain [%]

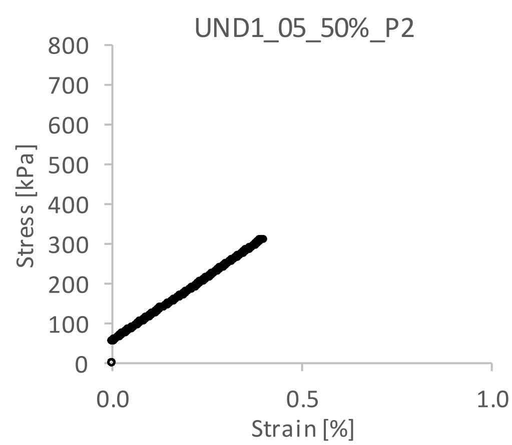
UND1_05_50%_P2
Stress [kPa]
Strain [%]

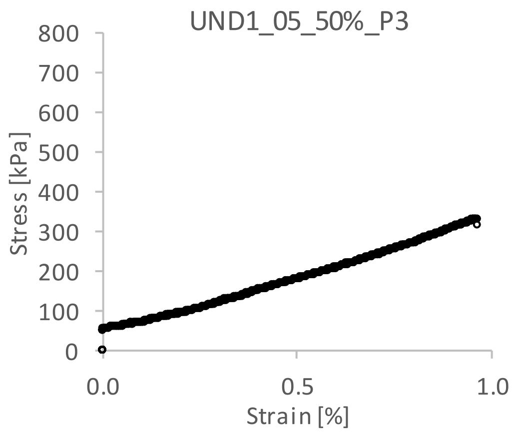
UND1_05_50%_P3
Stress [kPa]
Strain [%]
0
100
200
300
400
500
600
700
800
0.0
0.5
1.0

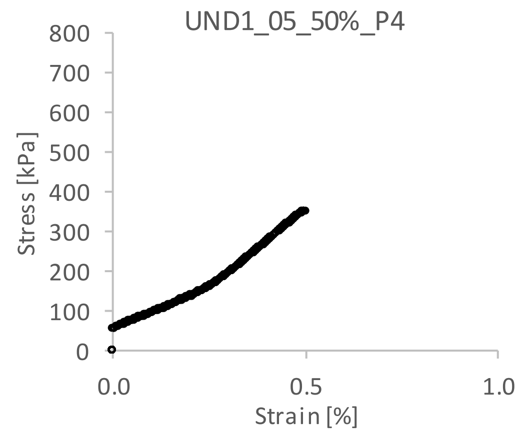
UND1_05_50%_P4
Stress [kPa]
Strain [%]
0
100
200
300
400
500
600
700
800
0.0
0.5
1.0

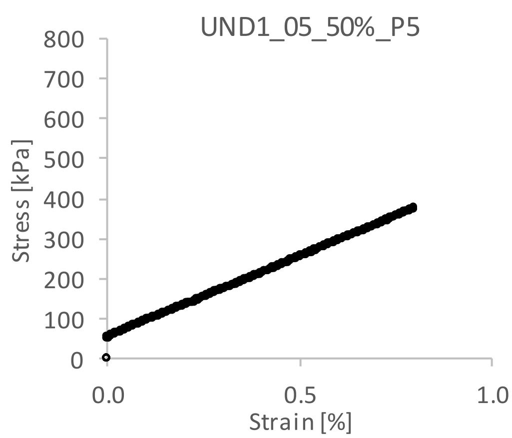
UND1_05_50%_P5
Stress [kPa]
Strain [%]
0
100
200
300
400
500
600
700
800
0.0
0.5
1.0

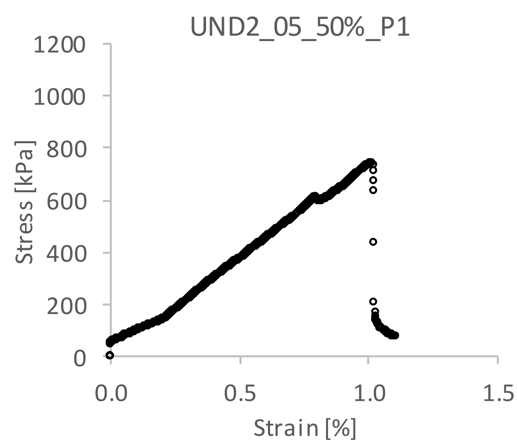
UND2_05_50%_P1
Stress [kPa]
Strain [%]
0
200
400
600
800
1000
1200
0.0
0.5
1.0
1.5

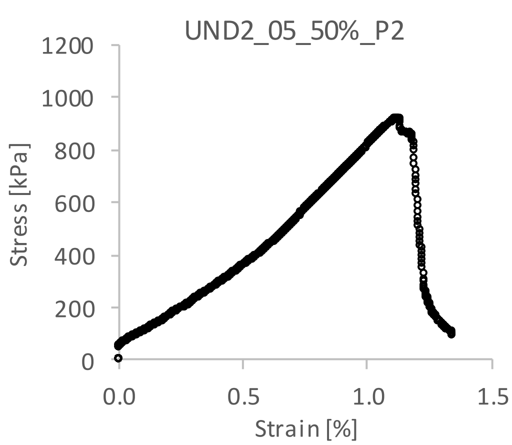
UND2_05_50%_P2
Stress [kPa]
Strain [%]
0
200
400
600
800
1000
1200
0.0
0.5
1.0
1.5

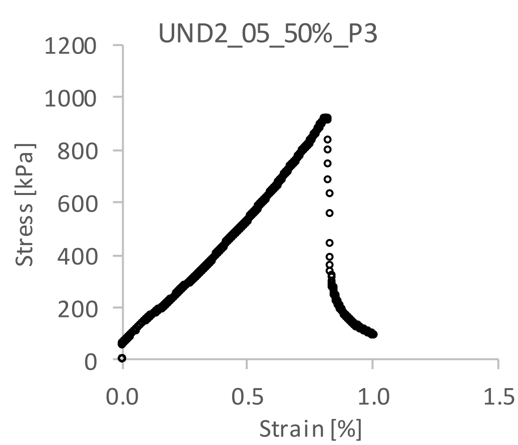
UND2_05_50%_P3
Stress [kPa]
Strain [%]
0
200
400
600
800
1000
1200
0.0
0.5
1.0
1.5

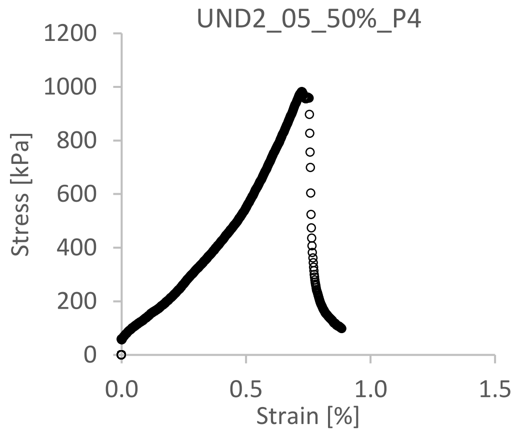
UND2_05_50%_P4
1200
1000
800
600
400
200
0
Stress [kPa]
0.0
0.5
1.0
1.5
Strain [%]

Stress-Strain curves for l/s = 0.4

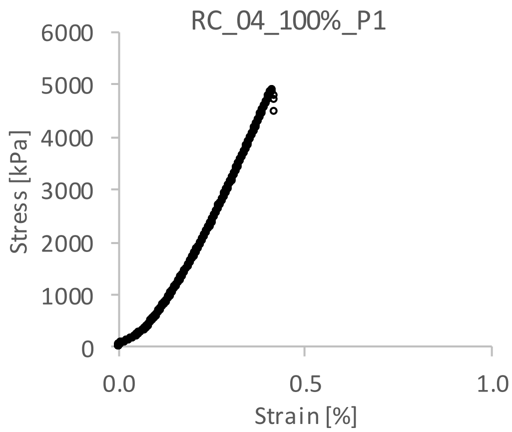

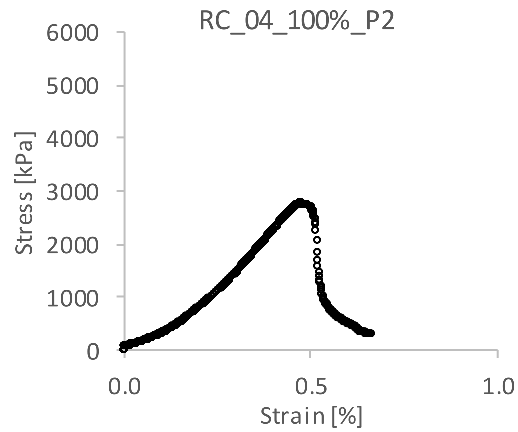

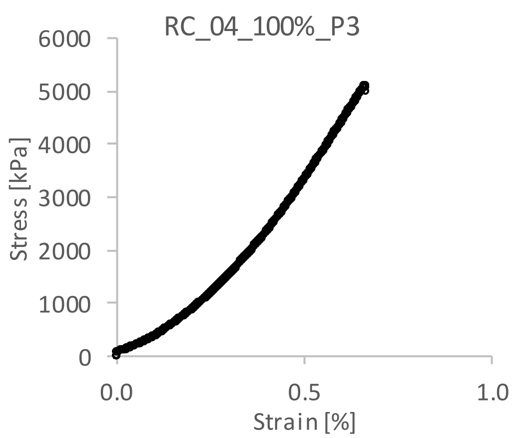

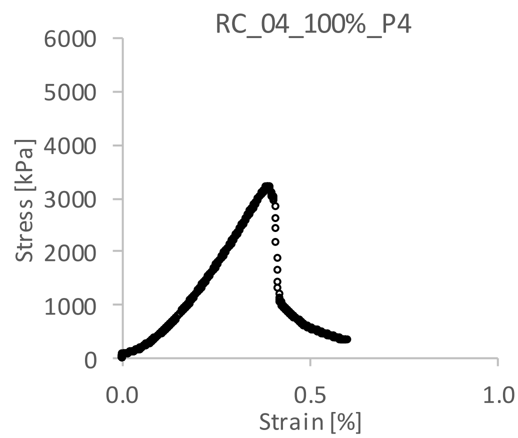

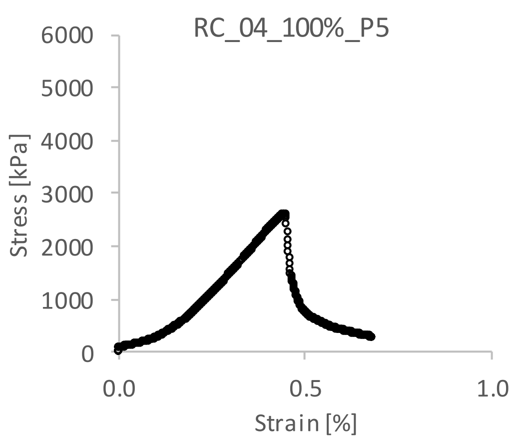

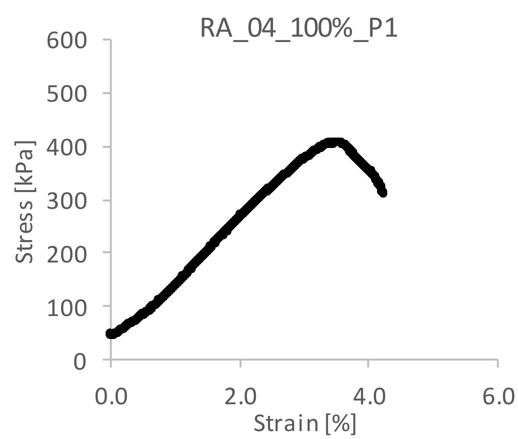

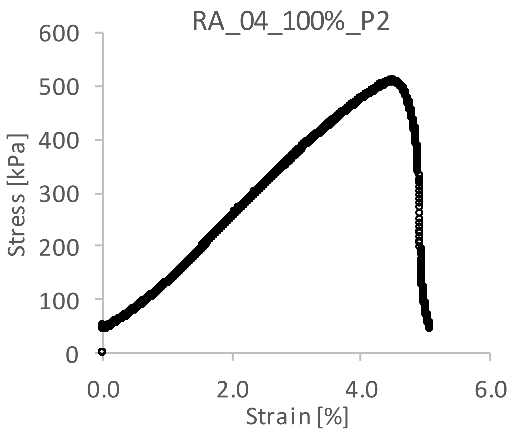
RA_04_100%_P2
Stress [kPa]
600
500
400
300
200
100
0
0.0
2.0
4.0
6.0
Strain [%]

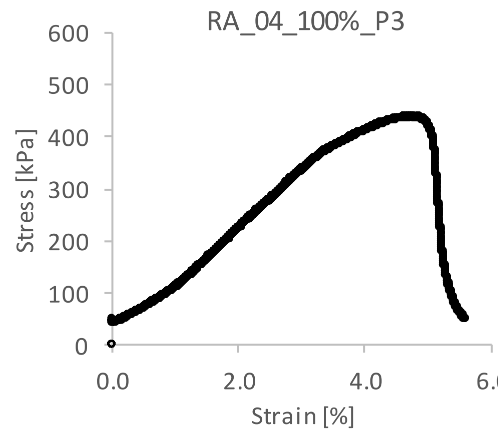
RA_04_100%_P3
Stress [kPa]
600
500
400
300
200
100
0
0.0
2.0
4.0
6.0
Strain [%]

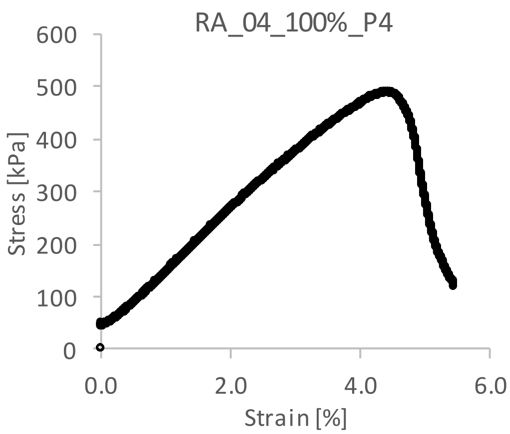
RA_04_100%_P4
Stress [kPa]
600
500
400
300
200
100
0
0.0
2.0
4.0
6.0
Strain [%]

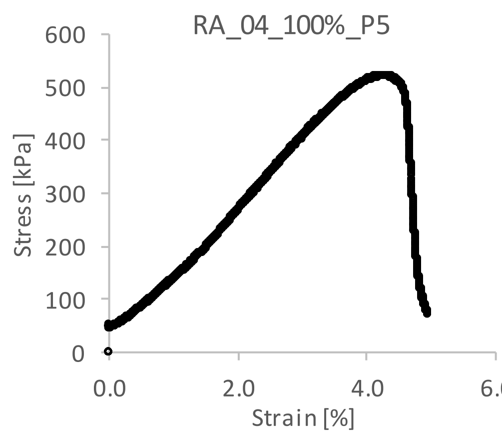
RA_04_100%_P5
Stress [kPa]
600
500
400
300
200
100
0
0.0
2.0
4.0
6.0
Strain [%]

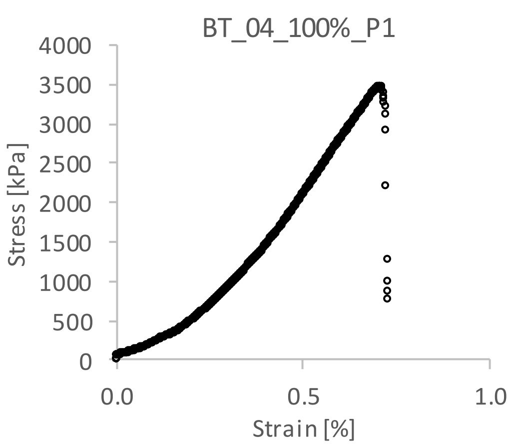
BT_04_100%_P1
Stress [kPa]
4000
3500
3000
2500
2000
1500
1000
500
0
0.0
0.5
1.0
Strain [%]

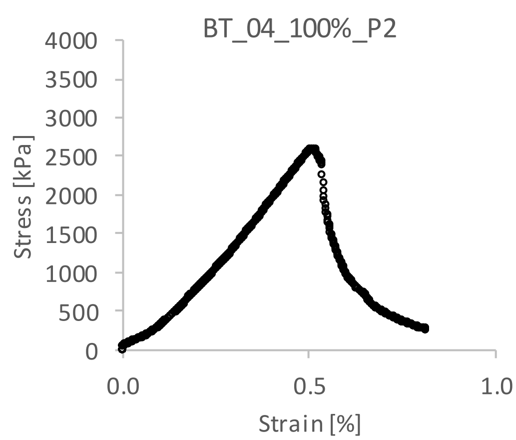
BT_04_100%_P2
Stress [kPa]
4000
3500
3000
2500
2000
1500
1000
500
0
0.0
0.5
1.0
Strain [%]

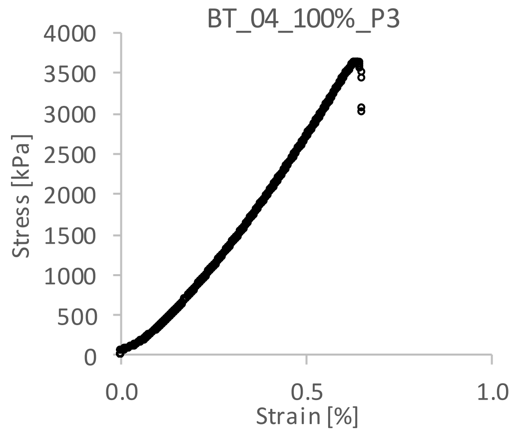
BT_04_100%_P3
Stress [kPa]
4000
3500
3000
2500
2000
1500
1000
500
0
0.0
0.5
1.0
Strain [%]

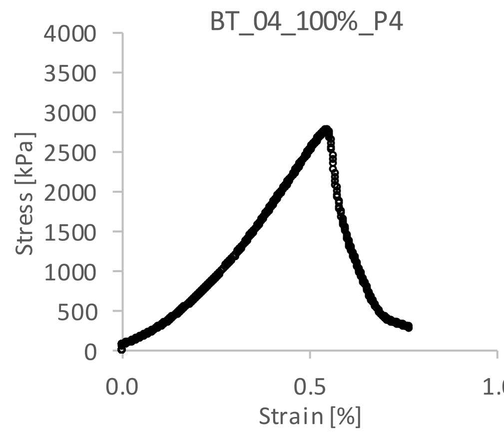
BT_04_100%_P4
Stress [kPa]
4000
3500
3000
2500
2000
1500
1000
500
0
0.0
0.5
1.0
Strain [%]

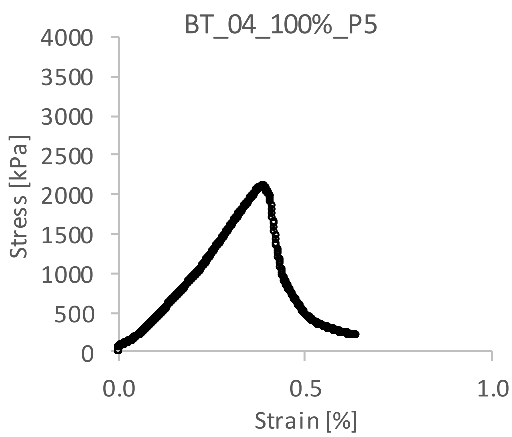
BT_04_100%_P5
Stress [kPa]
4000
3500
3000
2500
2000
1500
1000
500
0
0.0
0.5
1.0
Strain [%]

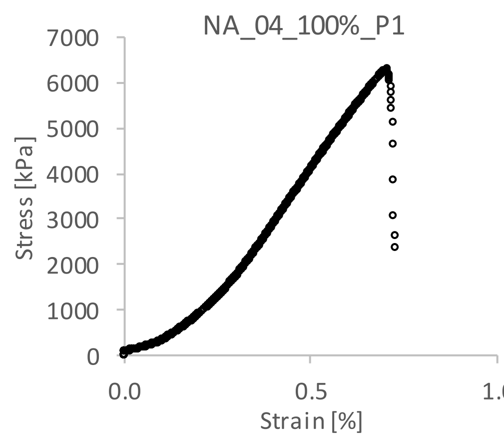
NA_04_100%_P1
Stress [kPa]
7000
6000
5000
4000
3000
2000
1000
0
0.0
0.5
1.0
Strain [%]

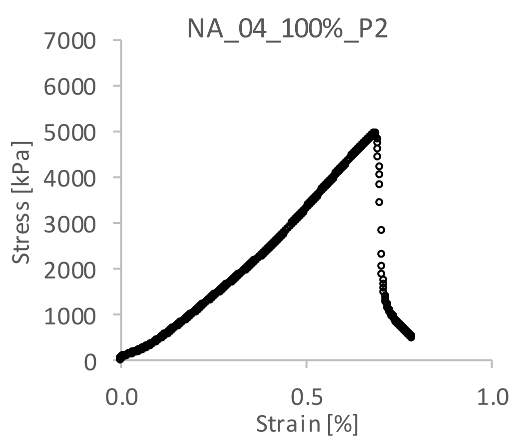
NA_04_100%_P2
Stress [kPa]
7000
6000
5000
4000
3000
2000
1000
0
0.0
0.5
1.0
Strain [%]

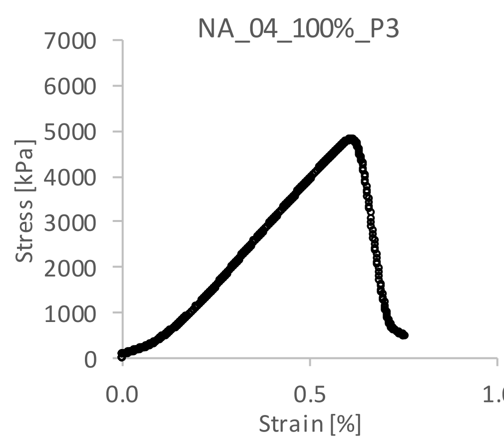
NA_04_100%_P3
Stress [kPa]
7000
6000
5000
4000
3000
2000
1000
0
0.0
0.5
1.0
Strain [%]

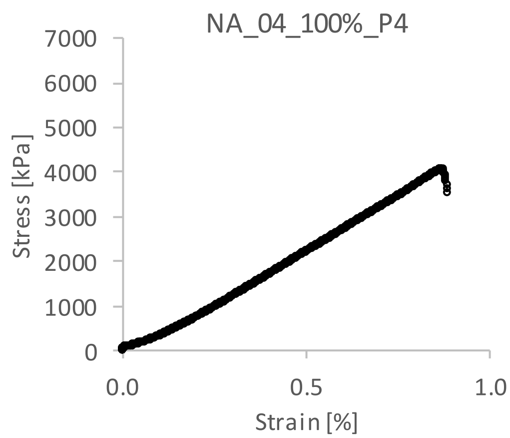
NA_04_100%_P4
Stress [kPa]
7000
6000
5000
4000
3000
2000
1000
0
0.0
0.5
1.0
Strain [%]

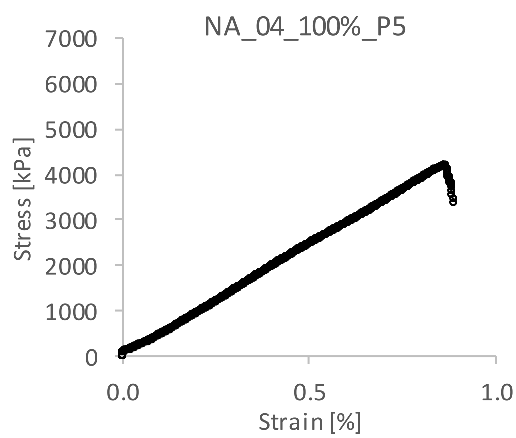
NA_04_100%_P5
Stress [kPa]
7000
6000
5000
4000
3000
2000
1000
0
0.0
0.5
1.0
Strain [%]

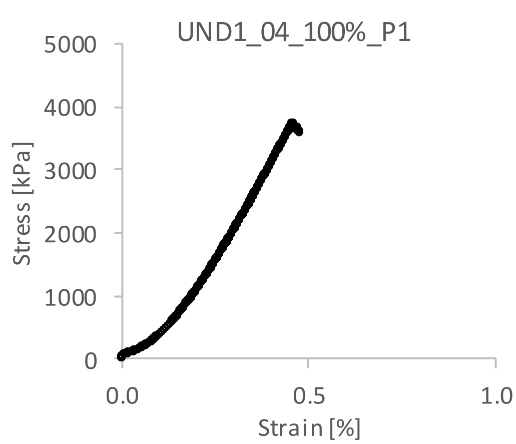
UND1_04_100%_P1
Stress [kPa]
5000
4000
3000
2000
1000
0
0.0
0.5
1.0
Strain [%]

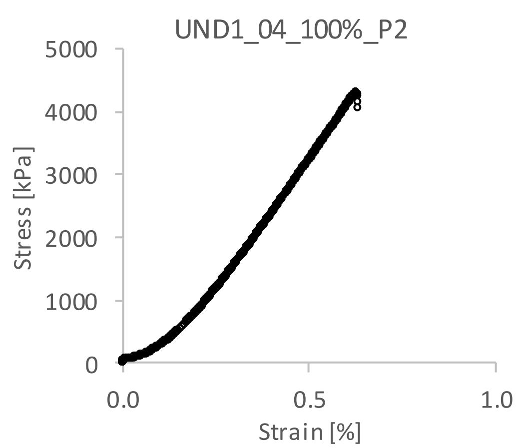
UND1_04_100%_P2
Stress [kPa]
5000
4000
3000
2000
1000
0
0.0
0.5
1.0
Strain [%]

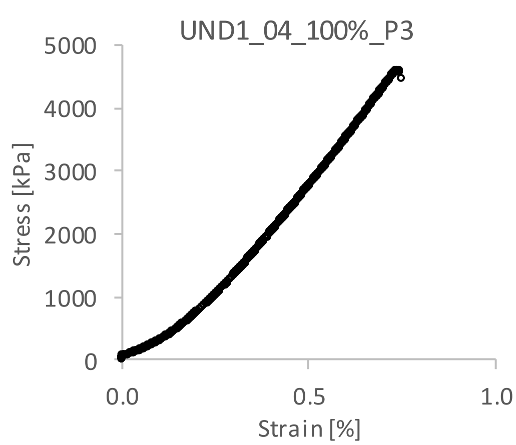
UND1_04_100%_P3
Stress [kPa]
5000
4000
3000
2000
1000
0
0.0
0.5
1.0
Strain [%]

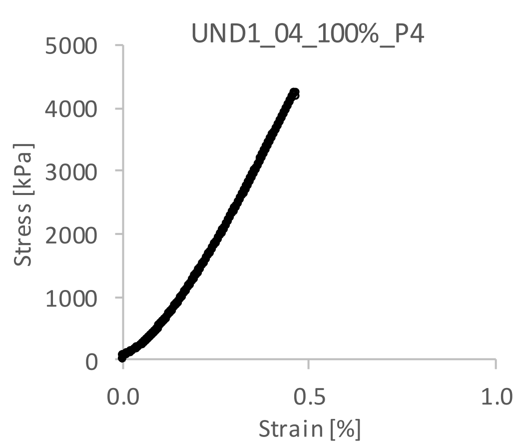
UND1_04_100%_P4
Stress [kPa]
5000
4000
3000
2000
1000
0
0.0
0.5
1.0
Strain [%]

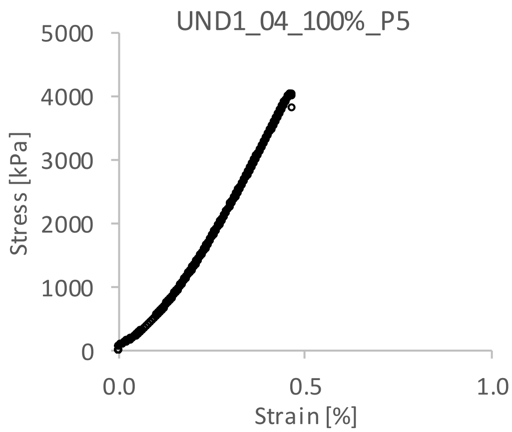
UND1_04_100%_P5
Stress [kPa]
Strain [%]

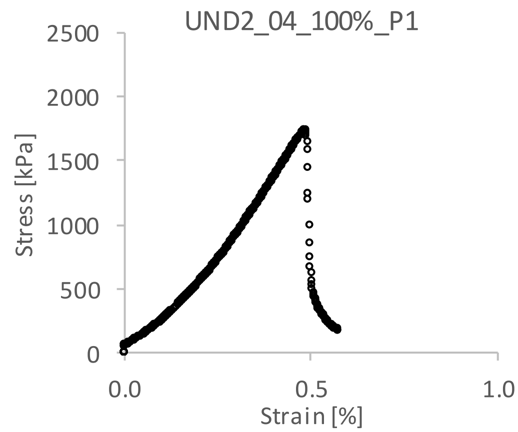
UND2_04_100%_P1
Stress [kPa]
Strain [%]

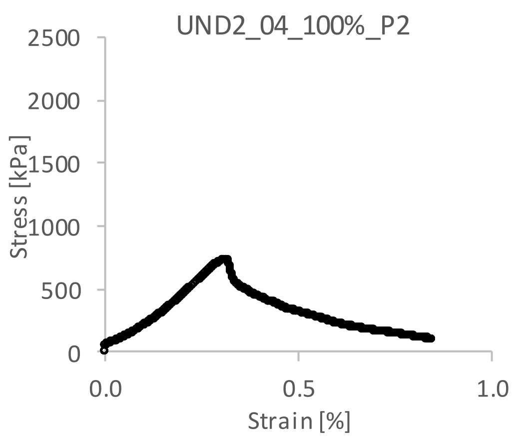
UND2_04_100%_P2
Stress [kPa]
Strain [%]

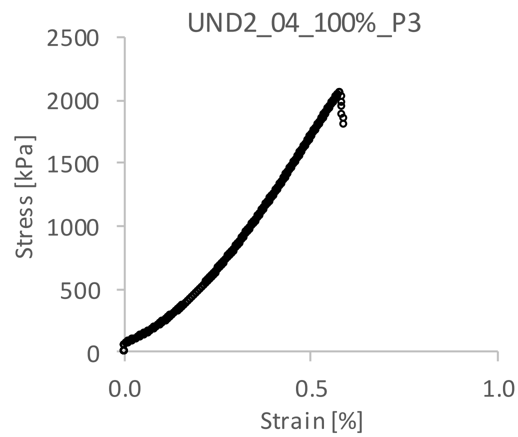
UND2_04_100%_P3
Stress [kPa]
Strain [%]

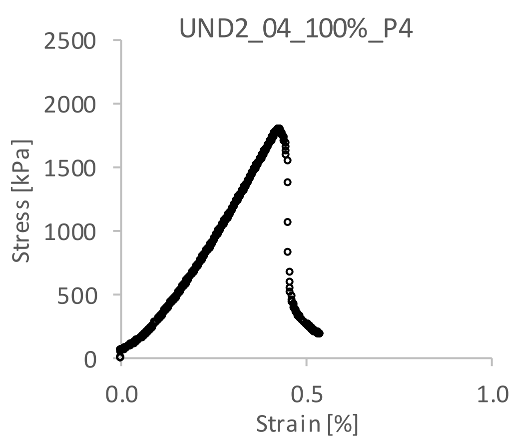
UND2_04_100%_P4
Stress [kPa]
Strain [%]

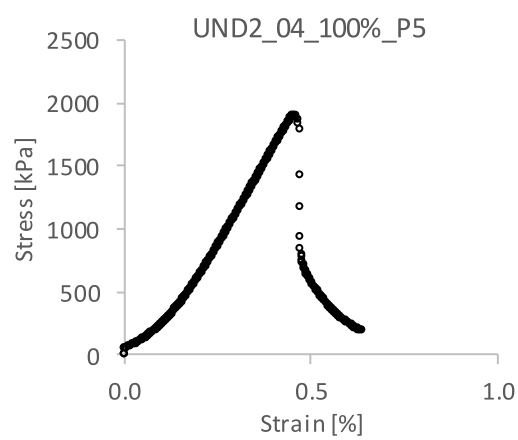
UND2_04_100%_P5
Stress [kPa]
Strain [%]